GENETIC AND EPIGENETIC EVALUATION OF THE CANDIDATE GENES IN HUMAN HEPATOCELLULAR CARCINOMAS

A THESIS SUBMITTED TO
THE DEPARTMENT OF MOLECULAR BIOLOGY AND GENETICS
AND THE INSTITUTE OF ENGINEERING AND SCIENCE
OF BILKENT UNIVERSITY
IN PARTIAL FULFILLMENT OF THE REQUIREMENTS
FOR THE DEGREE OF DOCTOR OF PHILOSOPHY

By
TOLGA ACUN
AUGUST 2010

Canım ailem,

SUMRU ACUN ve FİKRET ACUN'a

adıyorum...

I certify that I have read this thesis and that in my opinion it is fully adequate, in scope, and in quality, as a thesis for the degree of Doctor of Philosophy.

Assist. Prof. Dr. K. Can AKÇALI

I certify that I have read this thesis and that in my opinion it is fully adequate, in scope, and in quality, as a thesis for the degree of Doctor of Philosophy.

Assoc. Prof. Dr. M.Cengiz YAKICIER

I certify that I have read this thesis and that in my opinion it is fully adequate, in scope, and in quality, as a thesis for the degree of Doctor of Philosophy.

Assoc. Prof. Dr. İhsan GÜRSEL

I certify that I have read this thesis and that in my opinion it is fully adequate, in scope, and in quality, as a thesis for the degree of Doctor of Philosophy.

Assist. Prof. Dr. Ayşe Elif ERSON-BENSAN

I certify that I have read this thesis and that in my opinion it is fully adequate, in scope, and in quality, as a thesis for the degree of Doctor of Philosophy.

Assoc. Prof. Dr. Hilal ÖZDAĞ

Approved for the Institute of Engineering and Science

Prof. Dr. Levent ONURAL
Director of the Institute of Engineering and Science

ABSTRACT

GENETIC AND EPIGENETIC EVALUATION OF THE CANDIDATE GENES IN HUMAN HEPATOCELLULAR CARCINOMAS

Tolga Acun
Ph.D. in Molecular Biology and Genetics
Supervisor: Assist. Prof. Dr. K. Can AKÇALI
AUGUST 2010

Hepatocellular carcinoma (HCC) is the fifth most-common cancer and the third most common cause of cancer related mortality worldwide. HCC is also the most common type of liver cancer. Hepatocarcinogenesis is a multistep process that is not completely understood until today. In this study, we genetically and epigenetically evaluated candidate genes and molecular pathways which may act in hepatocarcinogenesis.

The RAS/RAF/MAPK pathway was genetically investigated and no mutation was described in HCC cell lines for the genes *MEK1* (*MAP2K1*), *MEK2* (*MAP2K2*), *ERK1* (*MAPK3*), *ERK2* (*MAPK1*) and *PTPN11* (*SHP2*).

TP53 pathway is also a common target for inactivation during liver carcinogenesis. Our analysis indicated that the presence of the *MDM2*-SNP309 G allele is inversely associated with the presence of somatic *TP53* mutations. This finding suggests that the *MDM2*-SNP309 G allele may functionally replace *TP53* mutations, and in addition to known etiological factors, may be partly responsible for differential HCC prevalence.

Epigenetic silencing of *SIP1* gene in HCC together with its reduced mRNA and protein level in tumors relative to normal liver tissue indicated *SIP1* as a potential tumor suppressor role. Inconsistent with previously published findings in other types of cancers, our results showed for the first time that *PTPRD* gene is epigenetically downregulated and mutated in liver cancers. Among other candidates our results suggest; *FBXL11*, *TUBA3C*, *TPTE2*, *IQSEC1*, *MIPOL1*, *CHUK*, *MCL1*, *MAGI-2* and *PTPRCAP* genes are involved in hepatocarcinogenesis.

ÖZET

İNSAN HEPATOSELÜLER KARSİNOMALARINDAKİ ADAY GENLERİN GENETİK VE EPİGENETİK OLARAK İNCELENMESİ

Tolga Acun
Moleküler Biyoloji ve Genetik Doktorası
Tez Yöneticisi: Yard. Doç. Dr. K. Can AKÇALI
AĞUSTOS 2010

Hepatoselüler karsinoma (HK) dünya çapında, diğer kanser türleri arasında 5. en yaygın kanser türü ve 3. en yaygın kanser ilişkili ölüm sebebi olarak sınıflandırılabilir. HK ayrıca en yaygın karaciğer kanseri tipidir. Hepatokarsinojeneziz çok adımlı bir süreçtir ve bu süreç bugüne kadar tam olarak anlaşılamamıştır. Bu çalışmada, hepatokarsinojenezizde rol oynayabilecek aday genler ve moleküler yolaklar genetik ve epigenetik bakımdan değerlendirilmiştir.

RAS/RAF/MAPK yolağı genetik bakımdan incelenmiş ve HK hücre hatlarında, *MEK1* (*MAP2K1*), *MEK2* (*MAP2K2*), *ERK1* (*MAPK3*), *ERK2* (*MAPK1*) ve *PTPN11* (*SHP2*) genlerinde hiçbir mutasyon saptanmamıştır.

TP53 yolağı karaciğer karsinojenezizinde genel bir inaktivasyon hedefidir. Analizimiz *MDM2*-SNP309 G aleli varlığının, somatik *TP53* mutasyonları varlığı ile ters orantılı olduğunu göstermiştir. Bu bulgu, *MDM2*-SNP309 G alel varlığnın fonksiyonel olarak *TP53* mutasyonlarının yerini alabileceğini ve etiyolojik faktörlere

ek olarak, HK yaygınlık farklılıklarının bir kısmından sorumlu olabileceğini düşündürmektedir.

SIP1 geninin epigenetik olarak susturulmuş olmasıyla beraber, bu genin karaciğer tümörlerinde normal karaciğer dokusuna göre düşük mRNA ve protein ifade seviyesine sahip olması, *SIP1* geninin potensiyel bir tümör baskılayıcı gen olabileceğini işaret etmektedir. Başka kanser türlerinde önceki yayımlanmış çalışmalarla uyumlu olarak, bizim sonuçlarımıza göre *PTPRD* geni ifadesinin epigenetik olarak baskılandığı ve mutasyona uğradığı karaciğer tümörlerinde ilk kez gösterilmiştir. Çalışmamız, diğer aday genler arasında, *FBXL11*, *TUBA3C*, *TPTE2*, *IQSEC1*, *MIPOL1*, *CHUK*, *MCL1*, *MAGI-2* ve *PTPRCAP* genlerinin hepatokarsinojenezizde rol oynadığını öne sürmektedir.

.

ACKNOWLEDGMENTS

I am grateful to my supervisor Dr. M.C. YAKICIER, for his valuable guidance, sharing his scientific knowledge, his patience and warm friendship. I would like to thank all my group mates, Özkan AYDEMİR, Yeliz YUVA AYDEMİR, Kubilay DEMİR, Atıl Çağdaş SAYDERE, for their friendship and help during my study.

I am grateful to Dr. K. Can AKÇALI and his group members; Zeynep TOKÇAER KESKİN, Fatma AYALOĞLU, Sumru BAYIN, for their endless technical and scientific support.

I am also deeply thankful to Dr. Tamer YAĞCI and Dr. Emin ÖZTAŞ for their big help and efforts during western and immunohistochemistry studies.

There are no groups or graduate students exist in the Bilkent MBG department that did not help me during my thesis study. I am very thankful to all Bilkent MBG group leaders and their graduate students, in other words my dear colleagues, not only for their help and for sharing their scientific knowledge and equipments with me but also for providing me a warm and cheerful environment. I will not forget this 7 years that I spent with you.

Thank to all MBG department personels, Sevim GÜRER BARAN, Füsun ELVAN KANBUR, Bilge ERDEM ÖZBAYOĞLU, Bilge KILIÇ, Tülay ARAYICI, Abdullah ÜNNÜ, Turan DAŞTANDIR and also thank to all our cleaning and security staff in behalf of Özcan KARA.

And finally I am very grateful to my family; my mother N. Sumru ACUN and my father Fikret ACUN, for their unconditioned and endless support during my education. Without their support this thesis will not be compelete.

This Ph.D. thesis research was supported by grants from TUBİTAK.

TABLE OF CONTENTS

LIST OF TABLES

LIST OF FIGURES

ABBREVIATIONS

AFB1	Aflatoxin B1
AKT	v-akt murine thymoma viral oncogene homolog
BRAF	v-raf murine sarcoma viral oncogene homolog B1
BRIT-1	BRCT-repeat inhibitor of TERT expression 1
bp	Base Pair
CDKN2A	cyclin-dependent kinase inhibitor 2A
cDNA	Complementary DNA
DAC	5-aza-2' deoxycytidine
ddH2O	Double Distilled Water
DMEM	Dulbecco's Modified Eagle's Medium
DMSO	Dimethylsulfoxide
DNA	Deoxyribonucleicacid
DNMT	Dna Methly Transferase
dNTP	Deoxyribonucleotide Triphosphate
dsDNA	Double-Stranded DNA
EDTA	Ethylene Diamine Tetra-Acetic Acid
ERK1	Mitogen-activated protein kinase 3
ERK2	Mitogen-activated protein kinase 1
EtBr	Ethidium Bromide
FBS	Fetal Bovine Serum
g	Gram
GAPDH	Glyceraldehyde-3-Phosphate Dehydrogenase
h	Hour
HBV	Hepatis B Virus
HBX	Hepatitis Virus Protein
HCC	Hepatocellular Carcinoma
HCV	Hepatis C Virus
HNPCC	Hereditary Nonpolyposis Colorectal Cancer
HRP	Horseradish peroxidase

hSIR2	Human SIR2-like protein 1
LOH	Loss of Heterozygosity
MAD1	Mitotic spindle assembly checkpoint protein
MAP/ERK	Mitogen activated protein/extracellular signal-regulated kinase
MAPK	Mitogen Activated Protein Kinase
MB	Mega base-pairs
MENIN	MEN1 (multiple endocrine neoplasia type 1)
MEK1	Mitogen-activated protein kinase kinase 1
MEK2	Mitogen-activated protein kinase kinase 2
mg	Miligram
miRNA	MicroRNA
MIN	Microsatellite Instability
min	Minute
ml	Mililiter
mm	Milimeter
mM	Milimolar
mRNA	Messenger RNA
MYC	Myelocytomatosis Viral Oncogene Homolog (Avian)
NaCl	Sodium Chloride
NAD	Nicotinamide Adenine Dinucleotide
NATs	Natural Antisense Transcripts
P21/CIP1	Cyclin Dependent Kinase Inhibitor 1A
PAGE	Polyacrylamide Gel Electrophoresis
PBS	Phosphate Buffered Saline
PCR	Polymerase Chain Reaction
PI3K	Phosphoinositide Kinase-3
PTEN	Phosphatase and tensin homolog
PTPN11	Protein tyrosine phosphatase, non-receptor type 11
PVDF	Polyvinylidene Difluoride
RAK	Fyn-related kinase (FRK)
RAF	Proto-oncogene serine/threonine-protein kinase

RAS	Rat sarcoma viral oncogene homolog
Rb	Retinoblastoma
RNA	Ribo Nucleic Acid
Rpm	Revolutions Per Minute
RT PCR	Reverse Transcription Pcr
Sec	Second
SNP	Single Nucleotide Polymorphism
TAE	Tris Acetate Edta Buffer
TBE	Tris Boric Acid Edta
TBS-T	Tris-Buffered Saline Tween-20
TGF-β	Transforming growth factor
TNFα	Tumor Necrosis Factor-α
Tm	Melting Temperature
TP53	Tumor Protein P53
Tris	Tris(Hydroxymethyl)-Methylamine
TSA	Trichostatin A
UV	Ultraviolet
v/v	Volume/Volume
VC	Vinyl Chloride
w/v	Weight/Volume
Wnt	Wingless
ZEB2	Zinc finger E-box binding homeobox 2
ZFHX1B	Zinc finger homeo box 1B
XC	Xylenecyanol
µg	Microgram
µl	Microliter
µm	Micrometer
µM	Micromolar
5-Aza-dC	5-aza-2′-deoxycytidine
5AzaC	5-aza-cytidine

CHAPTER 1
INTRODUCTION

1.1. Hepatocellular Carcinoma

1.1.1. Epidemiology

HCC is the fifth most-common malignancy in the world and is the third most-common cause of cancer-related mortality worldwide (Ferlay J. *et al*., 2001; Parkin D.M. *et al*., 2001). Among other types of histologically distinct primary hepatic neoplasms, such as intrahepatic bile duct carcinoma (cholangiocarcinoma), hepatoblastoma, bile duct cystadenocarcinoma, haemangiosarcoma and epitheliod haemangioendothelioma, HCC is the most common type of liver cancer, representing 83% of all cases ("Cancer Facts and FIGS", 2005; Anthony P., 2002).

Incidence of HCC vary according to geographical region. Most HCC cases are seen in sub-Saharan Africa or in Eastern Asia (Figure 1.1.1). China alone accounts for more than 50% of the world's cases. Incidence also vary according to sex. Males have higher HCC rates than females with a ratio between 2:1 to 4:1. High HCC incidence in males is thought to be not only due to sex-specific differences in exposure to risk factors but also due to androgens. (Rudolph KL *et al*., 2000; El-Serag H.B. and Rudolph K. L., 2007).

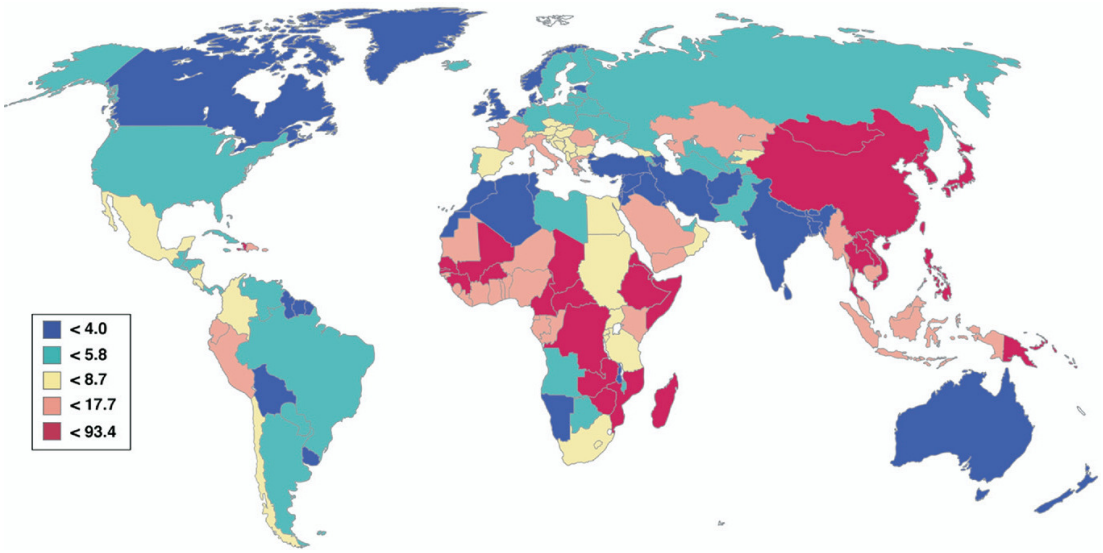

Figure 1.1.1 : Regional difference in the mortality rates of HCC categorized by age-adjusted mortality rates. The rates are reported per 100,000 persons (from "El-Serag H.B. and Rudolph K. L., 2007" with permission)

1.1.2. Aetiologies of hepatocellular carcinoma

Today, hepatocarcinogenetic process is much more better understood. It nearly always developes after chronic hepatitis or cirhosis during which many hepatocytes die and inflamatory cells invade the liver. Some agents that are known as causes of HCC and leading to marked variation in HCC incidence have been determined (Grisham J.W., 2001; Bosch F.X., *et al*. 1999; Buendia M.A., *et al*. 2000). These agents - hepatitis B virus (HBV), hepatitis C virus (HCV) and aflatoxin B1 (AFB) – are responsible for about 80% of all HCCs. There are several other risk factors that have also been associated with HCC. Such factors include exposure to vinyl chloride, tobacco, heavy alcohol intake, nonalcoholic fatty liver disease, diabetes, obesity, coffee, oral contraceptives and hemochromatosis (Aravalli R.N. *et al*., 2008). Prevalancy of these factors vary according to geographical regions. For instance, chronic hepatitis B virus (HBV) infection is prevalent in Africa and many Asian countries whereas hepatitis C virus (HCV) is dominant in Japan and the United States (El-Serag H.B. *et al*., 2007).

1.1.2.a. Hepatitis B Virus

Hepatitis B virus (HBV) infection is the most prominent cause of HCC with an estimated 320,000 deaths annualy. Previous studies have shown that HBV infection increased the risk of HCC 5- to 15-fold compared to general poulation (El-Serag H.B. *et al*., 2007).

HBV is a non-cytopathic, partially double-stranded hepatotropic DNA virus classified as a member of the *hepadnaviridae* family. The HBV genome encodes several viral proteins essential to its life cycle, including the capsid protein known as hepatitis B core antigen (HBcAg), a reverse transcriptase/DNA polymerase (pol), and the L, M and S envelope proteins that associate with the endoplasmic reticulum (ER) membrane as part of their replication process. HBV also encodes some other proteins whose functions are not fully understood, such as protein x (HBx) (Block T.M. *et al*., 2003)

Several studies have shown that HBV is directly involved in the transformation process. Integration of HBV genome to the host genome has been associated with host DNA microdeletions (Tokino T. *et al*., 1991). These deletions can target cancer-relevant genes including platelet-derived-growth-factor receptor-β (*PDGFRβ*), *PDGFβ*, mitogen activated protein kinase 1 (*MAPK1*) and telomerase reverse transcriptase (*TERT*) (Murakami Y. *et al*., 2001). HBx protein can bind and inactivate the tumor suppressor p53 in vitro, which increase cellular proliferation and survival (Feitelson M. A. *et al*., 2002; Ueda H. *et al*., 1995). The HCC inducing potential of HBx has been genetically validated in HBx transgenic mice. 90% of these mice have develop HCC (Kim C.M. *et al*., 1991; Yu D.Y. *et al*., 1999). Finally, HBx transcriptional activation can change the expression of growth-control genes, such as SRC tyrosine kinases, *RAS*, *RAF*, *MAPK*, *ERK*, *JNK* (Tarn C. *et al*., 2001; Nijhara R. *et al*., 2001; Feitelson M.A. *et al*., 2002).

1.1.2.b. Hepatitis C Virus

Chronic hepatitis C virus infection is an another major risk factor for HCC development. HCV-infected patients have 17-fold higher risk of getting HCC compared with HCV-negative controls (Donato F. *et al*., 2002). HCV have very high propensity to yield chronic infection than HBV (60-80% versus 10% respectively) Also propensity of HCV to promote liver cirrhosis is approximately 10–20-fold higher than HBV (Rehermann B. & Nascimbeni M., 2005).

HCV is classified as a member of the *flaviviridae* family. It is a non-cytopathic positive-stranded RNA virus. The HCV genome encodes non-structural proteins (NS2, NS3, NS5B, NS4A and NS5A) and viral envelope proteins (E1 and E2) (Farazi P.A. and DePinho R.A., 2006). This virus has no reverse transcriptase activity and does not integrate itself into the host genome (McKillop I.H. *et al*., 2006). It is suggested that HCV core protein is involved in the regulation of cell growth, as it can transcriptionaly regulate some cellular genes, including the proto-oncogene c-myc. Furthermore, the hepatic tumor inducing effect of HCV core protein has been seen in transgenic mice expressing the HCV core protein (Ray R.B. *et al*., 1995; Moriya K. *et al*., 1998). Another possible mechanism of HCV for HCC induction is its ability to inhibit apoptosis activators such as Fas and tumor necrosis factor-α (TNF- α) (Marusawa H. *et al*., 1999; Jin X., 2006)

Also, the HCV nonstructural proteins NS3 and NS5A have been shown to have direct oncogenic potential as indicated by their ability to promote anchorage independent growth when expressed in fibroblasts and tumor formation in nude mice (Sakamuro D. *et al*., 1995; Ghosh A.K. *et al*., 1999).

1.1.2.c. Aflatoxin B1

Aflatoxin B1 is a strong hepatocarcinogen and “International Agency for Research on Cancer” classified it as carcinogen (IARC, 1987). It is a fungal toxin (mycotoxin) produced by fungi *Aspergillus* that contaminate food such as nuts, grains and spices that are stored in humid conditions. In some areas, having high incidence of HCC such as South-East Asia and sub-saharan Africa, the rate of Aflatoxin B1 contamination together with HBV infection is also high. Aflatoxin B1

function as a mutagen and it induces G to T mutations. The most striking one is p53 hotspot mutation at codon 249 resulting in an Arg to Ser alteration in the p53 protein This mutation has been observed in 30%–60% of HCC tumors in aflatoxin-endemic areas (Ozturk M., 1991; Bressac B. *et al*., 1991; Turner P.C. *et al*. 2002). Aflatoxin B1 also have an mutational activation effect on HRAS oncogen (Riley J. *et al*., 1997). Aflatoxin B1 is metabolized by cytochrome p450 and converted to its exo-8,9-epoxide form which inturn react with guanine nucleotide and form DNA adducts. (Figure 1.1.2.) These DNA adducts result in heritable genetic changes that force the hepatocyte toward transformation (Smela *et al*., 2001; Essigmann J.M., *et al*. 1983). Aflatoxin B1 exposure often coexists with HBV infection, and such individuals have a 5–10-fold increased risk of developing HCC compared with exposure to only one of these factor (Kew, M.C., 2003).

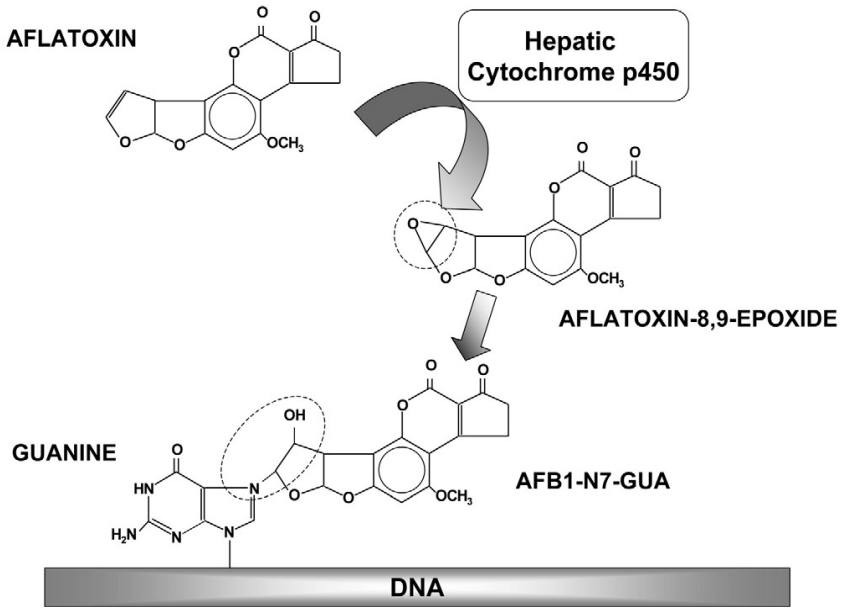

Figure 1.1.2 : Metabolic conversion of aflatoxin B1 to the 8,9-epoxide by cytochrome p450 and subsequent DNA adduct formation (from "Smela *et al*., 2001" with permission).

1.1.2.d. Alcohol

Heavy alcohol intake -more than 50–70 g/day for prolonged periods- is an another important HCC risk factor (Longnecker M.P., 1995; McKillop I.H., Schrum L.W., 2005). But the risk of HCC is not clear with low or moderate alcohol intake. Alcohol can damage the liver by three ways; inflammation, oxidative stress and cirrhosis. Alcohol causes the production of proinflammatory cytokines through monocyte activation and provokes increased concentrations of circulating endotoxin. Küpffer cells -specialized macrophages of the liver- become activated and releases many chemokines and cytokines such as TNFα, prostaglandin E2, interleukin-1β (IL1β), and IL6. These chemokines and cytokines have an adverse effect on hepatocyte survival. Chronic ethanol intake can increase the sensitivity of hepatocytes to the cytotoxic effects of TNFα which leads to chronic hepatocyte destruction, cirrhosis and finally HCC (McClain C.J. *et al*., 2002; Hoek J.B. & Pastorino J.G., 2002).

Ethanol metabolism is a two-step process involving the conversion of ethanol to acetaldehyde and conversion of acetaldehyde to acetate by the aldehyde dehydrogenase enzyme. In both process, NADH molecule is produced which result in the synthesis of reactive oxygen species (ROS) and hepatic oxidative stress (Figure 1.1.3). In addition, acetaldehyde, if accumulates in the cell, causes the formation of protein and DNA adducts and additional ROS generation (Ekstrom G. and Ingelman-Sundberg M., 1989).

Alcohol induced oxidative stress might be implicated in hepatocarcinogenesis in several ways. First, it provokes the development of fibrosis and cirrhosis which can lead to HCC. Second, it could have an effect on HCC-relevant signalling pathways. The loss of the protective effects of IFNγ results in hepatocyte damage (Osna N.A., 2005). Increased oxidative stress results from iron overload (hereditary haemochromatosis) might also be associated with the accumulation of oncogenic mutations such as *TP53* mutations (Marrogi A.J. *et al*, 2001). Alcohol induced oxidative stress may also contribute telomere shortening which help the process of chromosomal instability, liver cirrhosis and ultimately HCC (Kurz D.J. *et al*., 2004).

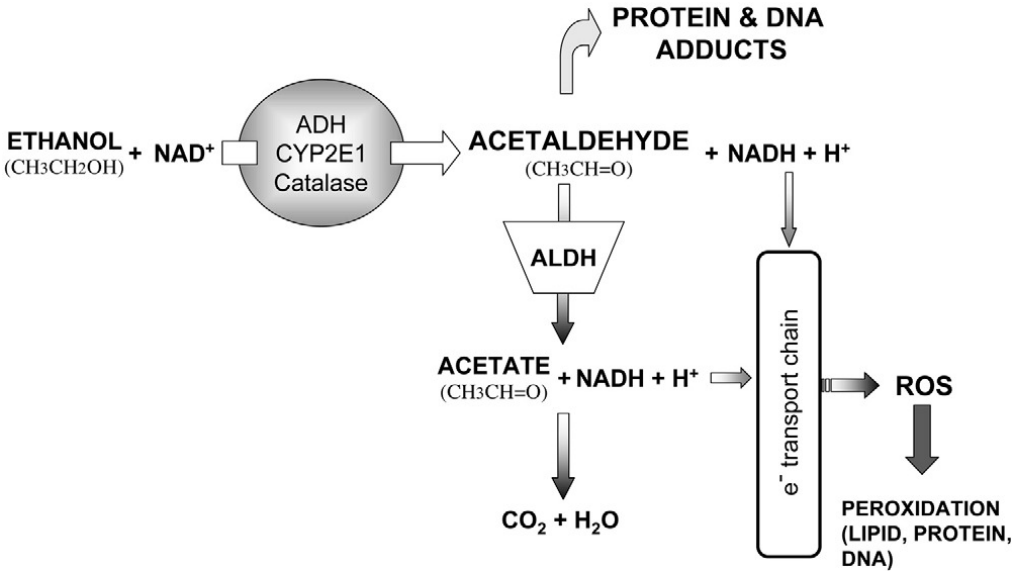

Figure 1.1.3 : Hepatic ethanol metabolism. Ethanol is metabolized to acetaldehyde which is then metabolized by acetaldehyde dehydrogenase to acetate (from "McKillop I.H. *et al*., 2006" with permission).

1.1.3. Molecular mechanisms and Genetic/Epigenetic Changes in HCC

Hepatocarcinogenesis is a multistep process which not only causes increased loss of differentiation, loss of normal cell adhesion and degradation of the extracellular matrix but also leads to progressive activation of some survival and growth-promoting pathways (McKillop I.H., 2006).

Chronic liver damage is a major driving factor of hepatocarcinogenesis as healthy liver rarely develops HCC during normal aging. High frequency of cell division helps hepatocarcinogenesis process to gain the genetic hits necessary for cellular transformation. But, this mechanism is unlikely to be a major mechanism of HCC. Chromosome copy number alterations and translocations are much more common in human HCCs. But, the most common condition associated with HCC is cirrhosis and it requires 20-40 years of chronic liver disease. Cirrhosis stage is characterized by low regenerarive capacity of the liver. There are 3 main mechanisms described which accelarate the HCC formation after the cirrhosis stage;

telomere shortening, slow hepatocyte proliferation, changes at the micro- and macro-environment of the liver. (El-Serag H.B., *et al*. 2007).

During the long preneoplastic stage, mitogenic pathways are upregulated partly by epigenetic mechanisms which leads to accelerated hepatocyte cycling. This stage is characterized by chronic hepatitis, cirrhosis, or both. Dysplastic hepatocytes form monoclonal populations which have telomere erosion, telomerase re-expression, microsatellite instability, and finally defective genes and chromosomes. Accumulation of these structural changes in genes and chromosomes form the basis of HCC. But the genomic changes that leads to malignant phenotype of the liver is heterogeneous. Many genes that are function in several different molecular pathways could be effected to cause HCC (Figure 1.1.4, Figure 1.1.5) (Thorgeirsson S.S. & Grisham J.W., 2002).

Molecular analysis of HCC show that Rb1, p53, and Wnt pathways are the most common pathways affected during hepatocarcinogenesis. Loss of $P16^{INK4A}$ and *RB1* expression through promoter methylation and amplification of *C-MYC* and *Cyclin D1* are the most common alterations (Table 1.1. and Table 1.2.) (Edamoto Y. *et al*., 2003). Also telomerase is shown to be activated in more than 90% of human HCC and up-regulated telomerase reverse transcriptase (*hTERT*) is a bonafide marker of human HCC (Llovet J.M. *et al*., 2006).

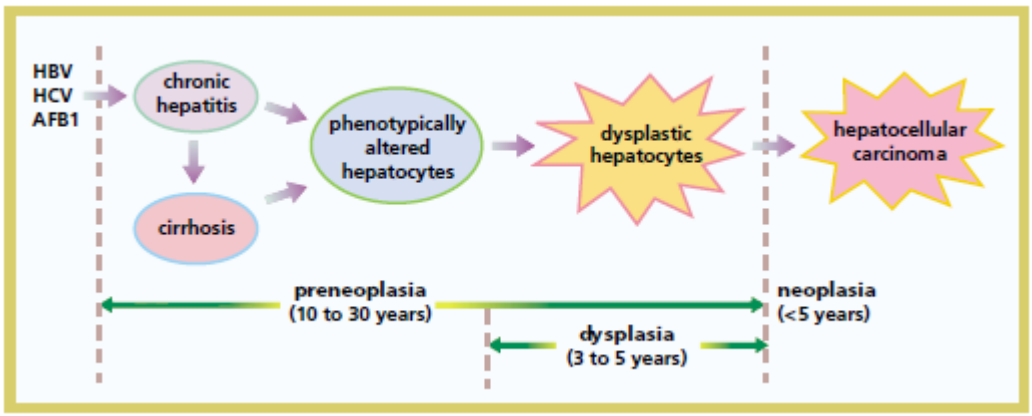

Figure 1.1.4 : Multistep process of hepatocarcinogenesis (from "Thorgeirsson S.S, 2002" with permission)

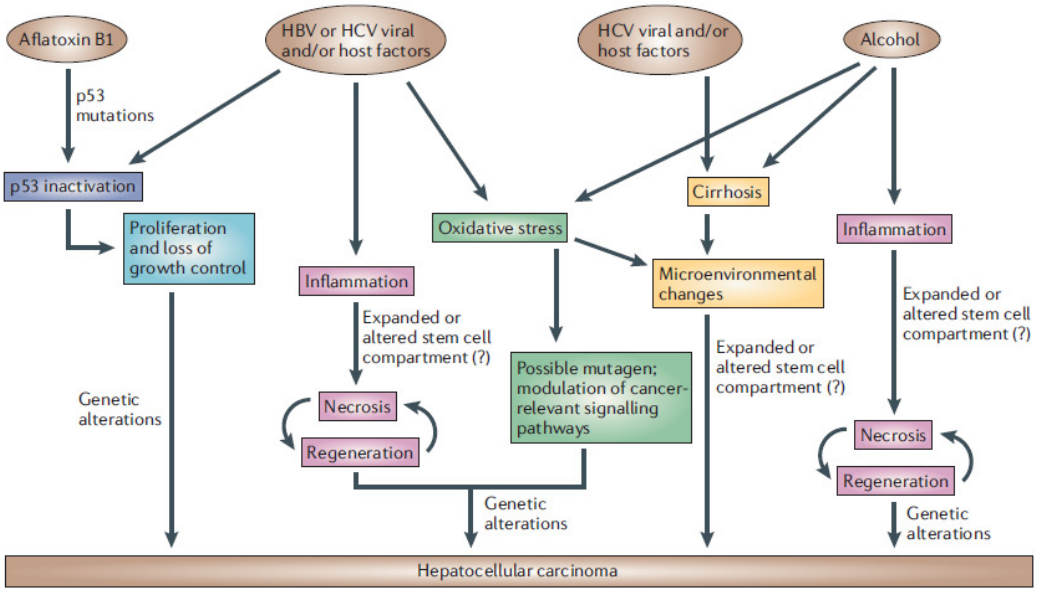

Figure 1.1.5 : Mechanisms of hepatocarcinogenesis for the various aetiologic factors (from "Farazi,P.A. and DePinho,R.A. 2006" with permission)

Genes	LOH (%)	Mutations (%)
TP53 (17p13)	~42	~27
M6P/*IGF2R* (6q27)	~42	~13
RB (13q)	~35	~22
P16 (9p21)	~30	~6
PTEN (10q)	~30	~17
RUNX3, *P73* (1p36)	~35	---
β-CATENIN	---	~22
SMAD2 & *SMAD4*	---	~10

Table 1.1 : Genes subjected to LOH, mutation or both in HCC (Thorgeirsson S.S, 2002; Xiao WH and Liu WW, 2004; Polakis P., 2000; Yakicier M.C. *et al.* 1999)

Alterations of Cell Cycle and Apoptosis Checkpoints		**Alterations of Developmental Pathways**		**Alterations of Oncogenic Pathways**	
Activation	**Inactivation**	**Activation**	**Inactivation**	**Activation**	**Inactivation**
Gankyrin (100%)	P16 (80%)	Hedgehog (50-60%)	Prickle 1 (55%)	Telomerase (>90%)	PTEN (41%)
MDM2 (45%)	IGF2R (>60%)	MET (30-40%)		MYC (30-60%)	
	P27 (50%)	WNT-β Cat. (26%)		PI3K/AKT (38%)	
	P53 (20-50%)				
	ARF (20%)				

Table 1.2 : Common alterations in cell cycle/apoptosis, developmental and oncogenic pathways in HCC (adapted from El-Serag HB, Rudolph KL., 2007).

Genetic and epigenetic events in HCC and their relationship to phenotype are poorly understood. During hepatocarcinogenesis gross genomic alterations occur such as chromosomal deletion or amplification, CpG methylation, DNA hypomethylation, DNA rearrangements. (Xu X.R. *et al*., 2001; Herath N.I., 2006). Chromosomal gains in 1q, 5p, 5q, 6p, 7q, 8q, 11q, 17q and 20q and losses in 1p, 4q, 6q, 8p, 10q, 13q, 16p, 16q, 17p can be listed as frequent genomic alterations in HCC (Farazi P.A. and DePinho R.A., 2006; Midorikawa Y. *et al*., 2006) (Table 1.3). Promoter hypermethylation has also been shown in HCC at tumor suppressor and tumor related genes such as *P16*, *P14*, *P15*, *SOCS-1*, *CASP8* and *E-CADHERIN*. (Table 1.4) *C-MYC* is overexpressed in HCC predominantly with promoter hypomethylation and with gene amplification (Herath N.I., *et al*. 2006; Tischoff I. and Tannapfel A., 2008; Yu J. et al., 2002).

Gain (%)	**LOH (%)**
1q (72.2%)	1p (22.2%)
5p (25%)	4q (27.7%)
5q (30.5%)	6q (27.7%)
6p (33.3%)	8p (55.5%)
7q (22.2%)	10q (33.3%)
8q (61.1%)	13q (47.2%)
17q (25%)	16p (25%)
20q (25%)	16q (36.1%)
	17p (66.7%)

Table 1.3 : Common chromosomal gain and losses in HCC (Farazi P.A. and DePinho R.A., 2006; Midorikawa Y. *et al*., 2006).

Gene	Location	Function	Methylation Frequency (%)
p16^{INK4a}	9q21	CDK inhibitor	17-83
p14^{ARF}	9q21	MDM2 inhibitor	25-30
CASP8	2q33	Apoptosis	72
TMS1/ASC	16p11.2	Apoptosis	80
E-Cadherin	16q22.1	Cell adhesion	33-67
M-Cadherin	16q24.1	Cell adhesion	55
H-Cadherin	16q24.2-3	Cell adhesion	21
TIMP3	22q12	MMP inhibitor	13-19
hMLH1	3p21.3	Mismatch repair	18-44
hMSH2	2p21-22	Mismatch repair	68
hMSH3	5q11-12	Mismatch repair	75
MGMT	10q26	DNA repair	22-39
GSTP1	11q13	Detoxification	41-58
SOCS-1	16p13.13	Cytokine inhibitor	60
SOCS-3	17q25.3	Cytokine inhibitor	33
RASSF1A	3p21.3	Apoptosis	54-95
SEMA3B	3p21.3	Apoptosis	80
FHIT	3p14.2	Histidine triad protein	71

Table 1.4 : Commonly methylated genes in HCC (adapted from Tischoff I. and Tannapfel A., 2008).

In this study, we genetically and epigenetically evaluated candidate genes that are fullfiil our selection criteria: (a) the gene must be shown to be a tumor suppressor or oncogene, but not studied in HCC; (b) it must have a role or be a member of a pathway in important cellular processes such as apoptosis, senescence or proliferation; (c) it must be located in commonly deleted or amplified regions in HCC and (d) alterations of it must be shown to trigger HCC in animal models. The chromosomal regions; 13q12, 11q13 and RAS/RAF/MAPK pathway genes genetically dissected. Other candidates either targeted by genetic events or indicated in the literature were evaluated. A total of 18 genes; *SIP1, PTPRD, MDM2, FBXL11, PTPRCAP, TUBA3C, ZNF198, TPTE2, IQSEC1, MIPOL1, CHUK, MCL1, MAGI-2, PTPN11, MEK1, MEK2, ERK1, ERK2* were evaluated in terms of their mRNA and protein expression and genetic/epigenetic alterations.

1.2. *SIP1*/*ZEB2*/*ZFHX1B* (Chr 2q22)

Carcinogenic process involves a series of events that allow cells to bypass senescence. Replicative senescence (telomere-dependent senescence, permanent growth arrest or M1 stage) is a potent anti-carcinogenic program and is believed to be initiated by the critically shortened telomers or by the loss of telomer integrity that activates cell cycle check point pathways involving p53, $p16^{INK4a}$, p21 and/or pRb proteins. In the absence of functional p53 and $p16^{INK4a}$/pRb pathway responses, telomeres continue to shorten resulting in crisis also called M2 stage. (Ozturk N. *et al*., 2006; Shay W.J. and Roninson I.B., 2004). During carcinogenesis, cancer cells bypass crisis by reactivating *hTERT* (human Telomerase Reverse Transcriptase) expression and gain the ability for indefinite cell proliferation, also called immortality. In recent studies, several genes including *SIP1*, *hSIR2*, *C-MYC*, *MAD1*, *MENIN*, *RAK* and *BRIT1* have been shown to be implicated in the mechanism of *hTERT* expression (Lin S.Y. and Elledge S.J., 2003; Wang J. *et al*., 1998) but only *SIP1* gene was strongly expressed in hTERT-negative senescent cells. Functional inactivation of *SIP1* in senescent cells has been shown to be enough to bypass the senescent arrest. *SIP1* is thought to serve as a molecular switch between replicative immortality and replicative senescence fates in HCC (Ozturk N. *et al*., 2006). SIP1 could also inhibit cell proliferation directly by downregulating *CYCLIN-D* expression (Mejlvang J. *et al*., 2007). Taken together with in vitro studies, these observations suggest that SIP1 may acts as a tumor suppressor gene in HCC but the mechanisms that contribute to the regulation of *SIP1* expression are not completely known.

SIP1 gene (2q22) (Smad Interacting Protein-1, *ZEB2* or *ZFHX1B*), encoding two-handed zinc finger homeodomain transcription factor protein, belongs to a small family of transcriptional repressors. ZEB2/SIP1 contains two Zn-finger clusters; at the N-terminal (N-ZF) and C-terminal (C-ZF) part of the protein (Figure 1.2.1). SIP1 is involved in TGF-β signaling by binding to MH2 domain of Smads. (Nelles L. *et al*., 2003; Verschueren K. *et al*., 1999).

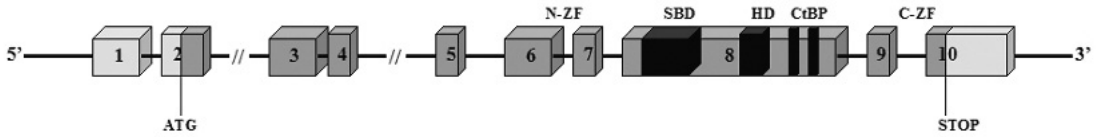

Figure 1.2.1 : *ZEB2* exons and functional domains. N-ZF, N-terminal zinc finger cluster; SBD, Smad-binding domain; HD, homeodomain; CtBP, C-terminal binding protein interacting domain; C-ZF, C-terminal zinc finger cluster (figure adapted from Dastot-Le Moal F. et al., 2007).

Beside its tumor suppressor activity through TGF-β dependent hTERT down regulation, SIP1 also have cell invasiveness and tumor progression effect by repressing E-CADHERIN expression through which it promotes epithelial-mesenchymal transition (EMT) (Comijn J., *et al*., 2001; Miyoshi A. *et al*., 2004) (Figure 1.2.2).

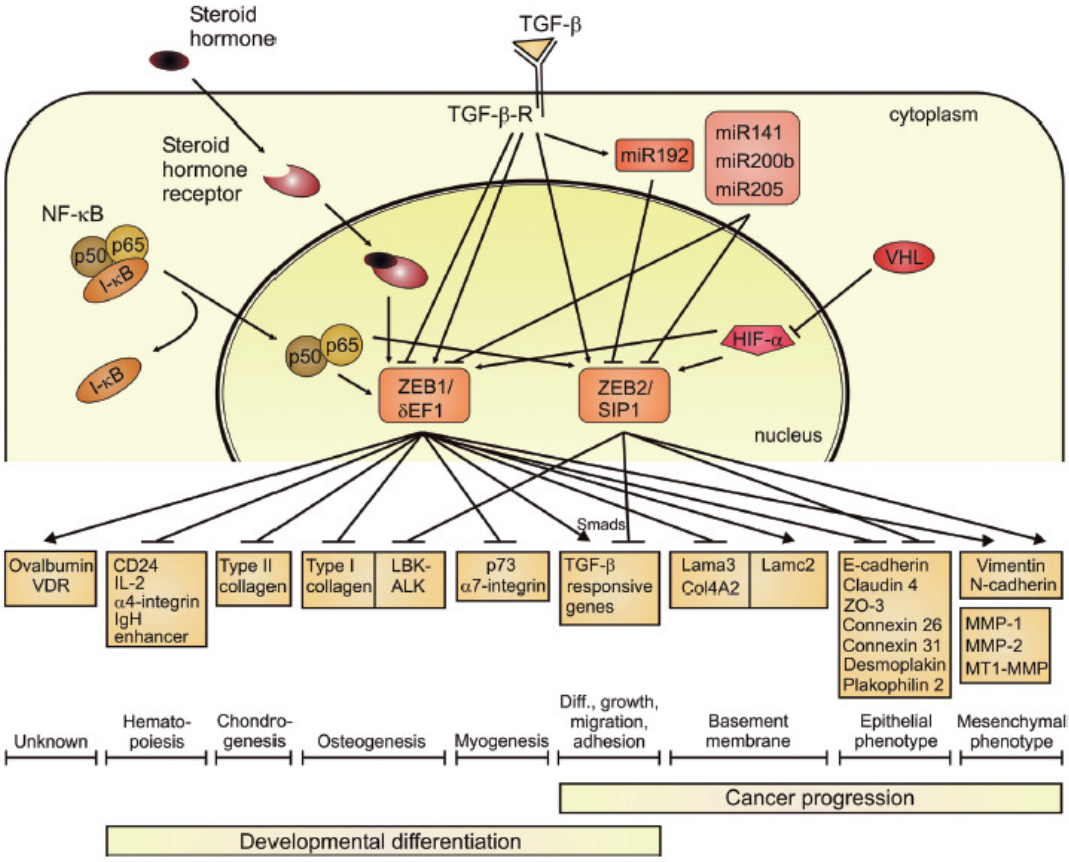

Figure 1.2.2 : Upstream signaling events and downstream targets of the ZEB family of transcription factors (ZEB1 and ZEB2) and their phenotypic effects are summerized. (from "Vandewalle C. *et al*., 2009" with permission)

SIP1 is essential for embryonic neural and neural crest development (Van de Putte T. *et al*., 2003) and its mutations cause severe defects in humans, namely Hirschsprung disease (Yamada K. *et al*., 2001; Wakamatsu N. *et al*., 2001) and Mowat-Wilson disease (Mowat D.R. *et al*., 2003; Moal DL. F. *et al*., 2007). Studies showed that the *SIP1* gene is expressed at high levels in almost all human somatic tissues tested, (heart, brain, placenta, lung, squeletal muscle) including liver and strongly positive in non-tumor liver samples, but its expression was significantly decreased in corresponding HCC samples (Ozturk N. *et al*., 2006; Cacheux V. *et al*., 2001).

Several studies showed that *SIP1* is epigeneticaly regulated, including miRNAs (Bracken C.P. *et al*., 2008; Cano A. and Nieto M.A., 2008; Christoffersen N.R. *et al*., 2007; Park SM. *et al*. 2008; Gregory P.A. *et al*., 2008) natural antisense transcripts (NATs) (Beltran M. *et al*., 2008) and hypermethylation (Rodenhiser D.I. *et al*., 2008). There is a double negative feedback loop between ZEB factors (ZEB1 and SIP1/ZEB2) and miR-200 family members. miR-200 family members inhibit ZEB factors at post-transcriptional level, ZEB factors inhibit miR-200 family members at the transcriptional level (Bracken C.P. *et al*., 2008). In a recent study, silencing of *SIP1* expression through promoter hypermethylation rather than miR-200 family was shown in most pancreatic cancer samples (90%). *SIP1* expression was restored by inhibiting the methylation with 5-Aza-dC in pancreatic cell lines (Li A. *et al.*, 2010).

There is a functional association between methylation status and expression level of the SIP1 gene in breast cancer cell lines. *SIP1* gene was found to be hypermethylated and silenced in poorly metastatic breast cancer cell line (Rodenhiser D.I. *et al*., 2008). *SIP1* genetic and epigenetic alterations is not known in HCC. In this study, genetic and epigenetic alterations of the *SIP1* gene was investigated in HCC including somatic mutation, mRNA and protein expression level, 5'CpG island methylation status and histone modification.

1.3. *PTPRD/PTPD/HPTP* (Chr 9p23)

Allelic loss on chromosome 9p has been reported in many tumor types including lung cancer, melanoma, gastric carcinoma, glioma, and head and neck cancer (Sato M. *et al*., 2005, Fountain J.W., *et al*. 1992; Sakata K. *et al*., 1995; Li Y.J. *et al*, 1995; Van der Riet P. *et al*., 1994). Frequent allelic loss on chromosome 9 in hepatocellular carcinoma has also been reported by Liew C.T. *et al*. (1999) and Kondo Y. *et al*. (2000). The tumor suppressor gene *CDKN2A* (*MTS1/P16*) located at chromosome 9p21 was shown to be deleted in various cancers. (Kondo Y. *et al*., 2000; Biden K. *et al*., 1997; Liew C.T. *et al*., 1999).

Kubilay Demir from our group also showed homozygous deletion in Mahlavu, Plc, Skhep1, Snu182, Snu387 and Snu423 HCC cell lines which maps to 9p23. This 1 MB region maps to a part of protein tyrosine phosphatase receptor type D gene (*PTPRD*) (Fig 1.3.1).

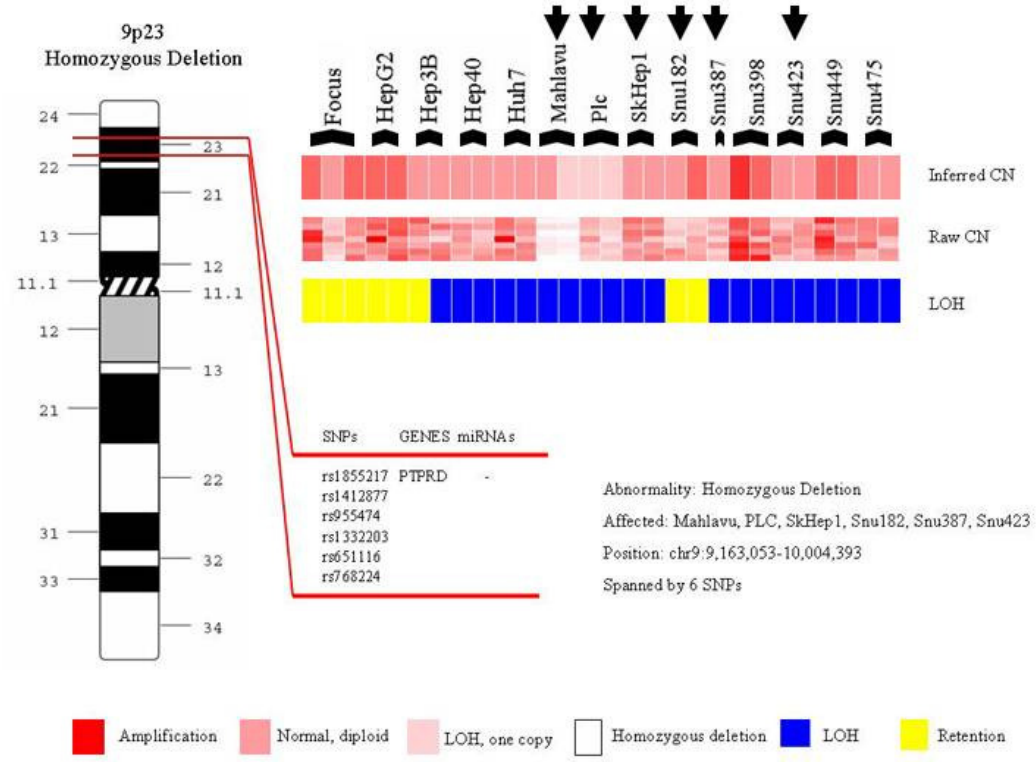

Figure 1.3.1 : Homozygous deletion at 9p23 in Mahlavu, PLC, SkHep1, Snu182, Snu387 and Snu423 HCC cell lines (adapted from Kubilay Demir thesis study).

PTPRD belongs to a protein-tyrosine phosphatases (PTPs) family which have a total of 107 members encoded by the human genome (Alonso, A. *et al*., 2004). PTPs constitute a large, highly specific enzymes having important regulatory roles. PTPs have both inhibitory and stimulatory effects on cancer-associated signalling processes. Deregulation of PTP function is associated with tumorigenesis in different types of human cancer. (Andersen, J. N. *et al*., 2001 ; Östman, A. & Böhmer, F. D., 2001; Alonso, A. *et al*., 2004).

PTPs are divided into non-receptor forms and receptor-like forms. The receptor-like PTPs have a single transmembrane domain and variable extracellular domains. The intracellular parts of most of the receptor-like PTPs contain two tandem PTP domains (D1 and D2). In many cases, the extracellular domains include immunoglobulinlike domains and fibronectin type III domains, similar to the extracellular domains of cellular adhesion molecules (Ostman A., 2006).

Candidacy of *PTPRD* as a tumor suppressor gene was first suggested by Urushibara *et al*. (1998). In Urushibara's study, mRNA levels of the four receptor-like protein tyrosine phosphatases (PTPases) (PTPalpha, PTPdelta, PTPgamma and LAR) were evaluated by Northern blot analysis in two types of chemically-induced rat primary hepatomas. PTPdelta mRNA was selectively reduced in these hepatoma tissues. Many other studies have reported homozygous deletions of *PTPRD* in a wide range of tumor types including lung cancer (Zhao X. *et al*., 2005; Kohno T. *et al*., 2010), neuroblastoma (Nair P. *et al*., 2008; Stallings R.L. *et al*., 2006), cutaneous squamous cell carcinomas (SCC) (Purdie K.J. *et al*., 2007), pancreatic cancer (Calhoun E.S., 2006), melanoma (Stark M. and Hayward N., 2007) and glioblastoma multiform (Solomon D.A., 2008).

SANGER CONAN (Copy Number Analysis) database also shows number of LOH and homozygous deletions in various cancer types (Figure 1.3.2). 5 HCC cell lines; PLC, SkHep1, Snu387, Snu449 and Snu475 are shown to have LOH in the region containing *PTPRD* gene. Homozygous deletion of *PTPRD* in Snu475 cell line was also shown in SANGER database (Figure 1.3.3).

Somatic mutations of *PTPRD* were first shown in a panel of 35 colorectal cancers by Sjoblom *et al*. (2006) who identified three missense substitutions. Mutations of *PTPRD* in lung adenocarcinoma (Ding *et al*., 2008; Weir *et al*., 2007), in glioblastoma multiforme (GBM), melonoma (Solomon *et al*., 2008), lung and squamous head and neck carcinoma (Veeriah S. *et al*., 2009) were also described.

Functional studies have recently showed that PTPRD has a tumor suppressive properties in human cancer cells. PTPRD inactivates STAT3 oncogene by dephosphorylating the 705^{th} tyrosine residue. Reconstitution of *PTPRD* expression in GBM and melanoma cells, that was alleviated by both the somatic and constitutional mutations, result in growth suppression and apoptosis (Solomon *et al*., 2008). Ectopic expression of *PTPRD* suppresses growth of human cancer cells HT29 (Human colon adenocarcinoma grade II cell line), SKMG3 (GBM cell line) and HCT-116 (colorectal carcinoma cell line). Knockdown of PTPRD with shRNAs results in increased growth rate of immortalized human astrocytes (Veeriah S. *et al*., 2009).

Veeriah *et al*. also showed that *PTPRD* is silenced or inactivated not only by deletions or somatic mutations, but also epigenetically. *PTPRD* was methylated in GBM (37%), breast (20%) and colon cancer (50%) but not in corresponding normal tissues. This study was also showed that *PTPRD* expression is restored in GBM cell line SKMG3 after treatment with the DNMT inhibitor DAC (Veeriah S. *et al*., 2009). Genetic and epigenetic alterations is not known in hepatocarcinoma.

View Selected Samples

Ensembl:9:8304246-9008735 | Cosmic:PTPRD

» Results for Gene 'PTPRD'

Tissues	High Level Amplification (>7)	Homozygous Deletion	LOH	Mutation
TOTAL (all tissues)	5	14	412	2
Adrenal gland (2)	0	0	2	0
Autonomic ganglia (37)	0	2	13	0
Biliary tract (6)	0	0	5	0
Bone (33)	1	0	16	0
Breast (45)	2	0	18	0
Central nervous system (59)	0	0	29	0
Cervix (12)	0	0	6	0
Endometrium (10)	0	0	1	0
Gastrointestinal tract (site indeterminate) (1)	0	0	1	0
Haematopoietic and lymphoid tissue (127)	0	1	46	0
Kidney (21)	0	0	17	0
Large intestine (39)	0	0	14	0
Liver (9)	0	1	5	0
Lung (149)	0	4	91	1
NS (1)	0	0	1	0
Oesophagus (22)	1	1	16	0
Ovary (22)	0	0	8	0
Pancreas (16)	0	0	15	0
Pleura (6)	0	0	4	0
Prostate (5)	0	0	2	0
Skin (51)	0	1	42	0
Soft tissue (19)	0	1	9	0
Stomach (21)	0	0	14	0
Testis (3)	0	0	1	0
Thyroid (12)	1	1	8	0
Upper aerodigestive tract (21)	0	2	14	0
Urinary tract (18)	0	0	11	1
Vulva (3)	0	0	3	0

Figure 1.3.2 : Homozygous deletion and LOH were described in the region containing *PTPRD* in many cancer types. Data an the photograph obtained from SANGER CONAN: Copy Number Analysis. (http://www.sanger.ac.uk/cgi-bin/genetics/CGP/conan/search.cgi).

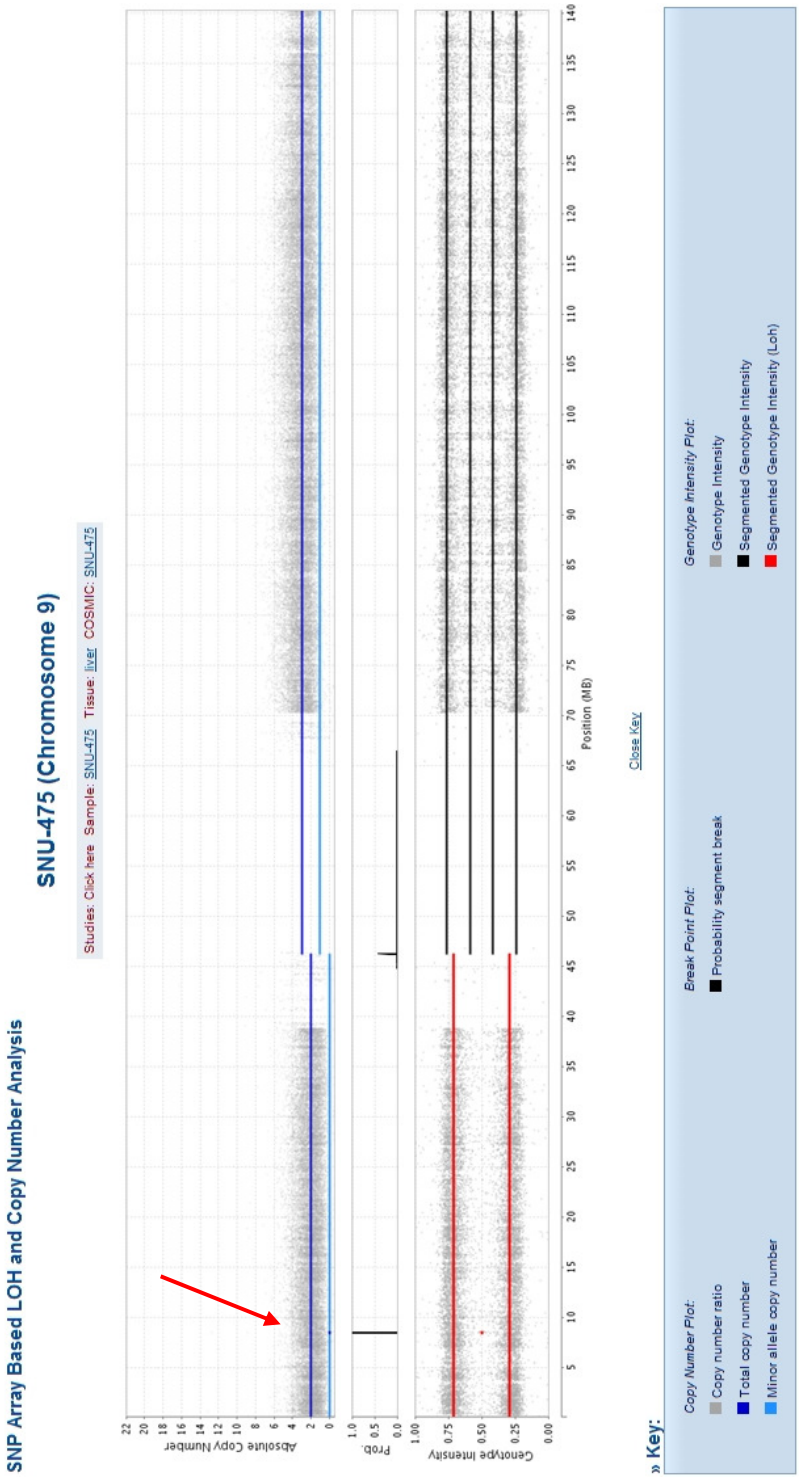

Figure 1.3.3: Copy number analysis of chromosome 9 in Snu475 HCC cell line. Homozygous deleted region (red arrow) containing PTPRD gene was also shown. Data and the photograph obtained from SANGER CONAN: Copy Number Analysis. (http://www.sanger.ac.uk/cgi-bin/genetics/CGP/conan/search.cgi).

1.4. *MDM2*

Germline polymorphisms of several genes have been studied as potential risk factors for HCCs (Sutton A., *et al*., 2006; Vogel A. *et al*., 2001; Yu M.W. *et al*., 1999). However, the pathogenesis of human HCC is a multistage process with the involvement of a series of genes, including oncogenes and tumor suppressor genes; germline polymorphisms of these genes may also determine individual susceptibility to HCC (Acun T., *et al.* 2010).

The p53 tumor suppressor gene (*TP53*) is of critical importance for regulating cell cycle and maintaining genomic integrity. *TP53* also is a common target for inactivation during liver carcinogenesis. Although this inactivation may be largely due to mutations in the *TP53* gene, recent evidence suggests that other mechanisms may be involved in *TP53* inactivation. For instance, the hepatitis B virus-encoded X antigen (HBxAg) binds to and inactivates wild-type TP53 (Ozturk M. *et al*., 1999; Puisieux A. *et al*., 1997). Interaction of TP53 with a cellular oncoprotein, MDM2, also inactivates TP53, via increasing its degradation and/or blocking TP53 transcriptional activation (Oliner J.D. *et al*., 1993; Momand J. *et al*., 1992; Haupt Y. *et al*., 1997; Acun T., *et al.* 2010) (Figure 1.4.1).

In a recent study, a functional single nucleotide polymorphism at nucleotide 309 (T>G) in the promoter region of *MDM2* has been reported. Interestingly, cells with the 309 G/G genotype have an enhanced affinity to bind stimulatory protein Sp1 and also show heightened *MDM2* expression and a significant attenuation of the p53 pathway compared with those carrying the 309 T/T genotype (Bond G.L. *et al*., 2004). Furthermore, SNP309 has been shown to be associated with earlier age of onset of certain hereditary and sporadic cancers in humans (Bond G.L. *et al*., 2004; Bougeard G. *et al*., 2006). In this study, we investigated the distribution of the SNP309 genotype in 99 human HCCs that were previously characterized for *TP53* alterations from HCC endemic and rare geographical areas (Acun T., *et al.* 2010).

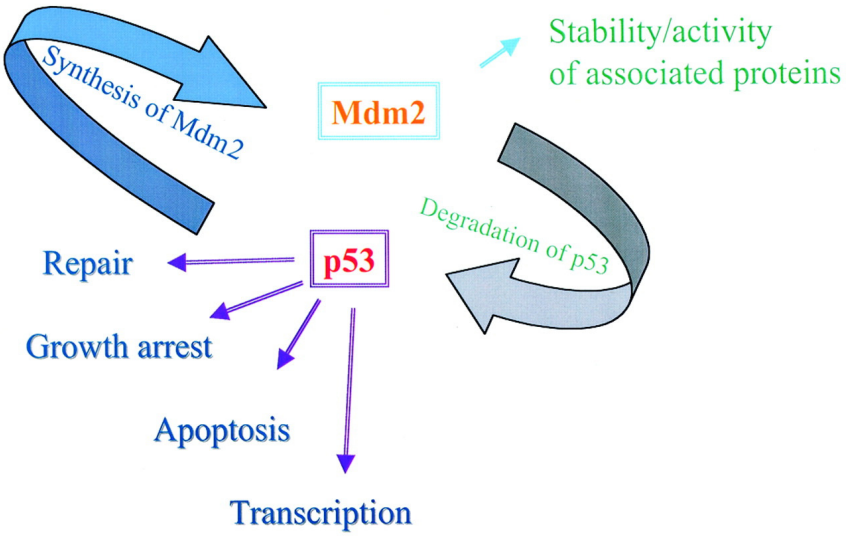

Figure 1.4.1 : p53, Mdm2 and their major activities **(**from "Alarcon-Vargas D., Ronai Z., 2002" with permission).

1.5. RAS/RAF/MAPK Pathway

RAS/RAF/MAPK pathway is one of the key signaling pathway in the transmission of signals from growth factor receptors to regulate cell proliferation and survival (Schubbert S. *et al.,* 2007). The MEK/ERK pathway is the best known MAPK pathways, having a key role in cell proliferation, and is known to be deregulated in approximately one-third of all human cancers. In this pathway ERK (extracellular signal-regulated kinase; ERK1 and ERK2) is activated upon phosphorylation by MEK (mitogen-activated and extracellular-signal regulated kinase kinase; *MEK1* and *MEK2*) which itself activated by Raf (Raf-1, B-Raf and A-Raf) (Dhillon A.S. *et al*., 2007) (Figure 1.5.1).

Many genes of these pathways are mutated or aberrantly expressed in several human cancers. Activating *RAS* mutations occur in ~30% of human cancers (Schubbert S. *et al.,* 2007). *RAS* mutations were described in many cancer types such as pancreas (90%), thyroid (60%), lung adenocarcinoma (non-small cell) (35%), liver (30%) and acute myelogenous leukemia (30%).

On the other hand, BRAF, which is the strongest MEK kinase followed by RAF-1, was shown to be mutated mostly in melanoma (66%) and colorectal cancer (12%) (Davies H. *et al*., 2002; Dhillon A.S. *et al*., 2007; Downward J., 2003). Mutations of BRAF were within the kinase domain, with a single substitution (V599E) accounting for 80% (Davies H. *et al*., 2002). Our ex group member Banu Sürücü was also showed activating BRAF mis-sense mutation (V599E) in SkHep1 cell line. She extended the analysis in HCC samples and found this mutation in one out of 53 HCC samples.

In contrast to *RAS* and *BRAF*, *MEK1* and *MEK2* mutations have not been reported in cancer or in any other human disease (Schubbert S. *et al.,* 2007; Greenman C. *et al*., 2007). In Greenman's study, the coding exons of 518 protein kinase genes were analysed in 10 different cancer types excluding liver and no somatic mutation was described for *MEK1 (MAP2K1) , MEK2 (MAP2K2), ERK1 (MAPK3)* and *ERK2 (MAPK1)* genes.

Genetic analysis of the other genes in RAS/RAF/MAPK pathway including *PTPN11 (SHP2)* would enlighten the role of RAS/RAF/MAPK pathway in HCC.

PTPN11 (protein tyrosine phosphatase, non-receptor type 11, *SHP2*) is a cytoplasmic protein tyrosine phosphatase and promotes the activation of the RAS/RAF/MAPK signaling pathway. Germline mutations of the *PTPN11* was shown in individuals with Noonan syndrome (NS) whereas somatic mutations in the same gene contribute myeloid and lymphoid malignancies. Mutations of *PTPN11* were also observed in melanoma, neuroblastoma, colon cancer and lung cancer (Matozaki T. *et al*., 2009; Tartaglia M. *et al*., 2006; Tartaglia M., Gelb B. D., 2005; Bentires-Alj M. *et al*., 2004). However there is no study showing *PTPN11* mutations in HCC.

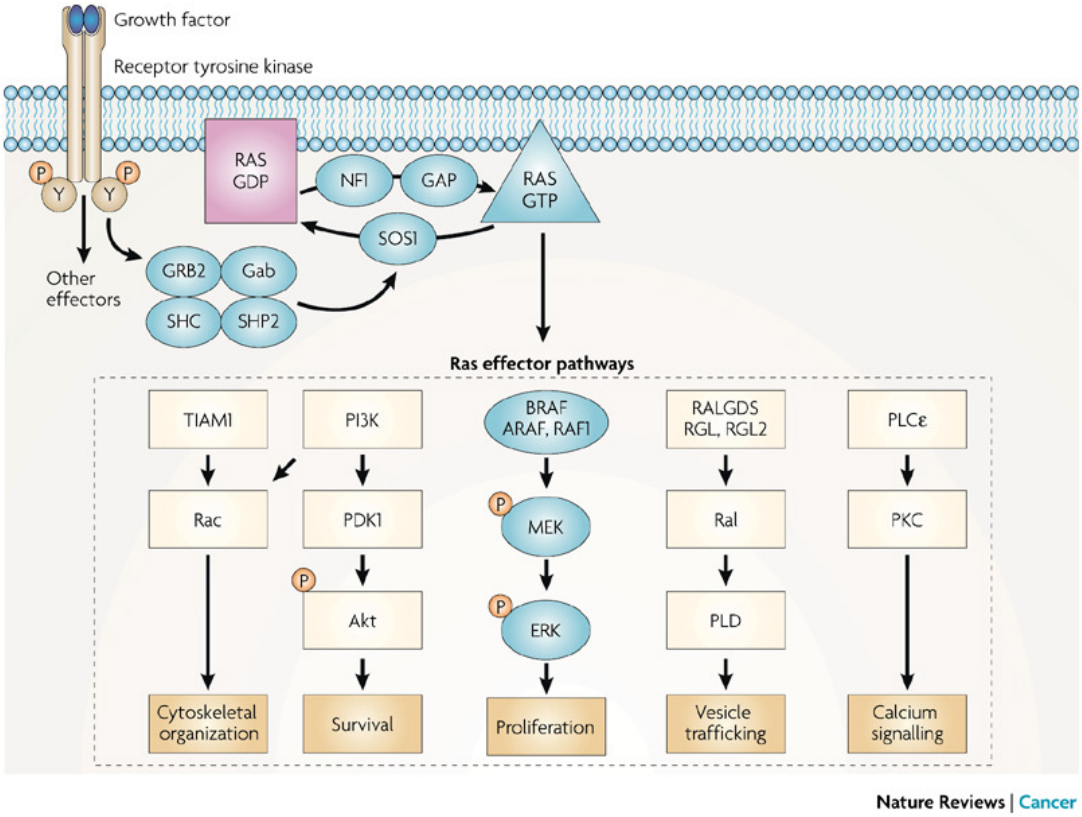

Figure 1.5.1 : RAS/RAF/MAPK pathway (from "Schubbert S. *et al*., 2007" with permission)

1.6. Chromosome 11q13 (*FBXL11*, *PTPRCAP*)

Several studies had been shown the amplification of chromosome 11q13 region in some cancer types including, bladder, esophageal, lung, hepatocellular carcinoma, breast and head and neck cancer. Chromosome 11q13 amplification has been reported in 13% of lung cancers, 15% of breast carcinomas, 21% of bladder tumors, 29% of head and neck cancer, about 45% of oral squamous cell carcinomas (OSCC) and squamous cell carcinomas of the head and neck and 50% of esophageal cancers (Zhang Y.J. *et al*., 1993; Schuuring E., 1995; Huang X. *et al*., 2002; Tanigami A. *et al*., 1992).

More than 10 genes are known to reside in the 11q13 amplicon and *CYCLIN D1, TAOS1, S14 (THRSP), CCND1* and *EMS1* have been reported to be amplified and identified as candidate oncogenes (Bekri S, 1997; Dickson C. *et al*., 1995; Huang X. *et al*., 2002; Schuuring E. *et al*., 1995; Zhang Y.J. *et al*, 1993; Moncur C.T. *et al*., 1998; Yuan B.Z., 2003) (Figure 1.6.1).

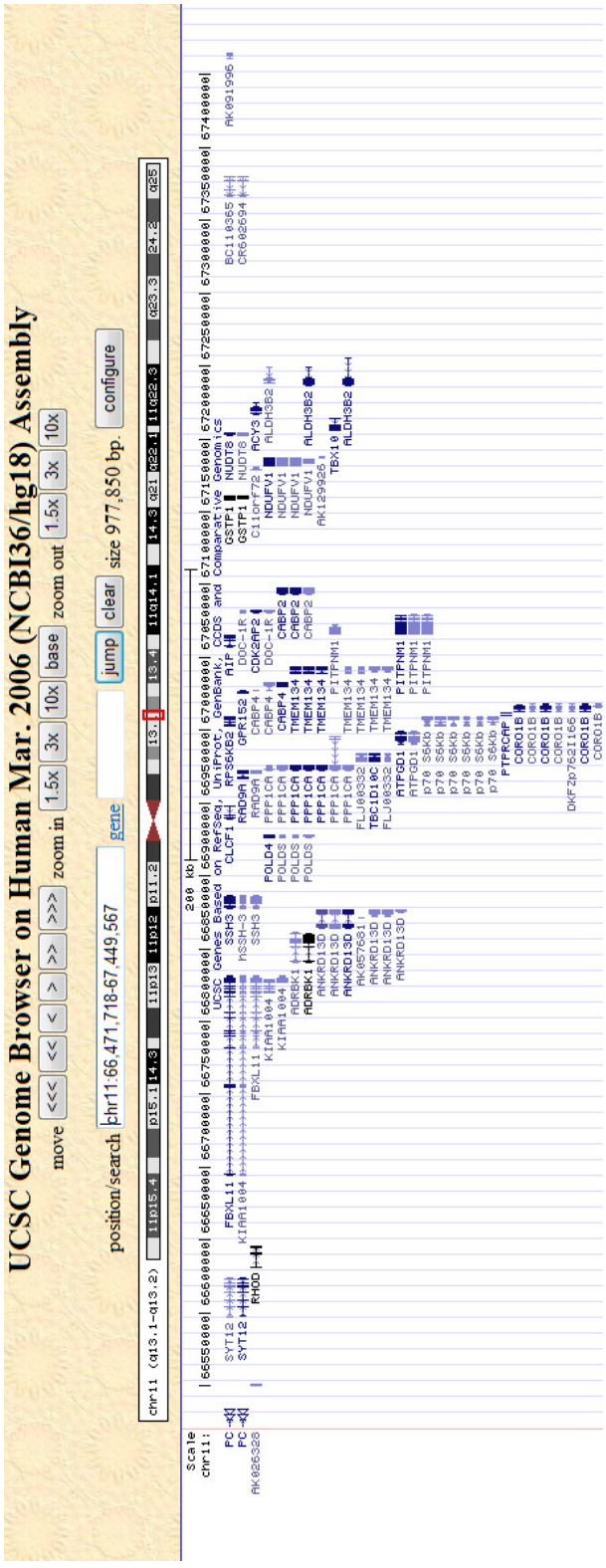

Figure 1.6.1 : Graphical view of chromosome 11(q13.1-q13.2) region and the genes reside in this region (UCSC Genome Browser: http://genome.ucsc.edu/cgi-bin/hgTracks)

1.6.1. *FBXL11*

FBXL11 (F-box and leucine-rich repeat protein 11), *KDM2A*, *JHDM1A* or *NDY1* is a lysine histone demethylase and contains a JmjC-domain and an F-box motif. *FBXL11* is required to maintain the heterochromatic state, centromeric integrity and genomic stability, particularly during mitosis (Frescas D. *et al*., 2008; Pfau R. *et al*., 2008). *FBXL11* is expressed primarily in testis, spleen, and thymus. *FBXL11* and its homolog *FBXL10* (*JHDM1B*, *NDY2*) is a target of provirus integration site in retrovirus-induced lymphomas and had been shown to contribute to the induction and/or progression of virus (MoMuLV) induced T cell lymphomas in rodents. (Pfau R. *et al*., 2008). *FBXL11* localizes at the nucleolus and binds ribosomal DNA repeats to inhibit the expression of ribosomal RNAs. (Tanaka Y. *et al*., 2010; Frescas D. *et al*., 2008). Significant downregulation in prostate carcinomas compared to normal prostate tissue suggest a role for *FBXL11* in cancer progression (Frescas D. *et al*., 2008). Many JmjC group of histone demethylases were regarded as candidate tumor suppressors and many of them were shown to involved in senescence, cancer and some diseases such as ; acute myeloid leukemia (AML), prostate cancer, squamous cell carcinoma, schizophrenia, congenital heart disease (CHD), multiple self-healing squamosus epitheloma (ESS1), arthricia with popular lesion (APL), alopecia universalis congenital (AUC), intractable epilepsy (IE), X-linked mental retardation (XLMR) (Cloos P.A.C. *et al*. 2008). On the other hand number of high level of copy number amplification were described in several tissues including liver (Sanger CONAN Database) (Figure 1.6.2, Figure 1.6.3). But, possible role of *FBXL11* in liver cancer remains to be resolved.

View Selected Samples

Ensembl:11:66698221-66781717 | Cosmic:FBXL11

» Results for Gene 'FBXL11'

Tissues	High Level Amplification (>7)	Homozygous Deletion	LOH	Mutation
TOTAL (all tissues)	10	0	103	1
Adrenal gland (2)	0	0	1	0
Autonomic ganglia (37)	0	0	4	0
Biliary tract (6)	0	0	1	0
Bone (33)	0	0	7	0
Breast (45)	1	0	5	0
Central nervous system (59)	0	0	11	0
Cervix (12)	0	0	1	0
Endometrium (10)	0	0	1	0
Haematopoietic and lymphoid tissue (127)	1	0	5	0
Kidney (21)	0	0	4	0
Large intestine (39)	0	0	5	0
Liver (9)	2	0	0	0
Lung (149)	3	0	24	0
Oesophagus (22)	1	0	4	0
Ovary (22)	0	0	1	0
Pancreas (16)	0	0	1	0
Pleura (6)	0	0	1	0
Skin (51)	1	0	12	1
Soft tissue (19)	0	0	4	0
Stomach (21)	0	0	2	0
Thyroid (12)	0	0	2	0
Upper aerodigestive tract (21)	0	0	4	0
Urinary tract (18)	1	0	2	0
Vulva (3)	0	0	1	0

Figure 1.6.2 : High level amplification, homozygous deletion and LOH were described in the region containing *FBXL11* in many cancer types. Data and the photograph obtained from SANGER CONAN: Copy Number Analysis. (http://www.sanger.ac.uk/cgi-bin/genetics/CGP/conan/search.cgi).

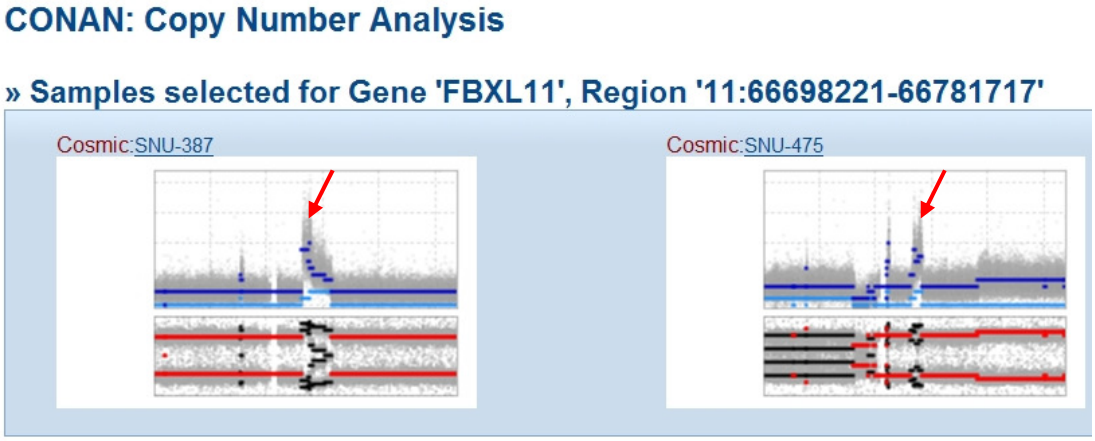

Figure 1.6.3 : Copy number analysis of chromosome 11 in Snu387 and Snu475 HCC cell lines. High level amplification were described in the region containing *FBXL11* and *PTPRCAP* (red arrows). Data and the photograph obtained from SANGER CONAN: Copy Number Analysis. (http://www.sanger.ac.uk/cgi-bin/genetics/CGP/conan/search.cgi).

1.6.2. *PTPRCAP*

The protein tyrosine phosphatase receptor type C (*PTPRC*), also known as *CD45*, activates Src family kinases (SFKs) by dephosphorylating the inhibitory tyrosine residue, which are implicated in tumor progression and metastasis (Ju H. *et al*., 2009; Penninger J.M. *et al*., 2001; Summy J.M. and Gallick G.E., 2003; Barraclough J. *et al*., 2007). *PTPRCAP* (PTPRC Associated Protein, CD45-AP or LPAP-lymphocyte phosphatase associated phosphoprotein) is a transmembrane protein that enhance the phosphatase activity of *PTPRC* (Kitamura K. *et al*., 1995; Motoya S. *et al*., 1999; Veillette A. *et al*., 1999; Takeda A. *et al*., 2004). An SNP in the promoter region of *PTPRCAP* shown to increase its expression and is associated with susceptibility to diffuse-type gastric cancer (Ju H. *et al*., 2009).

SANGER database revealed several cancer types having LOH or high level amplification in the region containing *PTPRCAP* (Figure 1.6.4). Snu387 and Snu475 have shown to be high level amplification in the region containing *PTPRCAP* (Figure 1.6.3).

View Selected Samples

Ensembl:11:66959557-66961729 | Cosmic:PTPRCAP

» Results for Gene 'PTPRCAP'

Tissues	High Level Amplification (>7)	Homozygous Deletion	LOH	Mutation
TOTAL (all tissues)	8	0	102	0
Adrenal gland (2)	0	0	1	0
Autonomic ganglia (37)	0	0	4	0
Biliary tract (6)	0	0	1	0
Bone (33)	0	0	6	0
Breast (45)	1	0	5	0
Central nervous system (59)	0	0	11	0
Cervix (12)	0	0	1	0
Endometrium (10)	0	0	1	0
Haematopoietic and lymphoid tissue (127)	1	0	4	0
Kidney (21)	0	0	4	0
Large intestine (39)	0	0	5	0
Liver (9)	2	0	0	0
Lung (149)	2	0	24	0
Oesophagus (22)	0	0	4	0
Ovary (22)	0	0	1	0
Pancreas (16)	0	0	1	0
Pleura (6)	0	0	1	0
Skin (51)	1	0	12	0
Soft tissue (19)	0	0	4	0
Stomach (21)	0	0	2	0
Testis (3)	0	0	1	0
Thyroid (12)	0	0	2	0
Upper aerodigestive tract (21)	0	0	4	0
Urinary tract (18)	1	0	2	0
Vulva (3)	0	0	1	0

Figure 1.6.4 : High level amplification and LOH were described in the region containing *PTPRCAP* in many cancer types.
Data and the photograph obtained from SANGER CONAN: Copy Number Analysis. (http://www.sanger.ac.uk/cgi-bin/genetics/CGP/conan/search.cgi).

1.7. Chromosome 13q12 (*TUBA3C,ZNF198,TPTE2*)

Our group member Kubilay Demir was found three homozygous and one hemizygous deletions which are in concordance with microarray expression data and confirmed by PCR. Homozygous deletions located at 9p23, 9p22.1-p21.2, and 13q12.11; hemizygous deletion located at Xq21.1-21.33. Homozygous deletion that mappep to 13q12.11 was found in two HCC cell lines, Huh7 and SkHep1. This deletion has a length of 1.5 MB. 13q12.11 deletion region was previously shown in HCC and other cancer types including colon cancer, esophageal squamous-cell carcinoma and non-small-cell lung cancer (Chen C.F. *et al*., 2005; Tamura *et al*., 1997; Li G. *et al*., 2001; Li SP. *et al*., 2001; Sivarajasingham *et al*., 2003; Zhang X. *et al*., 1994) (Figure 1.7.1). Chen *et al*. were identified more than 37 transcripts in this region, of them 18 are being known genes and 19 are being annotated transcripts. *LATS2, TG737, CRYL1*, and *GJB2* were shown to be downreguleted in 14%, 59%, 64% and 71% of HCC tissues, respectively (Chen C.F. *et al*., 2005).

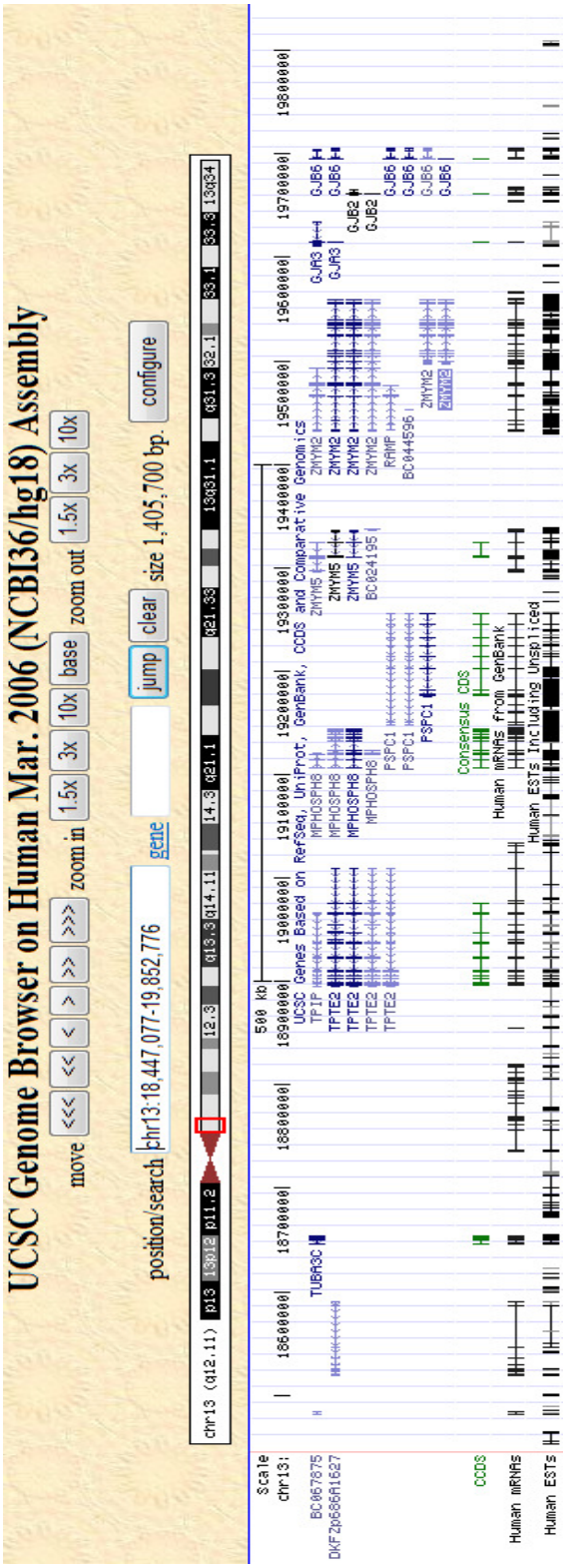

Figure 1.7.1 : Graphical view of chromosome 13q12.11 region and the genes reside in this region (UCSC Genome Browser: http://genome.ucsc.edu/cgi-bin/hgTracks)

1.7.1. *TUBA3C (TUBA2)*

Microtubules have an essential role in the eukaryotic cytoskeleton. They provide a backbone for cell organelles and determine cell shape. They are composed of a heterodimer of alpha and beta tubulin. Tubulin superfamily genes which are composed of six distinct families, encodes these micotubules. The alpha and beta tubulins represent the major components of microtubules, on the other hand gamma tubulin have a role in the nucleation of microtubule assembly. Two forms of human nonsyndromic deafness DFNA3 and DFNB1 are mapped to 13q11 (Chaib H. *et al*, 1994; Guilford P. *et al*., 1994).

TUBA3C (tubulin, alpha 3c) was studied in prostate tumor tissues and upregulation of *TUBA3C* in metastatic prostate tumor tissue compare to localized prostate tumor tissue was shown (Vila A.M.*et al*., 2010). Although little is known about the connection of *TUBA3C* and liver cancer, according to Affymetrix GeneChips HG-U95A-E and HG-U133A GNF data, *TUBA3C* expression is high in liver cancer compare to normal liver (Su AI *et al*., 2004).

1.7.2. *ZNF198 (ZMYM2)*

We previously shown that *ZNF198* is deleted in SkHep1 cell line. Copy number analysis of chromosome 13 in SkHep1 cell line also shows this deletion (Figure 1.7.1). *ZNF198* (Zinc finger protein 198) or *ZMYM2* (zinc finger, MYM-type 2) is a widely expressed gene containing five zinc-fingers. *ZNF198* is part of a protein complex that thought to have a role in DNA repair, and genome stability. Although there are not much information about its correlation with cancer, its translocation was shown in myeloproliferative disease. *ZNF198* is fused to *FGFR1* (fibroblast growth factor receptor I) by specific t(8;13)(p11;q12) translocation shown previously in atypical myeloproliferative disease patients. This fusion results in constitutive activation of the FGFRI kinase domain. It was also identified as a novel Smad binding protein (Kunapuli P. *et al*., 2003; Kulkarni S. *et al*, 1999; Warner D.R. *et al*., 2003). Copy number analysis of chromosome 13 in SkHep1 HCC cell line revealed homozygous deleted region, containing *ZNF198* (*ZMYM2*) gene (Figure

1.7.2). LOH was also showed in HLE, Snu387 and Snu449 HCC cell lines (Figure 1.7.3). Being a target of translocation and its location make *ZNF198* worth to study in HCC.

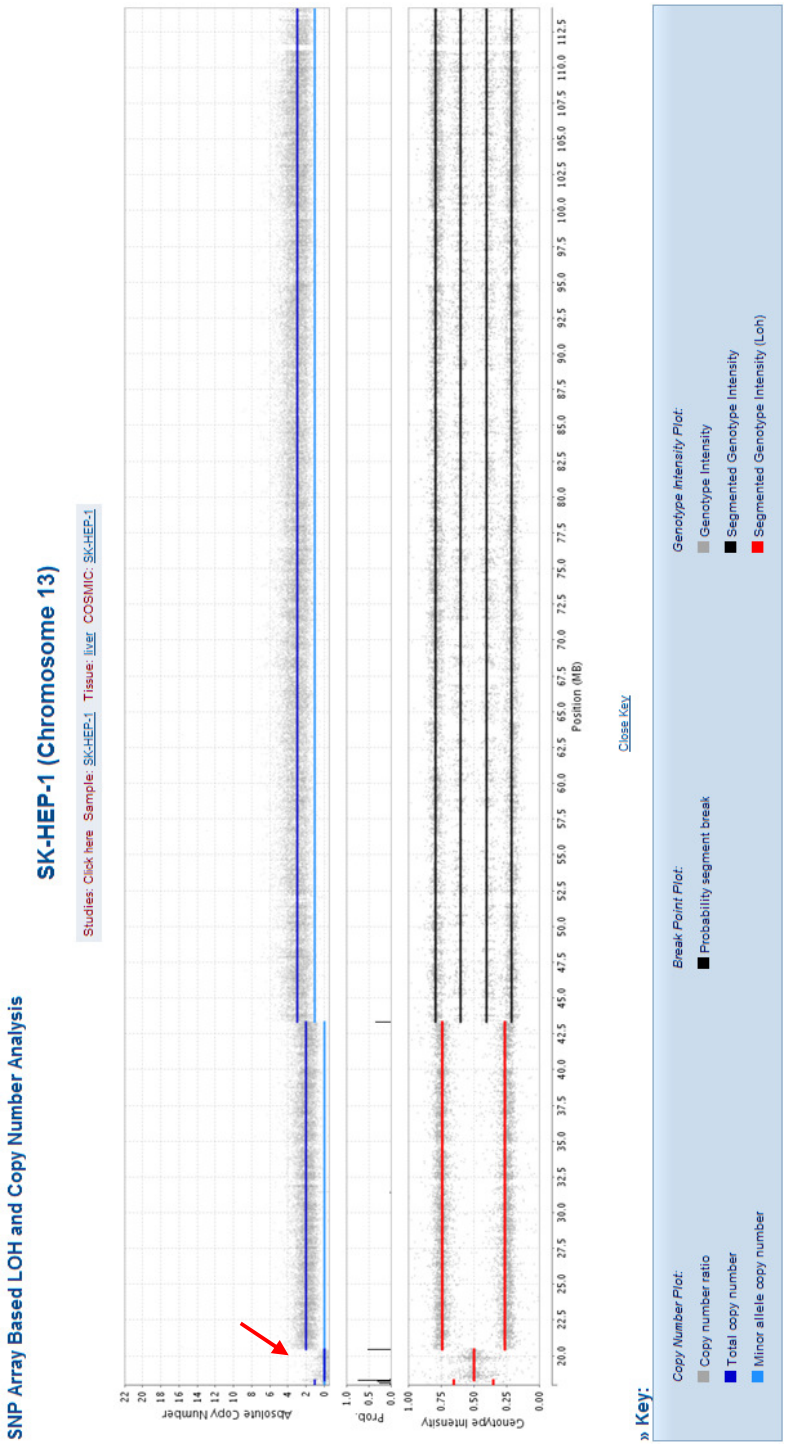

Figure 1.7.2: Copy number analysis of chromosome 13 in SkHep1 HCC cell line. Homozygous deleted region was shown by red arrow.
Data and the photograph obtained from SANGER CONAN: Copy Number Analysis. (http://www.sanger.ac.uk/cgi-bin/genetics/CGP/conan/search.cgi).

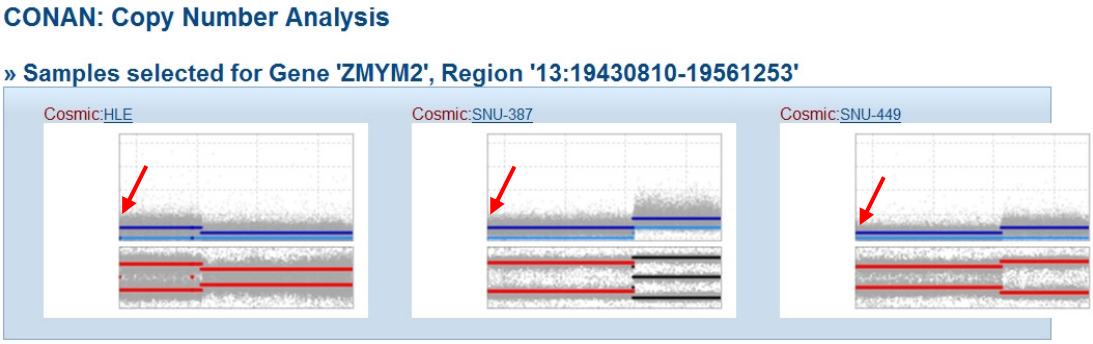

Figure 1.7.3 : Copy number analysis of chromosome 13 in HLE, Snu387 and Snu449 HCC cell lines. LOH (red arrows) was described in the region containing *ZNF198* (*ZMYM2*) and *TPTE2* genes.
Data and the photograph obtained from SANGER CONAN: Copy Number Analysis. (http://www.sanger.ac.uk/cgi-bin/genetics/CGP/conan/search.cgi).

1.7.3. *TPTE2*

TPTE2 (transmembrane phosphoinositide 3-phosphatase and tensin homolog 2), also known as *TPIP*, is a member of TPTE gene family. TPTE (*T*ransmembrane *P*hosphatase with *TE*nsin homology) gene family encodes a PTEN-related tyrosine phosphatases. There are multiple copies of the *TPTE* gene on chromosomes 13, 15, 21, 22 and Y but only the copies on 13 and 21 encode functional TPTE proteins, TPIP (TPTE and PTEN homologous Inositol lipid Phosphatase) and TPTE, respectively (Tapparel C. *et al*, 2003; Walker S.M. *et al*., 2001; Chen H. *et al*., 1999). *PTEN* is a well known tumor suppressor gene and by blocking the activation of AKT in the PI3K/AKT pathway, regulates several cellular processes like cell cycle and apoptosis. *PTEN* gene is frequently mutated or deleted in many cancer types (Li J. *et al*., 1997; Simpson L. *et al*., 2001). Copy number analysis of chromosome 13 in SkHep1 HCC cell line revealed homozygous deleted region, containing *TPTE2* gene (Figure 1.7.2). LOH was also showed in HLE, Snu387 and Snu449 HCC cell lines (Figure 1.7.3). There is no much information about *TPTE2* gene in liver cancer.

1.8. Chromosome 3p25.1 (*IQSEC1*)

IQSEC1 (IQ motif and SEC7 domain 1) also known as *ARF-GEP100* (ADP-Ribosylation Factor-Guanine nucleotide-Exchange Protein-100-kDa) or *BRAG2* is located in a minimal deleted region on 3p25.1 according to SNP analysis. It has been documented as a specific Guanine Exchange Factor (GEF) for ARF6 that not only regulates vesicular trafficking and structural organization at the plasma membrane but also induces invasion and metastasis through its effector Amap1 (Figure 1.8.1). Sabe *et al*. reported that *IQSEC1, ARF6* and *AMAP1* are highly overexpressed in malignant breast tumor. Sabe and colleagues also show that only *IQSEC1* is required for EGF-stimulated invasion (Sabe H. *et al*., 2009). Decreasing *IQSEC1* expression significantly reduces the metastasis of lung tumor cells in mice (Valderrama F. *et al*., 2008; Morishige M. *et al*., 2008). On the other hand, Someya and colleagues shown that, *IQSEC1* is also involved in the induction of apoptosis in monocytic phagocytes by Arf independent manner (Someya A. *et al*., 2006). It is postulated in Someya's study that *IQSEC1* may serve a positive regulator in *TNF-α* mediated apoptosis. Sanger copy number analysis of chromosome 3 in SkHep1 cell line shows homozygous deleted region, containing *IQSEC1* gene (Figure 1.8.2). Copy number analysis of chromosome 3 in PLC, SkHep1 and Snu475 HCC cell lines revealed LOH in the region containing *IQSEC1* gene (Figure 1.8.3).

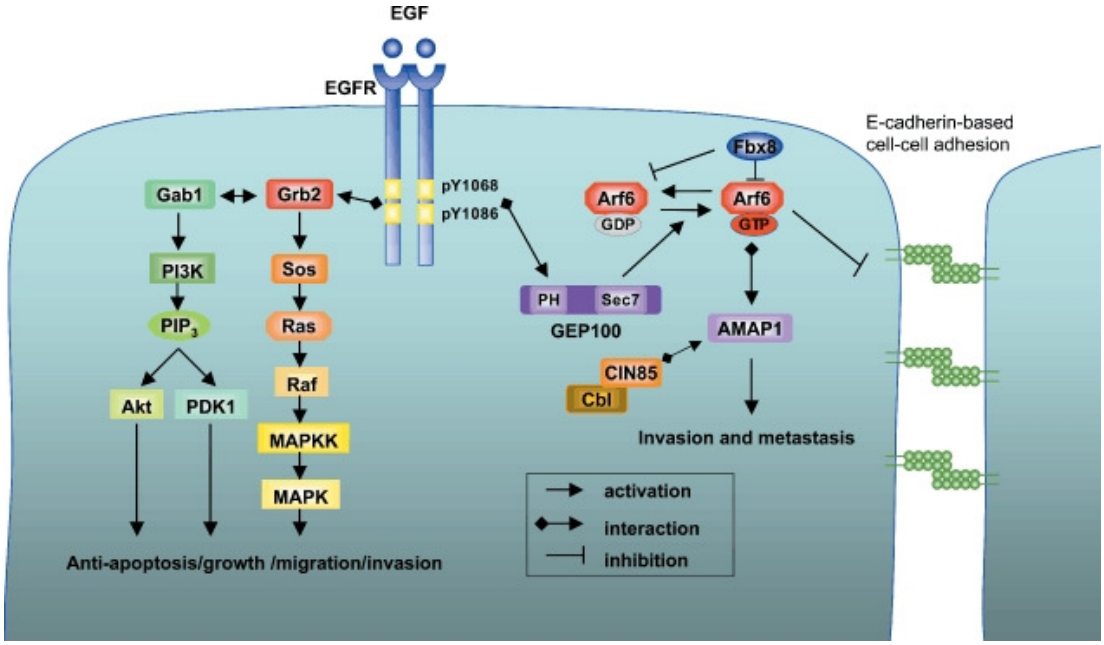

Figure 1.8.1 : EGF-induced *IQSEC1* activation and invasion through ARF6 (from "Sabe H. *et al*, 2009" with permission).

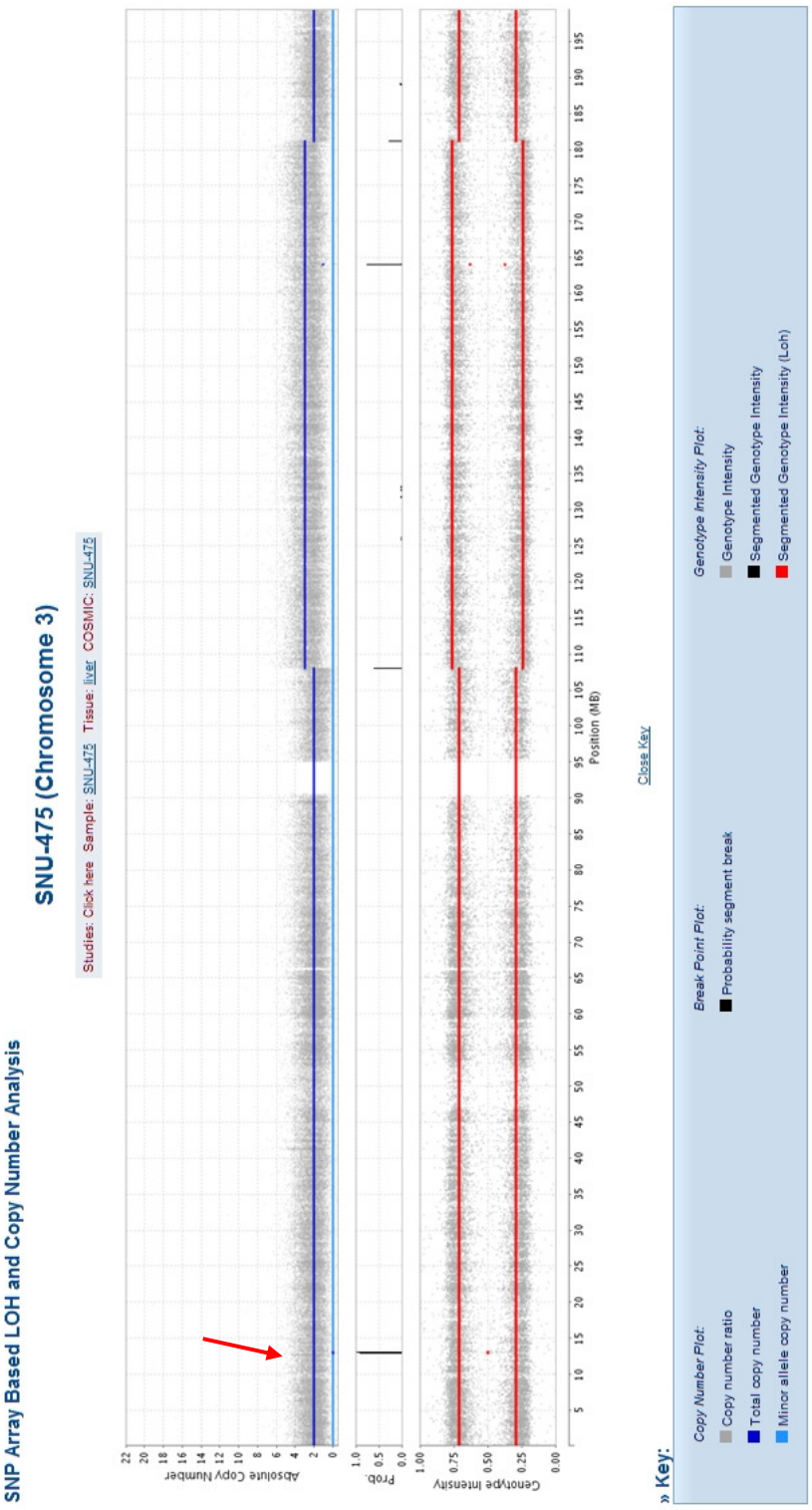

Figure 1.8.2: Copy number analysis of chromosome 3 in Snu475 HCC cell line. Homozygous deleted region (red arrow), containing *IQSEC1* gene, was shown. Data and the photograph obtained from SANGER CONAN: Copy Number Analysis. (http://www.sanger.ac.uk/cgi-bin/genetics/CGP/conan/search.cgi).

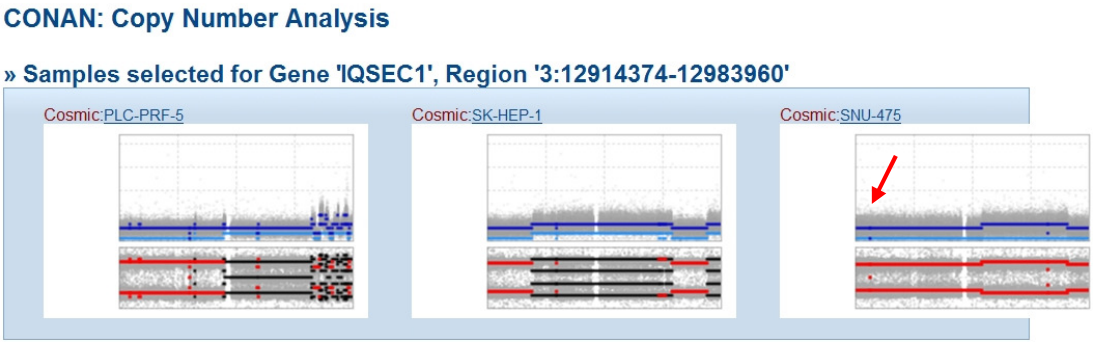

Figure 1.8.3 : Copy number analysis of chromosome 3 in PLC, SkHep1 and Snu475 HCC cell lines. LOH (red arrow) was described in the region containing *IQSEC1* gene. Data and the photograph obtained from SANGER CONAN: Copy Number Analysis. (http://www.sanger.ac.uk/cgi-bin/genetics/CGP/conan/search.cgi).

1.9. Chromosome 14q13.3 (*MIPOL1*)

MIPOL1 (mirror-image polydactyly 1) is first described by Kondoh S. and colleagues in a patient with mirror-image polydactyly of hands and feet (Kondoh S. *et al*., 2002). It is located at a 14q13 breakpoint of t(2;14). In 2009, Maher C.A. and colleagues showed *MIPOL1-DGKB* gene fusion in the prostate cancer cell line, LNCAP (Maher C.A. *et al*., 2009). Few months later, Cheung A.K.L. and colleagues argued that MIPOL1 might be a tumor suppressor gene in nasopharyngeal carcinoma (NPC) (Cheung A.K.L. *et al*., 2009). As all NPC cell lines have reduced levels of MIPOL1 and in 63% of NPC tumors via promoter hypermethylation and allelic loss. MIPOL1 tumor suppression effect is thought to involve up-regulation of the P21(WAF1/CIP1) and P27(KIP1) protein pathways (Cheung A.K.L. *et al*., 2009). Homozygous deletion of the region containing *MIPOL1* gene in PLC was shown in SANGER database (Figure 1.9.1). Copy number analysis of chromosome 14 in HLE, PLC and SkHep1 HCC cell lines revealed LOH in the region containing *MIPOL1* gene (Figure 1.9.2). There is still no information about *MIPOL1* gene regulation in HCC.

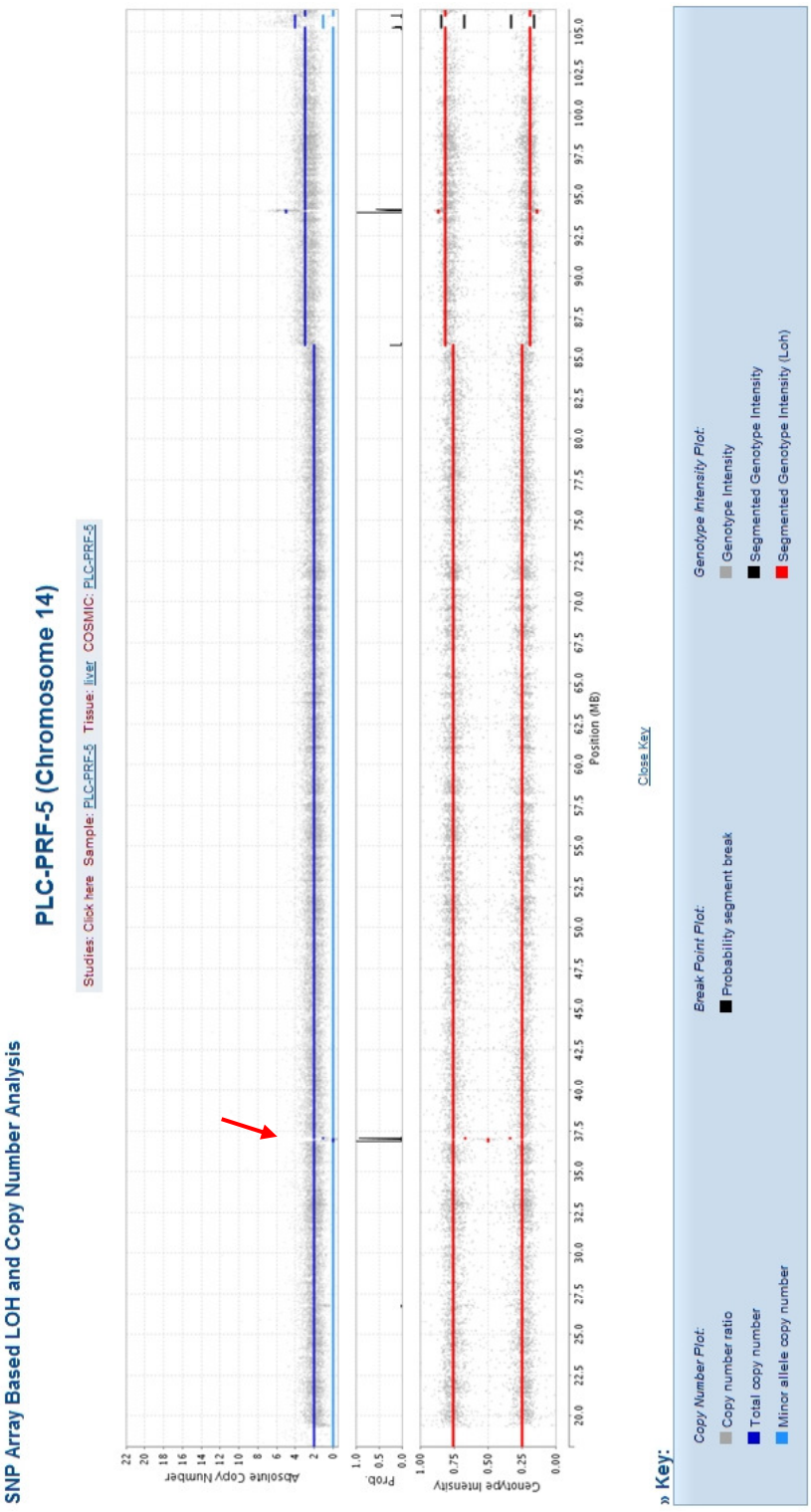

Figure 1.9.1: Copy number analysis of chromosome 14 in PLC HCC cell line. Homozygous deleted region (red arrow), containing *MIPOL1* gene, was shown. Data and the photograph obtained from SANGER CONAN: Copy Number Analysis. (http://www.sanger.ac.uk/cgi-bin/genetics/CGP/conan/search.cgi).

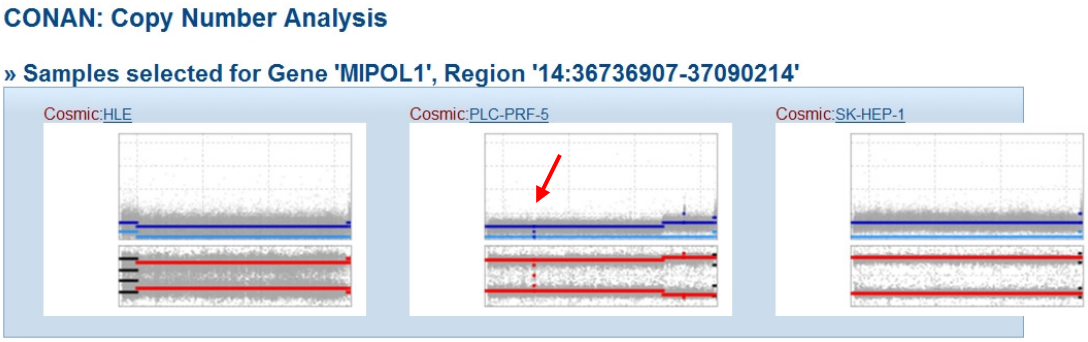

Figure 1.9.2 : Copy number analysis of chromosome 14 in HLE, PLC and SkHep1 HCC cell lines. LOH (red arrow) was described in the region containing MIPOL1 gene. Data and the photograph obtained from SANGER CONAN: Copy Number Analysis. (http://www.sanger.ac.uk/cgi-bin/genetics/CGP/conan/search.cgi).

1.10. Chromosome 10q24 (*CHUK*)

CHUK (conserved helix-loop-helix ubiquitous kinase) or *IKK1*(IKKA, I kappaB kinase alpha) is a part of an enzyme complex called IKK (IκB kinase) involved in the NF-κB activation. IKK enzyme complex is composed of three subunits, IKKalpha (*IKK1*), IKKbeta (*IKK2*) and IKKgamma (*NEMO*). IKKA together with IKKB are catalytically active, IKKgamma subunit serves a regulatory function (Mercurio F. *et al*., 1997; Zandi E. *et al*., 1997) (Figure 1.10.1)

Although CHUK (IKKA) was first described as a part of IKK complex in the the NF-κB pathway, it has also several unexpected functions. For example, in the epidermis, it serve as a cofactor for Smad2/3 in a Smad4-independent pathway and inhibits keratinocytes proliferation (Descargues P. *et al*, 2008). In previous studies, CHUK was identified as a tumor suppressor in squamous cell carcinoma (SCC). (Liu B, *et al*., 2006). Epigenetic inactivation of *CHUK* was also shown in oral carcinomas (Maeda G. *et al*., 2007) Copy number analysis of chromosome 10 in PLC and Snu475 HCC cell lines revealed LOH in the region containing *CHUK* gene (Figure 1.10.2).

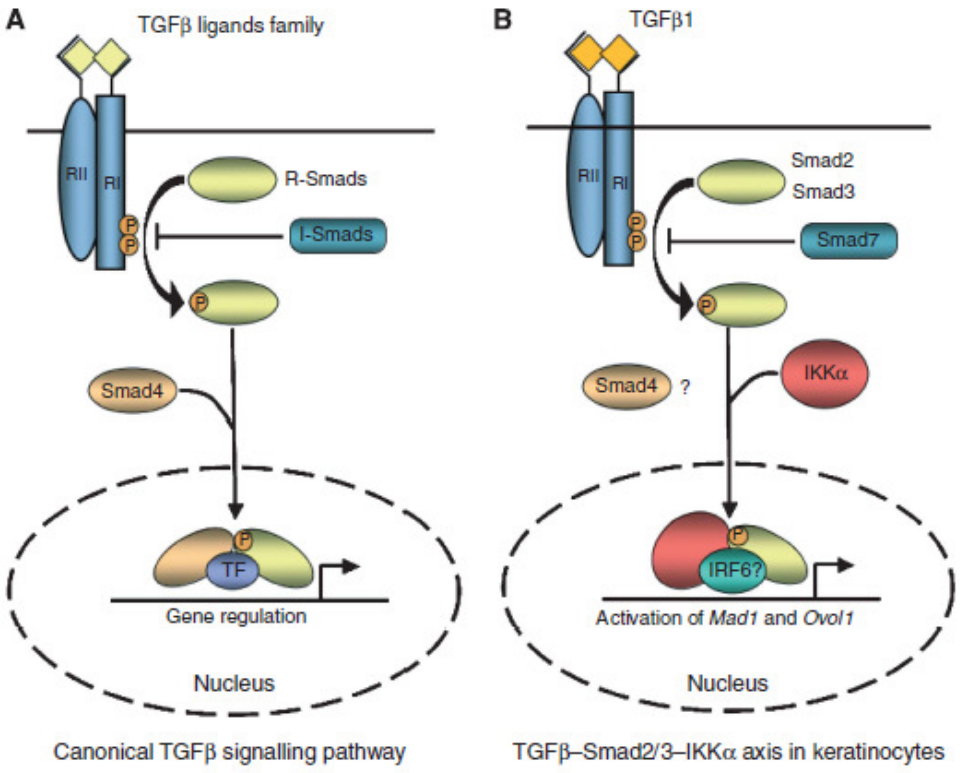

Figure 1.10.1: Smad4 independent activation of Mad1 and Ovol1 in non-canonical TGFβ pathway (from "Descargues P. *et al*, 2008" with permission).

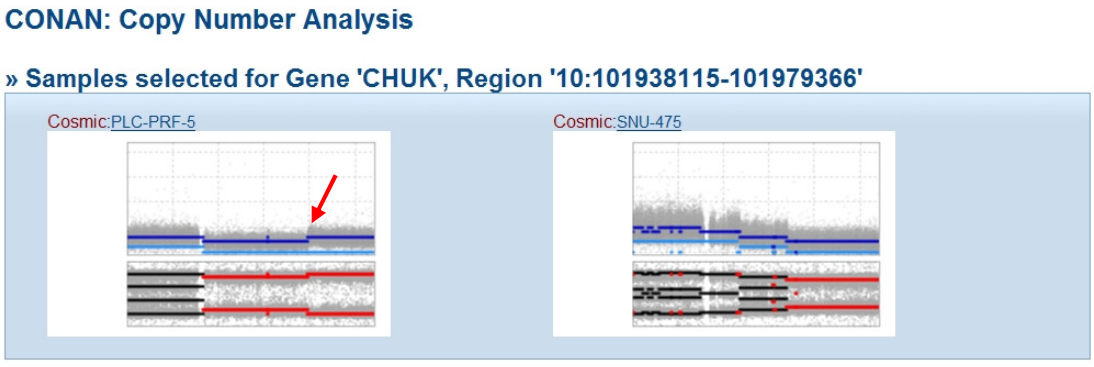

Figure 1.10.2 : Copy number analysis of chromosome 10 in PLC and Snu475 HCC cell lines. LOH (red arrow) was described in the region containing CHUK gene. Data and the photograph obtained from SANGER CONAN: Copy Number Analysis. (http://www.sanger.ac.uk/cgi-bin/genetics/CGP/conan/search.cgi).

1.11. Chromosome 1q21 (*MCL1*)

MCL1 (myeloid cell leukemia-1) gene is a member of the BCL2 (B-cell lymphoma 2) gene family which includes at least 15 members in mammalian cells. BCL2 family members categorized as oncogenes, but they do not promote cell proliferation like most other oncogenes, instead they either facilitate cell survival (pro-survival Bcl-2 subfamily) or promote cell death (Bax and Bcl-2 homologous 3 subfamilies) (Adams J.M. and Cory S., 1998; Danial N.N. and Korsmeyer S.J., 2004) (Figure 1.11.1). MCL1 was first discovered in 1993 by Kozopas *et al*., up-regulated during in the differentiation of a human myeloid leukemia cell line, ML-1 (Kozopas *et al*., 1993). MCL1 was shown to not only inhibit apoptosis but also inhibit cell cycle progression in the S-phase through its interaction with *PCNA* (proliferating cell nuclear antigen). *MCL1* has two unique features different from other BCL2 family members; first, *MCL1* can be induced upon proliferative and differentiating stimuli and second, short half-life probably because of its PEST sequence which is generaly present in cell cycle proteins (Fujise K. *et al*., 2000). There are few studies showing *MCL1* role in liver. One recent study showed that, *MCL1* inhibition through overactivation of the MEK/ERK pathway result in resistance to TGF-B–induced cell death in liver cells (Caja L. *et al*., 2009).

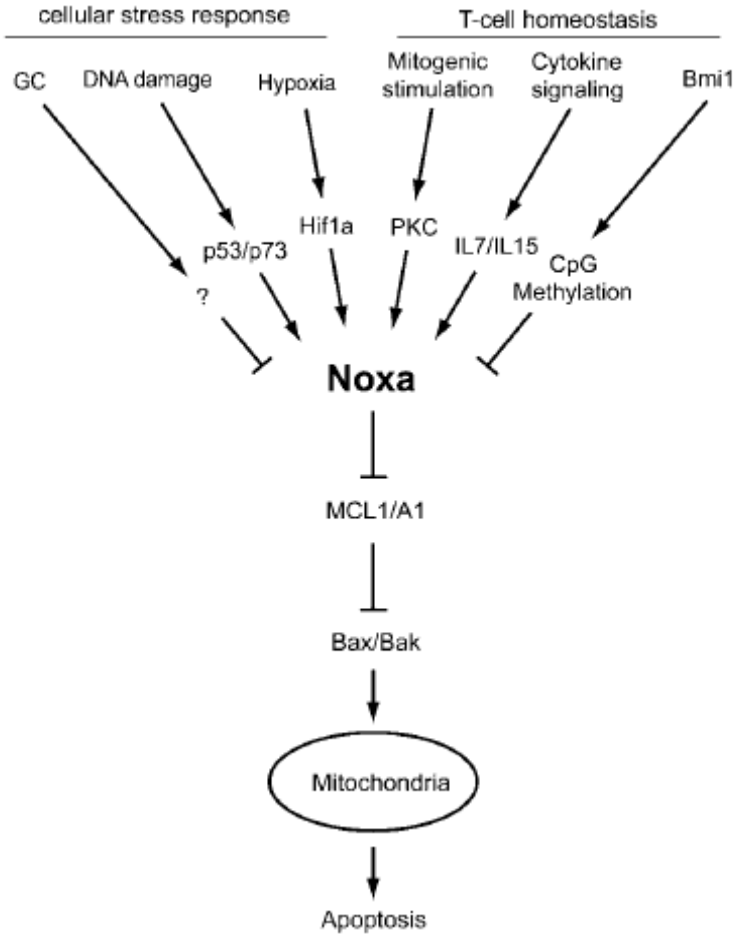

Figure 1.11.1: Upstream proteins regulating MCL1 through NOXA (from "Ploner C. *et al*., 2009" with permission).

1.12. Chromosome 7q21 (*MAGI-2*)

MAGI-2 (Membrane Associated Guanylate kinase Inverted-2) is located on chromosome 7q21, a region that was shown to be deleted in prostate cancer, glioblastoma and uterine leiomyomas (Ishwad C.S. *et al*., 1995; Cui J. *et al*., 1998; Kim D.H. *et al*., 1995). *MAGI-2* is expressed mainly in neuronal cells (Xu J.G. *et al*., 2001), but other family members (*MAGI-1* and *MAGI-3*) are widely expressed in both neuronal and non-neural cells including hepatic cells (Dobrosotskaya I. *et al*., 1997; Wu Y. *et al*., 2000, Lauraa R.P. *et al*. 2002).

MAGI-2 is a multidomain scaffolding protein belongs to MAGUKs (membrane associated guanylate kinases) superfamily. *MAGI-2* is involved in assembling and anchoring of several cellular signaling proteins such as β-CATENIN, ATROPHIN-1, NMDA glutamate receptors, β1-adrenergic receptor, neuroligins-1, NPRAP/δ-catenin, MAGUIN-1, nRAP-GEP, SAPAP and PTEN. MAGI-2 was shown to enhance PTEN tumor suppressor protein stability which result in inhibition of cell migration and proliferation in human hepatocarcinoma cells (Yali H. *et al*., 2007). Homozygous deletion of the region containing *MAGI-2* gene in HUH-6 cell line was shown in SANGER database (Figure 1.12.1). Copy number analysis of chromosome 7 in HLE and HUH-6 HCC cell lines revealed LOH in the region containing MAGI-2 (Figure 1.12.2). It was shown in Yali H. *et al*. study that *MAGI-2* was expressed only in one human hepatocarcinoma cell lines SMMC-7721 among eight cell lines tested (SMMC-7721, MHCC-97H, BEL-7404, HepG2, Huh7, LM6, 7402, Chang). Protein and mRNA expression profiles of *MAGI-2* in other 12 HCC cell lines and samples obtained from liver cancer patients was studied in this study.

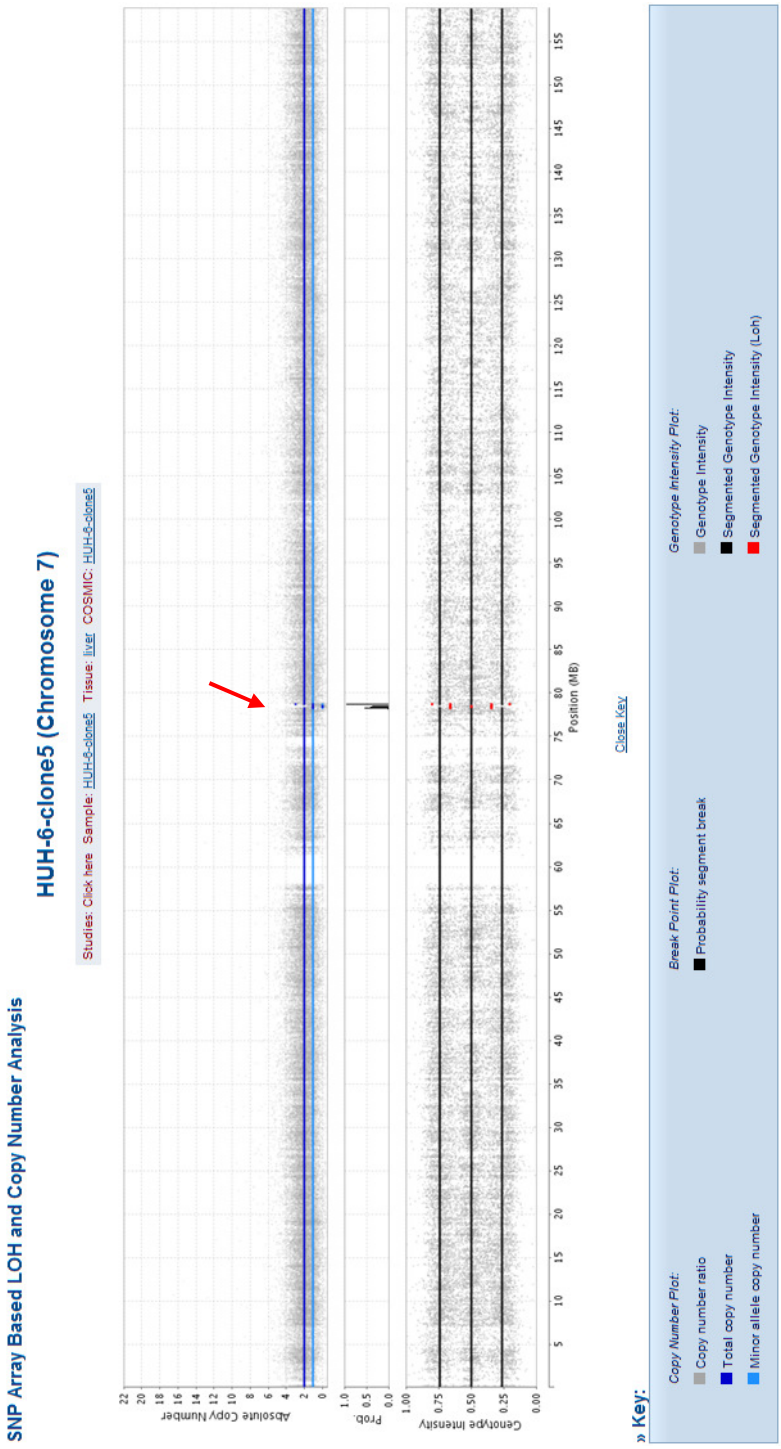

Figure 1.12.1: Copy number analysis of chromosome 7 in HUH-6 HCC cell line. Homozygous deleted region (red arrow), containing *MAGI-2* gene, was shown. Data and the photograph obtained from SANGER CONAN: Copy Number Analysis. (http://www.sanger.ac.uk/cgi-bin/genetics/CGP/conan/search.cgi).

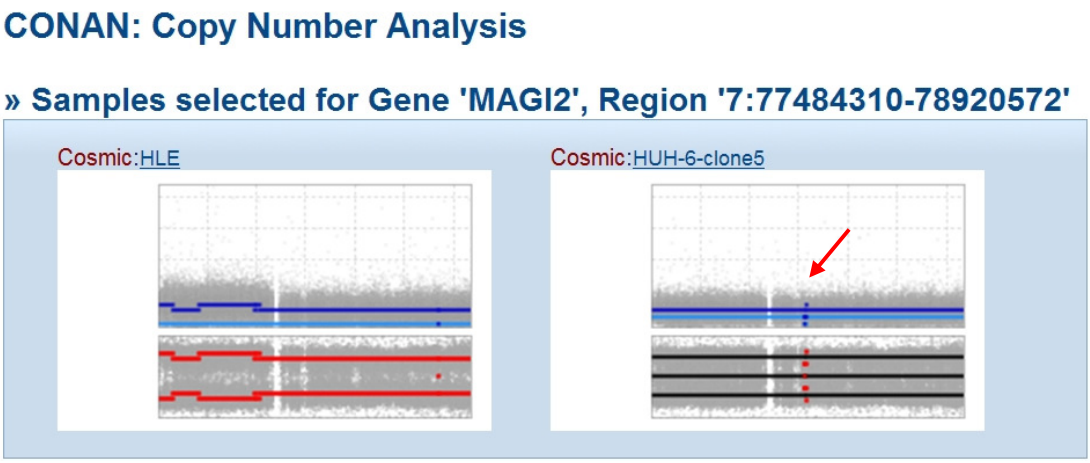

Figure 1.12.2 : Copy number analysis of chromosome 7 in HLE and HUH-6 HCC cell lines. LOH (red arrow) was described in the region containing *MAGI-2* gene. Data and the photograph obtained from SANGER CONAN: Copy Number Analysis. (http://www.sanger.ac.uk/cgi-bin/genetics/CGP/conan/search.cgi).

CHAPTER 2

OBJECTIVES and RATIONALE

Today, molecular mechanisms which lead to hepatocarcinogenesis are not completely resolved. Although many genes in cell cycle, apoptosis, developmental and oncogenic pathways were shown to have mutations, chromosome copy number alterations and translocations are much more common in human HCCs. Epigenetic mechanisms were also shown to be involved in hepatocarcinogenesis either as promoter hypermethylation or histone modifications.

In this study, several genes were selected as candidates for a detailed investigation. Genes were selected according to the following criterias: (a) the gene must shown to be a tumor suppressor or oncogene, but not studied in HCC; (b) it must have a role or being a member of a pathway in important cellular processes such as apoptosis, senescence or proliferation ; (c) it must be located in commonly deleted or amplified regions in HCC and (d) alterations of it must have been shown to trigger HCC in animal models. Analysis of the selected genes in terms of their genetic, epigenetic and expression status was revealed new candidate genes which may act in the process of hepatocarcinogenesis.

CHAPTER 3

MATERIALS AND METHODS

3.1. MATERIALS

3.1.1. Cell Lines and Patient Samples

In this study, 14 HCC cell lines were used (Table 3.1). 99 liver samples (29 paired normal/tumor) were also analyzed. These archival samples had previously been described (Ozturk M., 1991).

Cell Lines	Differentiation status	Origin	HBV-DNA	Tumorigenity in nude mice	Chromosome Ploidy
HepG2	WD	Argentina	Negative	Yes	Hyperdiploid
Hep3B	WD	USA	Positive	Yes	Hyperdiploid
Hep40	WD	China	Positive	No Data	Hyperdiploid
Huh-7	WD	Japan	Negative	Yes	Hypotetraploid
PLC/PRF/5	WD	S. Africa	Positive	Yes	Hyperdiploid
Mahlavu	PD				
Focus	PD	USA	Positive	Yes	Hypotriploid
Sk-Hep-1	PD	USA	Negative	Yes	Hyperdiploid
Snu182	PD	Korea	Positive	No Data	Hypertriploid
Snu387	PD	Korea	Positive	No Data	Hypertriploid
Snu398	PD	Korea	Positive	No Data	Hypertriploid
Snu423	PD	Korea	Positive	No Data	Hypertriploid
Snu449	PD	Korea	Positive	No Data	Hypertriploid
Snu475	PD	Korea	Positive	No Data	Hypertriploid

Table 3.1: Characteristics of the 14 Hepatocellular carcinoma (HCC) cell lines used in this study. WD, well differentiated; PD, poorly differentiated (adapted from Zimonjic D.B. *et. al.*, 1999)

TissueScan Liver Cancer Tissue qPCR Panel I were purchased from Origene Technologies (USA) (Catalog No:LVRT501). It contains ten identical plates. Each plate consists of pre-normalized cDNAs derived from 48 liver samples covering 8 tumor-adjacent normal, 27 tumors (grade I, II, IIIA, IV) and 13 lesions.

In immunohistochemistry (IHC) study, 15 formalin-fixed and paraffin-embedded liver tissues deriving from 2 normal, 1 HBV carrier, 3 chronic hepatitis B, 3 chronic hepatitis C, 3 cirrhosis and 3 HCC were obtained from the Department of Pathology of Gulhane Military Medical Academy. HCC tissue array consisting of 61 tumors and 5 normal cases was purchased from Biochain (Hayward, CA).

3.1.2. Tissue Culture Solutions

PBS (10X)

80 g NaCl, 14.4 g Na_2HPO_4, 2.4 g KH_2PO_4, 2 g KCl dissolved in 1 L of ddH_2O. pH of the 10X buffer should be around 6.8, when diluted to 1X, pH should be 7.2–7.4.

DMEM medium

500 ml Dulbecco's Modified Eagle Medium (Biochrom AG, Germany) supplemented with 3.7 g/L NaHCO3, 1 g/L D-Glucose and stable glutamine. Add 50 ml fetal calf serum (Sigma), 5 ml penicillin/streptomycin solution (Biological Industries, Israel) (50mg/ml), 5 ml non-essential aminoacids (Biochrom AG), store at 4°C, warm to 37°C prior to use.

RPMI 1640 medium

500 ml RPMI medium (Biological Industries), add 50 ml fetal calf serum (10% final concentration), 5 ml penicillin/streptomycin solution (1% final concentration), 5 ml non-essential aminoacids, store at 4°C, warm to 37°C prior to use.

Trypsin-EDTA

0.25% Trypsin-EDTA solution (Sigma-Aldrich, St. Louis, MO) was used.

3.1.3. Agarose gel solutions

Etidium bromide (EtBr)

Wear mask and gloves, prepare 10 mg/ml stock solution in ddH_2O (30 ng/ml working solution). Store at dark and 4°C.

TAE (50X)

242 g Tris base, 37.2 g Tritiplex III (EDTA), 57.1 ml glacial acetic acid bring to 1 L with ddH_2O, stir over night to dissolve.

Agarose gel (2%)

Weigh 2 g of agarose powder and add to 100 ml TAE buffer. Boil and cool down, add 1 μg/μL etidium bromide, swirl and pour onto gel casting apparatus.

DNA Markers

GeneRuler™ DNA Ladder Mix (Fermentas, #SM0331) and MassRuler™ DNA Ladder Mix (Fermentas, #SM0403) were used as markers for agarose gel electrophoresis (Figure 3.1.a,b)

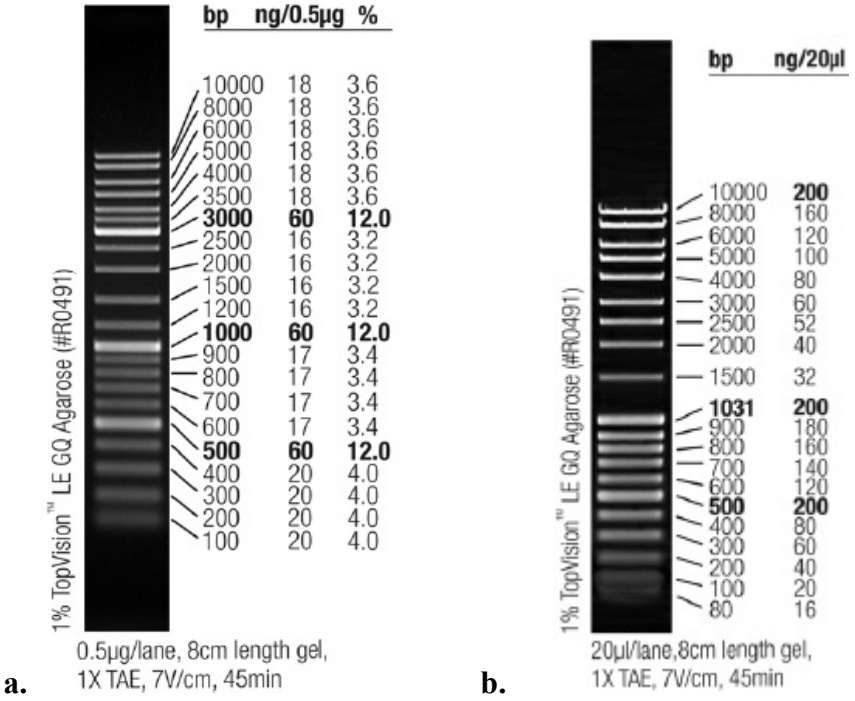

Figure 3.1 : Markers used for agarose gel electrophoresis. **a.** GeneRuler™ DNA Ladder Mix; **b.** MassRuler™ DNA Ladder Mix

3.1.4. Western Blot Solutions

Protein lysis buffer

50 µL Tris (1M, pH 8.0), 125 µL NaCl (2M), 40 µL proteinase inhibitor coctail (25X), 10 µL NP40, 775 µL filtered ddH_2O.

Bradford Solution

Dissolve 100mg coomassie brillant blue G-250 in 50ml 95% ethanol. Add 100ml 85% phosphoric acid, bring to 1lt with ddH_2O. Filter through whatman No:1. Store at 4°C in dark.

Transfer Buffer

2.25 g Glycine (1X), 5.81 g Tris base, 3.7 ml SDS (10%SDS solution), 200 ml methanol, bring to 1L with ddH_2O. Transfer buffer should be prepared freshly for each experiment.

Running Buffer

15.1 g Tris base (5X), 95 g glycine, 50 ml SDS (10% SDS solution), bring to 1 L with ddH_2O. Store at 4°C and do not adjust pH. pH should be around 8.3 for the 1X solution. When diluted to 1X, water should be added first in order to prevent excess bubbling.

Wet transfer buffer

6 g Tris base (1X), 28.8 g glycine, 1 ml SDS (10% SDS solution), 200 ml methanol, bring to 1 L with ddH_2O.

TBS (10X)

12.19 g Trisma base, 87 g NaCl, bring to 1 L with ddH_2O, adjust to pH 8.0 with 1N HCl.

Gel staining solution

100 mg Coomassie brilliant blue G.250, 50 ml absolute ethanol, 100 ml phosphoric acid (85%), bring to final volume of 1 L with ddH_2O. Filter the solution through Whatman paper, store at 4°C.

Gel de-stain solution

In ddH2O, add 20% methanol and 7% acetic acid. 30% acrylamide Wear mask, dissolve 146 g acrylamide and 4 g N'-N'-bismethylene acrylamide in 500 ml ddH_2O. Filter for 20 min, store at dark and 4°C.

APS 10% (w/v)

Dissolve 0.1 g ammonium persulfate in 1 ml ddH_2O .

Protein loading buffer (2X)

3.55 ml ddH_2O, 1.25 ml Tris HCl (0.5 M, pH 6.8), 2.5 ml glycerol, 2 ml SDS (10% w/v), 0.2 ml bromophenol blue (0.5% w/v). Store at room temperature. Add 5% ß-mercaptoethanol to buffer prior to use.

1.5 M Tris-HCl (pH 8.8)

27.23 g Tris base, 80 ml ddH_2O. Adjust pH with 6N HCl. Bring total volume to 150 ml with ddH_2O. Store at 4°C.

0.5 M Tris-HCl (pH 6.8)

6 g Tris base, 60 ml ddH_2O. Adjust pH with 6N HCl. Bring total volume to 100 ml with ddH_2O. Store at 4°C.

10% (w/v) SDS

Wear mask, dissolve 10 g lauryl sulfate in 90 ml ddH_2O with stirring, then bring to 100 ml final volume.

Blocking solution

2.5 g milk powder in 50 ml 1X TBS-T (contain 150 µL Tween-20)

Stripping solution

10 ml SDS (10% w/v), 3.125 ml Tris-HCl (1M, pH 6.8), 357 µL ß-mercaptoethanol, bring to final volume of 50 ml with ddH_2O.

Gel formulations (10 ml)

Mix 30% acrylamide, tris buffer, SDS and ddH_2O according to the gel percentage as described in the Table 3.2 and Table 3.3. Use 1.5 M Tris-HCl (pH 8.8) for resolving gel, 0.5 M Tris-HCl, (pH 6.8) for stacking gel. Add 50 µL 10% APS and 5 µL TEMED for the resolving gel; add 50 µL 10% APS and 10 µL TEMED for the stacking gel, immediately prior to pouring the gel. Swirl gently to initiate polymerization.

Percent Gel (%)	ddH_2O (ml)	30% Acyrlamide (ml)	Tris Buffer (ml)	10% SDS
5	5,7	1,7	2,5	0,1
8	4,7	2,7	2,5	0,1
10	4,1	3,3	2,5	0,1
12	3,4	4	2,5	0,1
15	2,4	5	2,5	0,1

Table 3.2: SDS-PAGE Gel Formulations

Percent Gel	ddH_2O (ml)	30% Acyrlamide (ml)	Tris Buffer (ml)	10% SDS	10% APS	Temed
7,5% (separating)	4,78	2,51	2,5	100 µl	100 µl	8 µl
6% (separating)	5,30	2	2,5	100 µl	100 µl	8 µl
4% (stacking)	3,60	0,664	0,63	50 µl	50 µl	5 µl

Table 3.3: SDS-PAGE Gel Formulations that were used in this study

Protein Markers

PageRuler™ Prestained Protein Ladder (Fermentas, #SM0671) and Spectra™ Multicolor Broad Range Protein Ladder (Fermentas, #SM1841) were used as protein markers for western blot experiments (Figure 3.2.a,b)

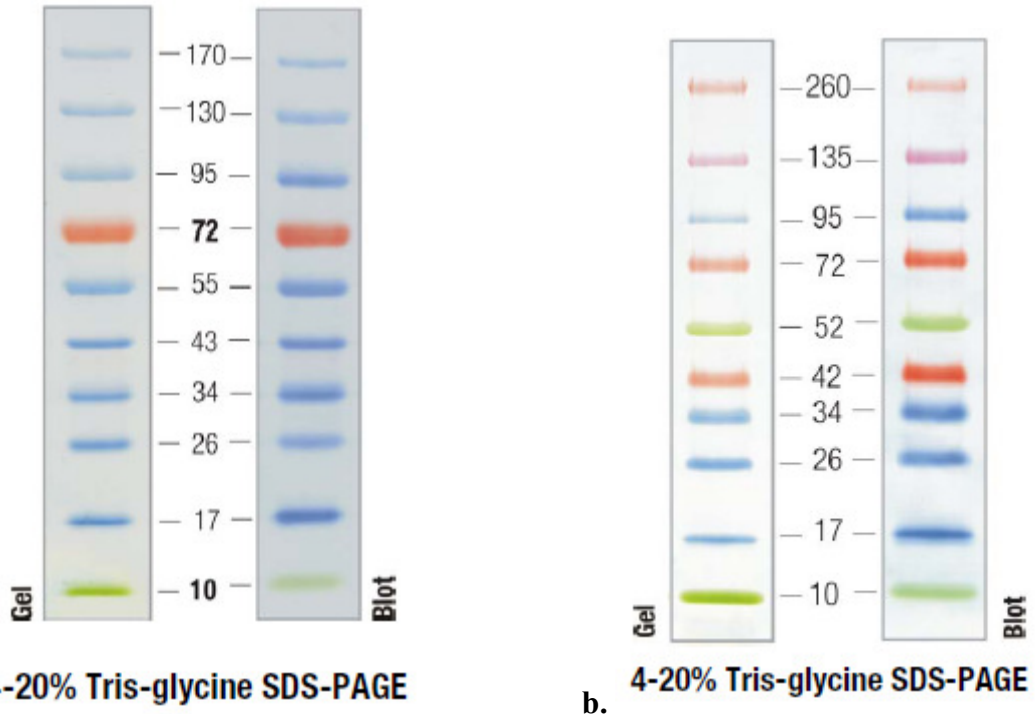

a. **b.**

Figure 3.2 : Markers used for western blotting **a.** PageRuler™ Prestained Protein Ladder; **b.** Spectra™ Multicolor Broad Range Protein Ladder.

3.2. METHODS

3.2.1. Tissue Culture Methods

3.2.1.a. Culturing of Adherent Cell Lines

14 Hepatocellular carcinoma (HCC) cell lines were used as shown in Table 3.1. HCC cell lines were grown as monolayer in DMEM or RPMI 1640 medium supplemented with 10% FBS, 1% penicillin/streptomycin solution and 5 ml non-essential aminoacids. The cells were incubated at 37°C in an incubator having an atmosphere of 5% CO_2 in air. Growth mediums were changed every other day. Old growth medium was aspirated with a vacuum pump and cells gently rinsed with 1X PBS, then fresh medium was added.

3.2.1.b. Sub-culturing of Adherent Cell Lines

Cells reaching a confluency of approximately 70-80% were sub-cultured to prevent the culture dying. Cells were brought into suspension with the help of trypsin/EDTA solution. First, cell monolayer washed with 1X PBS with a volume half the volume of growth medium. Trypsin/EDTA solution was then added (1ml/75cm^2) and cells were incubated at 37°C for 2-3 minutes. Cells were resuspended with a small volume of fresh medium and seeded into new flasks usually at a rate of 1:2-1:3.

3.2.1.c. Cyropreservation of Adherent Cell Lines

Cells were harvested with the help of trypsin/EDTA solution and resuspended with fresh growth medium to inactivate the trypsin. They were centrifuged at 1300 rpm/min for 4-5 min. and resuspended with 1X PBS. Cells again centrifuged and resuspended with freezing medium (90% FBS and 10% DMSO) at a concentration of 2-4.10^6 cells/ml. Cryotubes were kept in -20°C for 1h then in -80°C for overnight and put in liquid nitrogen tank for long term storage.

3.2.1.d. Resuscitation of Frozen Cell Lines

Cells were thawed in 37°C water bath and to get rid of the DMSO, mixed with 1-2 ml growth medium and centrifuged at 1300 rpm/min for 4-5 min. Cells were resuspended with 5ml growth medium and seeded into a 25cm^2 flask.

3.2.2. Genomic DNA isolation

Genomic DNA was isolated from HCC cell lines bu using "DNeasy Tissue Kit" (Qiagen) according to the manufacturer instructions. Cells were harvested with the help of trypsin/EDTA solution or scraper and resuspended with fresh growth medium to inactivate the trypsin. They were then washed with 1X PBS and pellets were stored at -80°C.

3.2.3. RNA isolation

"NucleoSpin RNA II Kit" (MN Macherey-Nagel) were used for RNA extraction from HCC cell lines. Cell pellets that were used for RNA isolation were obtained as above mentioned genomic DNA isolation procedure.

3.2.4. Quantification of Nucleic Acids

Concentrations and the ratio of absorbance at 260/280 of the isolated DNA and RNA samples were measured using NanoDrop ND-1000 spectrophotometer (NanoDrop Tech., USA).

3.2.5. cDNA synthesis

"RevertAid^{TM} First Strand cDNA synthesis kit" (MBI Fermentas) was used according to the manufacturer instructions. 2 μg RNA was used for cDNA synthesis. All reagents suppliled by the kit.

3.2.6. Multiplex Semi-Quantitative RT-PCR

Multiplex PCR is a technique in which more than one target is amplified and detected in the same PCR reaction. In multiplex semi-quantitative RT-PCR, one target gene was choosen as an housekeeping gene to asses the efficiency of cDNA synthesis and to normalize the quantity of input RNA and the other was the gene of interest. Housekeeping gene's primers designed so that they produce bigger PCR product than gene of interest's. After the reaction, PCR products were run on agarose gel to compare the intensity of housekeeping gene's products. In the second agarose gel, the PCR products load on the gel according to their corresponding housekeeping gene's product intensity determined in the first gel, in order to equalize the housekeeping gene's intensities.

Multiplex semi-quantitative RT-PCR was performed by using specific primers with an expected product size of 100-200 bp and GAPDH housekeeping gene spesific primers (GAPDH-RTF and GAPDH-RTR) with an expected product size of 611bp. Final primer concentrations were as ; 20 pmol for "gene of interest", 1.50 pmol for GAPDH. PCR cycling conditions were summarized in Table 3.4. PCR products were resolved on 1.5-2 % agarose gel.

	Multiplex Semi-Quantitative RT-PCR Conditions		
Initial Denaturation	94°C	5 min	
Denaturation	94°C	30 sn	
Annealing	58-62°C	30 sn	35 cycle
Extension	72°C	40-60 sn	
Final Extension	72°C	5 min	
	4°C	∞	

Table 3.4 : Multiplex Semi-Quantitative RT-PCR Conditions

3.2.7. Real-Time Quantitative RT-PCR

Quantitative Real-Time RT-PCR was performed with HCC cell lines and commercially available "TissueScan Liver Cancer Tissue qPCR Panel I" (catalog # LVRT501) (OriGene, USA) according to the manufacturer's instructions using Finnzymes DyNAmo^{TM} HS SYBR Green qPCR kit (Finnzymes, Finland) on a Stratagene MX3005P^{TM} real-time PCR system (Stratagene, USA). Dissociation (melt curve) protocol was also added after thermocycling protocol to check that if primer pair produce only a single product. GAPDH, ACTB and TBP genes were used as internal controls (FU LY. *et al*., 2009; Gur-Dedeoglu B. *et al*., 2009). Relative mRNA expression levels of HCC cell lines and samples in TissueScan liver cancer tissue qPCR panel were quantified by $2^{-\Delta\Delta Ct}$ method as previously described (Livak K.J. and Schmittgen T.D., 2001). Statistical analysis were perfomed by Student's t test and *P* value of < 0.05 was considered to be significant.

3.2.8. Sodium Bisulfite Treatment and COBRA Analysis

Genomic DNA was treated by Methylamp^{TM} DNA Modification Kit (Epigentek, USA) according to the instructions. Treated DNAs stored at –20°C. Bisulfite treated DNAs were amplified with nested primers (see appendix for primer list). The PCR products were incubated with BstUI at 60°C for overnight (COBRA, Combined Bisulfite Restriction assay). Digested DNAs were than size fractionated via 3% agarose gel to detect methylation status.

3.2.9. 5-azacytidine (5-AzaC) and Trichostatin A (TSA) Treatment

HCC cell lines (PLC, SkHep1, HepG2 and Hep3B) were seeded 6-well plates at a density of $3x10^5$ cells and treated 24h later with 2.5 μM of 5-AzaC (Sigma-Aldrich, A-2385) daily for 96 hours and with 1μM of trichostatin A (TSA) (Sigma-Aldrich, T8552) for last 24 hours. 5-AzaC is dissolved in DMEM to a concentration of 10 mM and stored at –20 °C in aliquots and used freshly. TSA is prepared as 10 mM stock solution dissolved in dimethyl sulfoxide (DMSO) stored at –20 °C in

small aliquots and a working solution of 1 mM was prepared just before use. Medium and 5-AzaC were replenished every 24h. Control cultures was left untreated or received a mock treatment with adequate volumes of DMSO in the case of TSA treatment. Treated cells were harvested by 0.25% Trypsin-EDTA incubation or by scraper and washed twice with phosphate-buffered saline (PBS) before used in DNA and RNA isolation.

3.2.10. Mutation Screening

The coding region of the gene of interest was amplified in 14 HCC cell lines. Primer sequences and their Tm values can be seen in appendix. PCR products were purified with PCR^{96} Cleanup Kit (Millipore, USA) and directly sequenced at Iontek (www.iontek.com.tr). Mutation screening was performed by Mutation Surveyor Demo V3.25 program (http://www.softgenetics.com). The software automatically forms contigs, performs alignments and mutation detection comparing both forward and reverse sample traces to reference or normal traces. Homozygous and heterozygous mutations are indicated by sharp peaks in electropherogram. Insertions and deletions are found by monitoring the mobility of the sample DNA fragments, in comparison to the reference.

3.2.11. Western Blot

To obtain total protein lysates from cells, cells scraped from culture flasks and cell pellets washed with 1X PBS. Cell pellets suspended in 200 µl "protein lysis buffer" followed by the 30 min. incubation on ice and then centrifuge at 13000 rpm for 20 min at 4°C. Supernatants were taken into a new tube and stored in -20°C.

Bradford assay was used to measure the concentration of the proteins in solution. First, a series of protein standarts were prepared. 2.5, 5, 7.5, 10, 12.5, 15, 17.5, 20 µl of bovine serum albumin (BSA) (1mg/ml) was mixed with adequate ddH_2O to bring them 100 µl. 900 µl bradford solution was then added each of them. 900 µl bradford solution mixed with 100 µl ddH_2O and used as a blank (Table 3.5). After 5 min. incubation at room temperature solutions were measured at 595nm by using spectrophotometer (Beckman, DU640). Second, 2 µl of protein solution from

each sample was mixed with 98 µl ddH_2O and 900 µl bradford solution. 2 µl of lysis buffer solution was mixed with 98 µl ddH_2O and 900 µl bradford solution and used as a blank. After 5 min. incubation at room temperature, solutions were measured at 595 nm by using spectrophotometer (Beckman, DU640). Bradford values of the samples and BSA standarts were plotted and unknown sample protein concentrations were calculated from the standart curve.

Equal amounts (µg) of protein mixed with protein loading buffer (cracking buffer) and denatured at 95°C for 5 min. follwed by incubation on ice. Samples and pre-stained protein ladder were then loaded on SDS-polyacrylamide gel. Samples were run at 70 volt during stacking gel and 85 volt during seperating gel. EC120 Mini Vertical Gel System was used for vertical PAGE (Thermo EC). Proteins were then transferred to PVDF membranes (Thermo Scientific, #88518) by wet transfer method. Bio-Rad's Mini-PROTEAN® Tetra cell apparatus was used for wet transfer. PVDF membrane soaked in methanol for 20 sec. then rinsed in ddH_2O for 2 min. and then kept in wet transfer buffer until used. Whatman papers and gel were also kept in wet transfer buffer at least 5 min. Whatman papers, gel, PVDF membrane were placed on transfer apparatus. Wet transfer was performed overnight at a constant voltage of 16 volt, in cold room (4°C). After the transfer, gel was stained with coomassie brilliant blue to ensure efficent transfer of proteins to PVDF membrane.

Membrane was soaked in blocking solution for 2 h. at room temperature to block non-specific binding. Primary antiboy was diluted in blocking solution (Table 3.6). Membrane was immersed in primary antibody solution for 2 h. at room temperature. Membrane was then washed three times with 1X TBS-T (10 min for each wash). Secondary antibodies were also diluted in blocking solution. Membrane was soaked in secondary antibody for 1h. at room temperature, then washed there times with 1X TBS-T (10 min each wash). Membrane was then incubated in HRP substrate for 5 min (SuperSignal West Femto Maximum Sensitivity Substrate, Thermo Scientific, #34095) for 5 min. and chemiluminescence emitted was captured on X-ray film for various exposure times (10 sec.-5 min.).

	Tubes								
	1	**2**	**3**	**4**	**5**	**6**	**7**	**8**	**9**
Bradford solution (µl)	900	900	900	900	900	900	900	900	900
ddH_2O (µl)	100	97,5	95	92,5	90	87,5	85	82.5	80
BSA (µl)	0	2,5	5	7,5	10	12,5	15	17,5	20

Table 3.5: Preparation of series of protein (BSA) standarts. 1st tube used as blank.

Antibody	Source	Company	Catalog No	Dilution	Size (kDa)
SIP1(ZEB2)	Mouse monoclonal	1C6, monoclonal antibody is produced by Dr. T. Yagci (Oztas E. *et al.* 2010)	-	-	~190
PTPRD (C-18)	Goat polyclonal	Santa Cruz Biotech., Inc.	sc-10867	1/200	175
FBXL11	Rabbit polyclonal	Abcam	ab31739	1/300	132
MIPOL1	Rabbit polyclonal	Sigma	HPA002893	1/300	50
MCL1	Rabbit polyclonal	Abcam	ab32087	1/1000	37
Calnexin (C-20)	Goat polyclonal	Santa Cruz Biotech., Inc.	sc-6465	1/2500	95
Anti-Mouse IgG-HRP linked	Donkey	Santa Cruz Biotech., Inc.	sc-2318	1/2000	-
Anti-Goat IgG-HRP linked	Donkey	Santa Cruz Biotech., Inc.	sc-2033	1/2500	-
Anti-Rabbit IgG-HRP linked	Goat	Cell Signalling	#7074	1/2500	-

Table 3.6 : Primary and secondary antibodies used in western blot.

3.2.12. Immunohistochemistry (IHC)

Immuno histochemistry was performed on human liver tissues to determine expression of Sip1 and Ptprd. Following a pathologist's review, immuno histochemistry was performed. In brief, tissue sections were deparaffinized at 70ºC and then in xylene. After rehydration in graded alcohol series, glass slides were immerged in 10 mM citrate buffer, pH 6.0 and transferred into microwave for 20 minutes for antigen retrieval. Endogenous peroxidase was blocked by incubation of slides in 0.3 % H2O2 for 30 minutes. Phosphate buffered saline (PBS) was used in all washing steps. Tissue sections were incubated with Sip1 hybridoma supernatant (1C6, monoclonal antibody is produced by Dr. T. Yagci at Molecular Biology and Genetics, Bilkent University, Ankara, Turkey) (Oztas E. *et al*., 2010) , for 2 hours and after washing, universal staining kit (LabVision) was used according to manufacturer recommendations. Diamino benzidine (DAB) was used as chromogen, and the slides were counterstained using Mayer's hematoxylin. Normal serum or phosphate buffered saline were used as negative controls, instead of the primary antibodies. Both positive and negative control slides were processed in parallel. Dark brown staining in section was taken as positive reaction. Immunoreactivity was registered semiquantitatively, and the intensity of immunostaining in each section was assessed independently by two observers (Dr. Emin Öztaş and Dr. Tamer Yağcı). The staining intensity was graded relatively from no staining to positive staining (Chen CL. *et al*., 2006).

CHAPTER 4

RESULTS

4.1. Chromosome 2q22; *SIP1*(*ZEB2*)

4.1.1. *SIP1* Expression in HCC Cell Lines

To explore the candidature of *SIP1* as a suppressor in hepatocarcinogenesis, its mRNA expression was checked in 14 HCC cell line by multiplex semi-quantitative RT-PCR. *SIP1* mRNA was not expressed in two cell lines, Hep3B and HepG2, very low in PLC/PRF/5 and weak in Hep40 and Huh7 cell lines. Other nine cell lines; Snu449, Snu475, Mahlavu, Snu423, Snu398, SkHep1, Focus, Snu387 and Snu182 displayed much stronger *SIP1* mRNA expression (Figure 4.1.1). We also confirmed this expression pattern with the Real-Time RT-PCR experiment (Figure 4.1.2).

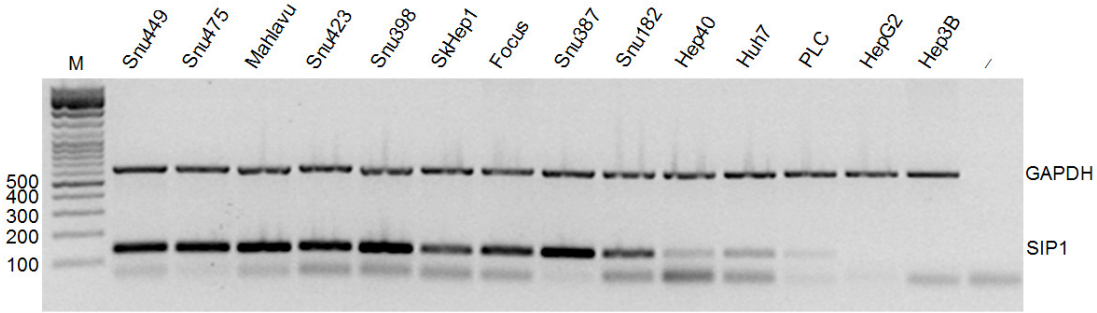

Figure 4.1.1 : Multiplex semi-quantitative RT-PCR result for *SIP1* in 14 HCC cell lines. SIP1 RTF / SIP1 RTR primer pair with an expected product size of 132 bp and GAPDH RTF / GAPDH RTR primer pair with an expected product size of 611 bp were used. M, marker (bp); (-) Negative control. *GAPDH* was used as an internal control.

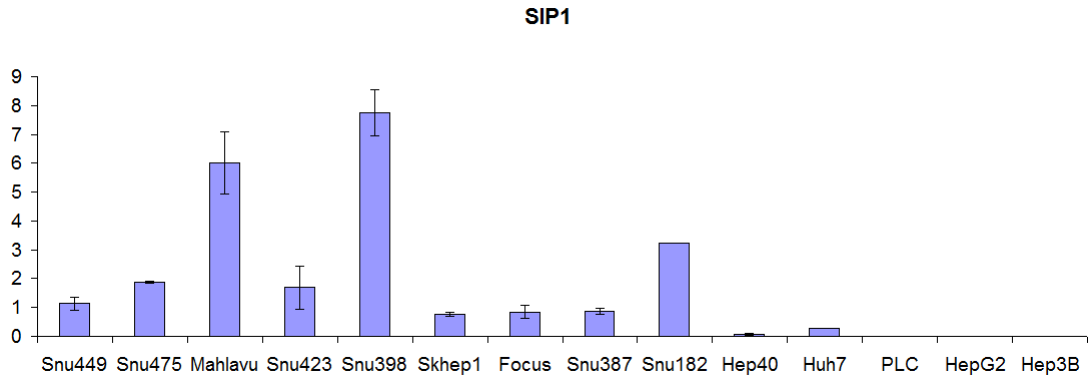

Dissociation Curves

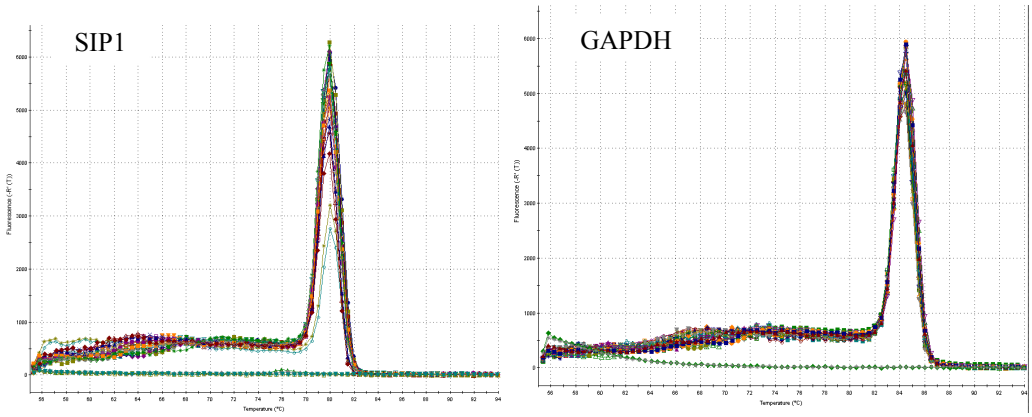

Figure 4.1.2: *SIP1* expression in 14 HCC cell lines was also checked by Real-Time RT-PCR. *GAPDH* was used as an internal control. Experiment conducted two times and standart deviations is shown. Dissociation curves of both genes are also presented.

SIP1 expression at the protein level was also checked by western blotting. 35 μg protein was loaded into each well. Among 11 HCC cell lines tested, only Snu398 cell line and normal liver was shown to have SIP1 protein. Snu387, Snu475 and Mahlavu cell lines show hardly detectable protein bands. Calnexin was used as an equal loading control (Figure 4.1.3.a,b).

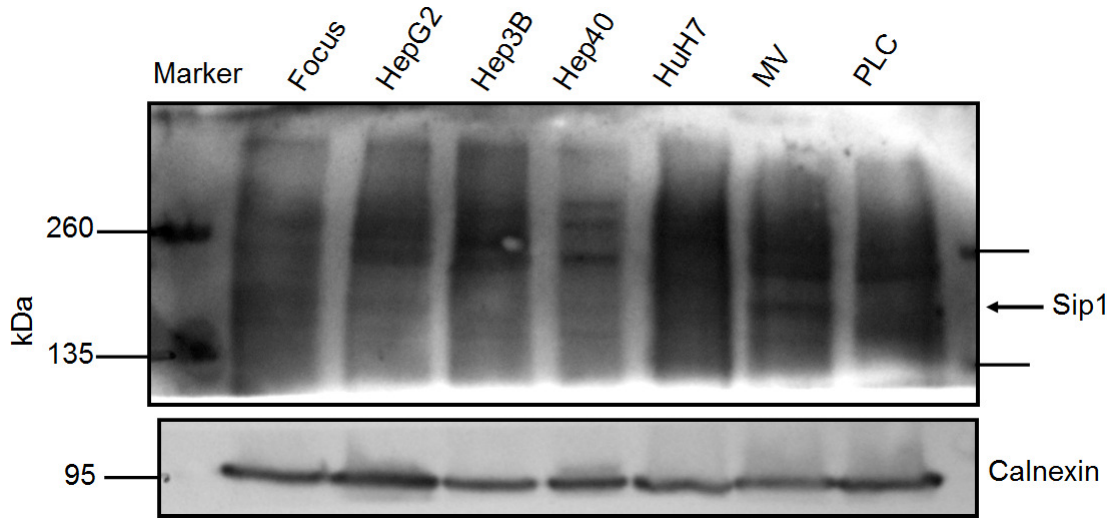

a.

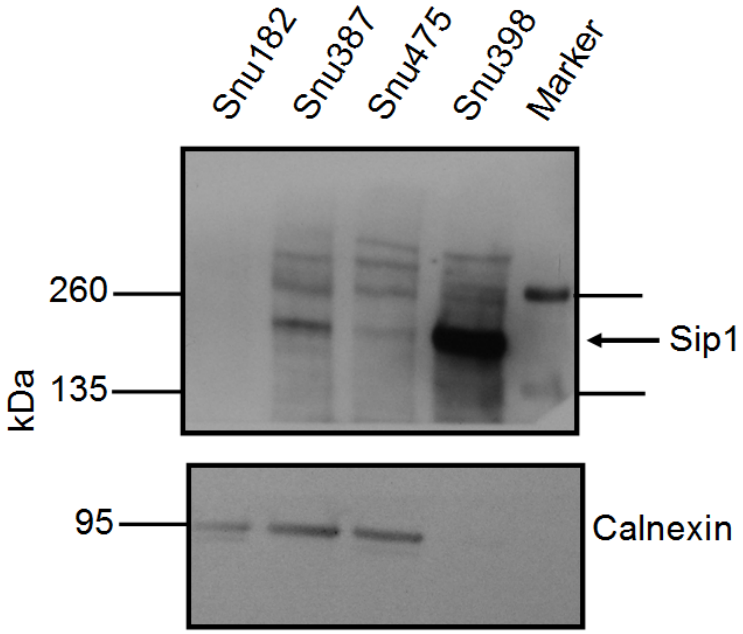

b.

Figure 4.1.3 : Western blot analysis of SIP1 in HCC cell lines. SIP1 was expected to give band at ~190 kDa (Oztas E. *et al.*,2010). Calnexin (90 kDa) was used as a loading control.

a. 35 µg protein was loaded to each well.

b. 15 µg protein was loaded to each well.

Spectra^{TM} Multicolor Broad Range Protein Ladder (Fermentas,USA) was used as a marker.

4.1.2. *SIP1* Expression in Human HCCs

We further expended our analysis to clinical samples in order to confirm that our finding is not an in vitro phenomenon restricted to the cell lines and might be relevant to human HCCs samples. We analyzed the expression of *SIP1* mRNA in a panel of human HCCs (TissueScan Liver Cancer Tissue qPCR panel I, Origene) by quantitative real time RT-PCR analysis (Figure 4.1.4). The samples were also analysed for TBP expression to normalize the *SIP1* expression (FU LY. *et al.*, 2009; Gur-Dedeoglu B. *et al.*, 2009). We observed significantly reduced Sip1 expression in 17 of 23 (73.91%) primary HCCs (GI, GII, GIIIA, GIV) as compared with eight normal liver tissues from the same panel as calculated by the student's t-test (*P* value=0,01) (Figure 4.1.5). Other six primary HCC samples displayed either normal, 3 of 23 (13.04%) or high, 3 of 23 (13.04%) mRNA levels of *SIP1*. The two repeated experiments showed consistent results. These results are consistent with our cell line data showing that *SIP1* mRNA is reduced in a subset of HCCs and downregulation of the *SIP1* occurs also invivo. Our data are also consistent with previous microarray data which shows downregulation of *ZEB2* in early and advanced HCC (Wurmbach E, 2007).

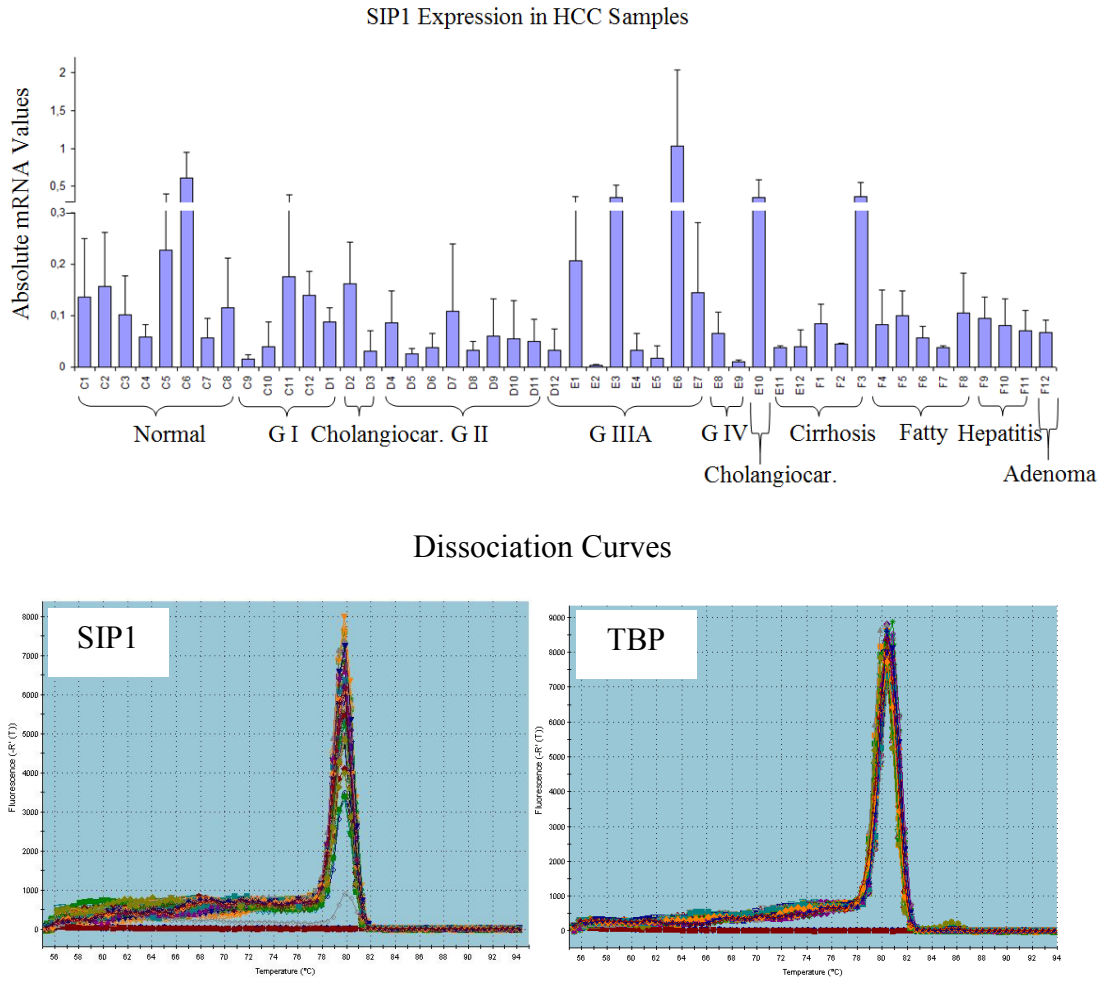

Figure 4.1.4 : *SIP1* mRNA expression in HCC samples. SIP1 RTF / SIP1 RTR primer pair was used. cDNAs from human liver tissues of normal and various stages of liver cancers were subjected to real-time reverse transcription–PCR for detection of *SIP1* mRNA expression. The data represent mRNA levels of *SIP1* normalized to *TBP*. The experiment was conducted two times and the standard deviation was shown. Dissociation curves of both genes are also presented.

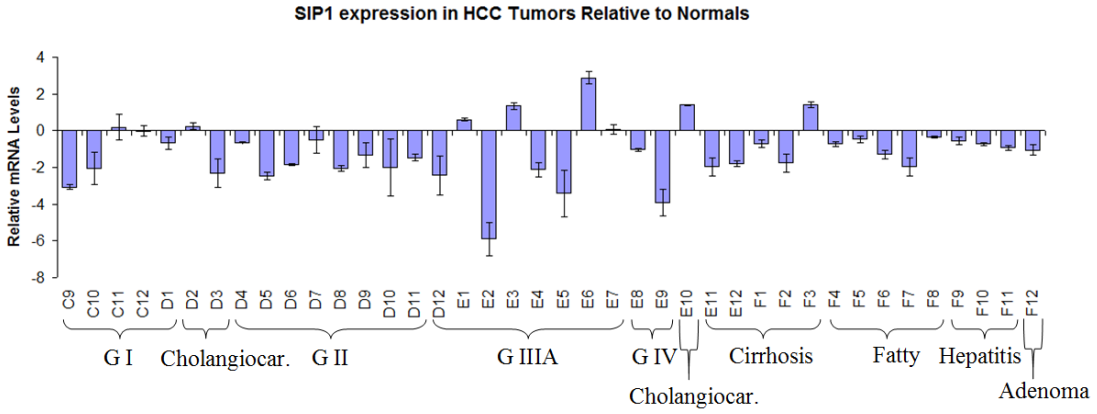

Figure 4.1.5 : *SIP1* mRNA expression in HCC tumors relative to normals.

4.1.3. Expression of the *SIP1* in human liver tissues

In order to assess whether reduced level of *SIP1* mRNA in HCCs is associated with SIP1 protein expression, we performed immunohistochemistry in human liver tissues including non HCC (normal liver, chronic hepatitis, cirrhosis) and HCC samples. We observed differential expression of SIP1 between non HCC and HCC cases. In all 17 cases of non HCC hepatocytes showed strong SIP1 expression which localized to the cytoplasm. SIP1 protein expression was missed (53 of 64 cases 82.8%) or low (11 of 64 cases, 17.2%) in HCCs (Figure 4.1.6). The results of immunostaining of the tissues are summarized in Table 4.1.1. Our data are in agreement with previous reports by Cacheux (Cacheux V. *et al*., 2001), Ozturk (Ozturk N. *et al*., 2006) and Oztas (Oztas E. et al., 2010). These reports showed that SIP1 was expressed in most of the adult human tissues as well as liver (Cacheux V. *et al*., 2001), it has decreased expression in small number of HCCs (Ozturk N. *et al*., 2006), its localized predominantly in cytoplasm and it has a stronger staining pattern in normal tissues (liver, stomach, colon, rectum and esophagus) compare to their tumors (Oztas E. et al., 2010). Our IHC data shows that downregulation of SIP1 protein expression in HCCs was more frequent than downregulation of *SIP1* transcript. This discordance might be explained by the posttranscriptional regulation mechanisms of Sip1 by non-coding RNAs such as miR-200 family (Park SM. *et al*.,

2008) and/or by natural antisense transcripts (Beltran M. *et al*., 2008). It would be interesting to analyse the expression level of these regulators in HCCs.

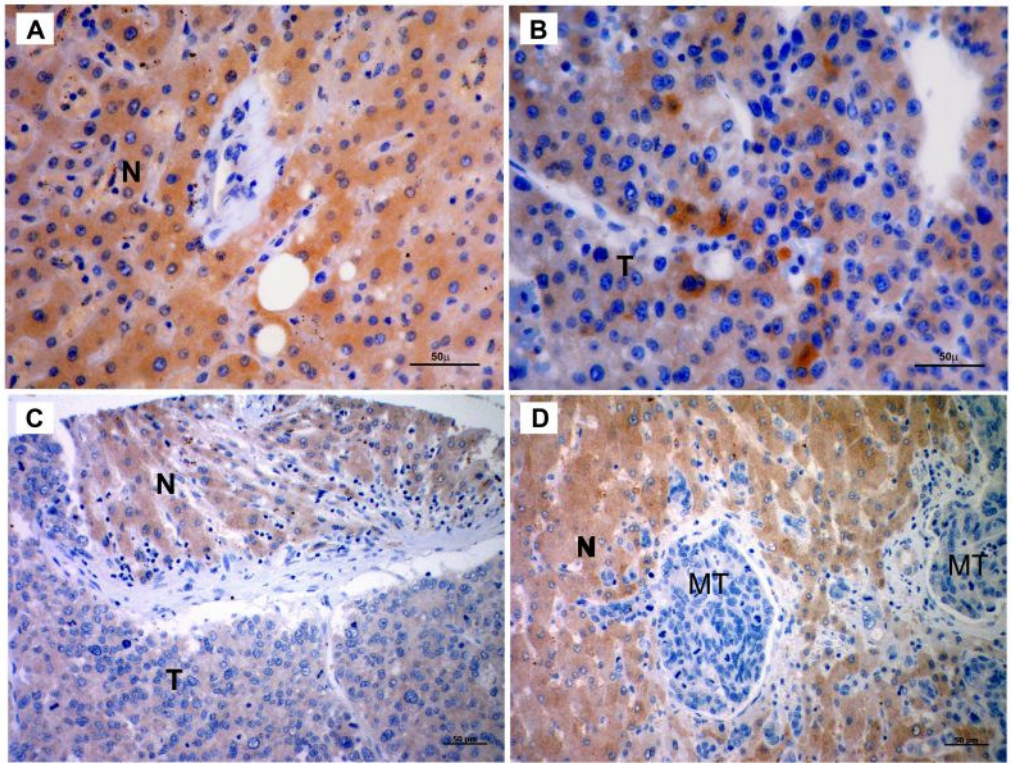

Figure 4.1.6: Representative photographs of immunohistochemistry of SIP1 in human liver tissues. **A**; Normal tissue shows strong, uniform cytoplasmic staining (brown) throughout the tissue. **B**; HCC specimen shows faint SIP1 immunoreactivity. **C**; Tissue array case shows differential expression pattern of SIP1 in HCC and non tumoral-normal hepatocytes. **D**; A metastatic adenoma case in normal liver tissue. Metastatic tumor cells shows negative staining of SIP1, but extensive SIP1 expression is seen in normal area. N, Normal liver hepatocytes; T, HCC tumor cells; MT, Metastatic adenocarcinoma cells (Scale Bars: 50µm).

	Sip1 Expression (staining intensity)		
Pathological Diagnosis	**No staining Cases**	**Faint (+) Cases**	**Positive (++/+++) Cases**
HCC (n=64)	53 (82.8%)	11 (17.2%)	-
Normal Liver (n=7)	0	-	7 (100%)
Cirrhosis (n=3)	0	-	3 (100%)
HBV Carrier (n=1)	0	-	1 (100%)
Choronic Hepatitis			
HBV (n=3)	0	-	3 (100%)
HCV (n=3)	0	-	3 (100%)

Table 4.1.1 : Immunostaining of SIP1 antibody in human liver tissues.

4.1.4. Absence of *SIP1* Mutations in HCCs

To investigate whether *SIP1* is inactivated by allelic deletions and/or somatic mutations we performed direct sequence analysis using genomic DNA from 14 HCC cell lines. PCR of genomic DNA was carried out using 13 sets of intronic primers that amplify the entire coding region (exons 2-10) of *SIP1* and included splice acceptor and donor sites. We failed to detect any types of somatic mutations leading to amino acid substitutions or frameshift except for previously described polymorphisms indicating that mutational alterations of *SIP1* is not a main genetic event in hepatocarcinogenesis (Figure 4.1.7).

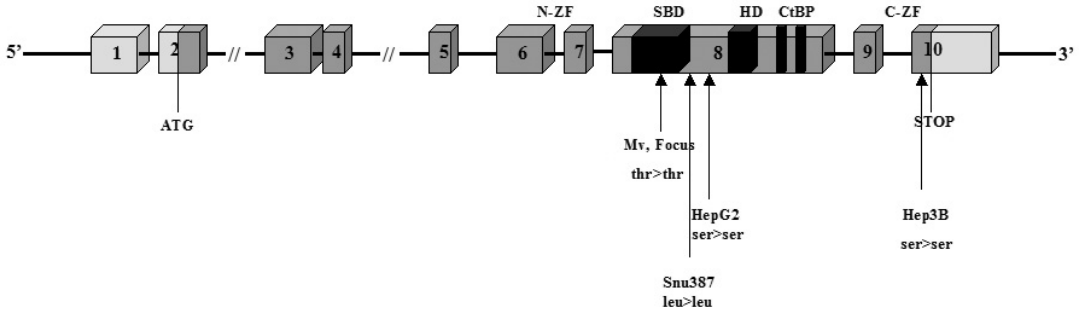

Figure 4.1.7: *SIP1* silent mutations was found in HCC cell lines and their locations are indicated (GeneID:9839, Ensembl:ENSG00000169554).

4.1.5. *In Silico* Analysis of CpG-rich *SIP1* promoter

CpG island analysis of *SIP1* gene was performed *in silico* starting from 3rd exon to the 20kb upstream of the 1st exon (a total of ~100kb region) by using MethPrimer software (http://www.urogene.org/methprimer/index1). It was found that the DNA sequences 5' upstream of the first exon (UTR), first exon and 5' upstream and 3' downstream of the second exon contain 7 CpG islands. These regions fulfilled the CpG island prediction criterias; CpG island size >100 bp, GC contents of >50% and an observed/expected CpG ratio of >0,6 according to MethPrimer software (Figure 4.1.8). Analysis of these regions by a specific promoter prediction program showed that some of them are also strong promoter candidates (Promoter2.0; http://www.cbs.dtu.dk/services/Promoter). The first candidate region (P2) reside in 1st exon (UTR) between -3006 to -3288 bp and contain TATA box, GC

box and initiator element (GAGACT). The second candidate region (P3) reside upstream of the 2nd exon between +1 to -576 bp and contain TATA and GC box. Previously, SIP1 promoter has been studied in mouse and the promoter activities of these two candidate regions and one additional candidate region (P1) in -7074 to 7782 bp have also been demonstrated (Nelles, 2003). The sequences of P2 and P3 are extremely conserved between human, mouse, rhesus, chimp, fugu, zebrafish and frog according to GenomeVista (http://pipeline.lbl.gov/cgi-bin/GenomeVista) analysis (Figure 4.1.9). In concordance with our results Sip1 gene is also the most upstream-conserved orthologue between humans and mice (Iwama H, 2004).

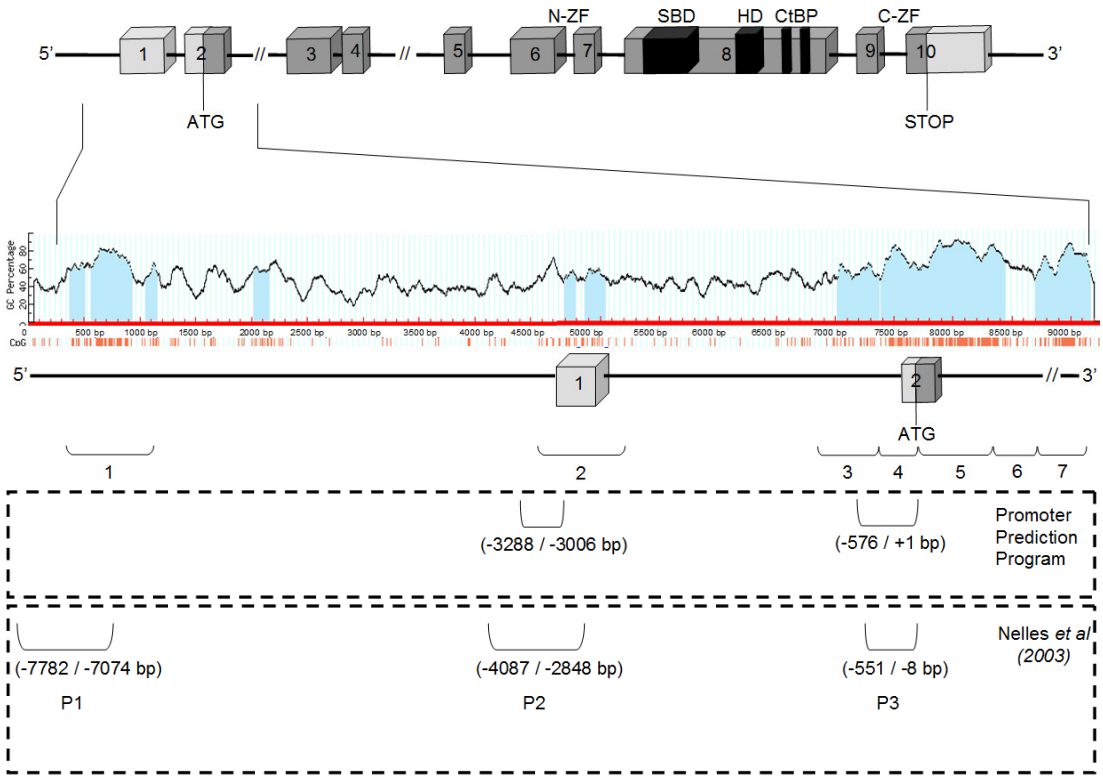

Figure 4.1.8: *In Silico* analysis of CpG-rich *SIP1* promoter. Genomic structure, CpG island prediction (MethPrimer) and promoter predictions (Promoter2.0 and Nelles *et al*., 2003 study) were represented.

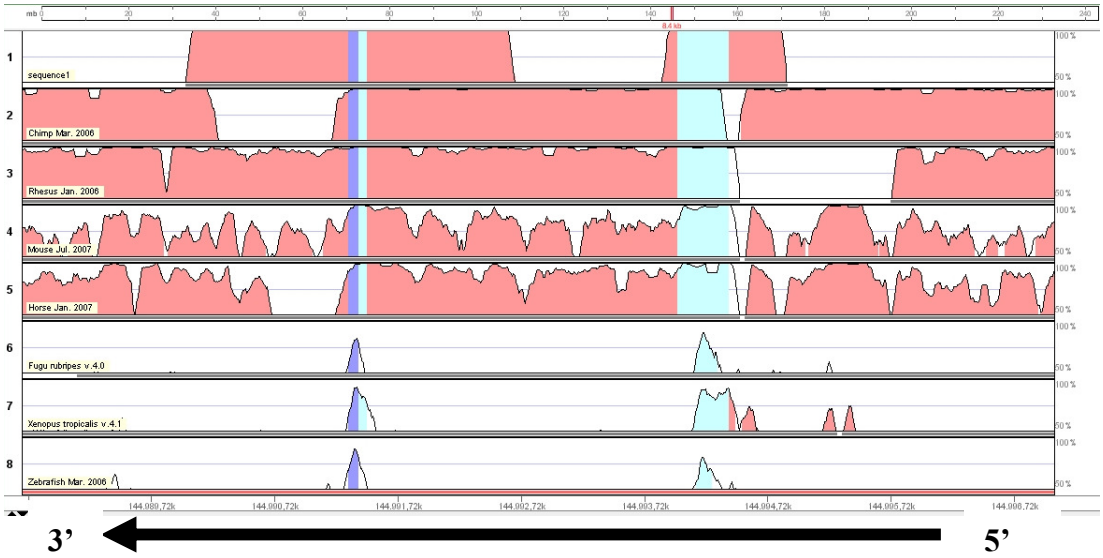

Figure 4.1.9: Conservation of 5' region of SIP1 gene according to GenomeVista analysis. (1:Human, 2:Chimp, 3:Rhesus, 4:Mouse, 5:Horse, 6:Fugu, 7: Xenopus, 8: Zebrafish) Light blue boxes shows UTR, blue boxes shows exons (1st exon UTR and 2nd exon, respectively).

4.1.6. Restoration of *SIP1* mRNA expression by 5'-AzaC and TSA treatment

Epigenetic mechanisms that involve DNA methylation and alterations of chromatin structure represent an important way of transcriptionally silencing many genes, especially tumor suppressor genes, and act as alternatives to genetic defects in human cancers (Esteller M., 2007). To investigate if the repressed expression of Sip1 in HCC cell lines was due to DNA methylation and/or histon deacetylation we treated three Sip1 negative or downregulated cell lines with DNA methyltransferase inhibitor (5-AzaC) alone and with histone deacetylase inhibitor trichostatin A (TSA).

To study the possible regulation mechanism of Sip1 expression in HCC cell lines we first treated HepG2 (*SIP1* mRNA negative) cell line with DNA methyltransferase inhibitor (5-AzaC) alone and/or with histone deacetylase inhibitor trichostatin A (TSA) (Figure 4.1.10.a). 5-AzaC and TSA alone could restore the expression of SIP1. 5-AzaC and TSA synergistically restored *SIP1* expression much more than that restored by 5-AzaC and TSA alone. We repeat the experiment with two another HCC cell lines Hep3B (*SIP1* mRNA negative) and PLC (very low

mRNA expression). 5-AzaC and TSA were succesfuly restored or increased the expression respectively (Figure 4.1.10.b). These results suggest that methylation together with histone deactylation play a role in *SIP1* gene silencing rather than genetic alterations.

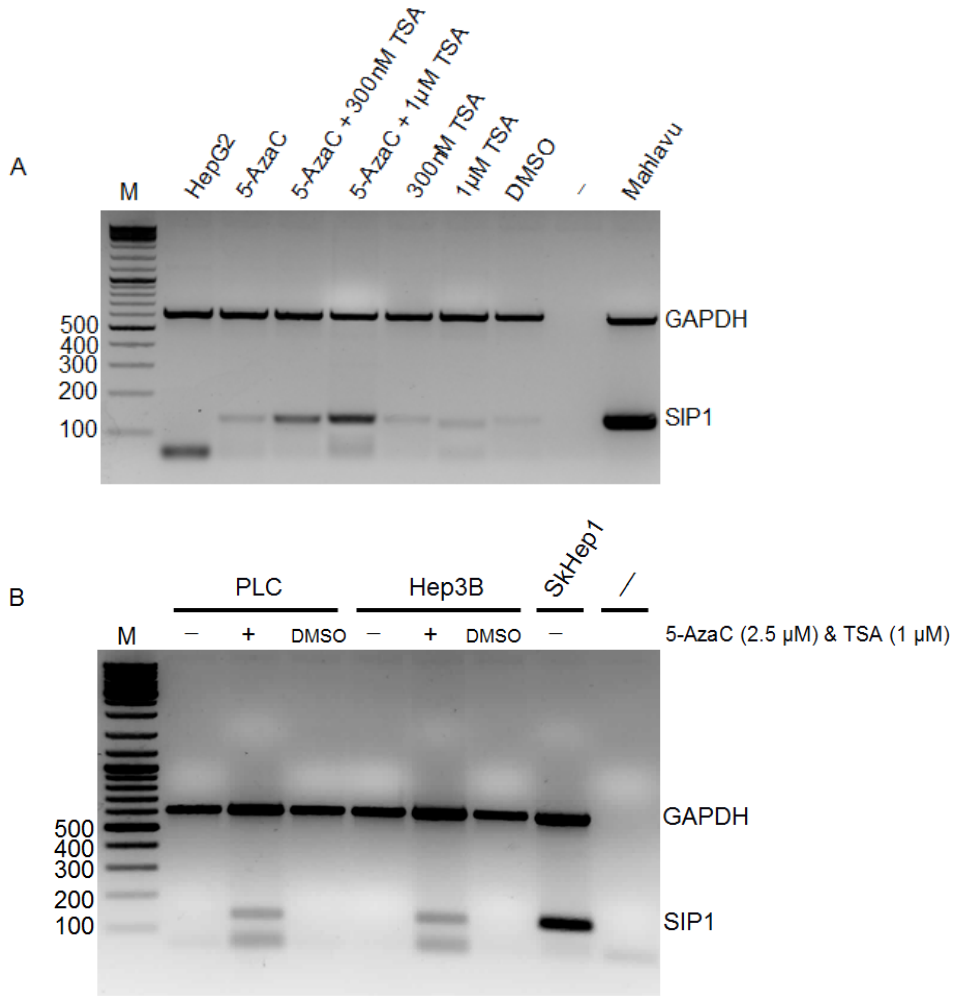

Figure 4.1.10: Restoration of *SIP1* mRNA expression in HCC cell lines.
SIP1 mRNA expression in HCC cell lines was restored by 5-AzaC and/or TSA treatment. SIP1 RTF/SIP1 RTR primer pair with an expected product size of 132 bp and GAPDH RTF/GAPDH RTR primer pair with an expected product size of 611 bp were used. M, marker (bp); (-), negative control **a)** HepG2 cell line was treated with 2.5 µM 5-AzaC and/or 300 nm and 1 µM TSA. Mahlavu cell line was used as a positive control for multiplex semi-quantitative RT-PCR. **b)** PLC and Hep3B cell lines were treated with 2.5 µM 5-AzaC and 1 µM TSA. SKhep1 cell line was used as a positive control.

4.1.7. Frequent metylation of *SIP1* promoter in primary HCC samples

To determine the overall frequency of Sip1 methylation in clinical HCC samples we performed combined bisulfite restriction analysis (COBRA), a semiquantitative methylation assay. We examined 29 tumor and paired normal liver tissue samples and nearly half of the tumors (48% for P1, 42% for P3) demonstrate an increase in methylation when compared to their corresponding normal tissue (Figure 4.1.11 and Figure 4.1.13). According to our results P2 region is not a site of methylation, as 4%-18% of the tumors were methylated according to *BstU*I and TaqI restriction analysis, respectively (Figure 4.1.12).

In total, COBRA analysis demonstrated that about half the primary carcinomas were methylated. Because, the promoter methylation was frequently detected in tumor samples but not in adjacent non-tumor tissue samples, our results suggest a tumor-specific hypermethylation of the *SIP1* promoter.

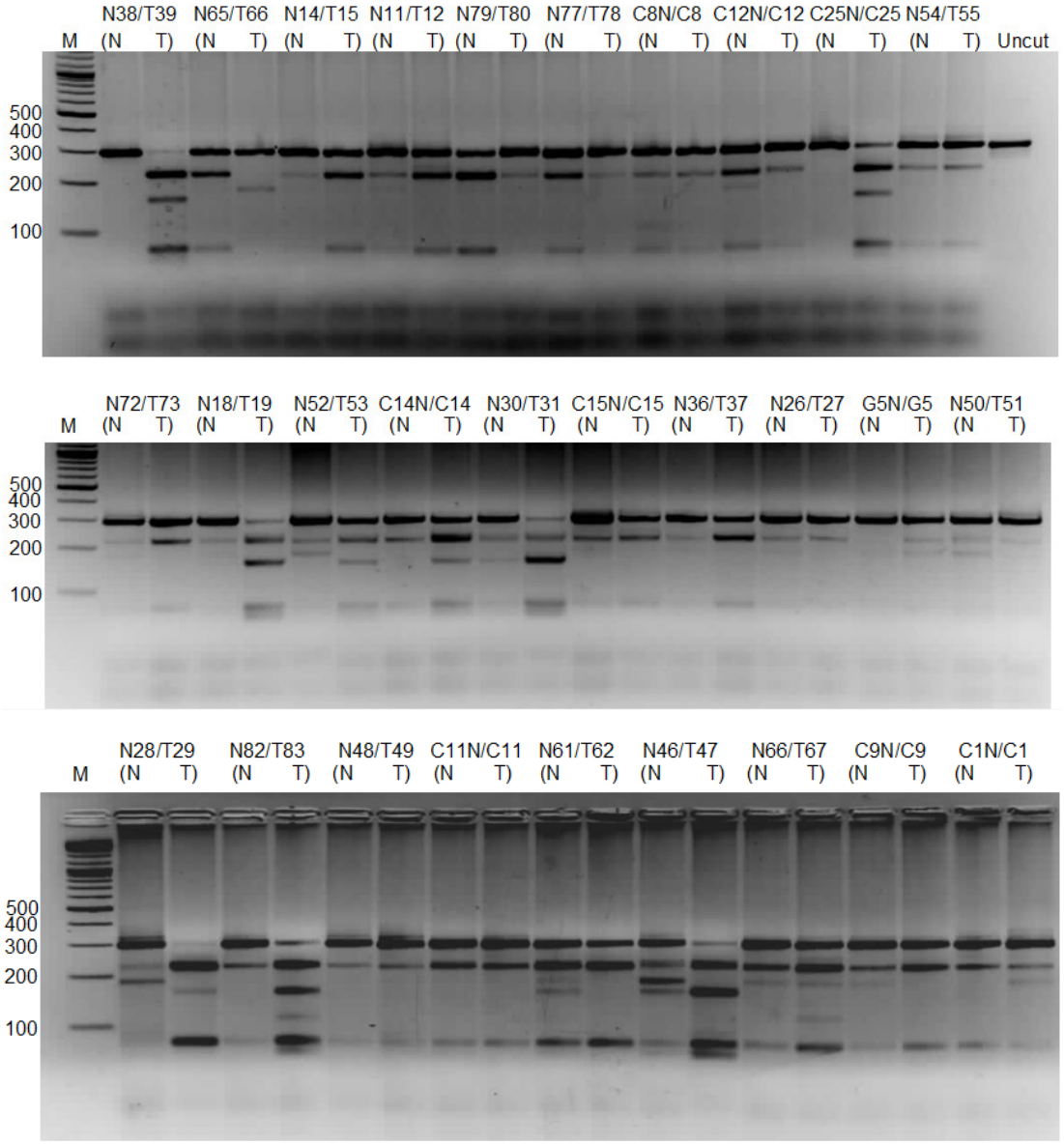

Figure 4.1.11 : *BstU*I restriction analysis of P1 region amplified by SIPM1dF / SIPM1iyR1 and SIPM1iF / SIPM1iyR1 semi-nested primer pairs. 14 out of 29 normal-tumor paired samples (48%) were methylated. M, marker (bp).

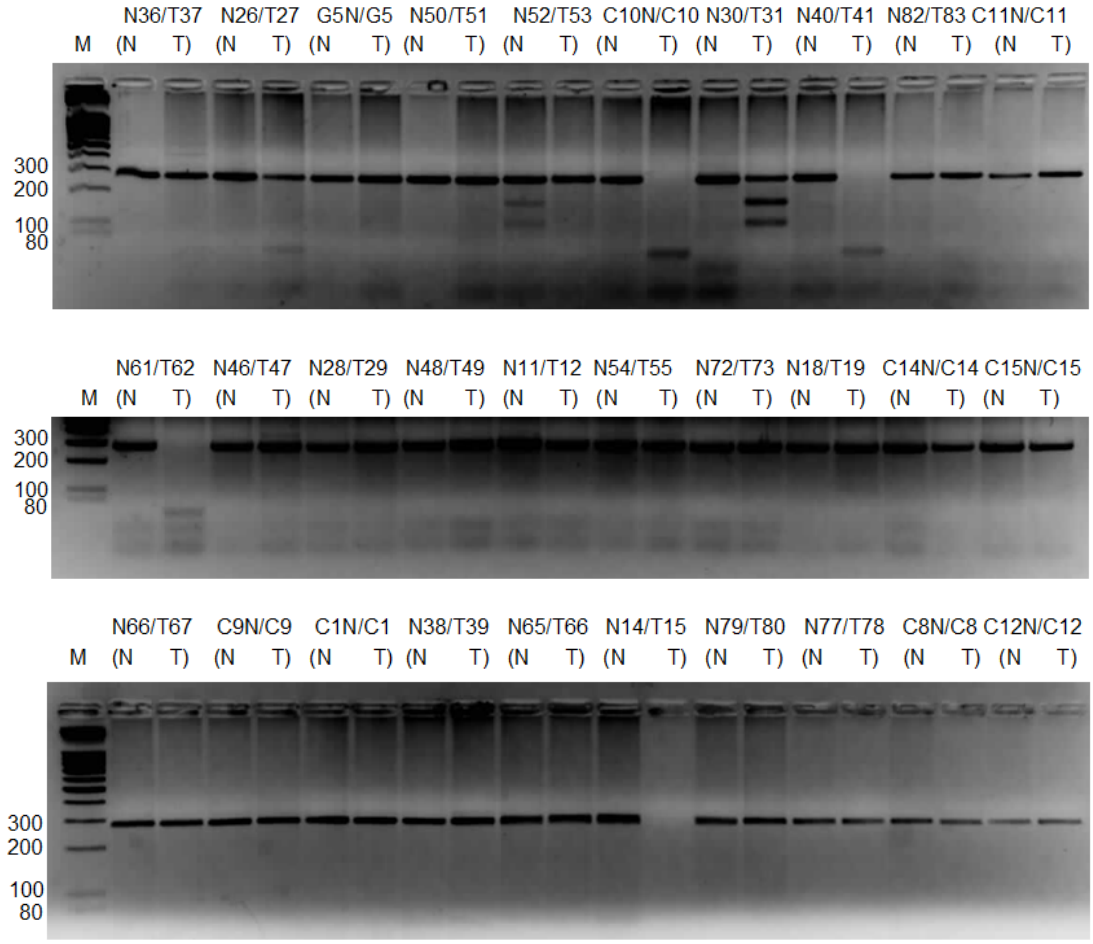

Figure 4.1.12 : *BstU*I restriction analysis of P2 region amplified by SIPM2iyF1 / SIPM2iR and SIPM2iyF1 / SIPM2iyR2 semi-nested primer pairs. 1 out of 26 normal-tumor paired samples (4%) were methylated. M, marker (bp).

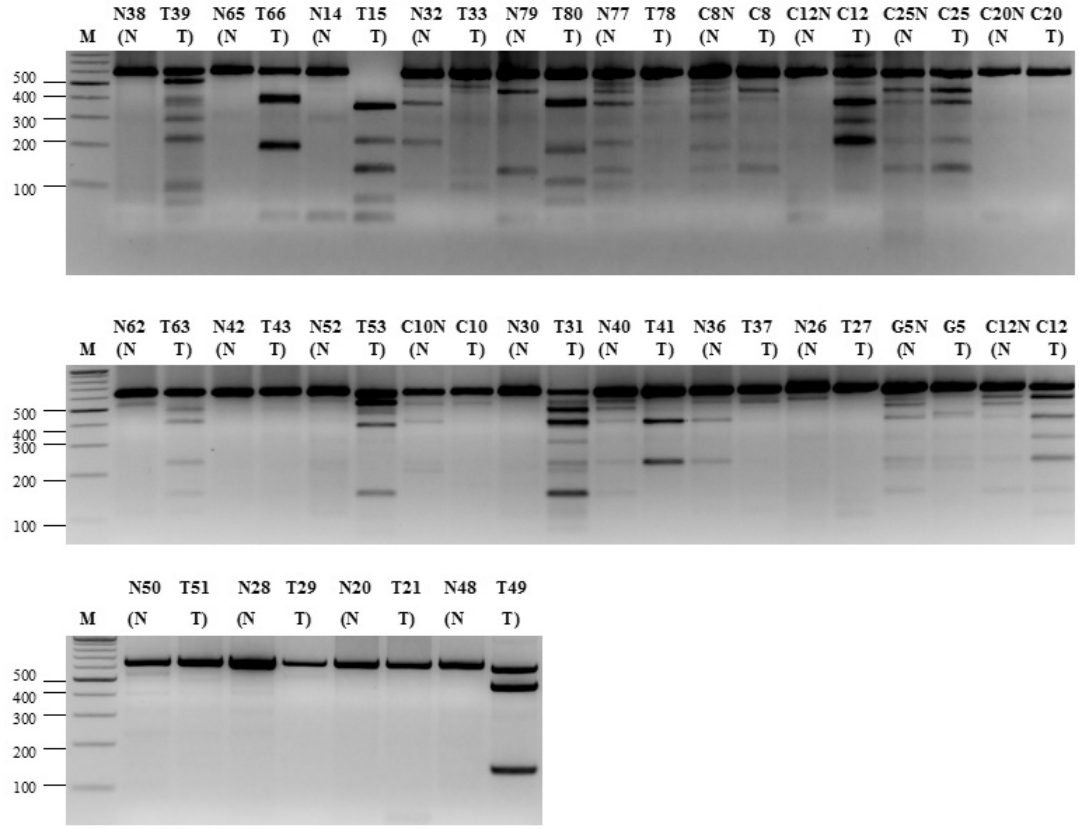

Figure 4.1.13 : *BstU*I restriction analysis of P3 region amplified by SIPM3dF / SIPM3dR and SIPM3iF / SIPM3iR nested primer pairs. 10 out of 24 normal-tumor paired samples (42%) were methylated. M, marker (bp).

4.2. Chromosome 9p23; *PTPRD*

4.2.1. *PTPRD* Expression in HCC Cell Lines

PTPRD mRNA expression was checked in 14 HCC cell line by quantitative real-time RT-PCR. *PTPRD* mRNA expression was found to be high in Snu449, Hep40, SkHep1; low in MV, PLC, Snu398, Hep3B, Snu182, Snu475. Almost no expression was observed in Focus, HepG2, Huh7, Snu387 and Snu423 cell lines (36%, 5/14) (Figure 4.2.1).

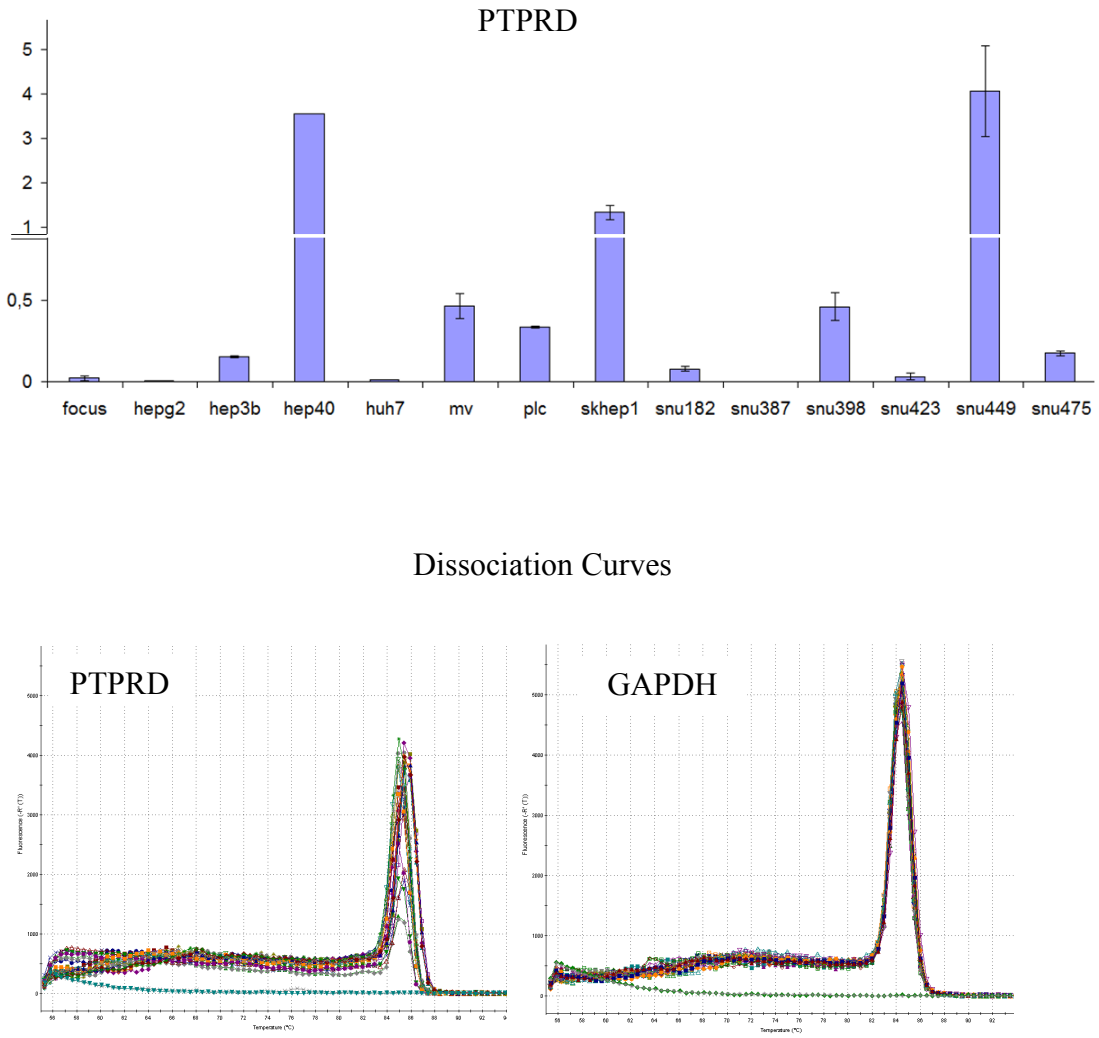

Figure 4.2.1 : Quantitative Real-Time Analysis of *PTPRD* in HCC Cell lines. PTPRDcd4F / PTPRDcd3R primer pair was used. *GAPDH* was used as an internal control. Experiment conducted two times and standart deviations are indicated. Dissociation curves of both genes are also presented.

PTPRD expression was also checked by multiplex semi-quantitative RT-PCR. First, we used primers (PTPRDcd3F/cd3R) designed to amplify 5' region of the *PTPRD* cDNA covering exon 10 and 11. *GAPDH* was used as an internal control. Results are almost consistent with the real-time RT-PCR result. Hep40 and SkHep1 cell lines and normal liver sample have high levels of *PTPRD* mRNA (Figure 4.2.2.a).

PTPRD gene encoded a mRNA bigger than 6000 bp. We also wanted to amplify 3' region of the *PTPRD* cDNA, covering exons 30 to 36 (PTPRDcd9F/cd9R) as there might be internal deletion/s or splice variants effecting the mRNA expression. *GAPDH* was used as an internal control. Results were still almost consistant with our real-time RT-PCR result. But there were some exceptions such as Snu182, Snu387 and Huh7 cell lines, which have higher *PTPRD* mRNA level compared to 5' PCR product. Also, HepG2 cell line had undetectable 3' *PTPRD* mRNA PCR product, which had low level of 5' PCR product (Figure 4.2.2.b).

a)

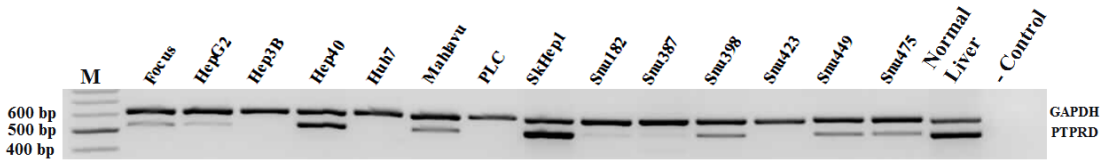

b)

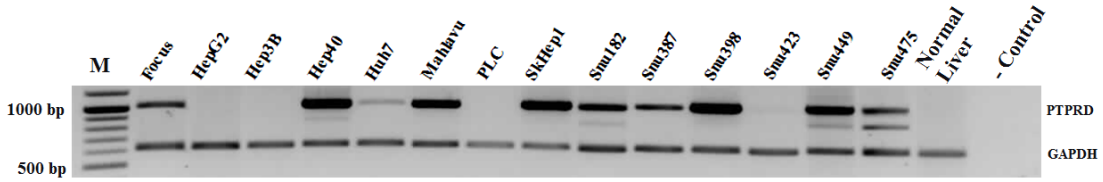

Figure 4.2.2 : Multiplex semi-quantitative RT-PCR of *PTPRD* in HCC Cell Lines. *GAPDH* was used as an internal control. M, marker (bp).

a) Multiplex semi-quantitative RT-PCR of the 5' region of the *PTPRD* cDNA. PTPRDcd3F / PTPRDcd3R primer pair with an expected product size of 517 bp and GAPDH RTF / GAPDH RTR pair with an expected product size of 611 bp were used.

b) Multiplex semi-quantitative RT-PCR of the 3'region of *PTPRD* cDNA. PTPRDcd9F / PTPRDcd9R primer pair with an expected product size of 1004 bp and GAPDH RTF / GAPDH RTR pair with an expected product size of 611 bp were used.

PTPRD expression at the protein level was also checked by western blotting. 35 µg protein were loaded into each well. 14 HCC cell lines were checked and all of the cell lines except Snu182, were shown to have PTPRD protein at different levels according to equal loading control calnexin. PLC have PTPRD protein band at a lower kDa suggested that PLC cell line might be expressing different *PTPRD* isoform (Figure 4.2.3).

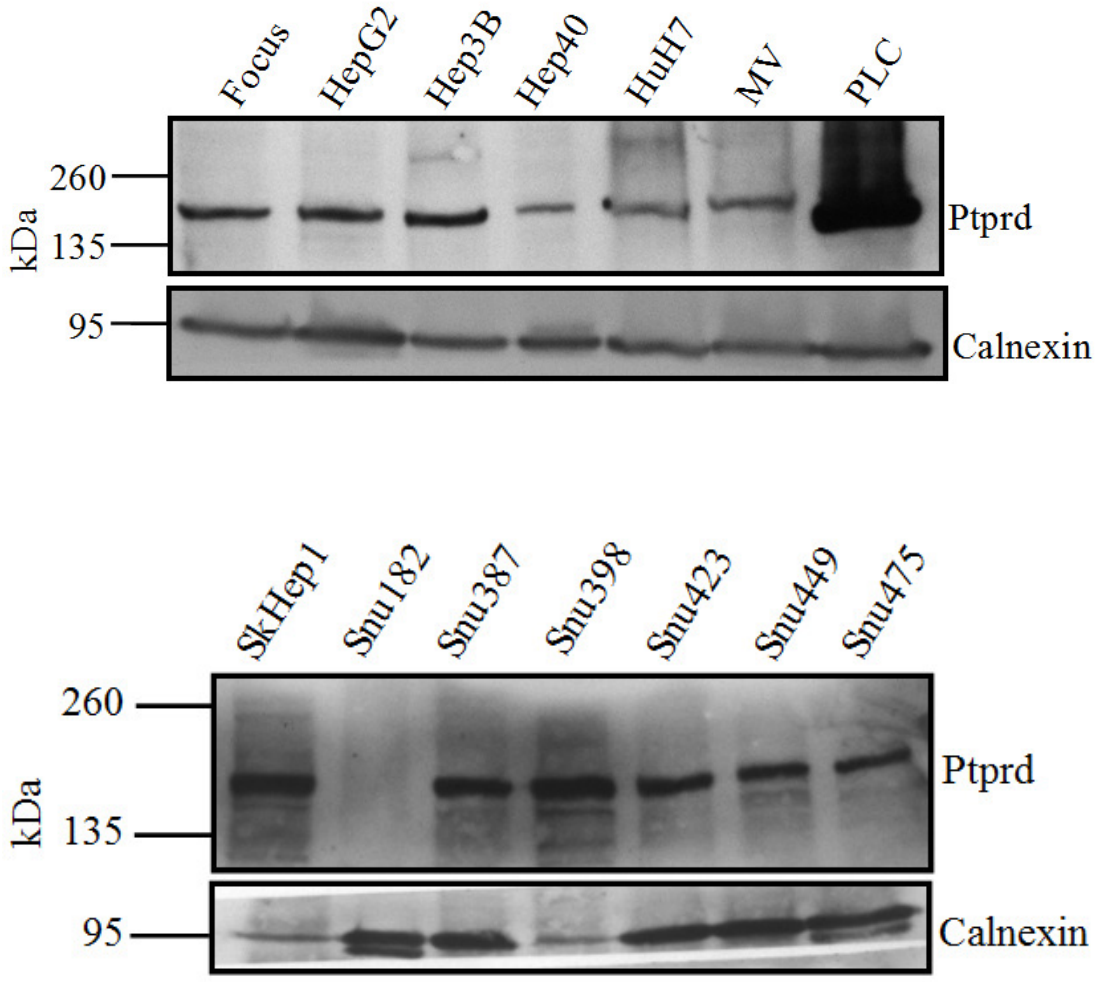

Figure 4.2.3 : Western blot analysis of PTPRD in 14 HCC Cell lines. PTPRD was expected to give band at 175 kDa. Calnexin (90 kDa) was used as a loading control. 35 µg protein were loaded each well. Spectra^{TM} Multicolor Broad Range Protein Ladder (Fermentas, USA) was used as a marker.

4.2.2. *PTPRD* Expression in Human HCCs

We also checked the expression analysis in clinical samples in order to verify that first findings in HCC cell lines is not restricted to the cell lines. We analyzed the expression of *PTPRD* mRNA in a panel of human HCCs (TissueScan Liver Cancer Tissue qPCR panel I, Origene) by quantitative real time RT-PCR analysis (Figure 4.2.4, 4.2.5). To normalize the *PTPRD* expression, samples were also analysed for *TBP* expression (FU LY. *et al.*, 2009; Gur-Dedeoglu B. *et al.*, 2009).

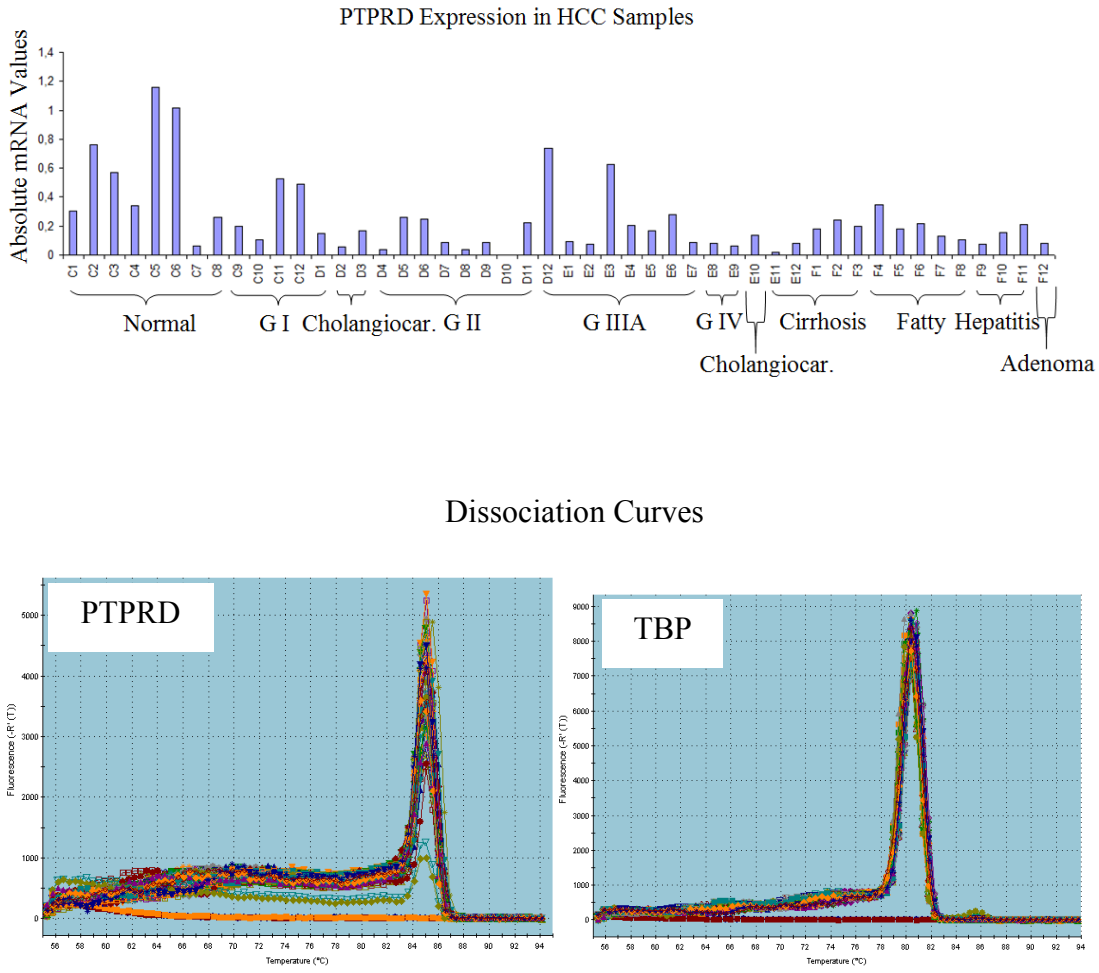

Figure 4.2.4.: *PTPRD* mRNA expression in HCC samples. PTPRDcd4F / PTPRDcd3R primer pair was used. cDNAs from human liver tissues of normal and various stages of liver cancers were subjected to real-time reverse transcription–PCR for detection of *PTPRD* mRNA expression. The data represent mRNA levels of *PTPRD* normalized to *TBP*. Dissociation curves of both genes are also presented.

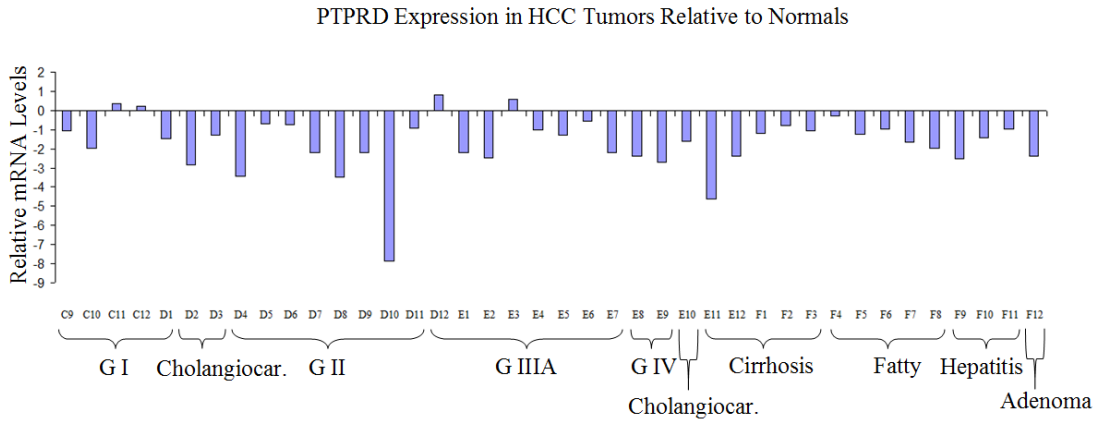

Figure 4.2.5. : *PTPRD* mRNA expression in HCC tumors relative to normals.

We observed significantly reduced *PTPRD* expression in 19 of 23 (82.6%) primary HCCs (GI, GII, GIIA, GIV) compared with eight normal liver tissues from the same panel as calculated by the student's t-test (*P* value=0,013). These results are consistent with our cell line data showing that *PTPRD* mRNA is reduced in a subset of HCCs and downregulation of the *PTPRD* occurs also in vivo.

4.2.3. Expression of the *PTPRD* in human liver tissues

To check if low level of *PTPRD* mRNA in HCCs is associated with PTPRD protein expression, we performed immunohistochemistry in human liver tissues containing non HCC and HCC samples. We observed strong PTPRD expression in non HCC hepatocytes and, low PTPRD protein expression in HCCs (Figure 4.2.6). Our IHC data shows that *PTPRD* expression is also downregulated in HCC at the protein level.

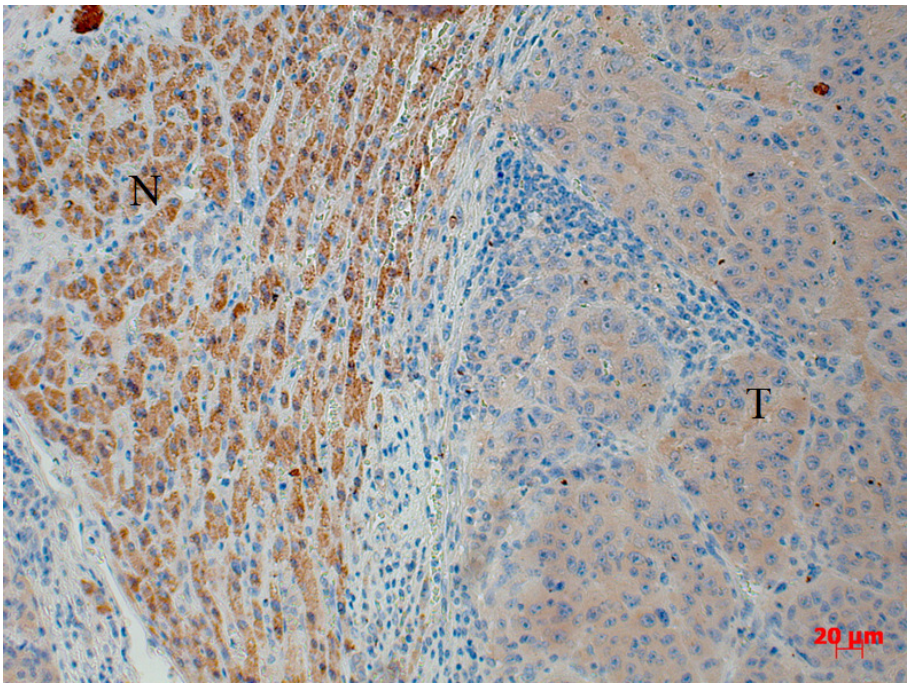

Figure 4.2.6: Representative photograph of immunohistochemistry of PTPRD in human liver tissue. Normal part of the tissue (N) shows strong, uniform cytoplasmic staining (brown) throughout the tissue. Tumor part of the tissue shows faint Sip1 immuno reactivity. N, Normal liver hepatocytes; T, HCC tumor cells (Scale Bars: 20µm).

4.2.4. *PTPRD* Mutations in HCCs

Somatic mutations of *PTPRD* were previously shown in colorectal cancers (Sjoblom *et al*., 2006), in lung adenocarcinoma (Ding *et al*., 2008; Weir *et al*., 2007), in glioblastoma multiforme (GBM), melanoma (Solomon *et al*., 2008)), lung and squamous head and neck carcinoma (Veeriah S. *et al*., 2009) were also described. But there is no information about mutations in HCC. *PTPRD* mutations were shown to accumulate in 11^{th} exon which encodes for a fibronectin III domain. Therefore, 11^{th} exon of *PTPRD* in 14 HCC cell lines was analysed first, by direct sequence analysis using genomic DNA and two sets of overlapping primers covering the 11^{th} exon. We could only detect an SNP (rs10977171) (Q447E) in one HCC cell line; Snu182 and one liver sample; C12 (Figure 4.2.7 a and b, respectively).

a.

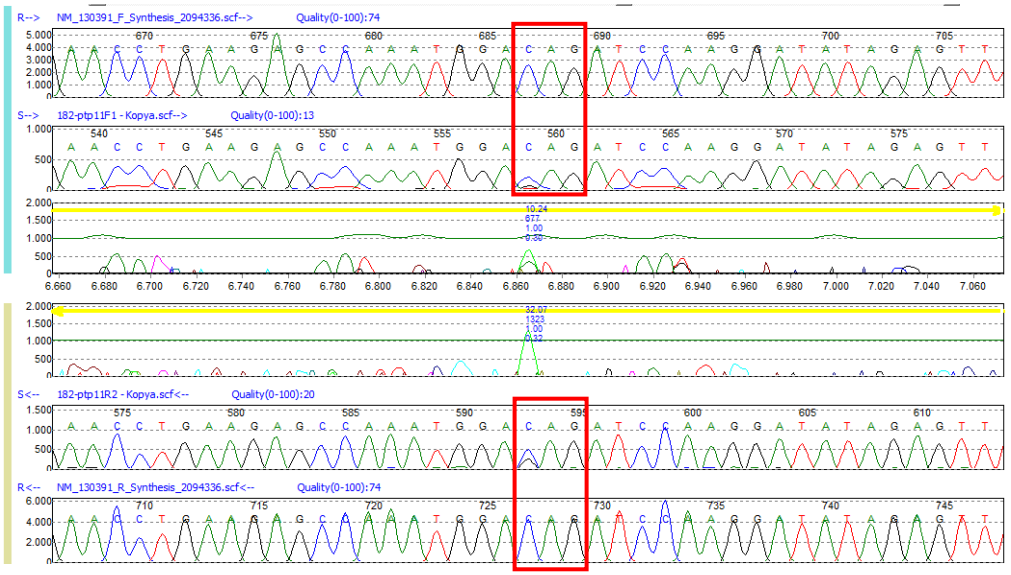

b.

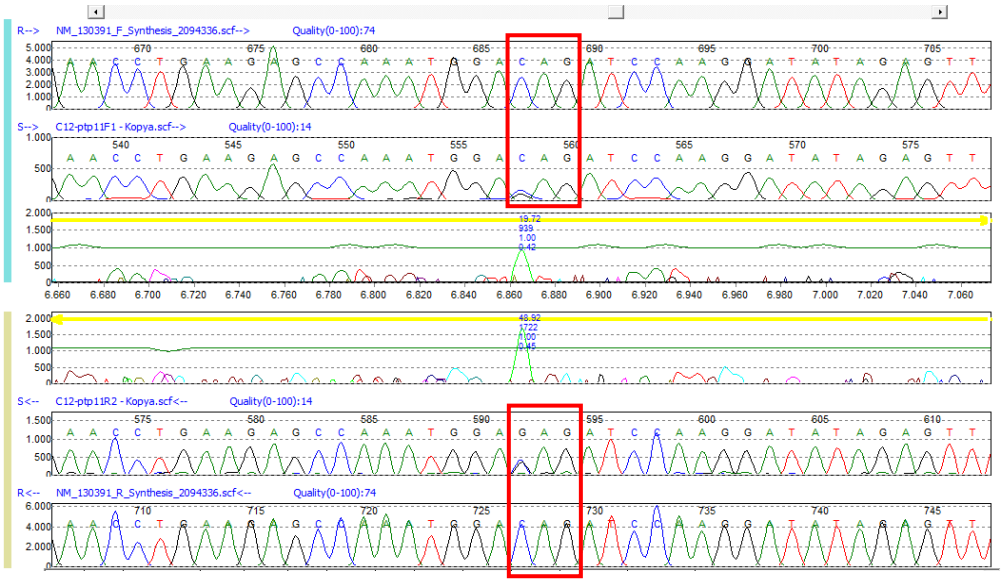

Figure 4.2.7 : Q447E SNP (rs10977171) mutation in *PTPRD*. Figures presented were captured from DNA Variant Analysis Software, Mutation Surveyor® Version 3.25 (www.softgenetics.com) showing an Q447E SNP (rs10977171) which result from "cag" to "gag" change. The uppermost and bottom sequence in each figures are *PTPRD* reference sequences downloaded from GenBank database. Between are the sequences of Snu182 cell line and C12 samples from both directions, forward and reverse.
a. Snu182 HCC cell line,
b. C12 HCC sample.

As *PTPRD* is a big gene having 35 coding exons, so it would be more feasible to analyse mutations using the cDNA rather than genomic DNA. Remaining coding exons were checked in four HCC cell lines; Hep40, Focus, MV and SkHep1, which were shown to express *PTPRD* mRNA. 35 coding exons were covered by 9 cDNA specific overlapping primers (Fig 4.2.8). We could not detect any mutation in these four cell lines (Ensembl transcript ENST00000356435 was used).

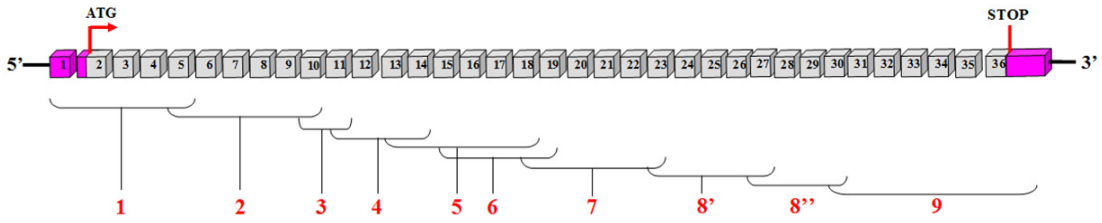

Figure 4.2.8: Primers were designed to cover all 36 exons in cDNA.

4.2.5. Homozygous Deletion of *PTPRD* Gene

As it is mentioned in details the introduction, *PTPRD* gene is localized in commonly deleted chromosomal region 9p23 in many cancer types including liver cancer, shown by our group study (Kubilay Demir, M.Sc.) and by several previous studies. Deleted region in Snu475 cell line (Figure 1.3.3) were analysed *in-silico* in SANGER CONAN database and deletion was mapped to between 8.455.500-8.490.500 bp. Deletion covers eight exons of *PTPRD* (Figure 4.2.9). To fine mapping the deletion of *PTPRD* gene in 14 HCC cell lines, 36 exons were amplified one by one by genomic PCR with the primers that were located in introns close to exon-intron splice sites. Ensembl transcript ENST00000356435 was used for genomic screening. It was clearly shown in Figure 4.2.10 that all exons except for the ones between 15^{th}-22^{th} were amplified in Snu475 cell line. This deletion result in a 1586 bp lost in *PTPRD* cDNA and 37683 bp lost in genomic DNA. All 36 exons were succesfully amplified in remaining 13 HCC cell lines and in normal liver (Figure 4.2.10).

Figure 4.2.9: Deleted region (red rectangle) in *PTPRD* gene. (ENSEMBL Genome Browser, NCBI36 database)

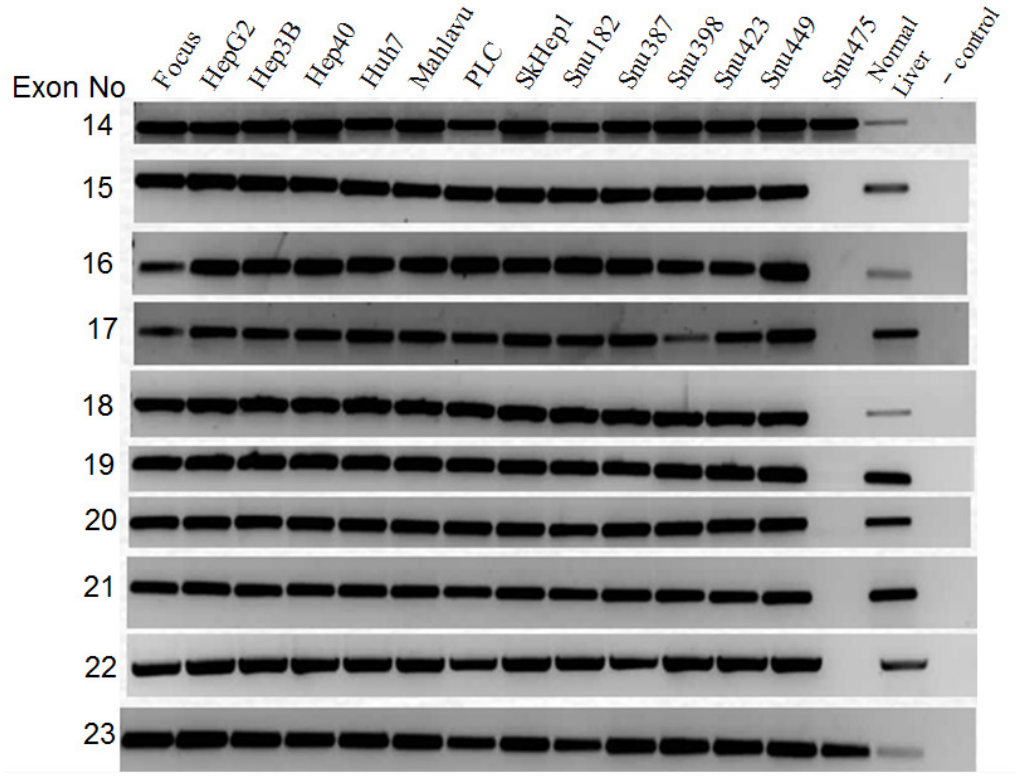

Figure 4.2.10: Homozygot deletion on Snu475 HCC cell line between exons 15-22.

4.2.6. *In Silico* Analysis of *PTPRD* promoter

Tumor suppressor genes can be inactivated by genetic mechanisims, such as deletion, or epigenetic mechanism such as promoter hypermethylation (Ponder B.A. , 2001; Jones P.A., Baylin S.B., 2002) Promoter hypermethylation has been show to be a major inactivation mechanism of the tumor suppressor genes in cancers (Herman J.G., Baylin S.B., 2003). As *PTPRD* has been shown to be downregulated by epigenetically in GBM, breats and colon cancer but not in corresponding normal tissues, and its expression can be restored after treatment with the DNMT inhibitor DAC, we want to search in HCC (Veeriah S. *et al*., 2009). *PTPRD* promoter region contains CpG island as studied in Veeriah S. *et al*. study (Figure 4.2.11). Nested primers were designed in order to amplify the region of CpG sites. Same region was also investigated previously by Veeriah S. *et al*. and methylation was found in 37% of GBM tumors (Ensembl Transcript ID: ENST00000381196) (Veeriah S. *et al*., 2009).

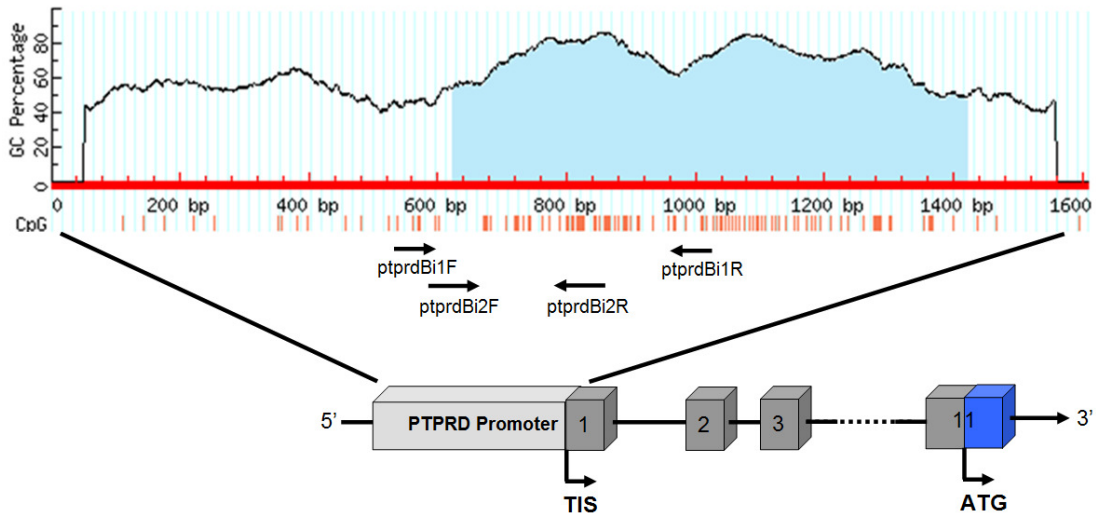

Figure 4.2.11 : Promoter region of the *PTPRD* gene. CpG island (light blue area) predictted by MethPrimer program and location of the primers used for the analysis of methylation status were shown. Red lines denote CpG sites, numbered boxes denote exons and TIS denotes the transcriptional start site (Ensembl Transcript ID: ENST00000381196).

4.2.7. Restoration of *PTPRD* mRNA expression by 5'-AzaC and TSA treatment

As mentioned previously, many genes, especially tumor suppressor genes transciptionally silenced via epigenetic mechanisms including promoter hyper-methylation and histone modifications (Esteller M., 2007). To clarify if *PTPRD* expression in HCC cell lines was reduced due to DNA methylation and/or histon deacetylation, cell lines having reduced level of *PTPRD* expression was treated with DNA methyltransferase inhibitor (5-AzaC) alone and with histone deacetylase inhibitor trichostatin A (TSA). PLC and Hep3B cell lines did not express *PTPRD* mRNA that was shown in both 5' and 3' multiplex semi-quantitative RT-PCR experiment but HepG2 cell line was shown to have low level of *PTPRD* mRNA expression in 5' (Figure 4.2.2). *PTPRD* mRNA expression was succesfully restored after 5-AzaC treatment alone (in PLC and Hep3B cell lines) or together with trichostatin A (TSA) (in Hep3B and HepG2 cell lines) (Figure 4.2.12, Figure 4.2.13).

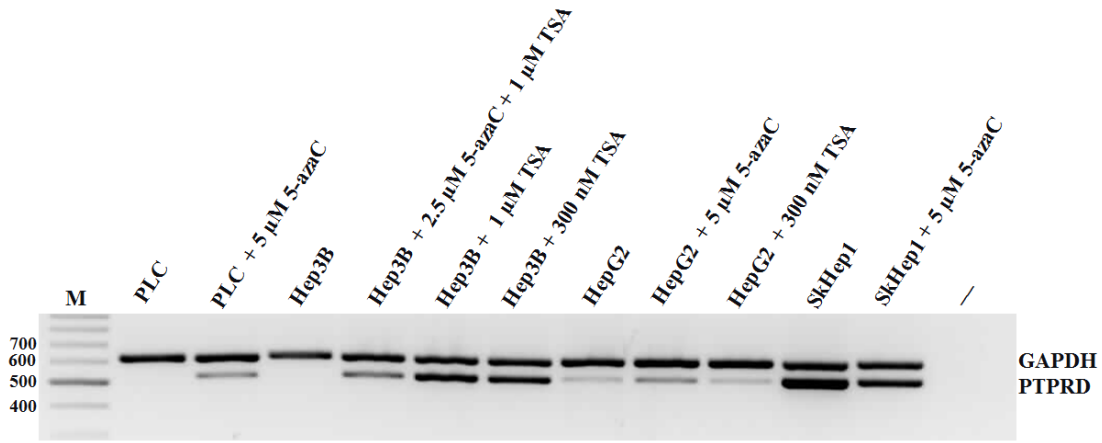

Figure 4.2.12 : Restoration of *PTPRD* mRNA expression by 5'-AzaC and TSA treatment. PTPRDcd3F/PTPRDcd3R primer pair with an expected product size of 517 bp and GAPDH RTF/GAPDH RTR pair with an expected product size of 611 bp were used. M, marker (bp); (-), negative control. SkHep1 cell line was used as a *PTPRD* positive control. *GAPDH* was used as an internal control of multiplex semi-quantitative RT-PCR.

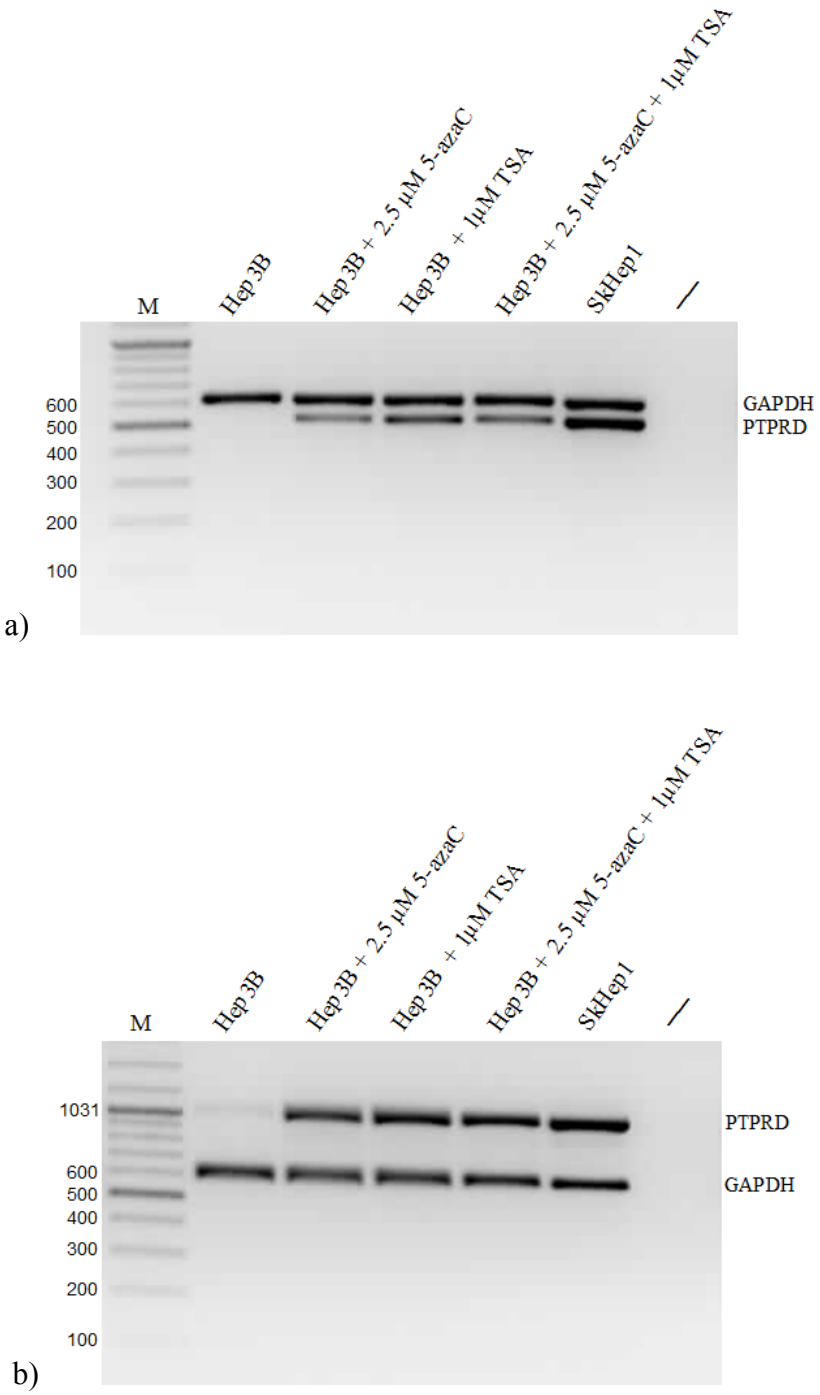

Figure 4.2.13 : Restoration of *PTPRD* mRNA expression in Hep3B cell line after 5'-AzaC and/or TSA treatment shown by multiplex semi-quantitative RT-PCR.
M, marker (bp); (-), negative control. SkHep1 cell line was used as a *PTPRD* positive control. *GAPDH* (with an expected product size of 611 bp) was used as an internal control. **a)** PTPRDcd3F/PTPRDcd3R primer pair with an expected product size of 517 bp and **b)** PTPRDcd9F / PTPRDcd9R primer pair with an expected product size of 1004 bp was used.

HepG2 and Hep3B was previously shown to have PTPRD protein when 35 µg protein were loaded (Figure 4.2.3). But, these cell lines could not be shown to have protein when loaded 12 µg and 3 µg protein respectively. Even more interestingly, they restored PTPRD protein after 5-AzaC/TSA treatments. It could be suggested that these cell lines have PTPRD protein, but only at the basal level (Figure 4.2.14).

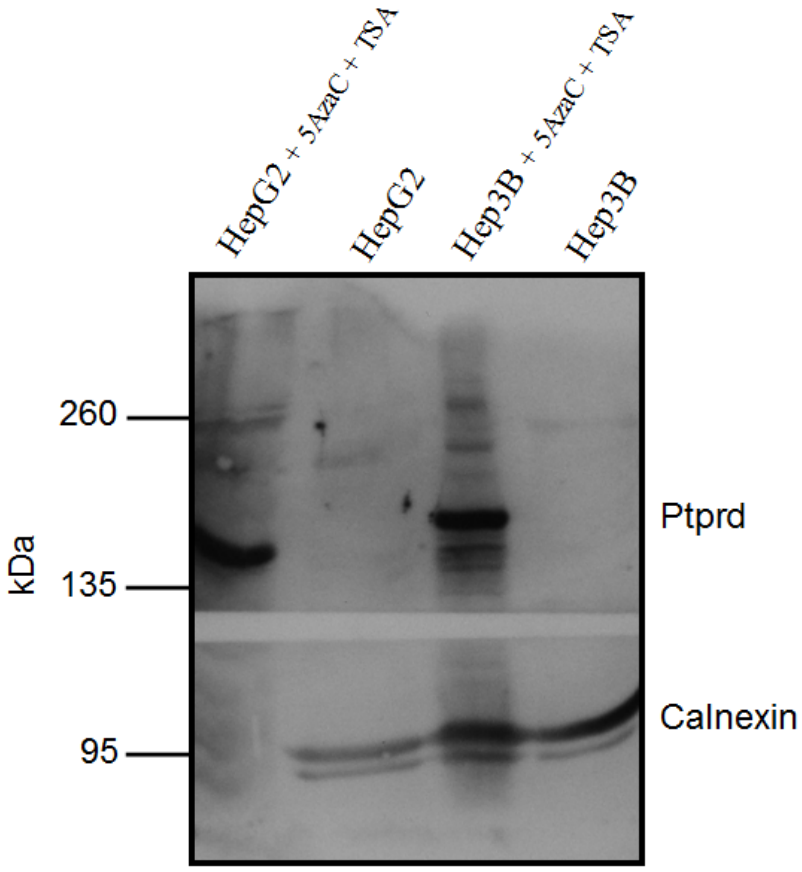

Figure 4.2.14 : Western blot analysis of PTPRD in HepG2 and Hep3B cell lines and same cell lines after 5-AzaC and TSA treatments. Calnexin was used as a equal loading control. 12 µg protein were loaded for HepG2 and HepG2 + (5-AzaC+TSA). 3 µg protein were loaded for Hep3B and Hep3B + (5-AzaC+TSA). Spectra^{TM} Multicolor Broad Range Protein Ladder (Fermentas, USA) was used as a marker.

4.2.8. Frequent metylation of *PTPRD* promoter in primary HCC samples

PTPRD promoter was previously shown to be methylated (37%) in GBM (glioblastoma multiforme) tumors, breast cancer (20%) and colon cancer (50%) (Veeriah S. *et al*., 2009). CpG island in the promoter of *PTPRD* gene (Figure 4.2.11) was investigated in clinical HCC samples. Combined bisulfite restriction analysis (COBRA) was performed to determine the level of *PTPRD* methylation. 29 tumors and paired normal liver tissue samples were examined and 20.7% of the tumors was shown to have high level of methylation compared to their corresponding normal tissues (Figure 4.2.15).

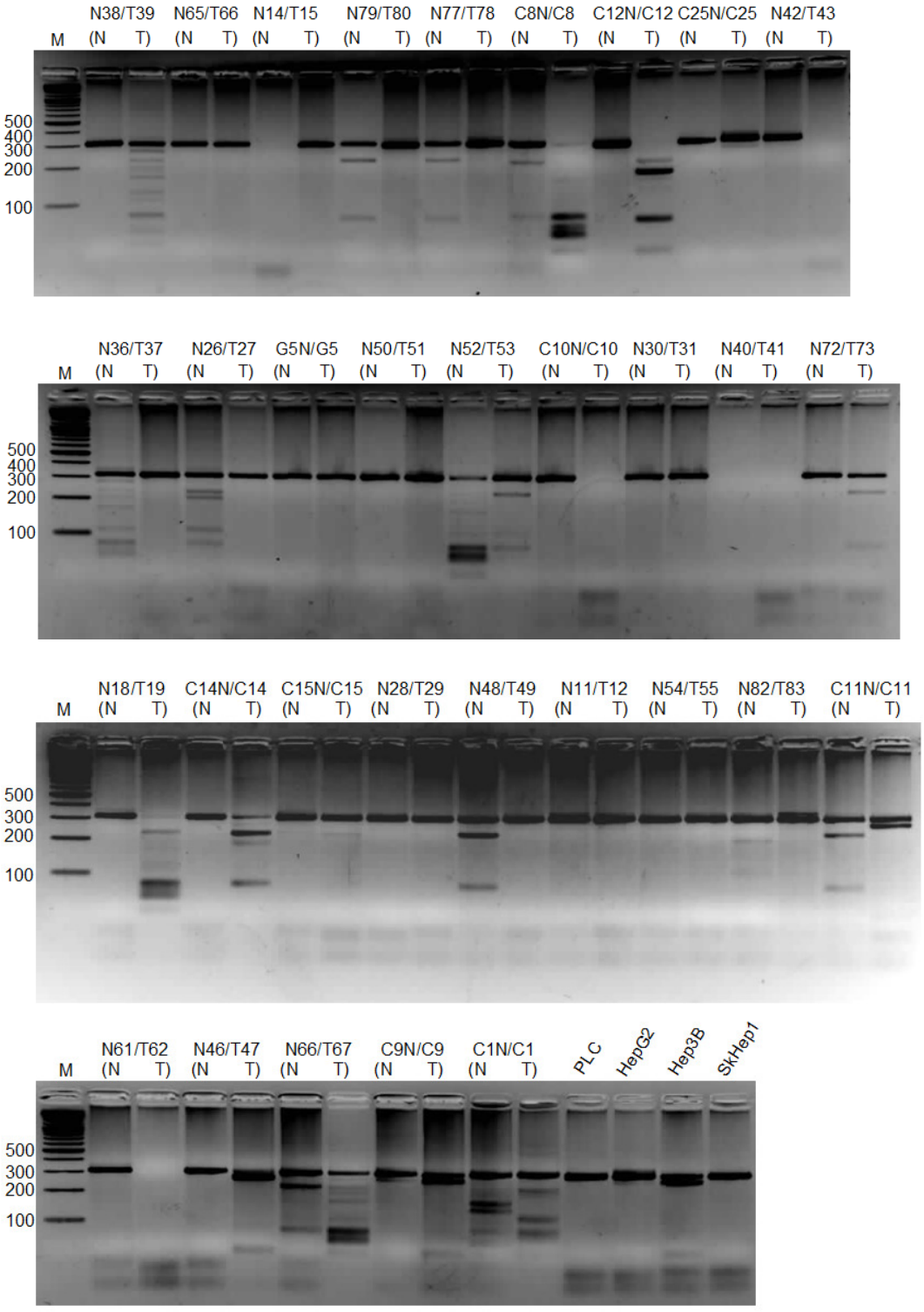

Figure 4.2.15 : *BstU*I restriction analysis of *PTPRD* promoter region amplified by ptprdBi2F / ptprdBi1R primer pair. 6 out of 29 normal-tumor paired samples (20,7%) were methylated. M, marker (bp).

4.3. *MDM2* (Chromosome 12q15)

In our published study, the distribution of the SNP309 genotype was investigated in 99 human HCCs that were previously characterized for *TP53* alterations from HCC endemic and rare geographical areas (Acun T., *et al.* 2010).

A total of 99 DNA samples with known *TP53* status isolated from histologically confirmed tumor and nontumor liver tissue of the patients from HCC patients living in different geographical regions, including Mozambique (n=16), South Africa (excluding Mozambique: n=17), China (n=21), Japan (n=13), Europe (Germany, France, Spain, Turkey, Israel and USA: n=32) were analysed. Characteristics of these tumors and methods for DNA isolation have been described previously (Unsal H. *et al*., 1994; Cagatay T. *et al*., 2002).

SNP309 (T/G) of *MDM2* were genotyped using PCR amplification of the first intron by MDM2-F / MDM2-R primer pair (304 bp), followed by *MspA1*I (Promega) digestion as described elsewhere (Sotamaa K. *et al*., 2005) (Figure 4.3.1).

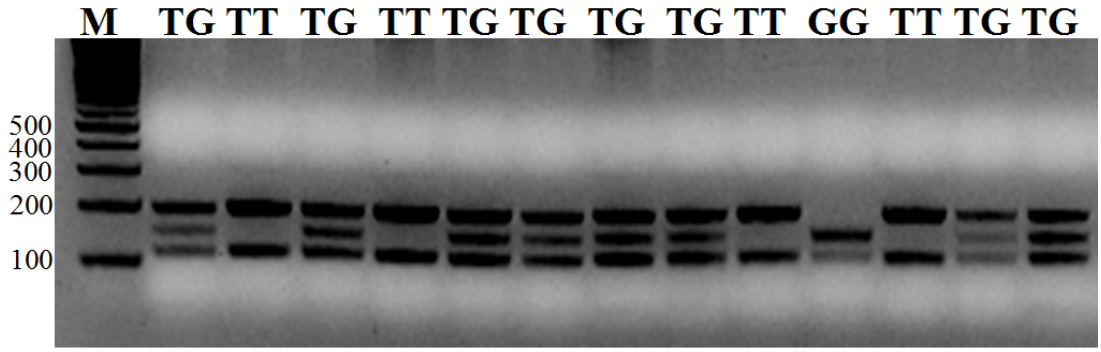

Figure 4.3.1: Representative photograph of *MspA1*I digested PCR products of HCC samples resolved on 3% agarose gel .Three distinct patterns were observed representing T/T wild type, T/G heterozygote, G/G homozygote. M, marker (bp).

All statistical analyses were conducted using R functions in 'genetics' and 'stats' packages (http://www.r-project.org) (Foulkes A.S., 2009; Cohen Y. Cohen J.Y., 2008). Pearson's Chi-squared test with simulated *P*-value (based on 10,000 replicates) was applied to test whether the populations were in Hardy–Weinberg equilibrium with respect to MDM2 SNP309 polymorphism. The association between the P53 mutation status and the SNP309 genotypes was assessed using Fishers' exact tests.

Ninety-nine samples with known *TP53* status (n=99) were genotyped for SNP309. The observed genotypic frequency of SNP309 in HCC patients was distributed as 49% T/T genotype carriers (n=49), 31% T/G genotype carriers (n=31) and 19% G/G genotype carriers (n=19) (Table 4.3.1).

Remarkable differences in the allele frequencies for each SNP309 genotype between patients from different geographical regions were observed. The G allele was the most common in the 13 Japanese HCC patients (100%); three of them were homozygous (23%) and 10 of them (77%) were heterozygous (Table 4.3.1). Interestingly, there was no wild-type SNP309 genotype carrier (T/T) among Japanese HCC patients (n=13), although the Japanese population was in HW equilibrium (*P*-value = 0.08).

Contrastingly, 31 out of 33 South African patients were wild-type for SNP309 (94%), but only two were heterozygous (6%), while there was no patient with the G/G genotype. Genotypic distributions of African and European populations did not exhibit HW disequilibrium. The allele frequencies were highly divergent between African and other populations in which G allele was frequent (Table 4.3.1).

Distribution of T/T and T/G−G/G genotypes together was similar between patients from two geographically distant regions: China and Europe [wild-type genotype frequency 33% (7/21) vs. 34% (11/32); mutant genotype frequency 67% (14/21) vs. 66% (21/32), respectively]. However, heterozygote genotype frequency varied drastically between Chinese and European HCC patients [15% (3/21) vs. 50% (16/32)].

Samples	P53 Mutant	MDM2 SNP309 Genotypes			Hardy-Weinberg Equilibrium			
		T/T	T/G	G/G	p	q	Chi-square	*P*-value
Africa (n=33)	11(33%)	31	2	0	0.97	0.03	0.03	1
Japan (n=13)	1(8%)	0	10	3	0.38	0.62	5.08	0.08
China (n=21)	5(23%)	7	3	11	0.40	0.60	10.39	0.001
Europe (n=32)	5(16%)	11	16	5	0.59	0.41	0.04	1
Total (n=99)	22(22%)	49	31	19	0.65	0.35	9.54	0.0015

Table 4.3.1: Distribution of *TP53* mutations and SNP309 genotypes in HCC samples from different geographical regions and Hardy–Weinberg equilibrium states of *MDM2* genotypes. Mut, mutations; p and q refer to allele frequencies of T and G, respectively (Acun T., *et al.* 2010).

		Genotype Frequency		OR (95%CI)	*P*-value
		T/T	TG/GG		
All HCC Samples	**p53 Wt**	31	46	0.15 (0.03 to 0.52)	0,0006
	p53 Mut	18	4		
African Samples Excluded	**p53 Wt**	11	44	0.15 (0.03 to 0.7)	0.0065
	p53 Mut	7	4		

Table 4.3.2: Inverse relationship between *TP53* mutation and SNP309 G genotype of *MDM2* gene in all HCC samples and without african samples. Wt, wild type; Mut, mutant; OR, odds ratio; CI, confidence interval (Acun T., *et al.* 2010).

We then analyzed whether a significant correlation between the *TP53* mutation and SNP309 genotypes existed. Interestingly, 18 of 22 (82%) *TP53* mutations were concentrated in 49 (37%) HCC cases displaying the T/T genotype (Table 4.3.2). Among the 19 cases homozygous for G/G, three of them had TP53 mutations (16%) and only one of 31 cases of heterozygous T/G displayed somatic *TP53* mutations (3%) (Table 4.3.2). Considering both T/G and G/G genotypes together (dominant model), only 4% of the 99 HCCs were positive for both p53 gene mutation and the G genotype (Table 4.3.1 and Table 4.3.2).

We next examined whether there was a statistical interaction between the G genotype and *TP53* mutations using Fisher's exact test. There was a highly significant inverse relationship between the presence of *TP53* mutation and the G allele (*P*-value, two-sided = 0.0006; odds-ratio = 0.153; 95% CI = 0.03–0.52).

We next excluded African patients from the statistical analysis to prevent the potential bias from the high percentage of *TP53* mutations and SNP309 wild-type genotype carriers in Africa. The inverse relationship between the presence of *TP53* mutation and the G genotype was sustained (*P*-value, two-sided = 0.0065; odds-ratio = 0.148; 95% CI = 0.03–0.7).

Given the functional role of SNP309 in the inhibition of the TP53 pathway, the mutant genotype of this SNP may be functionally equivalent to the inactivating *TP53* mutations in hepatocarcinogenesis (Figure 4.3.2). Either germline mutations at MDM2 SNP 309 or somatic mutations in *TP53* gene seems to occur to inactivate TP53 pathway. Both alteration classify about 70% (68/99) of the HCCs, remaining 30% of tumors that lack of TP53 pathway inactivation are not inlcuded in the figure (Figure 4.3.2).

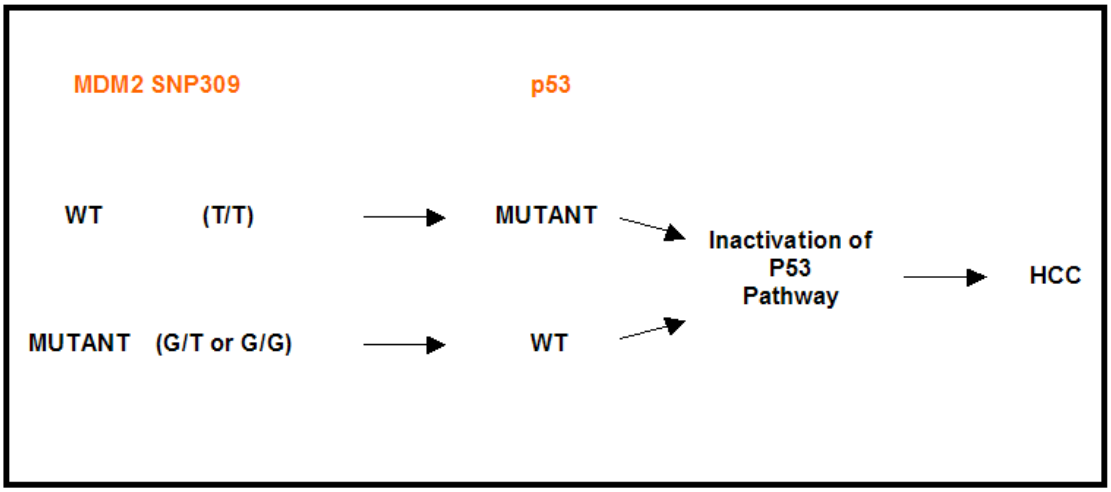

Figure 4.3.2: Model for TP53 pathway inactivation during hepatocellular carcinoma development.

4.4. RAS/RAF/MAPK Pathway

Mutation analysis of the *MEK1* (*MAP2K1*) , *MEK2* (*MAP2K2*), *ERK1* (*MAPK3*) and *ERK2* (*MAPK1*) genes in HCC cell lines were performed by using overlapping cDNA specific primers and direct sequencing of the amplified PCR products (Figure 4.4.1). No mutations were described in these genes in 14 HCC cell lines.

PTPN11 (*SHP2*), on the other hand, was analysed by using genomic DNA because of difficulties of amplifying its cDNA. As, *PTPN11* was previously shown to have mutations described in noonan syndrome (NS), clinically related leopard syndrome (LS) and leukemia (Tartaglia M. *et al*., 2006), which are accumulated on exon 3,4,7,8,12 and 13. These exons were analysed first but no mutations were described in these exons in 14 HCC cell lines (Figure 4.4.2). But, mutation analysis was extended to remaining exons, as there might be some mutations specific for HCC. As no mutation was found in HCC cell lines for the genes *MEK1* (*MAP2K1*) , *MEK2* (*MAP2K2*), *ERK1* (*MAPK3*), *ERK2* (*MAPK1*) and *PTPN11* (*SHP2*), mutation analysis was not extended to HCC samples.

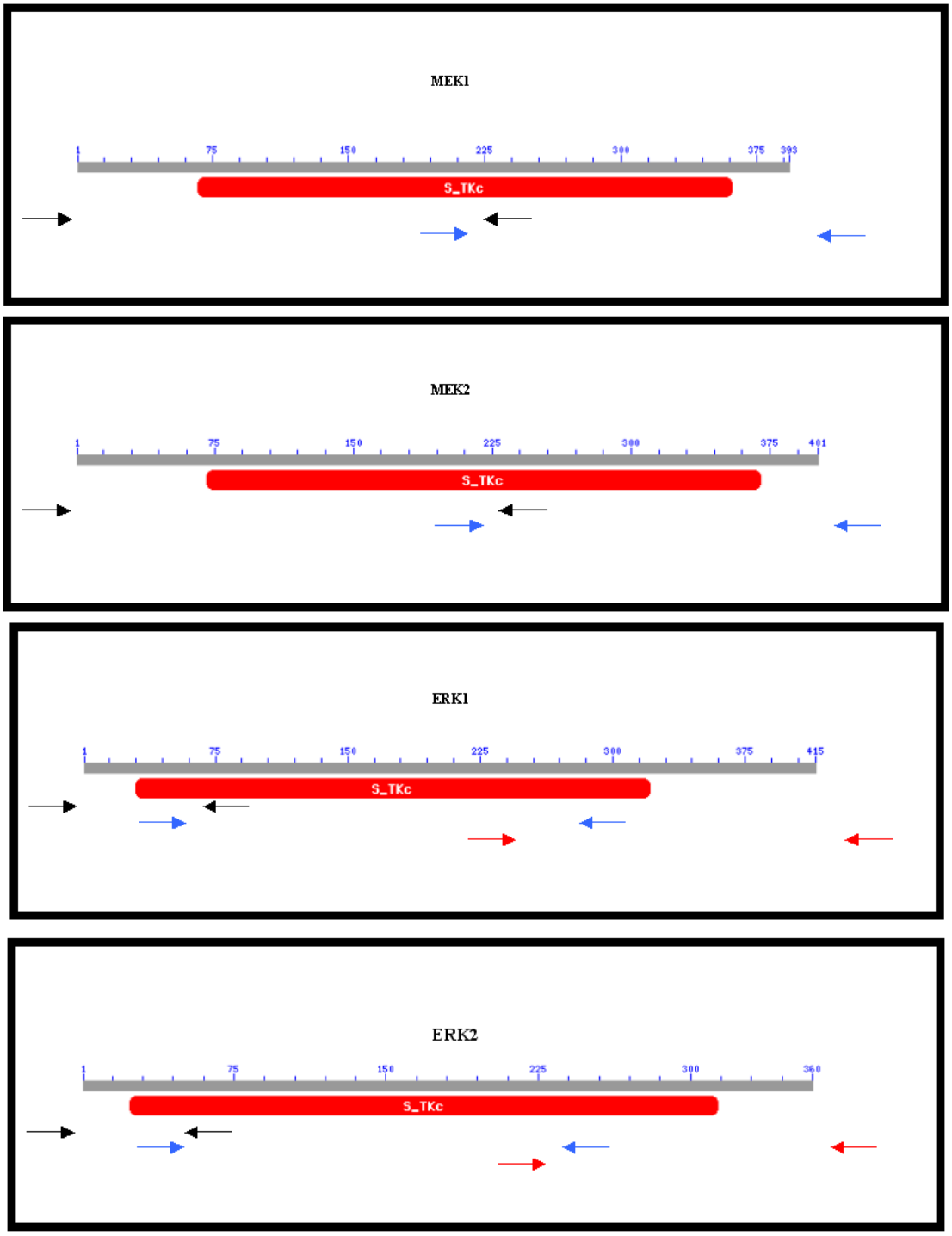

Figure 4.4.1: Representative figures showing functional domains and locations of the primers used for amplification of each gene cDNA. Each F/R primer pairs represented in same color.

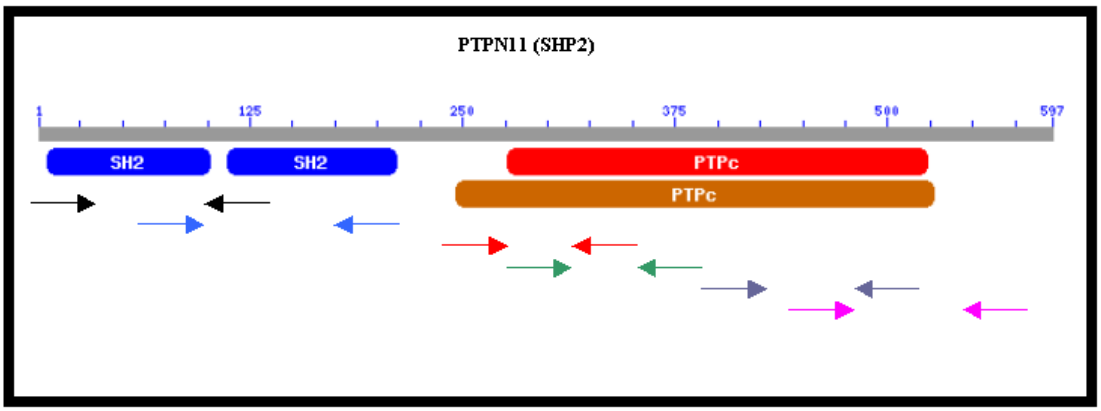

Figure 4.4.2: Representative figure showing functional domains and locations of the primers used to amplify *PTPN11* gene. Each F/R primer pairs specific for exons 3, 4, 7, 8, 12, 13 are represented in same color.

4.5. Chromosome 11q13 (*FBXL11*, *PTPRCAP*)

4.5.1. *FBXL11* Expression in HCC Cell Lines

FBXL11 mRNA expression was analysed in 14 HCC cell line by quantitative real-time RT-PCR. *FBXL11* mRNA expression was found to be high in Huh7, Hep40 and Snu387; low in Focus, HepG2, MV, PLC, Snu398, Snu423 and Snu475. Hep3B, SkHep1 and Snu182 cell lines shown very little expression (Figure 4.5.1).

FBXL11 expression was also observed at the protein level in eight HCC cell lines tested (Figure 4.5.2).

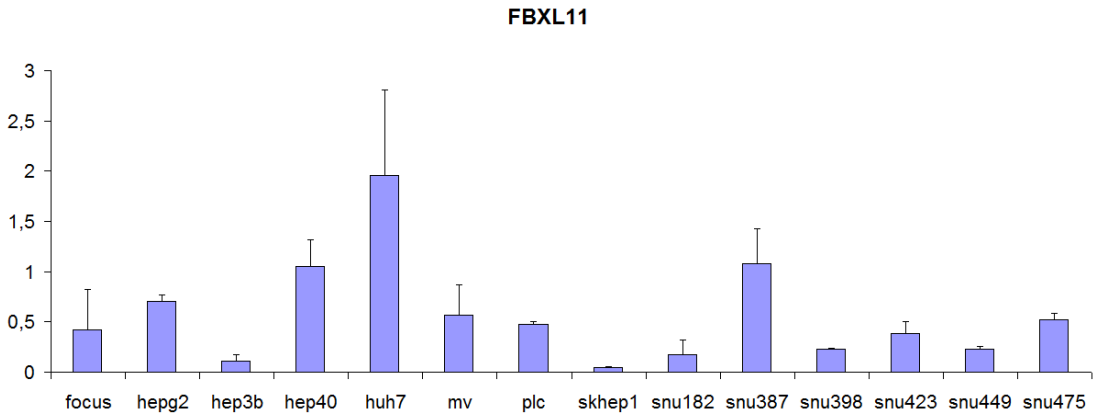

Dissociation Curves

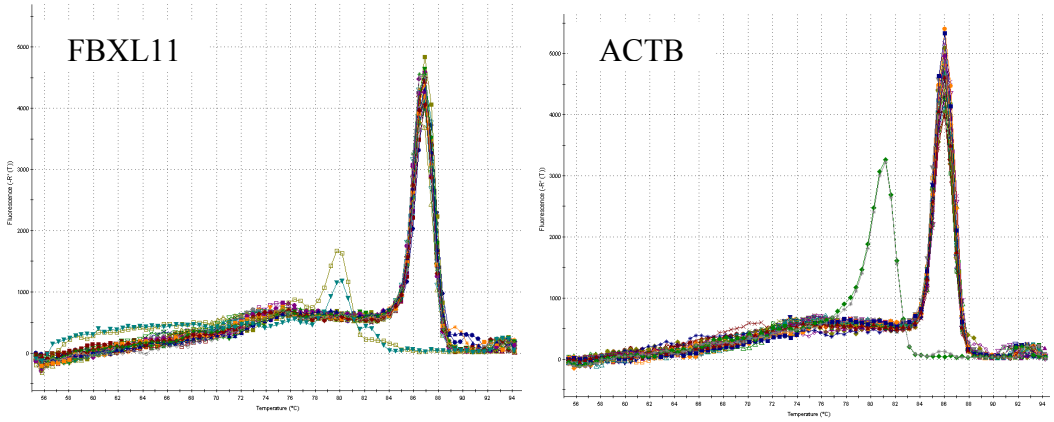

Figure 4.5.1: Quantitative Real-Time Analysis of *FBXL11* in HCC cell lines. *ACTB* was used as an internal control. Experiment conducted two times and standart deviations are indicated. Dissociation curves of both genes are also presented.

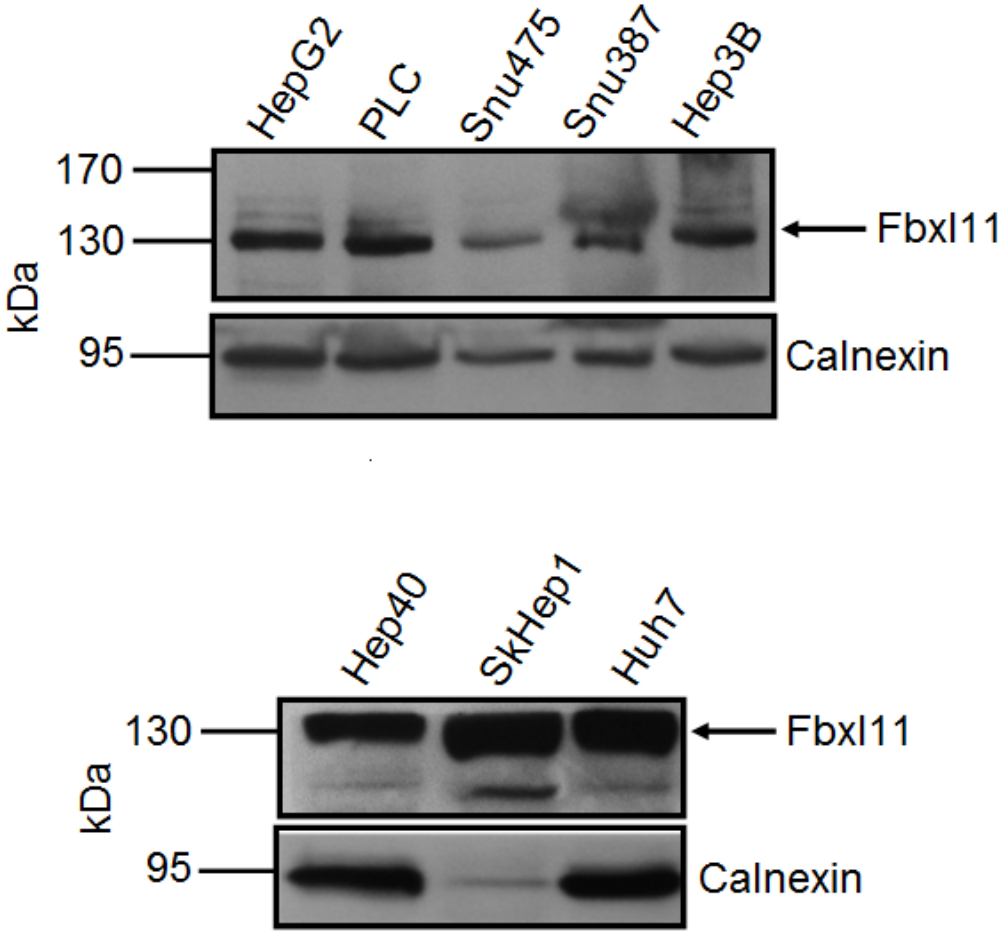

Figure 4.5.2 : Western blot analysis of FBXL11 in HCC cell lines. FBXL11 was expected to give band at 132 kDa. Calnexin (90 kDa) was used as a loading control. 35 µg protein were loaded each well. PageRuler™ Prestained Protein Ladder (Fermentas, USA) was used as a marker.

4.5.2. *FBXL11* Expression in Human HCCs

FBXL11 mRNA expression was analysed in clinical samples (TissueScan Liver Cancer Tissue qPCR panel I, Origene) by quantitative real time RT-PCR analysis (Figure 4.5.3, 4.5.4). To normalize the *FBXL11* expression, samples were also analysed for *TBP* expression (FU LY. *et al.*, 2009; Gur-Dedeoglu B. *et al.*, 2009).

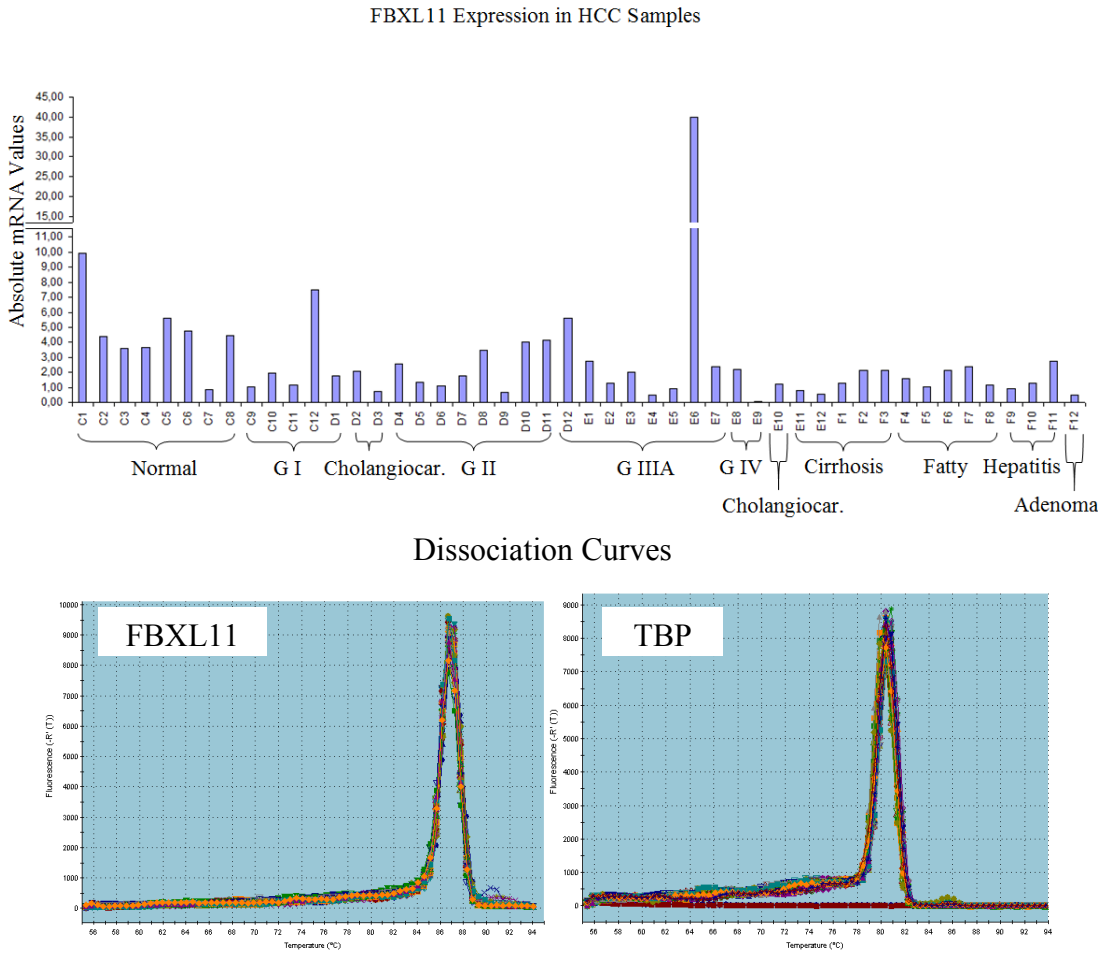

Figure 4.5.3 : *FBXL11* mRNA expression in HCC samples. cDNAs from human liver tissues of normal and various stages of liver cancers were subjected to real-time reverse transcription–PCR for detection of *FBXL11* mRNA expression. The data represent mRNA levels of *FBXL11* normalized to *TBP*. Dissociation curves of both genes are also presented.

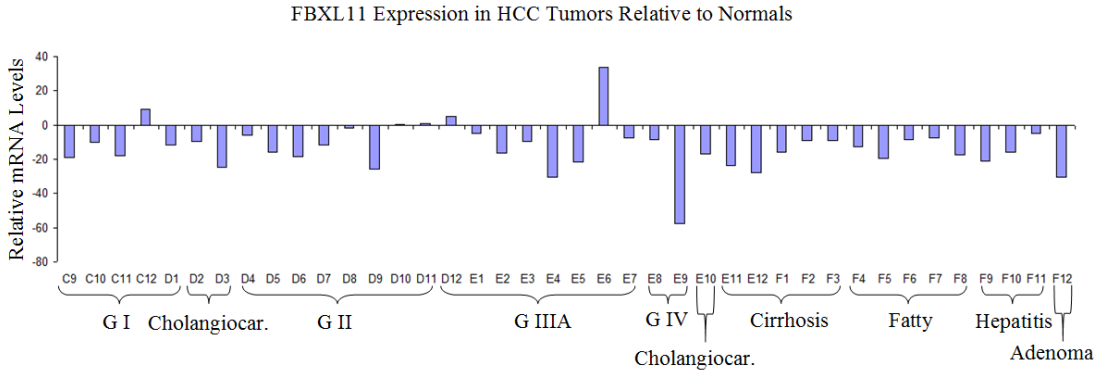

Figure 4.5.4 : *FBXL11* mRNA expression in HCC tumors relative to normals.

We observed significantly reduced *FBXL11* mRNA expression in 18 of 23 (78.3%) primary HCCs (GI, GII, GIIIA, GIV), compared with eight normal liver tissues from the same panel as calculated by the student's t-test (*P* value=0,0043).

4.5.3. Absence of *FBXL11* Mutations in HCC Cell Lines

Coding region of *FBXL11* gene (exon 10 to exon 21) was also investigated by using genomic primers and direct sequencing of the amplified PCR products. No mutations were described in 14 HCC cell lines.

4.5.4. *PTPRCAP* Expression in HCC Cell Lines

PTPRCAP mRNA expression was analysed in 14 HCC cell line by quantitative real-time RT-PCR by using PTPRCAP-F/PTPRCAP-R primer pair with an expected product size of 132 bp. *PTPRCAP* mRNA expression was found to be high in Snu182, Snu387 and Snu475. Focus, HepG2, MV, SkHep1 and Snu449 cell lines shown very little expression (Figure 4.5.5).

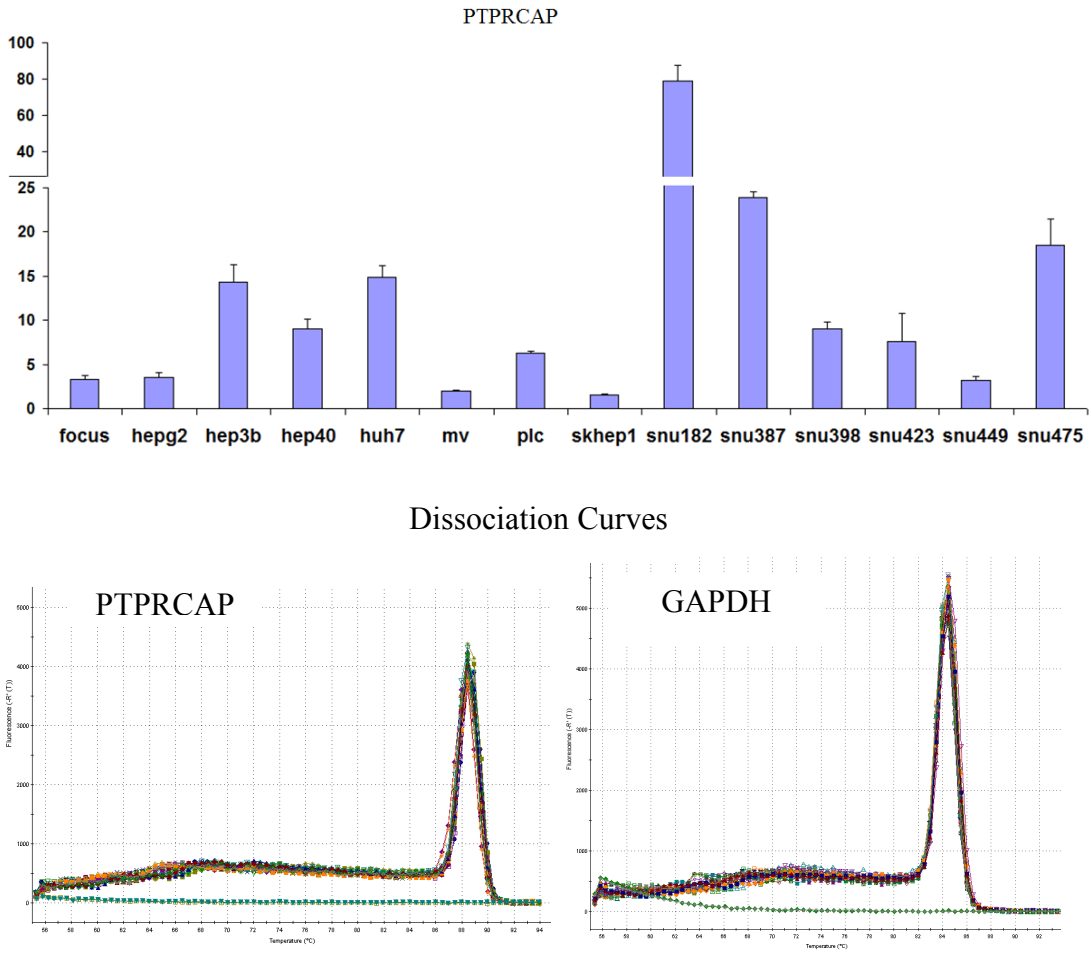

Figure 4.5.5: Quantitative Real-Time Analysis of *PTPRCAP* in HCC cell lines. *GAPDH* was used as an internal control. Experiment conducted two times and standart deviations are indicated. Dissociation curves of *PTPRCAP* and *GAPDH* primers are also presented.

4.5.5. *PTPRCAP* Expression in Human HCCs

PTPRCAP mRNA expression was analysed in clinical samples (TissueScan Liver Cancer Tissue qPCR panel I, Origene) by quantitative real time RT-PCR analysis (Figure 4.5.6, 4.5.7). PTPRCAP-F/PTPRCAP-R primer pair was used. To normalize the *PTPRCAP* expression, samples were also analysed for *TBP* expression (FU LY. *et al.*, 2009; Gur-Dedeoglu B. *et al.*, 2009).

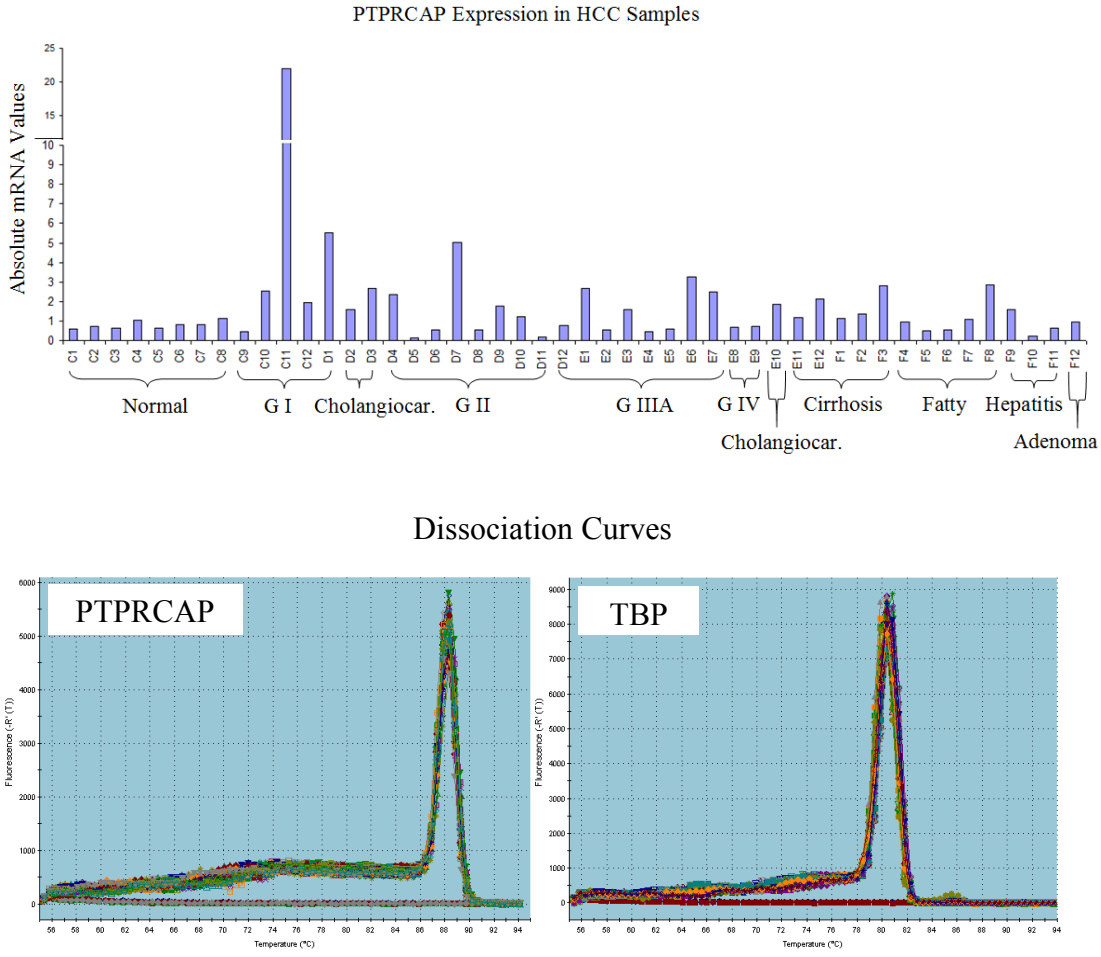

Figure 4.5.6 : *PTPRCAP* mRNA expression in HCC samples. cDNAs from human liver tissues of normal and various stages of liver cancers were subjected to real-time reverse transcription–PCR for detection of *PTPRCAP* mRNA expression. The data represent mRNA levels of *PTPRCAP* mRNA normalized to *TBP*. Dissociation curves of both genes are also presented.

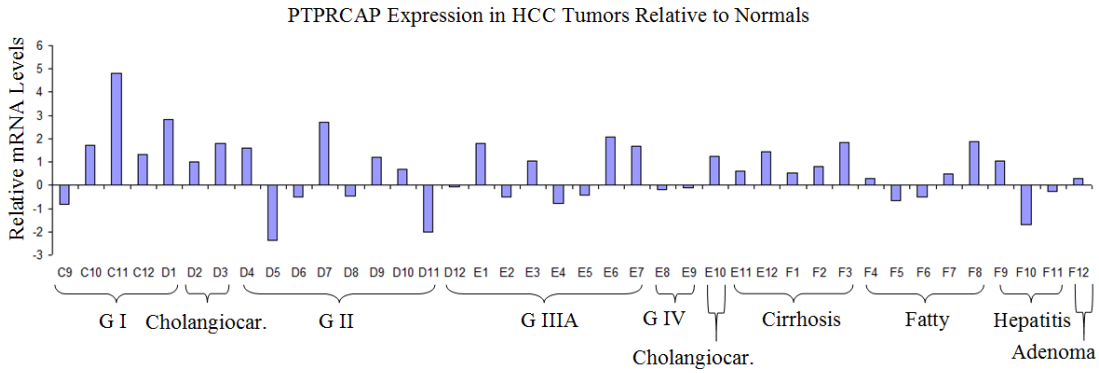

Figure 4.5.7 : *PTPRCAP* mRNA expression in HCC tumors relative to normals.

We observed high *PTPRCAP* mRNA expression in 12 of 23 (52,1%) primary HCCs (GI, GII, GIIA, GIV), compared with eight normal liver tissues from the same panel.

4.6. Chromosome 13q12 (*TUBA3C,ZNF198,TPTE2*)

4.6.1. Detailed Genetic Analysis of 13q12.11 Region

13q12.11 region in Huh7 and SkHep1 cell lines was previously shown to be deleted (Kubilay DEMIR, M.Sc.). 10K chip was used to analyse the region which was covered by 9 SNP markers. These markers are not enough to investigate the deleted region gene-by-gene. To better understand the deletion borders and to determine the deleted genes, we use fine-mapping starategy. 9 genes (predicted and defined) were analysed in 14 HCC cell lines by using genomic primers (Figure 4.6.1).

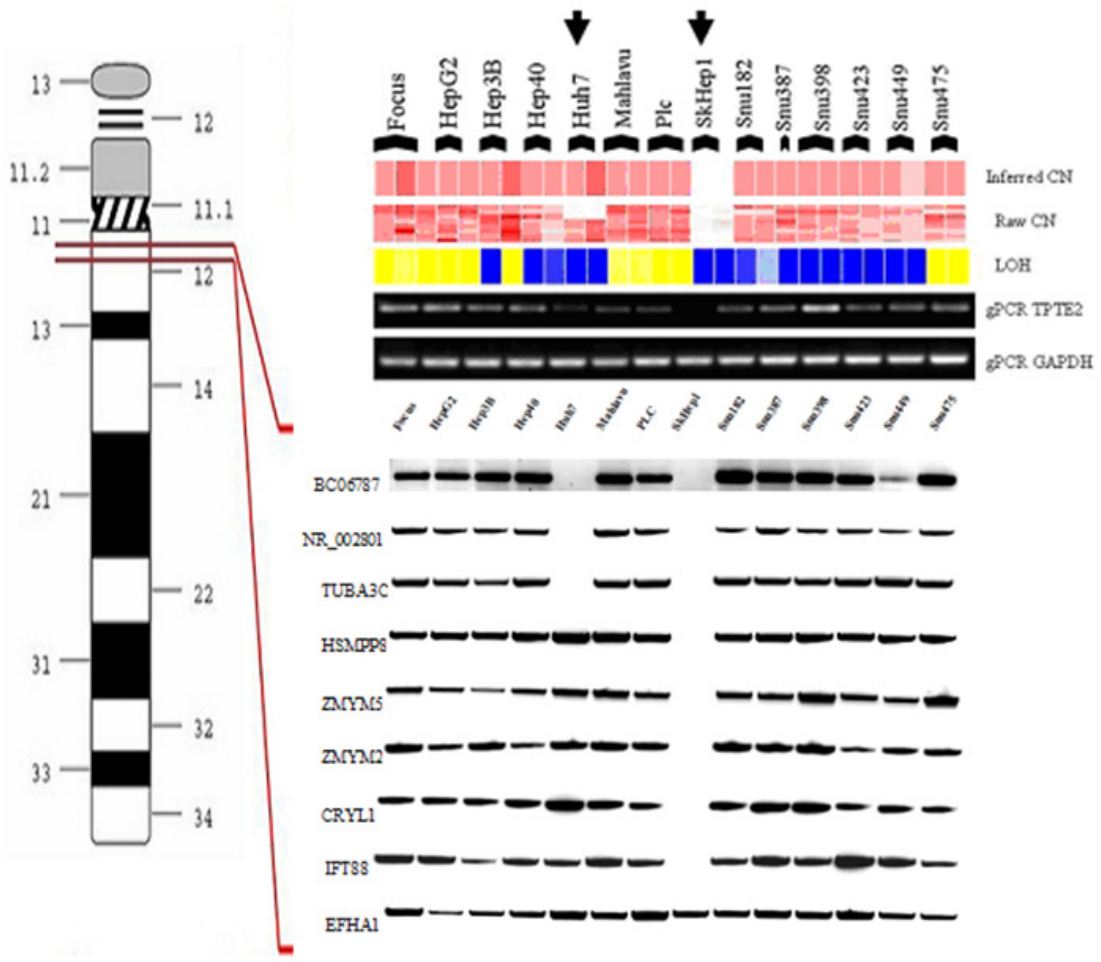

Figure 4.6.1: PCR results of the genes located in the deleted region (Figure was adapted from Kubilay Demir, M.Sc.).

The genes; *BC06787*, *NR_002801*, *TUBA3C*, *HSMPP3*, *ZMYM5*, *ZMYM2*, *CRYL1*, *IFT88*, were shown to be deleted in SkHep1. *BC06787*, *NR_002801* and *TUBA3C* genes were deleted in both Huh7 and SkHep1 cell lines (Figure 4.6.1). Preliminary bioinformatic studies on *BC06787* and *NR_002801* genes showed that these genes does not code for protein. So, it appears that *TUBA3C* is the only gene to be deleted in both Huh7 and SkHep1 cell lines.

According to SANGER CONAN (Copy Number Analysis) database, in the case of liver tissue, the deleted region is between around 13:18,310,000 and 13: 20,455,000 bp (Figure 4.6.2).

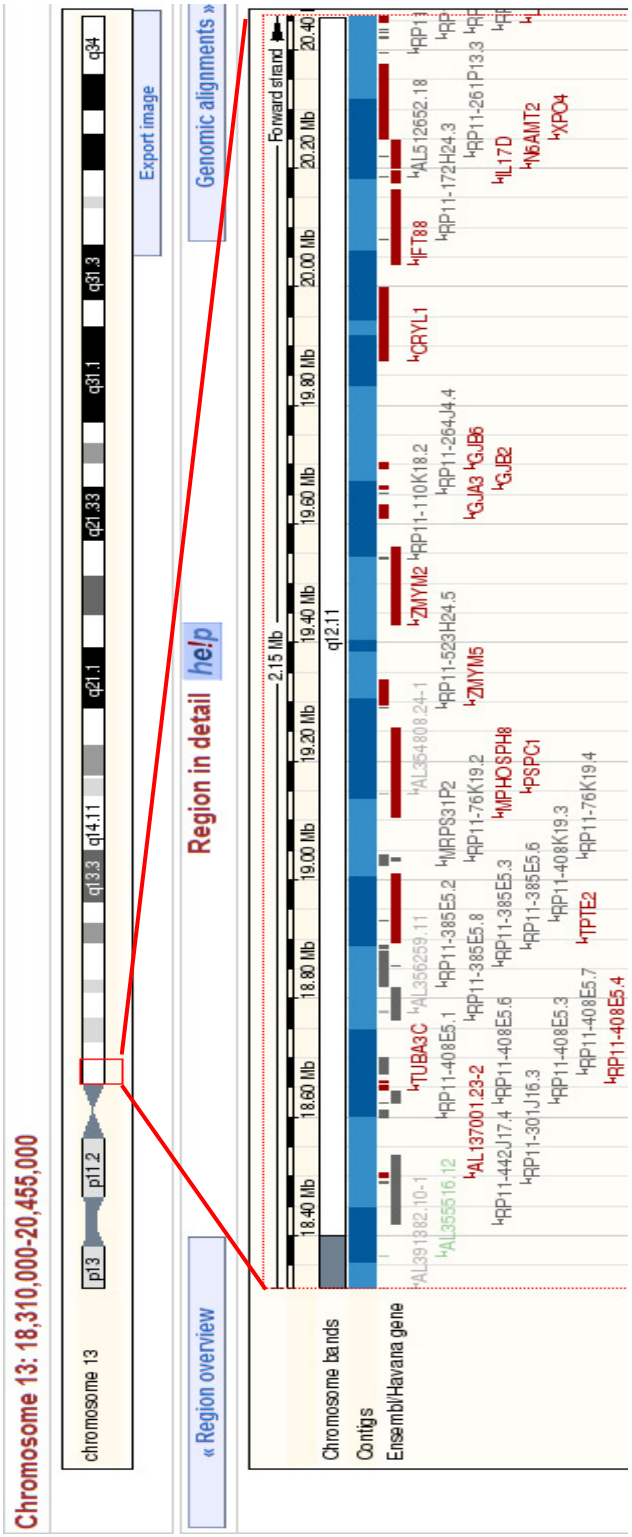

Figure 4.6.2: Deleted region in 13q12 (red rectangle) and residing genes was represented in detail (Photograph from Ensembl database, NCBI36).

4.6.2. *TUBA3C*

4.6.2.a. *TUBA3C* Expression in HCC Cell lines

To investigate *TUBA3C* mRNA expression pattern in HCC cell lines, multiplex semi-quantitative RT-PCR were preformed. Only 4 out of 14 cell lines were shown to express *TUBA3C* mRNA, being Focus is the highest. Thus, expression of *TUBA3C* is reduced 71,4 % (10/14) of HCC cell lines (Figure 4.6.3).

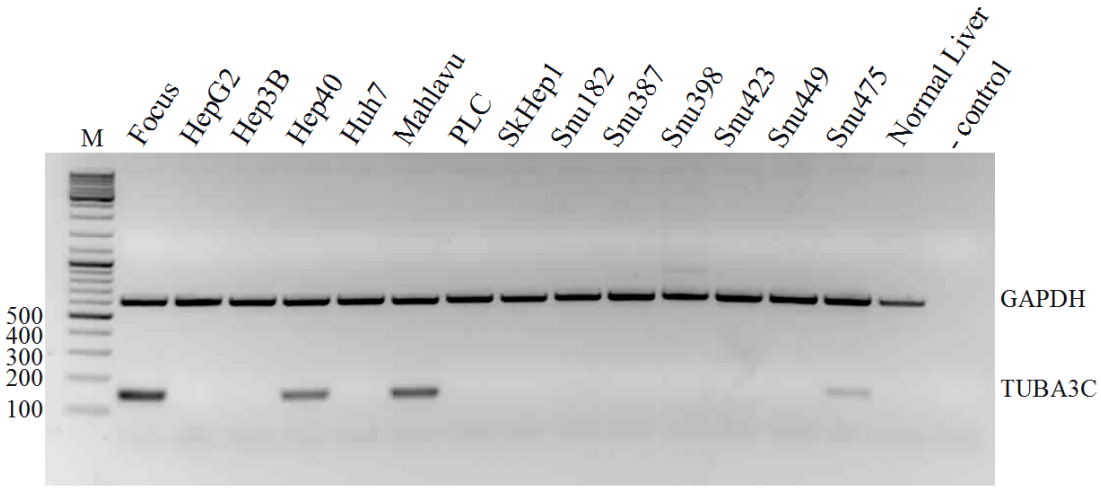

Figure 4.6.3: Multiplex semi-quantitative RT-PCR result for *TUBA3C* in 14 HCC cell lines. Tuba3CRTF/tuba3CRTR pirmer pair with an expected product size of 145 bp and GAPDH RTF/GAPDH RTR pair with an expected product size of 611 bp were used. M, marker (bp); (-), Negative control. *GAPDH* was used as an internal control.

TUBA3C mRNA expression pattern was also confirmed by Real-Time RT-PCR experiment (Figure 4.6.4).

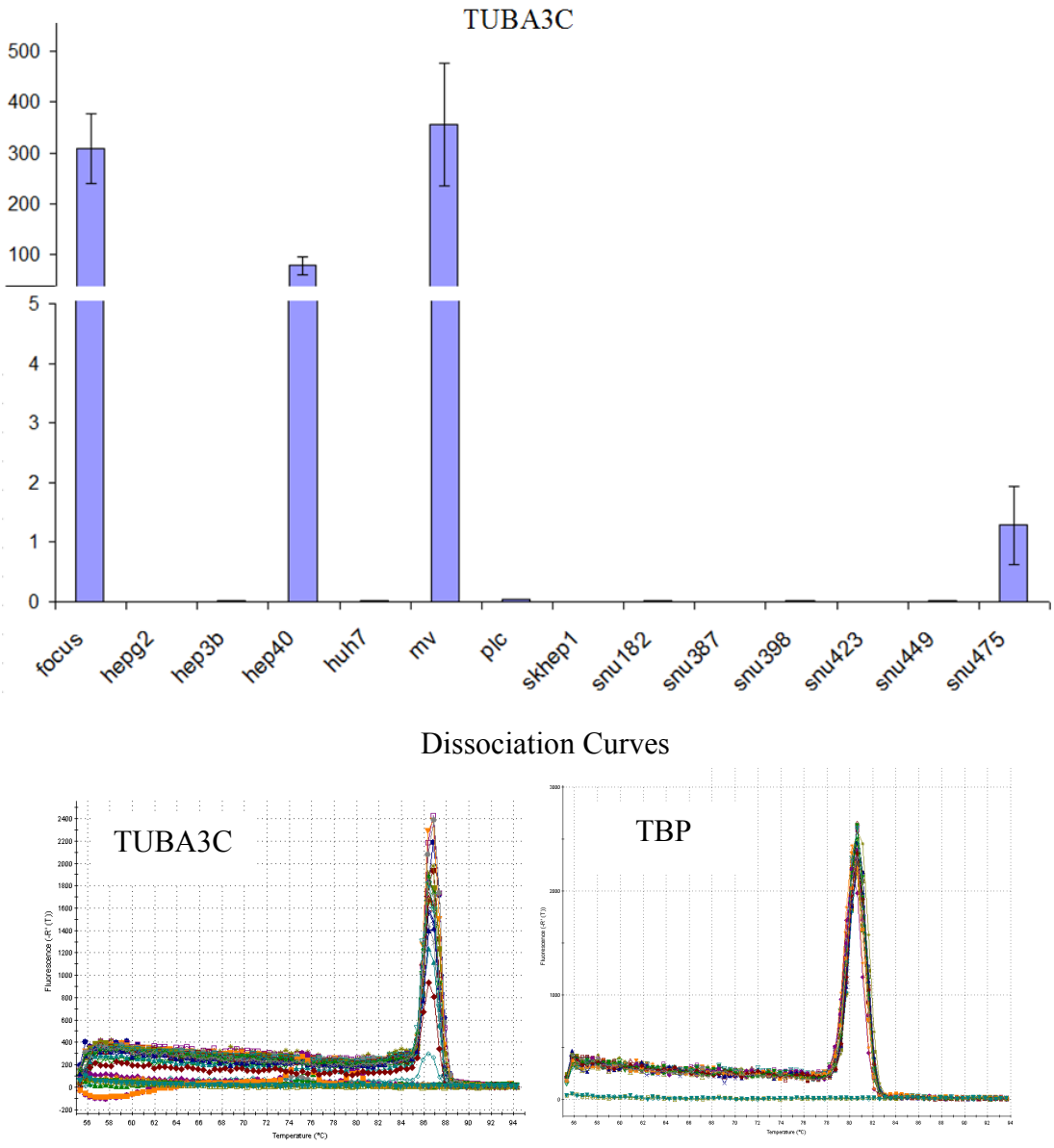

Figure 4.6.4 : Quantitative Real-Time Analysis of *TUBA3C* in HCC cell lines. Tuba3CRTF / tuba3CRTR primer pair was used. *TBP* was used as an internal control. Experiment conducted two times and standart deviations are indicated. Dissociation curves of *TUBA3C* and *TBP* primers are also presented.

4.6.2.b. *TUBA3C* Expression in Human HCCs

TUBA3C mRNA expression was analysed in clinical samples (TissueScan Liver Cancer Tissue qPCR panel I, Origene) by quantitative real time RT-PCR analysis (Figure 4.6.5). To normalize the *TUBA3C* expression, samples were also analysed for *TBP* expression (FU LY. *et al.*, 2009; Gur-Dedeoglu B. *et al.*, 2009).

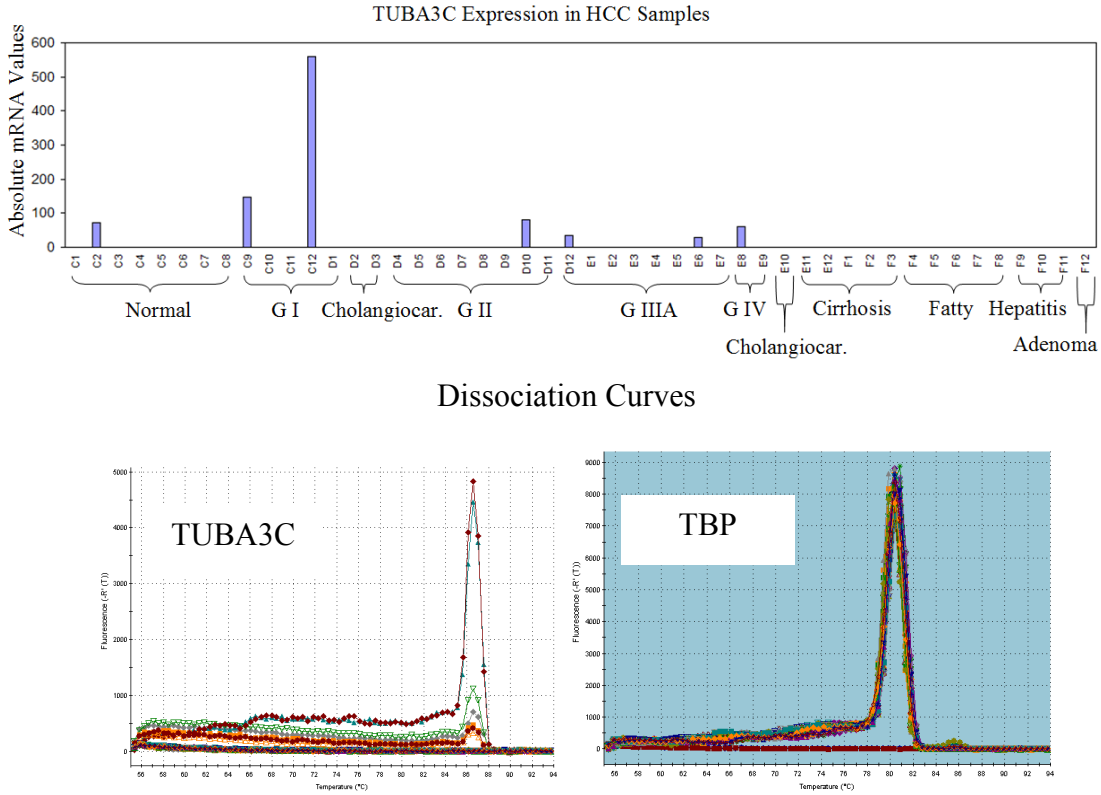

Figure 4.6.5 : *TUBA3C* mRNA expression in HCC samples. cDNAs from human liver tissues of normal and various stages of liver cancers were subjected to real-time reverse transcription–PCR for detection of *TUBA3C* mRNA expression. Tuba3CRTF / Tuba3CRTR primer pair was used. The data represent mRNA levels of *TUBA3C* mRNA normalized to *TBP*. Dissociation curves of both genes are also presented.

4.6.2.c. Genetic Analysis of *TUBA3C*

Each exon of *TUBA3C* were analysed in all HCC cell lines (except Huh7 and SkHep1) by genomic PCR followed by direct sequencing. This detailed mutation analysis was revealed one mutation (S38N) in Mahlavu cell line. Some silent mutations were also found (data not shown) (Figure 4.6.6).

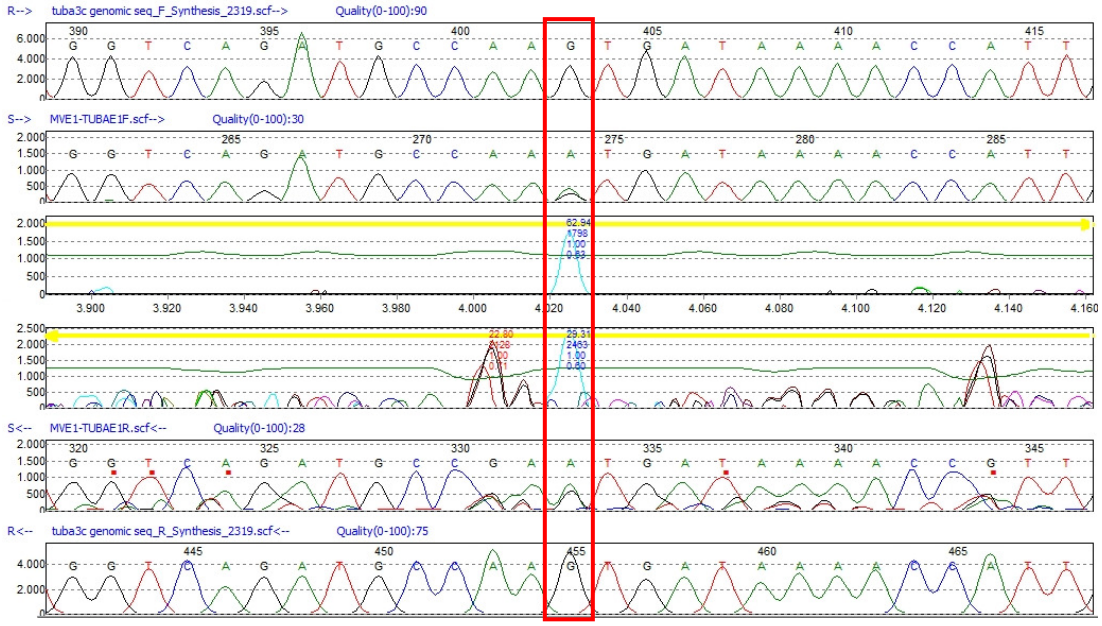

Figure 4.6.6: S38N mutation in *TUBA3C*. Figure presented here were captured from DNA Variant Analysis Software, Mutation Surveyor® Version 3.25 (www.softgenetics.com) showing an S38N mutation which result from "agt" to "aat" change. The uppermost and bottom sequence are *TUBA3C* reference sequences downloaded from GenBank database. Between are the sequences of MV cell line from both directions, forward and reverse.

4.6.2.d. Epigenetic events in the restoration of *TUBA3C* expression

Epigenetic mechanisms including promoter hypermethylation and histone modifications play an important role in the silencing of many genes, especially tumor suppessor genes (Esteller M., 2007). To better understand the possible role of epigenetic mechanisms in *TUBA3C* mRNA expression, PLC, HepG2 and Hep3B cell lines which does not have *TUBA3C* expression, was treated with DNA methyltransferase inhibitor (5-AzaC) alone and together with histone deacetylase inhibitor trichostatin A (TSA) (Figure 4.6.7, Figure 4.6.8). *TUBA3C* mRNA expression was succesfully restrored in these cell lines after the treatments. TSA alone was shown to restore the expression more than 5-AzaC alone in Hep3B cell line. Also, TSA together with 5-AzaC increase the *TUBA3C* expression more than 5-AzaC alone, in HepG2 and Hep3B cell lines. It can be suggested from these results that, not only DNA methylation but also histone modifications seems to have a role in the regulation of *TUBAC* expression. Together, these results strongly suggest a possible role of epigenetic control on the *TUBA3C* mRNA expression.

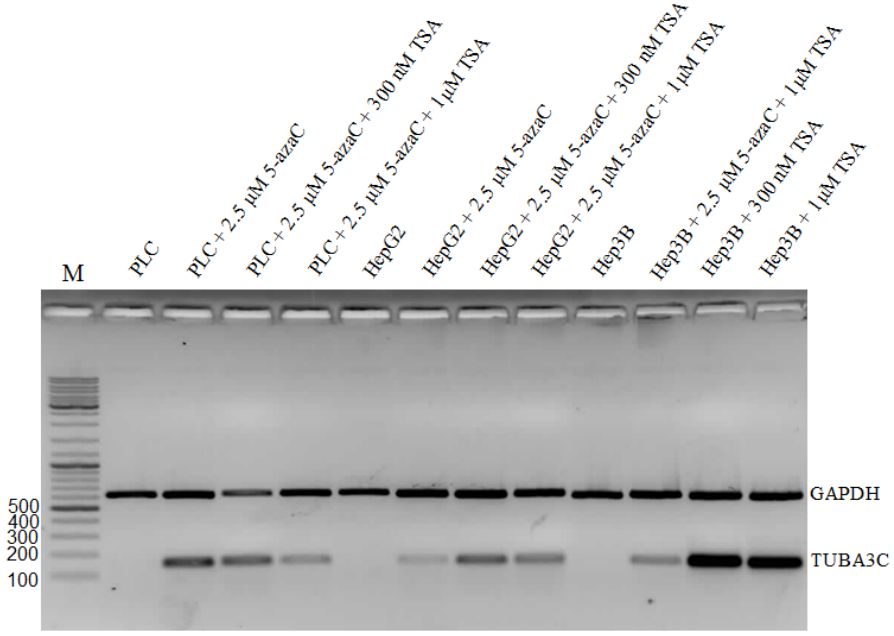

Figure 4.6.7: Restoration of *TUBA3C* mRNA expression after 5'-AzaC and TSA treatments. Tuba3CRTF/tuba3CRTR pirmer pair with an expected product size of 145 bp and GAPDH RTF/GAPDH RTR pair with an expected product size of 611 bp were used. M, marker (bp); *GAPDH* was used as an internal control.

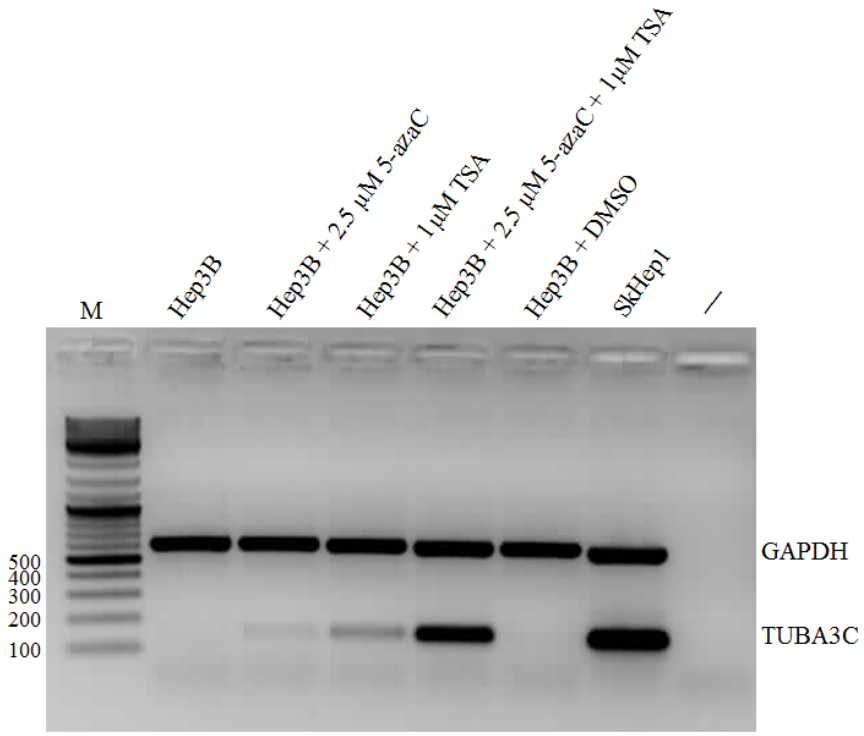

Figure 4.6.8 : Restoration of *TUBA3C* mRNA expression in Hep3B cell line after 5'-AzaC and TSA treatments. Tuba3CRTF/tuba3CRTR pirmer pair with an expected product size of 145 bp and GAPDH RTF/GAPDH RTR pair with an expected product size of 611 bp were used. *GAPDH* was used as an internal control of multiplex semi-quantitative RT-PCR M, marker (bp); (-) negative control.

4.6.3. *ZNF198* (*ZMYM2*)

ZNF198 was shown to be located in deleted region and PCR result also confirm its deletion only in SkHep1 cell line (Figure 4.6.1).

4.6.3.a. *ZNF198* Expression in HCC Cell lines

ZNF198 mRNA expression pattern in HCC cell lines was analysed by semi-quantitative RT-PCR. All HCC cell lines were shown to express *ZNF198* mRNA (Figure 4.6.9).

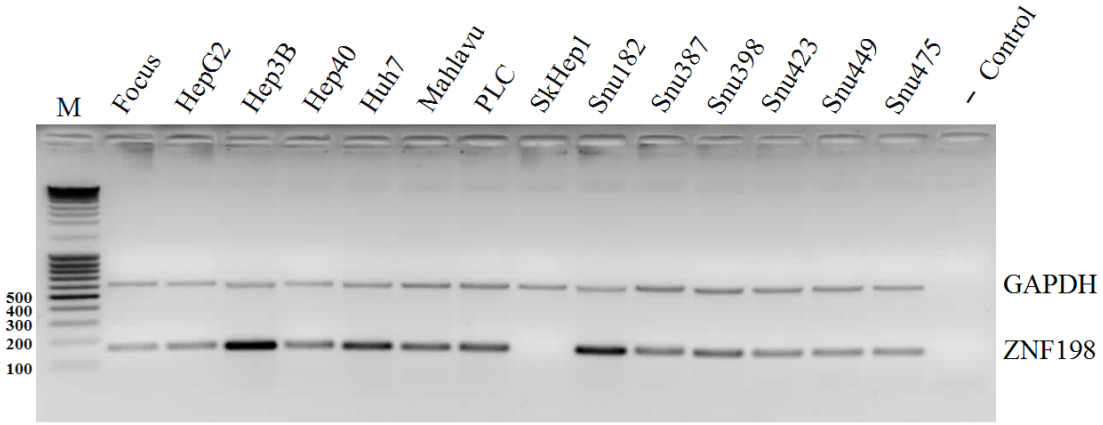

Figure 4.6.9: Multiplex semi-quantitative RT-PCR result for *ZNF198* in 14 HCC cell lines. ZNF198-Cd5F/ZNF198- Cd4R primer pair with an expected product size of 164 bp and GAPDH RTF/GAPDH RTR pair with an expected product size of 611 bp were used. *GAPDH* was used as an internal control. M, marker (bp).

4.6.3.b. Genetic Analysis of *ZNF198*

ZNF198 mutation analysis was performed by 1 genomic, 5 cDNA specific and overlapping primer pairs. They cover all coding region of the *ZNF198*. No mutation was found on 13 HCC cell lines.

4.6.4. *TPTE2*

4.6.4.a. *TPTE2* Expression in HCC Cell lines

TPTE2 mRNA expression pattern was analysed by quantitative real-time RT-PCR in 14 HCC cell lines (Figure 4.6.10). Only Hep40, Huh7 and PLC have *TPTE2* mRNA expression among other 11 HCC cell lines. SkHep1 did not express *TPTE2* mRNA as it is deleted in this cell line.

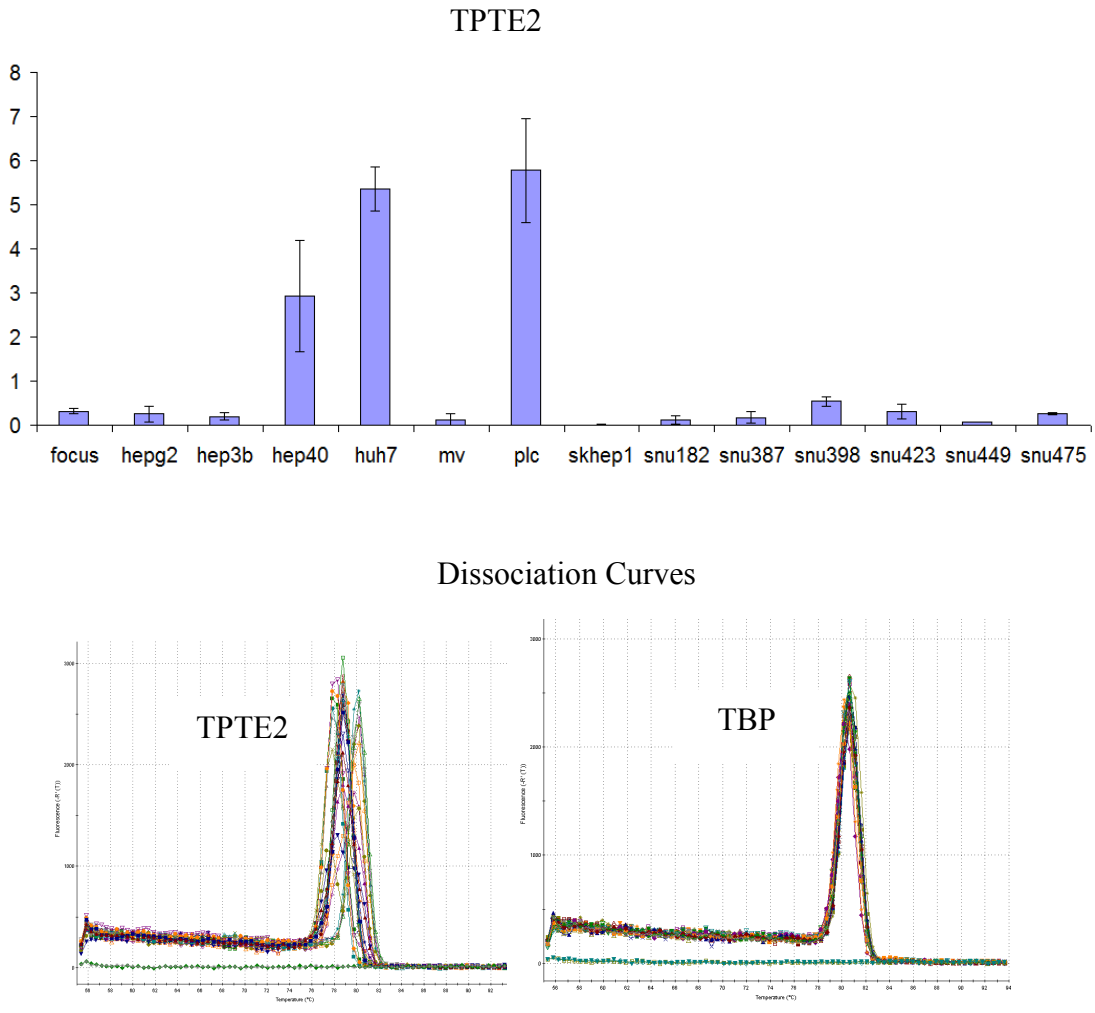

Figure 4.6.10 : Quantitative Real-Time Analysis of *TPTE2* in 14 HCC cell lines. TPTE2F/TPTE2R primer pair was used. *TBP* was used as an internal control. Experiment conducted two times and standart deviations are indicated. Dissociation curves of *TPTE2* and *TBP* primers are also presented.

4.6.4.b. *TPTE2* Expression in Human HCCs

TPTE2 mRNA expression was analysed in clinical samples (TissueScan Liver Cancer Tissue qPCR panel I, Origene) by quantitative real time RT-PCR analysis (Figure 4.6.11, 4.6.12). To normalize the *TPTE2* expression, samples were also analysed for *TBP* expression (FU LY. *et al.*, 2009; Gur-Dedeoglu B. *et al.*, 2009).

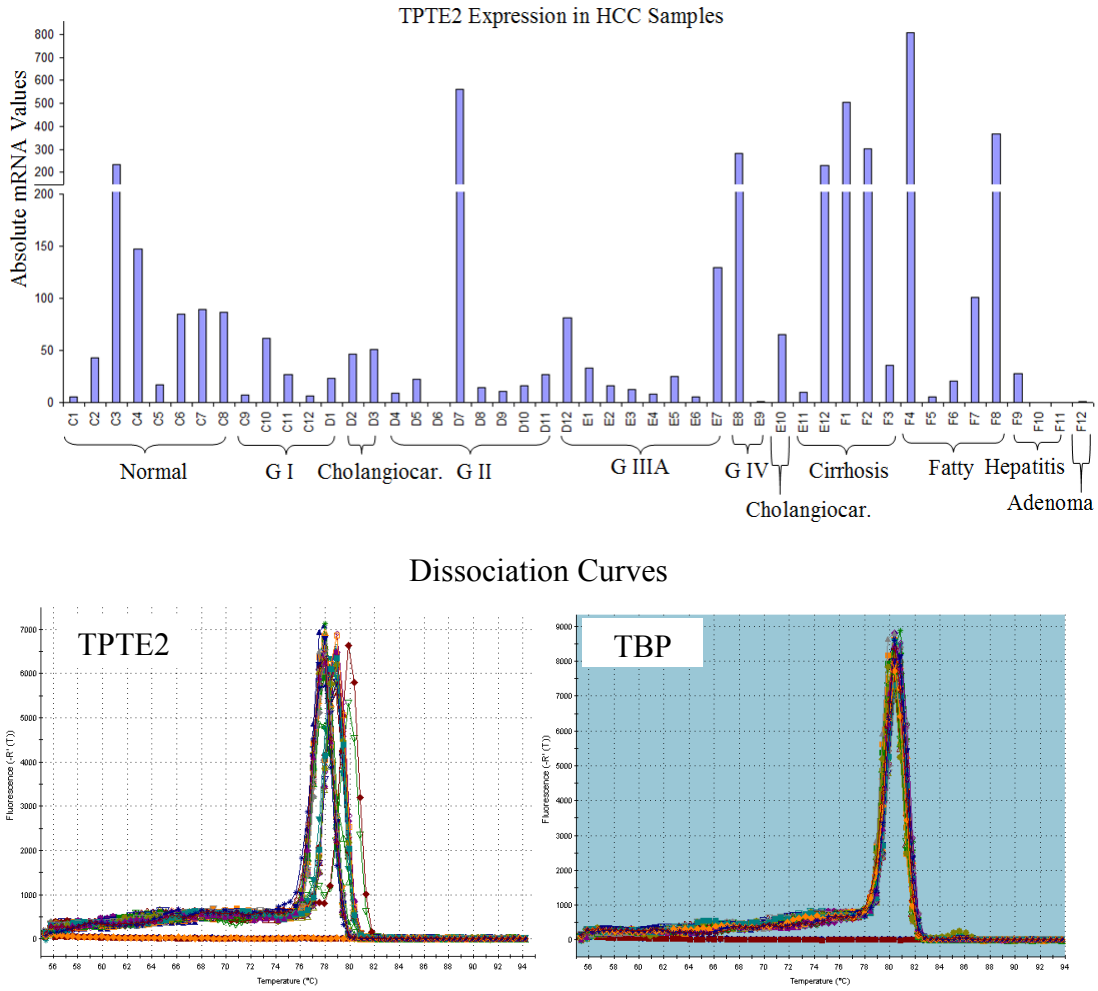

Figure 4.6.11 : *TPTE2* mRNA expression in HCC samples. cDNAs from human liver tissues of normal and various stages of liver cancers were subjected to real-time reverse transcription–PCR for detection of *TPTE2* mRNA expression. TPTE2F /TPTE2R primer pair was used. The data represent mRNA levels of *TPTE2* mRNA normalized to *TBP*. Dissociation curves of both genes are also presented.

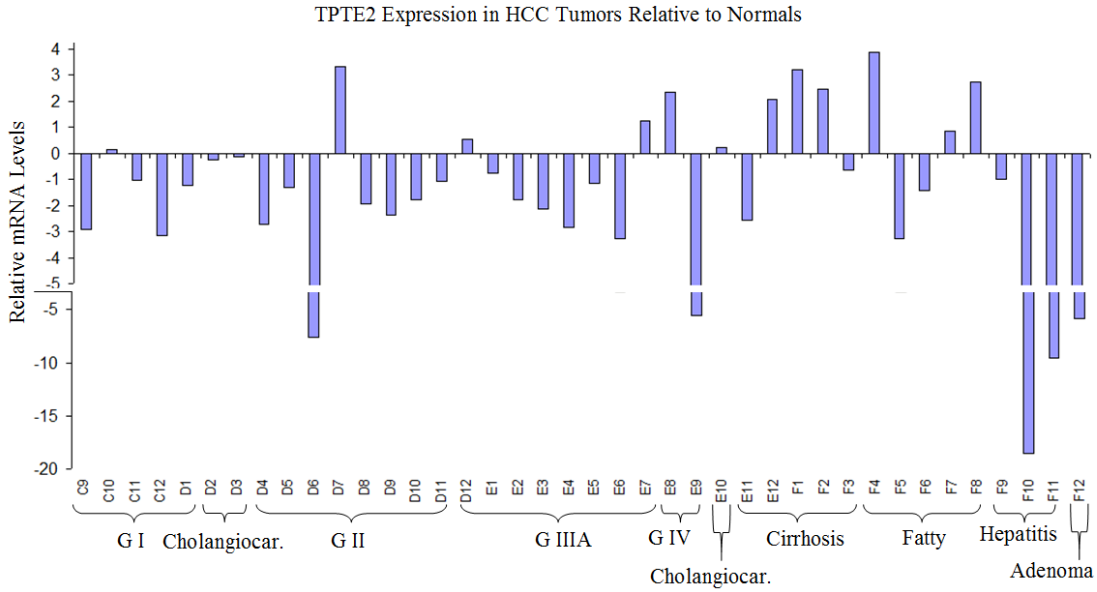

Figure 4.6.12 : *TPTE2* mRNA expression in HCC tumors relative to normals.

We observed low *TPTE2* mRNA expression in 18 of 23 (78,2%) primary HCCs (GI, GII, GIIA, GIV), compared with eight normal liver tissues from the same panel as calculated by the student's t-test (*P* value=0.057).

4.7. Chromosome 3p25.1 (*IQSEC1*)

4.7.1 *IQSEC1* Expression in HCC Cell lines

IQSEC1 mRNA expression was analysed in 14 HCC cell lines by quantitative real-time RT-PCR (Figure 4.7.1). Hep40, Huh7 and Snu398 have highest *IQSEC1* mRNA expression among other 11 HCC cell lines. HepG2, PLC, SkHep1 and Snu475 cell lines were shown to almost no *IQSEC1* expression.

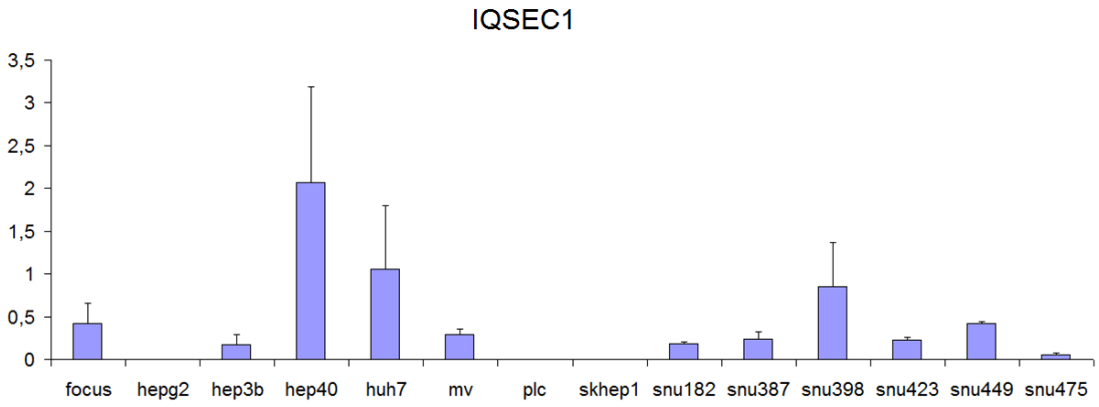

Dissociation Curves

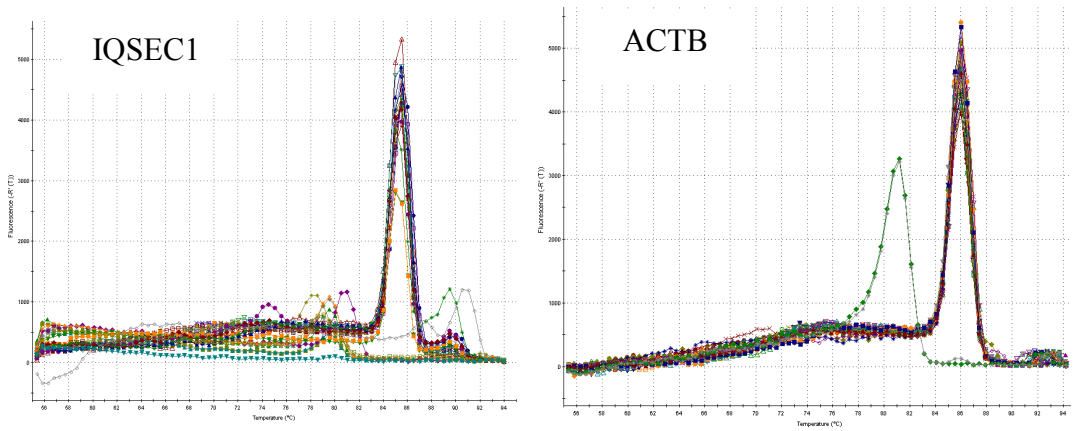

Figure 4.7.1: Quantitative Real-Time Analysis of *IQSEC1* in 14 HCC cell lines. *ACTB* was used as an internal control. Experiment conducted two times and standart deviations are indicated. Dissociation curves of *IQSEC1* and *ACTB* primers are also presented.

4.7.2 *IQSEC1* Expression in Human HCCs

IQSEC1 mRNA expression was analysed in clinical samples (TissueScan Liver Cancer Tissue qPCR panel I, Origene) by quantitative real time RT-PCR analysis (Figure 4.7.2, 4.7.3). To normalize the *IQSEC1* expression, samples were also analysed for *TBP* expression (FU LY. *et al.*, 2009; Gur-Dedeoglu B. *et al.*, 2009).

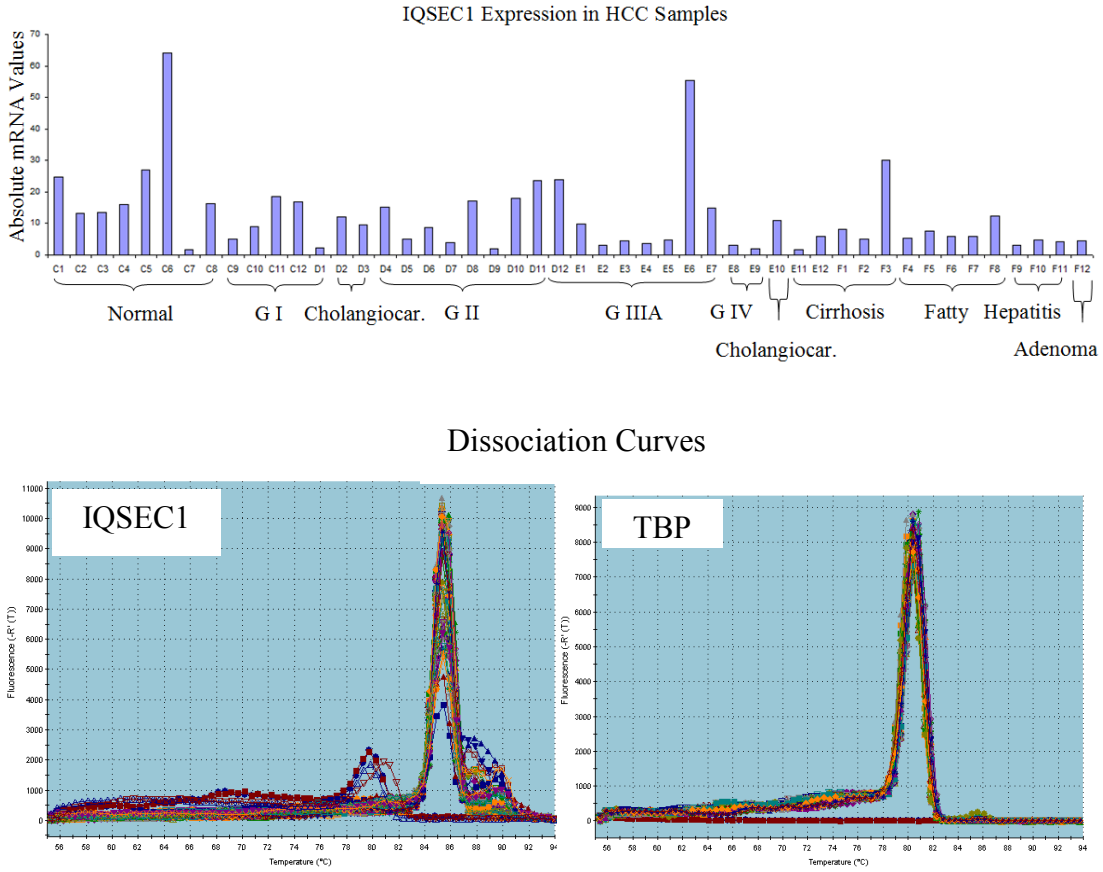

Figure 4.7.2: *IQSEC1* mRNA expression in HCC samples. cDNAs from human liver tissues of normal and various stages of liver cancers were subjected to real-time reverse transcription–PCR for detection of *IQSEC1* mRNA expression. The data represent mRNA levels of IQSEC1 mRNA normalized to *TBP*. Dissociation curves of both genes are also presented.

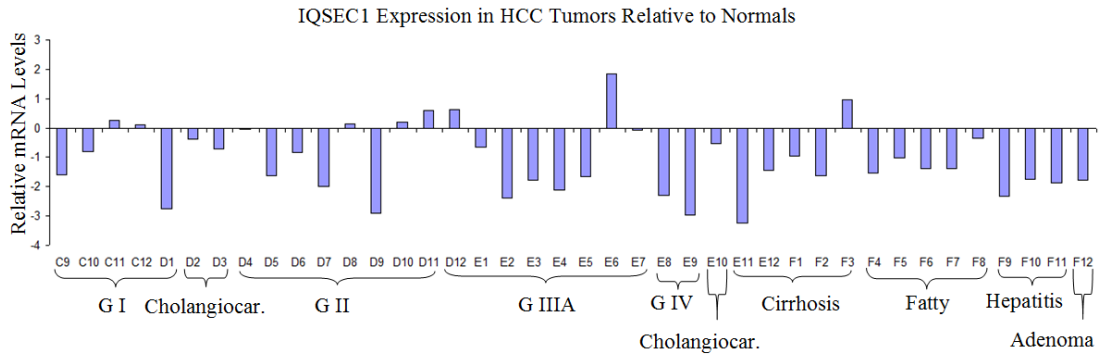

Figure 4.7.3 : *IQSEC1* mRNA expression in HCC tumors relative to normals.

We observed low *IQSEC1* mRNA expression in 16 of 23 (69,5%) primary HCCs (GI, GII, GIIA, GIV), compared with eight normal liver tissues from the same panel.

4.8. Chromosome 14q13.3 (*MIPOL1*)

4.8.1 *MIPOL1* Expression in HCC Cell lines

MIPOL1 mRNA expression was analysed in 14 HCC cell lines by quantitative real-time RT-PCR (Figure 4.8.1). Snu398 and Snu449 cell lines have highest *MIPOL1* mRNA expression among other 12 HCC cell lines.

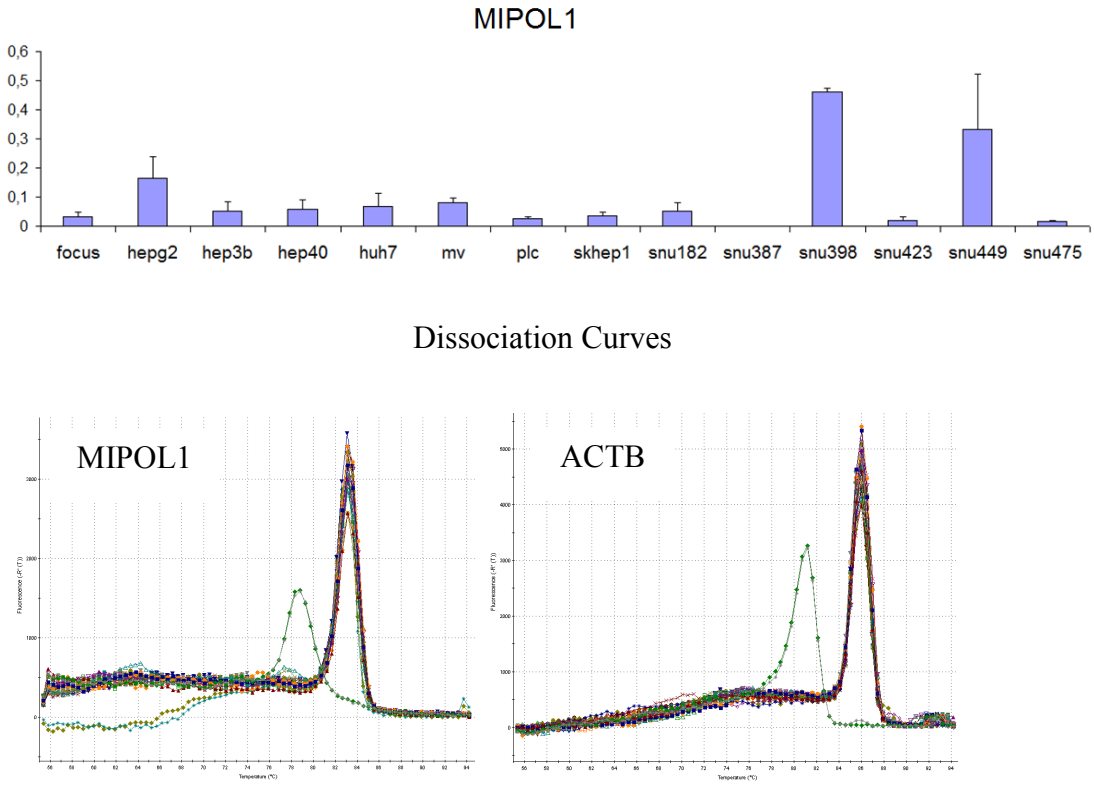

Figure 4.8.1: Quantitative Real-Time Analysis of *MIPOL1* in 14 HCC cell lines. *ACTB* was used as an internal control. Experiment conducted two times and standart deviations are indicated. Dissociation curves of *MIPOL1* and *ACTB* primers are also presented.

MIPOL1 expression was also checked at the protein level (Figure 4.8.2). HepG2, Snu475, Snu387 and Hep3B was in concordance with the real-time results. PLC was previously shown to be reside in the homozygous deletion region (Figure 1.9.1), but western results showed MIPOL1 protein in PLC cell line. In silico analysis on SANGER CONAN database revealed that this deletion was between 36,887,100-37,030,900 bp (143.800 bp) and result in ~67 aminoacid loss in protein (Figure 4.8.3).

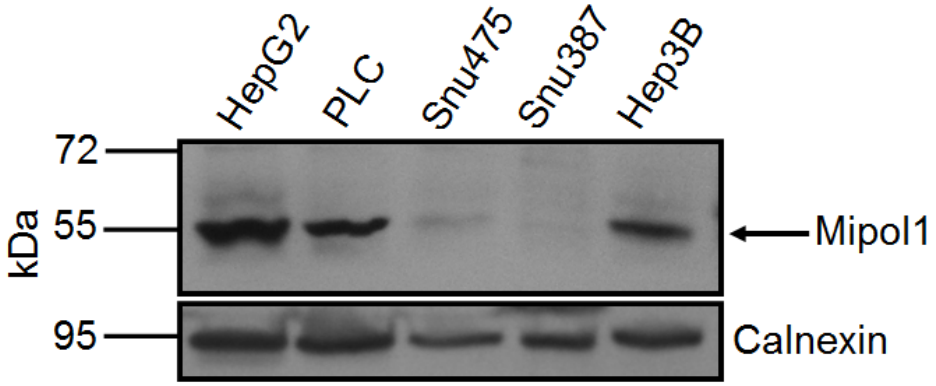

Figure 4.8.2 : Western blot analysis of MIPOL1 in 5 HCC cell lines. MIPOL1 was expected to give band at 50 kDa. Calnexin (90 kDa) was used as a loading control. 35 µg protein were loaded each well. PageRuler™ Prestained Protein Ladder (Fermentas, USA) was used as a marker.

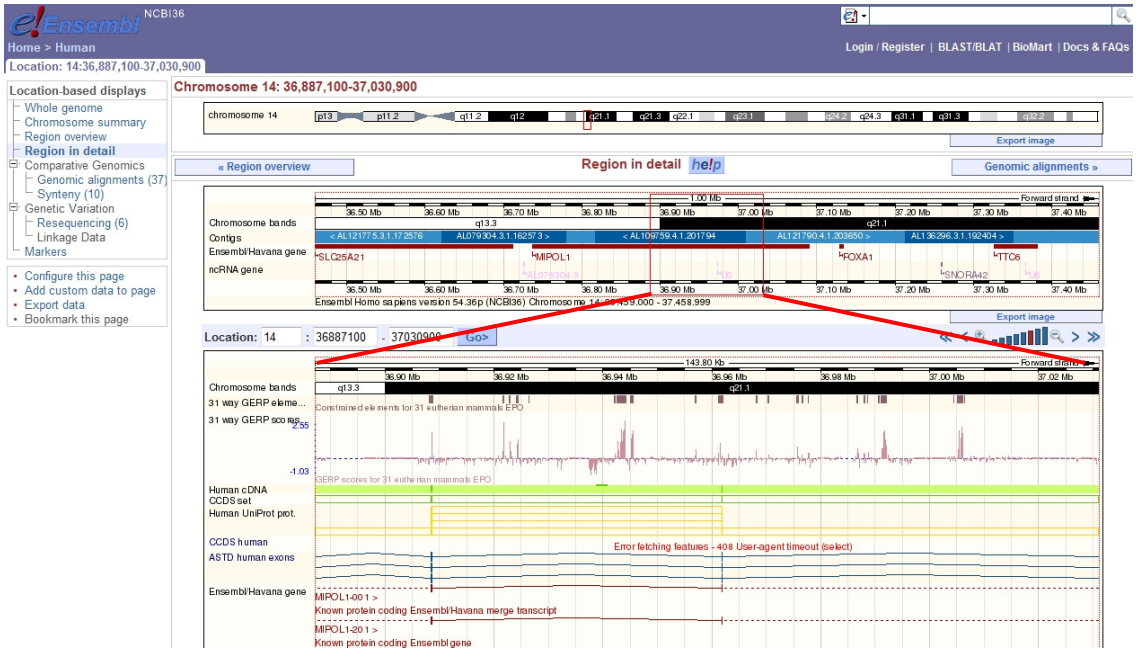

Figure 4.8.3: Deleted region (red rectangle) in *MIPOL1* gene. (ENSEMBL Genome Browser, NCBI36 database).

4.8.2 *MIPOL1* Expression in Human HCCs

MIPOL1 mRNA expression was analysed in clinical samples (TissueScan Liver Cancer Tissue qPCR panel I, Origene) by quantitative real time RT-PCR analysis (Figure 4.8.4, 4.8.5). To normalize the *MIPOL1* expression, samples were also analysed for *TBP* expression (FU LY. *et al.*, 2009; Gur-Dedeoglu B. *et al.*, 2009).

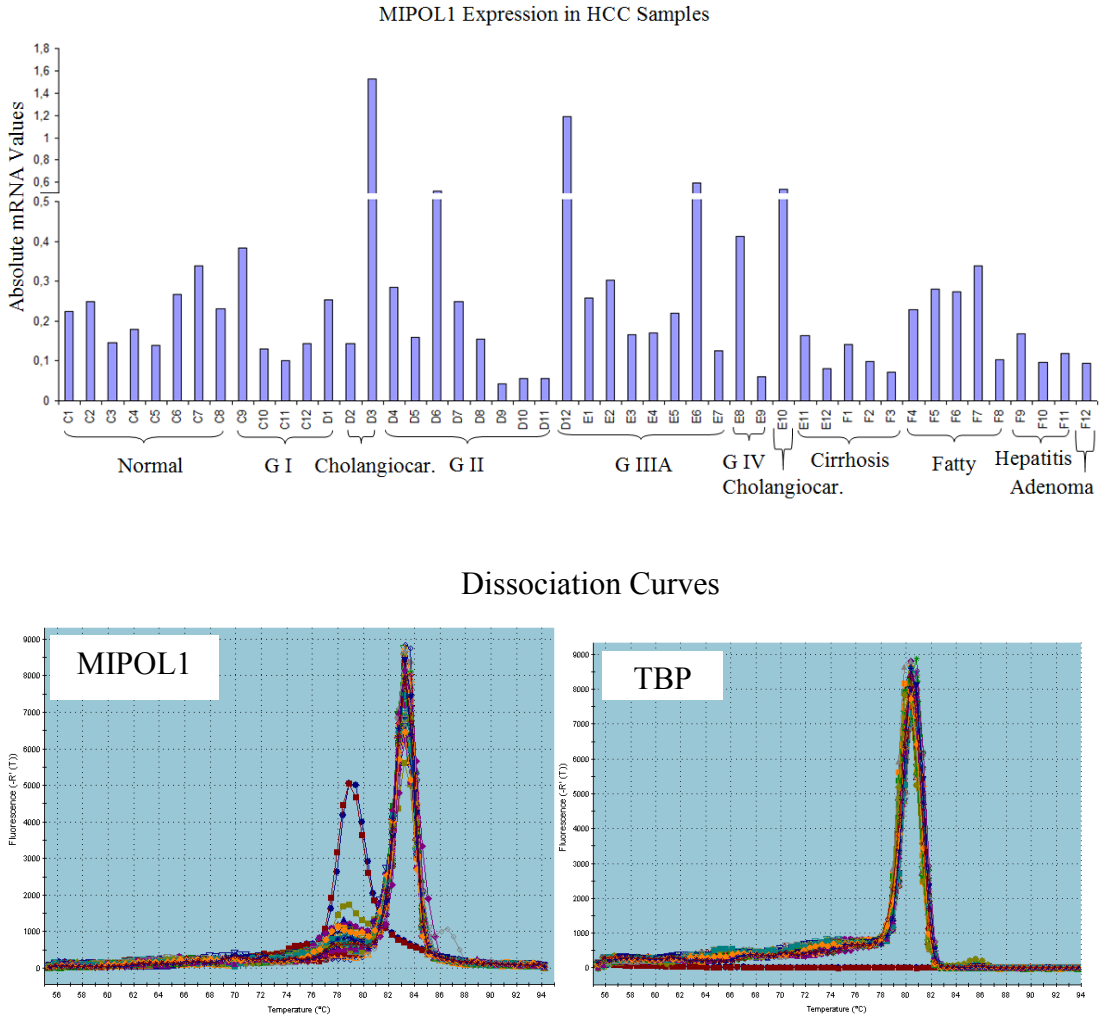

Figure 4.8.4: *MIPOL1* mRNA expression in HCC samples. cDNAs from human liver tissues of normal and various stages of liver cancers were subjected to real-time reverse transcription–PCR for detection of *MIPOL1* mRNA expression. The data represent mRNA levels of *MIPOL1* mRNA normalized to TBP. Dissociationcurves of both genes are also presented.

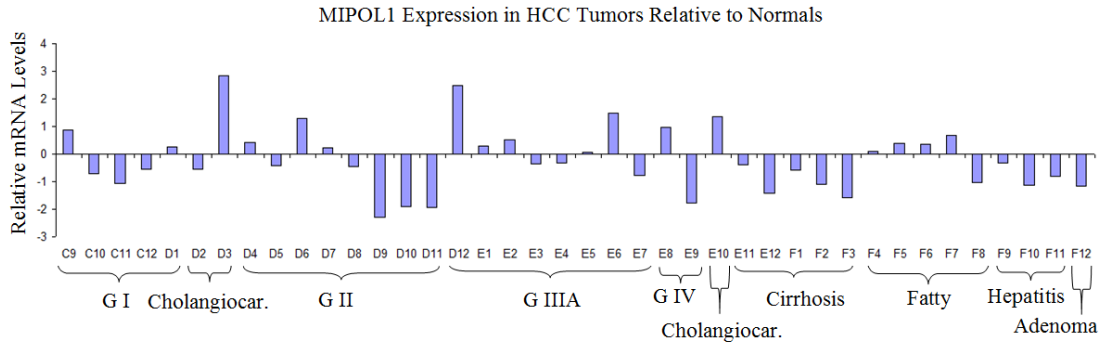

Figure 4.8.5 : *MIPOL1* mRNA expression in HCC tumors relative to normals.

We observed low *MIPOL1* mRNA expression in 12 of 23 (52,17%) and high *MIPOL1* mRNA expression in 11 of 23 (47,8%) primary HCCs (GI, GII, GIIA, GIV), compared with eight normal liver tissues from the same panel.

4.9. Chromosome 10q24 (*CHUK*)

4.9.1 *CHUK* Expression in HCC Cell lines

CHUK mRNA expression was analysed in 14 HCC cell lines by quantitative real-time RT-PCR (Figure 4.9.1). Snu398, PLC, MV, HepG2, Hep40 and Huh7 cell lines have highest *CHUK* mRNA expression among other HCC cell lines. Hep3B, SkHep1, Snu182, Snu387 and Snu475 cell lines have very low amount of *CHUK* mRNA.

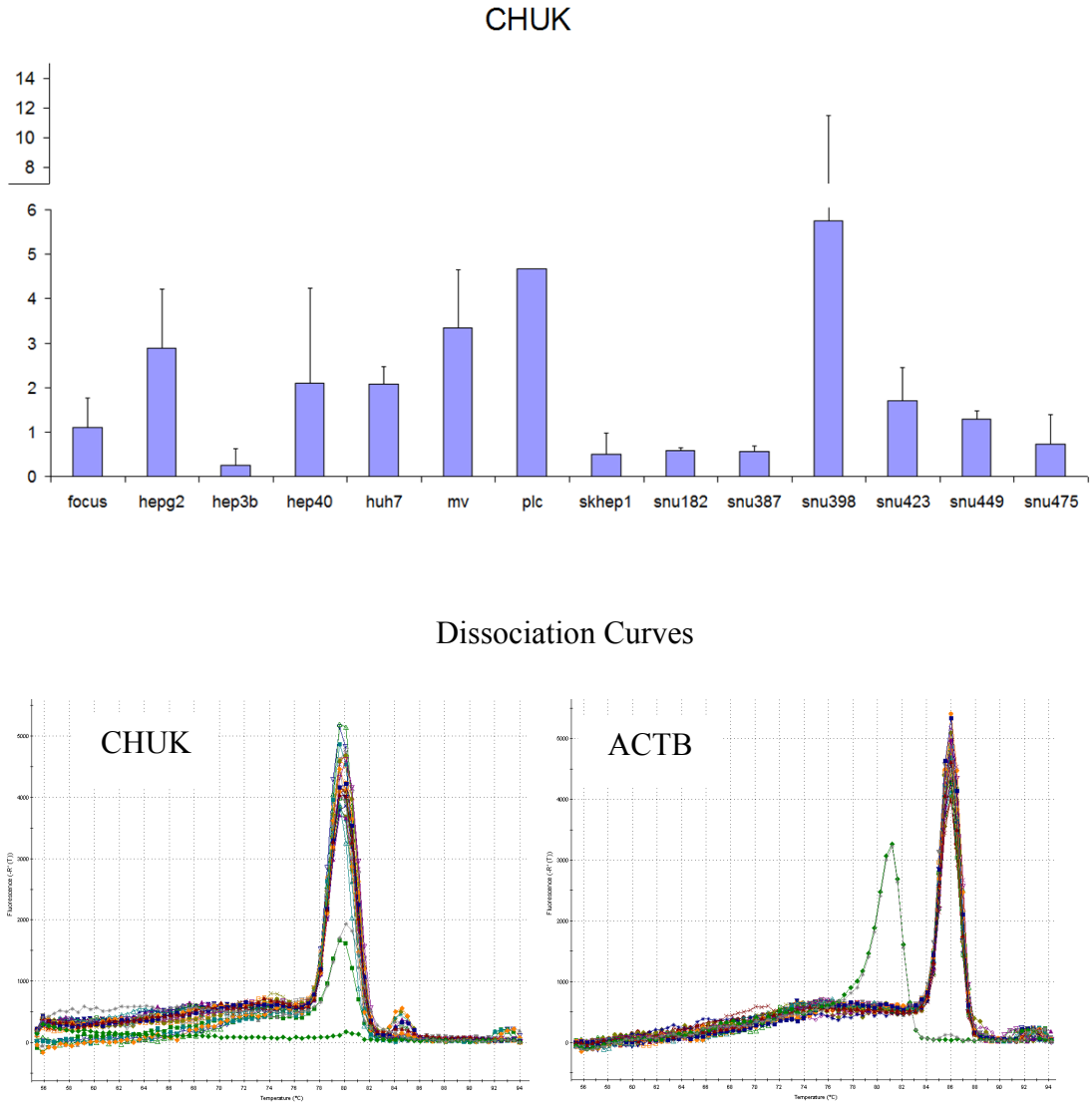

Figure 4.9.1: Quantitative Real-Time Analysis of *CHUK* in 14 HCC cell lines. *ACTB* was used as an internal control. Experiment conducted two times and standart deviations are indicated. Dissociation curves of *CHUK* and ACTB primers are also presented.

4.9.2 *CHUK* Expression in Human HCCs

CHUK mRNA expression was analysed in clinical samples (TissueScan Liver Cancer Tissue qPCR panel I, Origene) by quantitative real time RT-PCR analysis (Figure 4.9.2, 4.9.3). To normalize the *CHUK* expression, samples were also analysed for *TBP* expression (FU LY. *et al.*, 2009; Gur-Dedeoglu B. *et al.*, 2009).

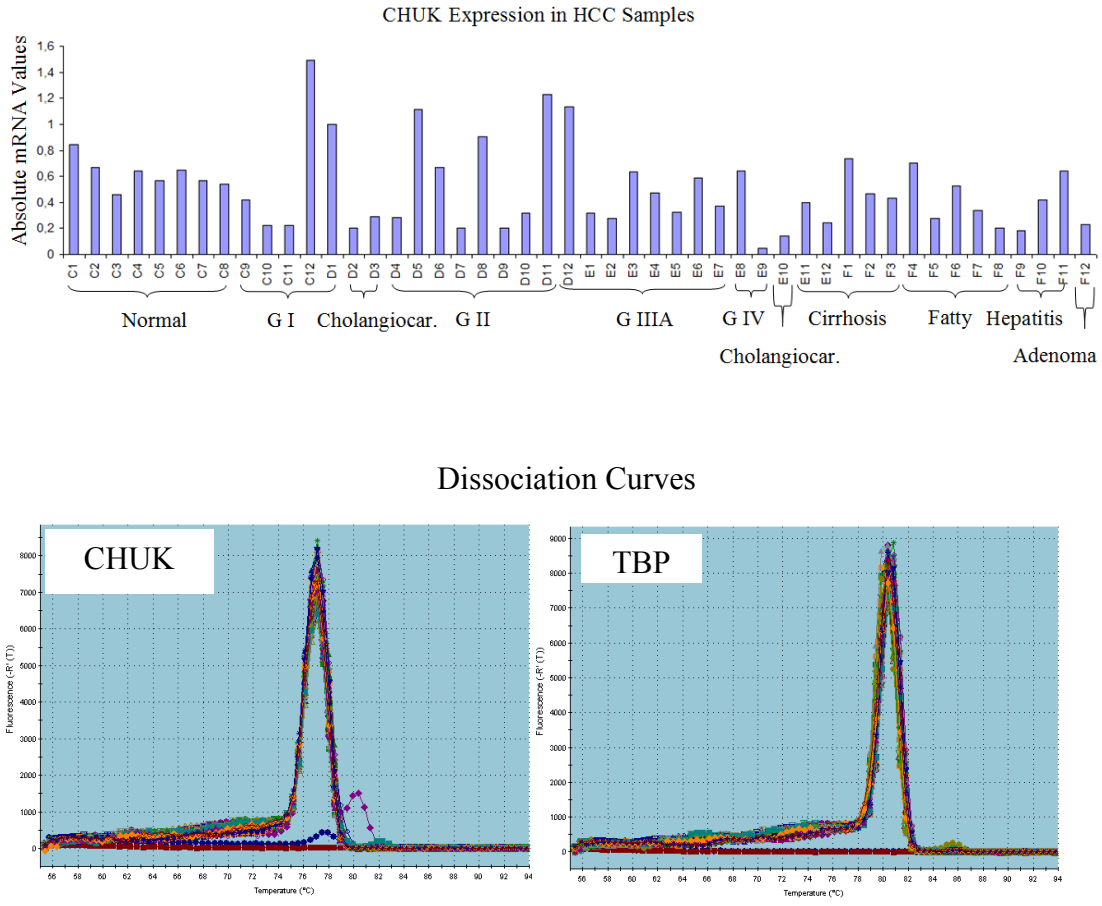

Figure 4.9.2: *CHUK* mRNA expression in HCC samples. cDNAs from human liver tissues of normal and various stages of liver cancers were subjected to real-time reverse transcription–PCR for detection of *CHUK* mRNA expression. The data represent mRNA levels of *CHUK* mRNA normalized to *TBP*. Dissociation curves of both genes are also presented.

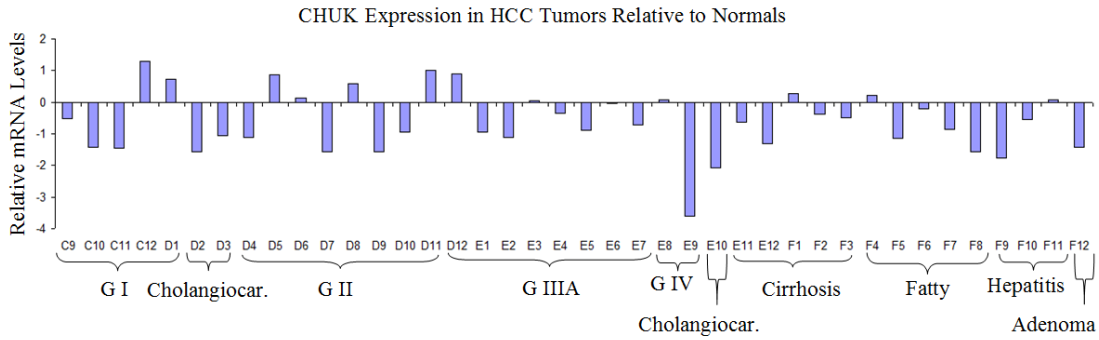

Figure 4.9.3 : *CHUK* mRNA expression in HCC tumors relative to normals.

We observed low *CHUK* mRNA expression in 14 of 23 (60,86%) primary HCCs (GI, GII, GIIA, GIV), compared with eight normal liver tissues from the same panel.

4.10. Chromosome 1q21 (*MCL1*)

4.10.1 *MCL1* Expression in HCC Cell lines

MCL1 mRNA expression was analysed in 14 HCC cell lines by quantitative real-time RT-PCR (Figure 4.10.1). Snu182 and Hep3B cell lines have highest *MCL1* mRNA expression among other HCC cell lines. Hep40, Mahlavu, SkHep1, Snu398 and Snu423 cell lines have reduced level of *MCL1* mRNA.

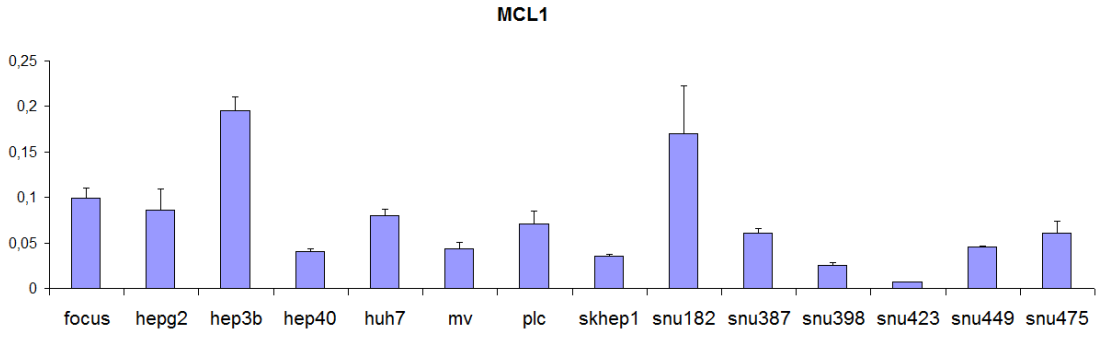

Figure 4.10.1: Quantitative Real-Time Analysis of *MCL1* mRNA expression in 14 HCC cell lines. *GAPDH* was used as an internal control. Experiment conducted two times and standart deviations are indicated.

MCL1 expression at the protein level was also checked by western blot analysis (Figure 4.10.2). Western blot analysis was confirmed real-time analysis result.

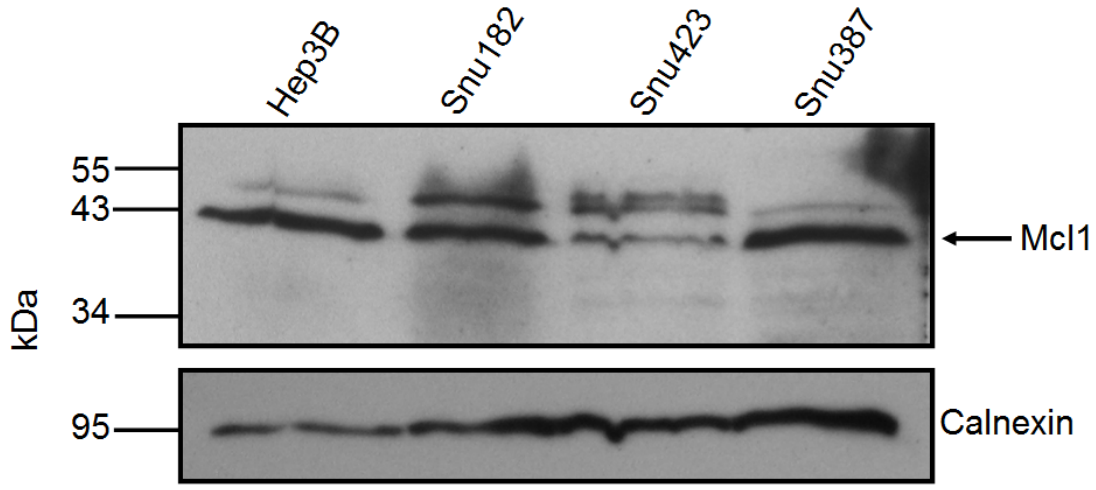

Figure 4.10.2 : Western blot analysis of MCL1 in 4 HCC cell lines. MCL1 was expected to give band at 37 kDa. Calnexin (90 kDa) was used as a loading control. 35 µg protein were loaded each well. PageRuler™ Prestained Protein Ladder (Fermentas, USA) was used as a marker.

4.10.2 *MCL1* Expression in Human HCCs

MCL1 mRNA expression was analysed in clinical samples (TissueScan Liver Cancer Tissue qPCR panel I, Origene) by quantitative real time RT-PCR analysis (Figure 4.10.3, 4.10.4). To normalize the *MCL1* expression, samples were also analysed for *TBP* expression (FU LY. *et al.*, 2009; Gur-Dedeoglu B. *et al.*, 2009).

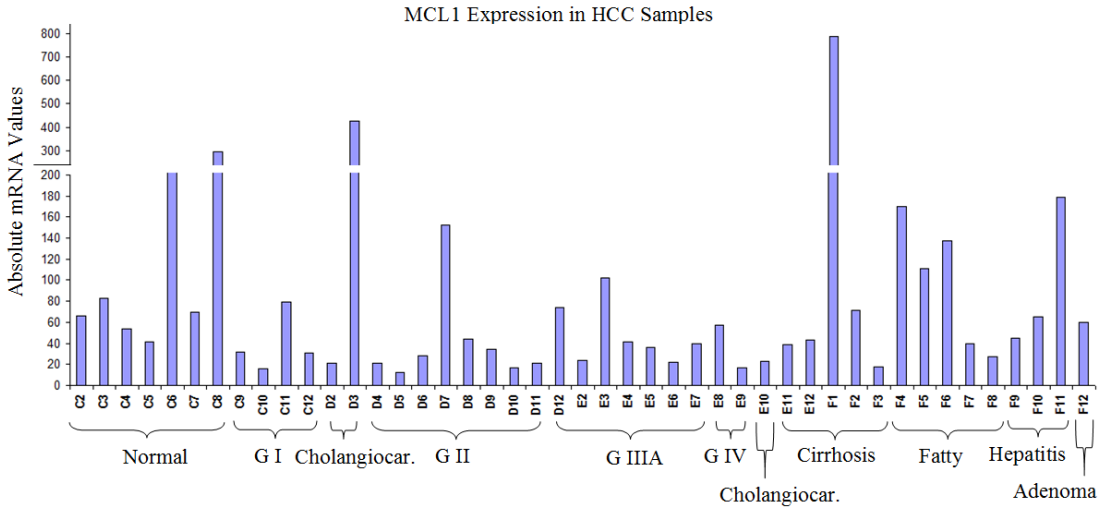

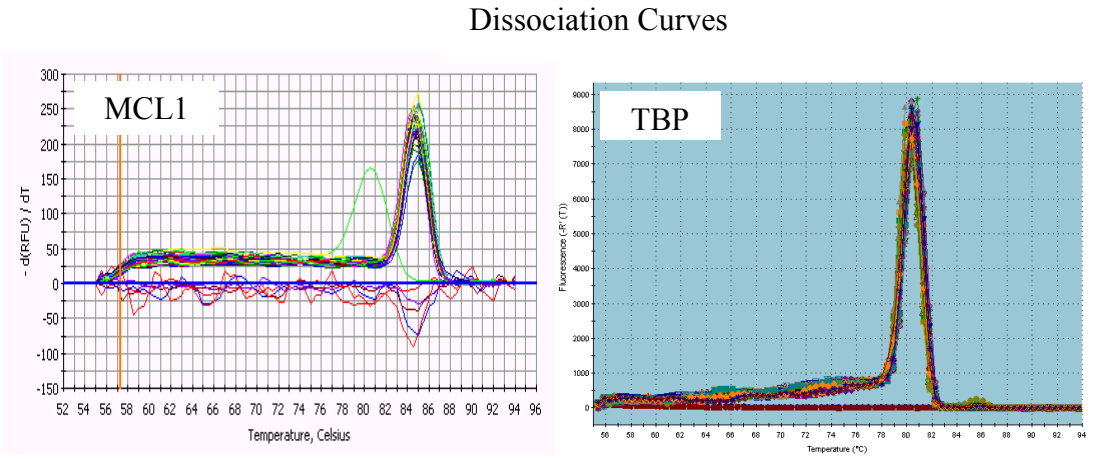

Figure 4.10.3: *MCL1* mRNA expression in HCC samples. cDNAs from human liver tissues of normal and various stages of liver cancers were subjected to real-time reverse transcription–PCR for detection of *MCL1* mRNA expression. The data represent mRNA levels of *MCL1* mRNA normalized to *TBP*. Dissociation curves of both genes are also presented.

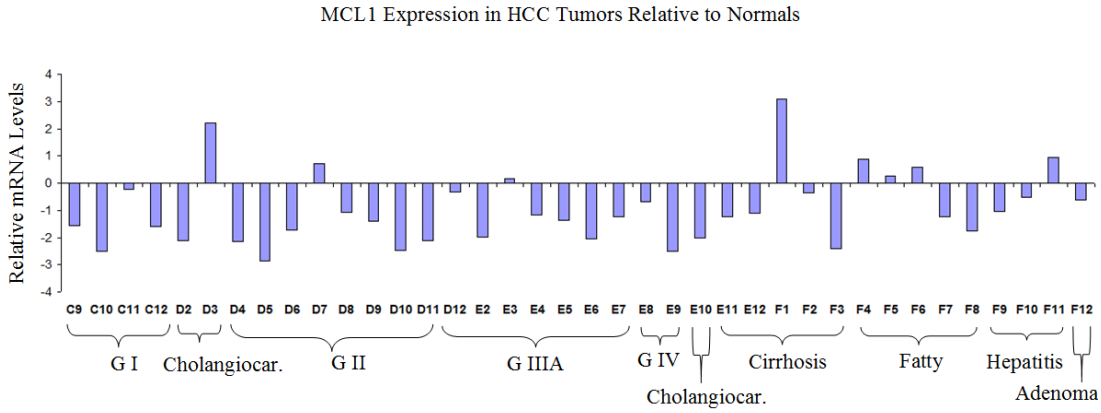

Figure 4.10.4 : *MCL1* mRNA expression in HCC tumors relative to normals.

We observed significantly low *MCL1* mRNA expression in 21 of 23 (91,30%) primary HCCs (GI, GII, GIIA, GIV), compared with eight normal liver tissues from the same panel as calculated by the student's t-test (*P* value=0.011).

4.11. Chromosome 7q21 (*MAGI-2*)

4.11.1 *MAGI-2* Expression in HCC Cell lines

MAGI-2 mRNA expression was analysed in 14 HCC cell lines by multiplex semi-quantitative RT-PCR (Figure 4.11.1) and quantitative real-time RT-PCR (Figure 4.11.2). Focus, HepG2, Hep3B, PLC, Snu387 and Snu475 cell lines have low level of *MAGI-2* mRNA in both RT experiments.

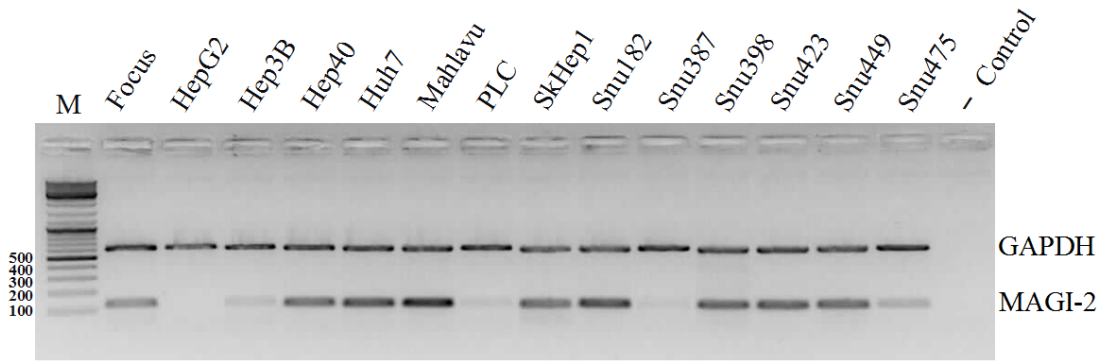

Figure 4.11.1: Multiplex semi-quantitative RT-PCR result for *MAGI-2* in 14 HCC cell lines. MAGI-2 F/R primer pair with an expected product size of 129 bp and GAPDH RTF/GAPDH RTR pair with an expected product size of 611 bp were used. *GAPDH* was used as an internal control. M, Marker; (-), Negative control.

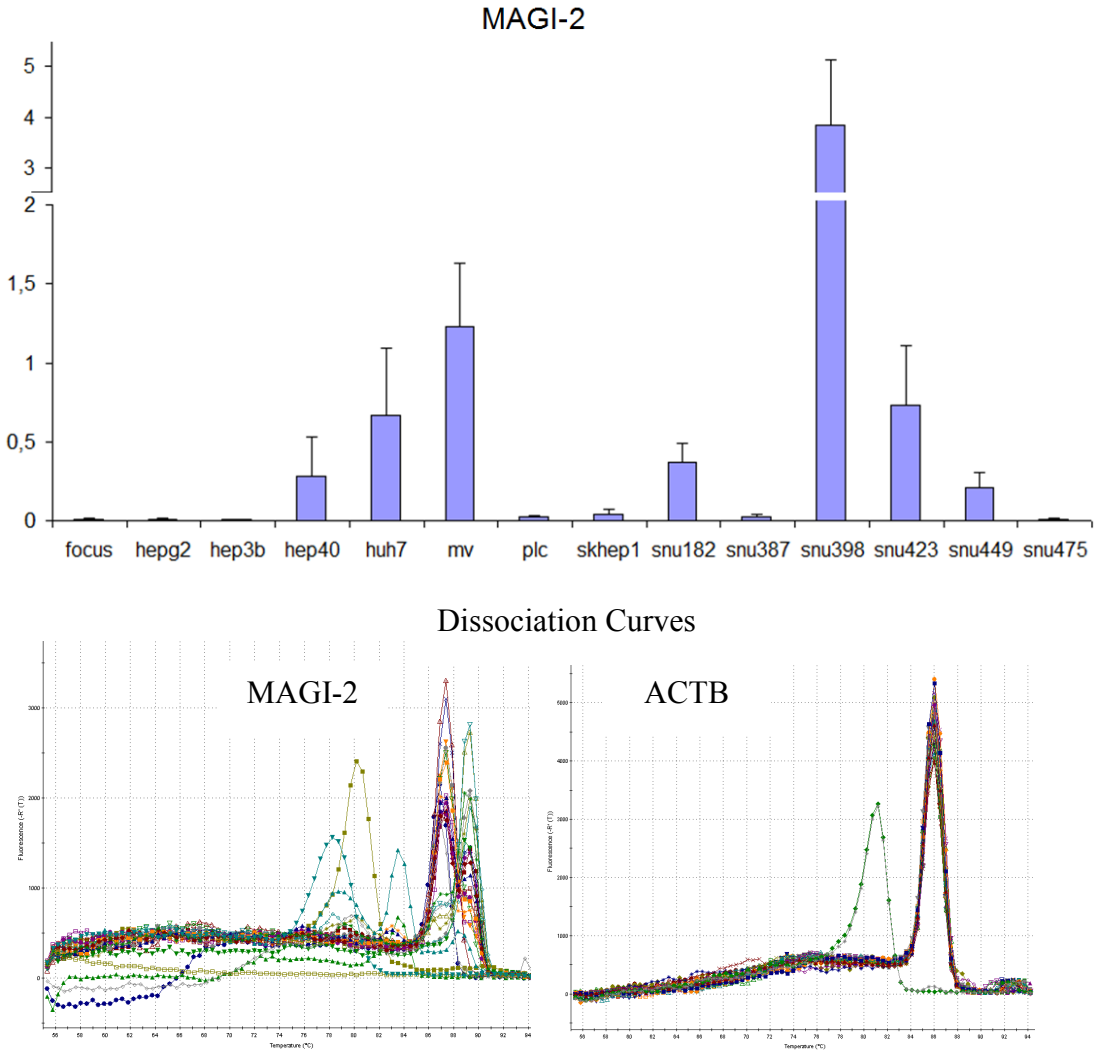

Figure 4.11.2: Quantitative Real-Time Analysis of *MAGI-2* mRNA expression in 14 HCC cell lines. *ACTB* was used as an internal control. Experiment conducted two times and standart deviations are indicated. Dissociation curves of *MAGI-2* and *ACTB* primers are also presented.

4.11.2 *MAGI-2* Expression in Human HCCs

MAGI-2 mRNA expression was analysed in clinical samples (TissueScan Liver Cancer Tissue qPCR panel I, Origene) by quantitative real time RT-PCR analysis (Figure 4.11.3, 4.11.4). To normalize the *MAGI-2* expression, samples were also analysed for *TBP* expression (FU LY. *et al.*, 2009; Gur-Dedeoglu B. *et al.*, 2009).

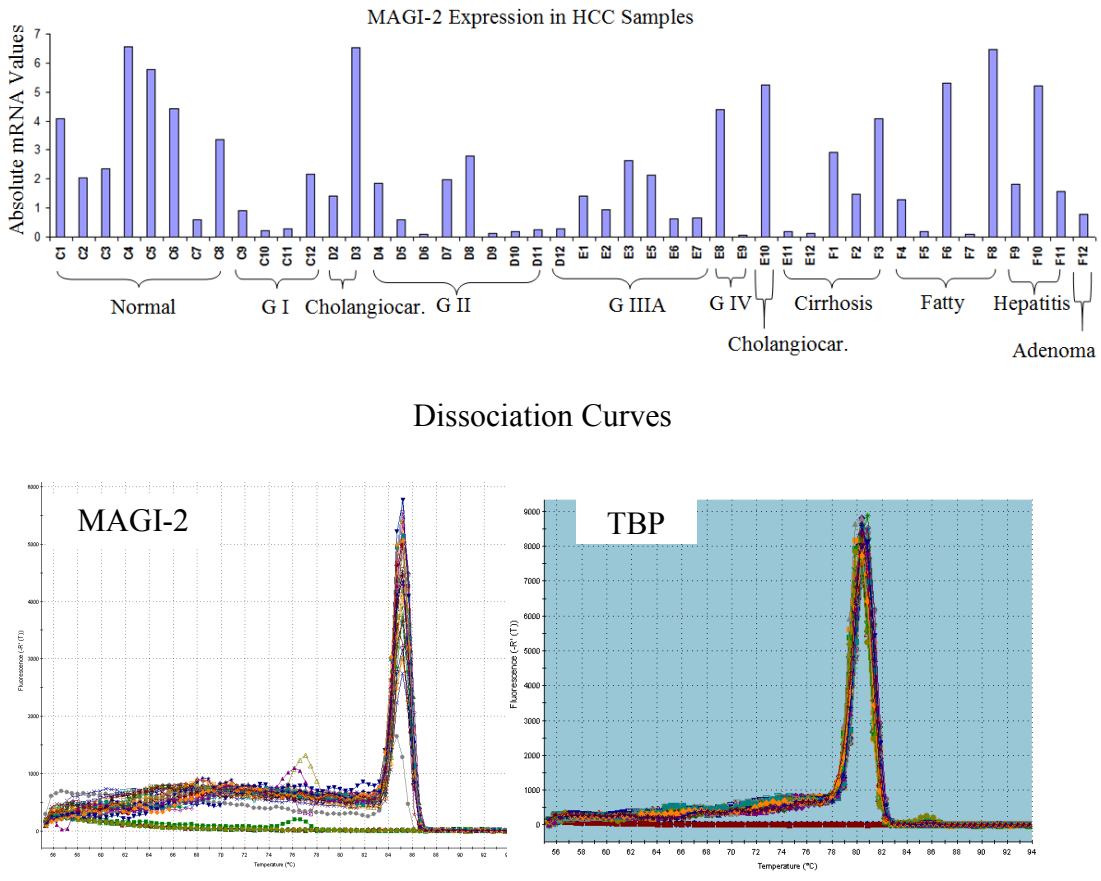

Figure 4.11.3 : *MAGI-2* mRNA expression in HCC samples. cDNAs from human liver tissues of normal and various stages of liver cancers were subjected to real-time reverse transcription–PCR for detection of *MAGI-2* mRNA expression. The data represent mRNA levels of *MAGI-2* mRNA normalized to *TBP* (D1 and E4 samples were excluded from the analysis). Dissociation curves of both genes are also presented.

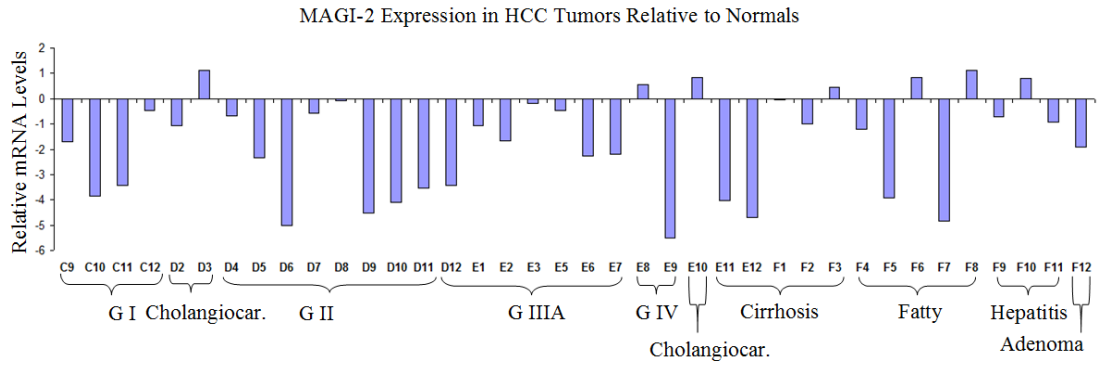

Figure 4.11.4 : *MAGI-2* mRNA expression in HCC tumors relative to normals. (D1 and E4 samples were excluded from the analysis).

We observed significantly reduced level of *MAGI-2* mRNA expression in 22 of 23 (95,65%) primary HCCs (GI, GII, GIIA, GIV), compared with eight normal liver tissues from the same panel as calculated by the student's t-test (*P* value=0.002).

CHAPTER 5
DISCUSSION

5.1. *SIP1* (*ZEB2*)

Upregulation of *SIP1* in different types of cancers have been described (Rosivatz E. *et al*., 2002; Elloul S. *et al*., 2005; Mejlvang J. *et al*., 2007). Comijn *et al*. (2001) showed that conditional *ZEB2*/*SIP1* expression in epithelial cells resulted in the specific loss of E-cadherin expression which strongly correlates with the loss of cell aggregation and induction of invasion in vitro. In addition, strong expression of SIP1 had previously been reported in some HCC cell lines (Miyoshi A. *et al*., 2004) but SIP1 protein level in HCC tissues was currently unknown.

Our data was seemingly contradictory to the role of *SIP1* as a promoter of invasion in HCC cell lines as proposed by Miyoshi *et al*., but the latter has not been yet confirmed with in vivo studies (Miyoshi A. *et al*., 2004). On the other hand, significant cancer tissue expression biases can be explained by cell context-dependent effect of *SIP1*.

It was previously reported that *SIP1* may induce senescence in HCC cells through *hTERT* repression, which in turn suggests that *SIP1* could act as a tumor suppressor (Ozturk N. *et al*., 2006). Consistent with Ozturk N. *et al*. study, *SIP1* has also been shown to be a negative regulator of *hTERT* transcription in breast cancer cells (Lin S.Y. *et al*., 2003). In this context, *ZEB2*/*SIP1* could act as a negative regulator of *hTERT* expression, and thus may exerce a tumor suppressive activity instead of its more commonly accepted role in EMT and metastasis. In support of this hypothesis, in A431 cells *SIP1* inhibits directly the expression of *cyclin D1*, a

known oncogene, and induced hypophosphorylation of the RB protein, a bona fida tumor suppressor and led to accumulation of cells in G1 phase (Mejlvang J. *et al*., 2009).

If *SIP1* acts as a tumor suppressor, one can expect its decreased expression in tumors. In a very recent study, silencing of *SIP1* expression through promoter hypermethylation was shown in most pancreatic cancer samples (90%) (Li A. et al., 2010). In case of hepatocarcinogenesis, here, we show that *SIP1* mRNA and protein levels decrease in HCC cell lines and tissues which supports our hypothesis that SIP1 contributes to the prevention of hepatocarcinogenesis.

The data presented here clearly demonstrate that Sip1 undergoes epigenetic silencing in a considerable proportion of HCC. Combined with previous in vitro and in vivo findings that shows the implication of Sip1 in *hTERT* repression and senescence arrest in a HCC cell line (Ozturk N. *et al*., 2006), our observations here suggest that inactivation of *SIP1* might contribute to hepatocarcinogenesis and Sip1 is a potential tumor suppressor gene.

5.2. *PTPRD*

PTPRD was suggested as a tumor suppressor gene because of its inactivation in many cancer types not only by deletions or somatic mutations, but also epigenetically. But, genetic and epigenetic alterations is not known in hepato carcinoma until our study.

PTPRD has previously shown to deleted in many cancer types including lung cancer (Zhao X. *et al*., 2005; Kohno T. *et al*., 2010) , neuroblastoma (Nair P. *et al*., 2008; Stallings R.L. *et al*., 2006), cutaneous squamous cell carcinomas (SCC) (Purdie K.J. *et al*., 2007), pancreatic cancer (Calhoun E.S., 2006), melanoma (Stark M. and Hayward N., 2007) and glioblastoma multiform (Solomon D.A., 2008). Kubilay Demir from our group was also showed homozygous deletion in Mahlavu, Plc, Skhep1, Snu182, Snu387 and Snu423 HCC cell lines which maps to 9p23. This 1 MB region maps to a part of protein tyrosine phosphatase receptor type D gene (*PTPRD*) (Fig 1.3.1).

Homozygous deletion of *PTPRD* in Snu475 cell line was also shown in SANGER CONAN database (Figure 1.3.3). Our detailed analysis of this deleted region by fine mapping study revealed that this deletion exist only in Snu475 cell line among 14 HCC cell lines studied and was covering 8 exons of *PTPRD* gene (Figure 4.2.9, Figure 4.2.10).

Many studies showed somatic mutations of *PTPRD* genes in colorectal cancers (Sjoblom *et al*., 2006), lung adenocarcinoma (Ding *et al*., 2008; Weir *et al*., 2007), glioblastoma multiforme (GBM) and melanoma (Solomon *et al*., 2008). *PTPRD* hot-spot mutations were also investigated in 14 HCC cell lines on exon 11 which encodes fibronectin III domain. But, we could only detect an SNP (rs10977171) (Q447E) in one HCC cell line, Snu182 and one liver sample, C12 (Figure 4.2.7 a. and b., respectively). Other exons of *PTPRD* gene were also analysed by cDNA specific primers in Hep40, Focus, MV and SkHep1 HCC cell lines (Figure 4.2.8). No somatic mutations were found in these cell lines. It is suggested that mutational inactivation could not be the major event in *PTPRD* silencing in HCC.

Loss of *PTPRD* mRNA expression in 5 out of 14 HCC cell lines (HepG2, Hep3B, Huh7, PL and Snu423) was shown by quantitative real-time and multiplex semi-quantitative RT-PCRs (Figure 4.2.1 and Figure 4.2.2). Although PLC mRNA expression was shown by quantitative real-time analysis, expression was undetectable on multiplex semi-quantitative RT-PCR of the 5' and 3' region of *PTPRD* cDNA (Figure 4.2.2). Also, *PTPRD* mRNA expression of Snu182 and Snu387 cell lines was only shown in multiplex semi-quantitative RT-PCR of the 3' region of *PTPRD* cDNA (Figure 4.2.2.b). Other 11 cell lines show almost consistent expression results in both experiments.

PTPRD expression was also checked at the protein level. All HCC cell ines, except Snu182 cell line, shown to have PTPRD protein (Figure 4.2.3).

Clinical HCC samples were analysed for their *PTPRD* mRNA expression (Figure 4.2.4.). Primary HCCs (GI, GII, GIIIA and GIV) were have significantly low levels of *PTPRD* mRNA compare to normals (*P* value=0.013) (Figure 4.2.5). IHC data was also consistent with our data from clinical HCC samples and showed stronger immunostaining in non-HCC hepatocytes compare to HCC (Figure 4.2.6.).

In a previous study, *PTPRD* was shown to be methylated in GBM (37%), breats (20%) and colon cancer (50%) but not in corresponding normal tissues (Veeriah *et al*., 2009). We analysed the metylation status of *PTPRD* promoter in clinical HCC samples by combined bisulfite restriction analysis (COBRA) method. 29 tumor and paired normal liver tissue samples were examined and 20,7% of the tumors was shown to have high level of methylaiton compared to their corresponding normal tissue (Figure 4.2.15).

Veeriah's study was also showed that *PTPRD* expression is restored in GBM cell line SKMG3 after treatment with the DNMT inhibitor DAC. In our study, *PTPRD* expression was shown to be restored in HCC after 5'-AzaC and TSA treatment at both mRNA and protein level, which indicates a possible promoter hypermethylation and/or histone modification (Figure 4.2.12, 4.2.13, 4.2.14). This western blot experiment was also showed high binding efficiency of the *PTPRD* antibody, because it could detect 3-12 µg protein used in this western study. In previous western experiment (Figure 4.2.3), 35 µg proteins were used and HepG2 and Hep3B were shown to have Ptprd protein. So, from these two western results, together with their mRNA expression analysis results, it could be suggested that HCC cell lines may have Ptprd protein but only at the basal level. 5'-AzaC and TSA treatment increases the level of Ptprd protein so much that Ptprd antibody can detect it even in 3 µg total protein.

Previous studies showing *PTPRD* tumor suppressor activities in other cancer types are in concordance with our results which suggests *PTPRD* as a tumor suppressor gene in HCC for the first time. To improve this suggestion, functional studies should be performed.

5.3. *MDM2*

Given the importance of the p53 pathway in HCC development, it is of interest to investigate the potential impact of the SNP309 genotype on its own and in combination with *TP53* mutation status in hepatocellular carcinomas. Here, we analyzed two genetic alterations, one of which is somatic and another of which is germline: *TP53* mutations and SNP309 polymorphism. We evaluated dominant and

additive models (G/G and G/T genotypes together) because Bond *et al*. showed a two fold increase in the MDM2 protein for cell lines with the heterozygous (G/T) genotype and a fourfold increase for cell lines with the homozygous variant (SNP309 G/G) genotype (Bond G.L. *et al*., 2004).

Our study provides evidence for an inverse association between the presence of the SNP309 mutant genotype and *TP53* mutation in HCC patients. However 4% of our HCC population displayed *TP53* mutations despite having SNP309G allele. The presence of the *TP53* mutations in these samples could at least partly be explained by direct affect of known and unknown environmental factors in the etiology of these four HCC samples. Indeed, one of these patients displays G> T mutation in codon 249 of TP53, which is strongly associated with diatery aflatoxin B1 intake (Ozturk M., 1999; Puisieux A. and Ozturk M., 1997).

Given the functional role of SNP309 in the inhibition of the p53 pathway, the mutant genotype of this SNP may be functionally equivalent to the inactivating *TP53* mutations in hepatocarcinogenesis. In fact, numerous studies have shown that overexpression of *MDM2* is an important event in carcinogenesis; in addition, *MDM2* amplification occurs mostly in the absence of *TP53* mutation, supporting the concept that MDM2 amplification and *TP53* mutation are alternative mechanisms of p53 dysfunction (Oliner J.D. *et al*., 1993; Momand J. *et al*., 1998; Reifenberger G. *et al*., 1993). In agreement with our hypothesis, a recent study shows that invasive bladder cancer patients with wild-type SNP309 (T/T) were prone to displaying p53 mutations (Sanchez-Carbayo M. *et al*., 2007).

On the other hand, our study also provides evidence that the p53 pathway was disrupted either by *TP53* mutation or the SNP309 G allele in 68/99 HCCs (68%). Thus, the p53 pathway may be more frequently altered in HCCs than previously thought. Previous studies proposed that high levels of *MDM2* resulting from the SNP309 G allele and just one wild-type p53 allele in Li-Fraumeni patients produce a severely weakened p53 tumor suppressor pathway, resulting in a higher mutation rate, poorer DNA repair processes and reduced apoptosis, which lead to faster and more frequent tumor formation (Bond G.L. *et al*., 2004 ; Bond G.L. *et al*., 2005). Because the G genotype might substitute the need for *TP53* gene mutation or weaken

the p53 tumor suppressor pathway,we suggest that this genotype may contribute to hepatocellular carcinoma risk. Because of lack of healthy control samples in corresponding ethnic groups or countries, we were not able to test this hypothesis with a case–control study. However, in a recent study, Dharel *et al*. reported that SNP309 is associated with the presence of hepatocellular carcinoma in Japanese patients with chronic hepatitisC[22]. In concordance with the study by Dharel *et al*., two recent studies indicated an association between the G genotype and risk for hepatocellular carcinoma in Moroccan and Korean patients with chronic hepatitis B infections (Ezzikouri S. *et al*., 2009; Yoon Y.J. *et al*. 2008).

Our study, together with the studies by Dharel *et al*., Yoon *et al*. and Ezzikouri *et al*., infers that the variations in HCC development not only depend on somatic mutations occurring in the tumor itself but also host genetic factors. Although additional work is necessary to confirm, these findings may raise the possibility that the high prevalence of HCC in some geographical regions, in addition to environmental factors, could be partly due to the high frequency of SNP309 G alleles in the people of these regions. For further information please see our published article (Acun T., *et al.* 2010).

5.4. RAS/RAF/MAPK Pathway

The MEK/ERK pathway is the best known MAPK pathways, having a key role in cell proliferation, and is known to be deregulated in approximately one-third of all human cancers (Figure 1.5.1) (Dhillon A.S. *et al*., 2007). Activating *RAS* mutations occur in ~30% of human cancers. RAS mutations were described in many cancer types suchas pancreas (90%), thyroid (60%), lung adenocarcinoma (non-small cell) (35%), liver (30%) and acute myelogenous leukemia (30%) (Schubbert S. *et al*., 2007).

BRAF, was shown to be mutated mostly in melanoma (66%) and colorectal cancer (12%) (Davies H. *et al*., 2002; Dhillon A.S. *et al*., 2007; Downward J., 2003). Activating *BRAF* mis-sense mutation (V599E) in SkHep1 cell line and in 1 out of 53 HCC samples were described by Banu Sürücü from our group. This mutation was

within the kinase domain and accounting for 80% in all *BRAF* mutations (Davies H. *et al*., 2002).

In contrast to *RAS* and *BRAF*, *MEK1* and *MEK2* mutations have not been reported in cancer or in any other human disease (Schubbert S. *et al*., 2007; Greenman C. *et al*., 2007). Mutation analysis of the *MEK1* (*MAP2K1*) , *MEK2* (*MAP2K2*), *ERK1* (*MAPK3*) and *ERK2* (*MAPK1*) genes in 14 HCC cell lines revealed no mutations (Figure 4.4.1).

PTPN11 (*SHP2*) was previously shown to have mutations described in noonan syndrome (NS), clinically related leopard syndrome (LS) and leukemia (Tartaglia M. *et al*., 2006), which are accumulated on exon 3,4,7,8,12 and 13. These exons were analysed first but no mutations were described in these exons in 14 HCC cell lines (Figure 4.4.2). But, mutation analysis was extended to remaining exons, as there might be some mutations specific for HCC.

As no mutation was found in HCC cell lines for the genes *MEK1* (*MAP2K1*), *MEK2* (*MAP2K2*), *ERK1* (*MAPK3*), *ERK2* (*MAPK1*) and *PTPN11* (*SHP2*), mutation analysis was not extended to HCC samples. Epigenetic and genetic analysis of the remaining genes in the RAS/RAF/MAPK pathway should be performed to enlighten the role of this pathway in the hepatocarcinogenesis.

5.5. Chromosome 11q13 (*FBXL11*, *PTPRCAP*)

5.5.1 *FBXL11*

FBXL11 is located in the region chromosome 11q13, which had been shown to be amplified in some cancer types including, bladder, esophageal, lung, hepatocellular carcinoma, breast and head and neck cancer (Zhang Y.J. *et al*., 1993; Schuuring E., 1995; Huang X. *et al*., 2002; Tanigami A. *et al*., 1992). On the other hand significant down regulation was shown in prostate carcinomas compared to normal prostate tissue which indicates its possible tumor suppressor role in tumorogenesis (Frescas D. *et al*., 2008).

Also, many JmjC group of histone demethylases (like *FBXL11*) were regarded as candidate tumor suppressors and many of them shown to involved in senescence, cancer and some diseases such as; acute myeloid leukemia (AML), prostate cancer, squamous cell carcinoma, schizophrenia, congenital heart disease (CHD), multiple self-healing squamosus epitheloma (ESS1), arthricia with popular lesion (APL), alopecia universalis congenital (AUC), intractable epilepsy (IE), X-linked mental retardation (XLMR) (Cloos P.A.C. *et al*. 2008).

Our results showed that, *FBXL11* mRNA is expressed almost all HCC cell lines except Hep3B, SkHep1 and Snu182 cell lines (Figure 4.5.1). According to SANGER copy number analysis of chromosome 11, in Snu387 and Snu475 HCC cell lines, there is a high level of amplification at the region containing *FBXL11* gene (Figure 1.6.3). But, the results of quantitative real-time RT-PCR and western blot analysis of Snu475 and Snu387 cell lines was not support the data from SANGER database (Figure 4.5.1, Figure 4.5.2 respectively). Actually, FBXL11 protein was shown to localized at the nucleolus where it binds ribosomal DNA repeats to inhibit the expression of ribosomal RNAs. (Tanaka Y. *et al*., 2010; Frescas D. *et al*., 2008). So, total cell lysates used in the western blot experiment might not reflect the actual protein level of FBXL11 in the cell.

FBXL11 mRNA expression was also analysed in clinical HCC samples by quantitative real-time RT-PCR (Figure 4.5.3). We observed significantly reduced *FBXL11* mRNA expression in 18 of 23 (78.3%) primary HCCs, compared with eight normal liver tissues from the same panel as calculated by the student's t-test (*P* value=0,0043) (Figure 4.5.4). Our findings support the notion that *FBXL11* might have a tumor suppressor role in the HCC tumorogenesis. But, this argument should be validated *in-vitro* and *in vivo* with the functional studies.

5.5.2 *PTPRCAP*

PTPRCAP is a transmembrane protein that enhance the phosphatase activity of PTPRC. PTPRC is known as an activator of Src family kinases (SFKs) which are implicated in tumor progression and metastasis (Kitamura K. *et al*., 1995; Motoya S.

et al., 1999; Veillette A. *et al*., 1999; Takeda A. *et al*., 2004; Ju H. *et al*., 2009; Penninger J.M. *et al*., 2001; Summy J.M. and Gallick G.E., 2003; Barraclough J. *et al*., 2007). Increased expression of *PTPRCAP* is associated with susceptibility to diffuse-type gastric cancer (Ju H. *et al*., 2009). Also, high level amplification in the region 11q13 containing *PTPRCAP* gene in Snu475 and Snu387 HCC cell lines was shown at SANGER CONAN database (Figure 1.6.3).

According to our results, 9 out of 14 HCC cell lines have high level of *PTPRCAP* mRNA (Figure 4.5.5). *PTPRCAP* mRNA expression was also analysed in clinical HCC samples by quantitative real time RT-PCR (Figure 4.5.6). We observed high PTPRCAP mRNA expression in 12 of 23 (52,1%) primary HCCs, compared with eight normal liver tissues from the same panel. Together with the copy number analysis (CONAN) data and our real-time RT-PCR results of HCC samples, indicates *PTPRCAP* as a candidate oncogene. Functional studies should be done and *PTPRCAP* expression at the protein level should be checked in the tumor samples by either IHC or western in order to strengthen its possible oncogenic role in hepatocarcinogenesis.

5.6. Chromosome 13q12 (*TUBA3C*,*ZNF198*,*TPTE2*)

5.6.1 *TUBA3C*

13q12.11 region was found to be homozygously deleted in two HCC cell lines, Huh7 and SkHep1 (Kubilay Demir, MSc). This 1.5 MB deletion region was previously shown in HCC and other cancer types including colon cancer, esophageal squamous-cell carcinoma and non-small-cell lung cancer (Chen C.F. *et al*., 2005; Tamura *et al*., 1997; Li G. *et al*., 2001; Li SP. *et al*., 2001; Sivarajasingham *et al*., 2003; Zhang X. *et al*., 1994) (Figure 1.7.1). There are more than 37 identified transcripts in this region, 18 are the known genes and 19 are the annotated transcripts. *LATS2*, *TG737*, *CRYL1*, and *GJB2* were shown to be downreguleted in 14%, 59%, 64% and 71% of HCC tissues, respectively (Chen C.F. *et al*., 2005).

There are few studies showing *TUBA3C* role in cancer development but upregulation of *TUBA3C* in metastaitic prostate tumor tissue was shown compare to

localized prostate tumor tissue (Vila A.M.*et al*., 2010) and according to Affymetrix GeneChips HG-U95A-E and HG-U133A GNF data, *TUBA3C* expression is high in liver cancer compare to normal liver (Su AI *et al*., 2004).

Our fine mapping study of the 13q12.11 region in 14 HCC cell lines revealed that *TUBA3C* is deleted in both Huh7 and SkHep1 cell lines (Figure 4.6.1, Figure 4.6.2). According to our real-time analysis, 4 out of 14 HCC cell lines; Focus, Hep40, Mahlavu, Snu475, have *TUBA3C* mRNA (Figure 4.6.3; Figure 4.6.4). *TUBA3C* mRNA expression was also analysed in clinical HCC samples by quantitative real time RT-PCR analysis. Only six primary HCC samples and one normal sample showed *TUBA3C* mRNA expression in total of 48 samples (Figure 4.6.5).

Genetic analysis of *TUBA3C* in all HCC cell lines (except Huh7 and SkHep1) revealed one mutation (S38N) in Mahlavu cell line (Figure 4.6.6). Some silent mutations were also found (data not shown).

Possible epigenetic regualation on the *TUBA3C* mRNA expression was also investigated. 5-AzaC and TSA treatments was restored the *TUBA3C* mRNA expression in PLC, HepG2 and Hep3B HCC cell lines (Figure 4.6.7, Figure 4.6.8).

Homozygous deletion in 2 out of 14 HCC cell lines together with epigenetic regulation of its mRNA expression suggest a possible tumor suppressor role of *TUBA3C* in hepatocarcinogenesis. NATs and miRNAs might also contribute the regulation of *TUBA3C* mRNA expression. Functional studies should be perfomed to prove this suggestion.

5.6.2 *ZNF198 (ZMYM2)*

ZNF198 (*ZMYM2*) was previously shown to be located in deleted region 13q12. Our fine mapping study was also confirmed this deletion in SkHep1 cell line (Figure 4.6.1). *ZNF198* mRNA expression in HCC cell lines was analysed by semi-quantitative RT-PCR. All HCC cell lines, except SkHep1 cell line, were shown to express *ZNF198* mRNA at different levels (Figure 4.6.9). Genetic analysis of *ZNF198* gene revealed no somatic mutation in 13 HCC cell lines. Our results indicate that *ZNF198* seems not involved in hepatocarcinogensis.

5.6.3 *TPTE2*

TPTE2 mRNA expression pattern was analysed in 14 HCC cell lines (Figure 4.6.10). Only Hep40, Huh7 and PLC have *TPTE2* mRNA expression among other 11 HCC cell lines. SkHep1 did not express *TPTE2* as it is deleted in this cell line. *TPTE2* mRNA expression was low in 18 of 23 (78,2%) primary HCCs, compared to eight normal liver tissues from the same panel (Figure 4.6.12). Being located in homozygously deleted region, being a homolog of *PTEN* tumor suppressor, downregulation in both HCC cell lines and HCC samples make *TPTE2* gene a strong tumor suppressor candidate. In order to better understand the role of *TPTE2* in HCC progression, western and IHC studies should be done in clinical samples and functional studies should be performed.

5.7. Chromosome 3p25.1 (*IQSEC1*)

IQSEC1 is located in a minimal deleted region on 3p25.1 according to SNP analysis. It is a specific Guanine Exchange Factor (GEF) for ARF6. ARF6 induces invasion and metastasis through its effector Amap1 (Figure 1.8.1). There are reports showing high expression of *IQSEC1*, *ARF6* and *AMAP1* in malignant breast tumor (Sabe H. *et al*., 2009). Also inhibition of *IQSEC1* expression shown to significantly reduces the metastasis of lung tumor cells in mice (Valderrama F. *et al*., 2008; Morishige M. *et al*., 2008). On the other hand, it is postulated in Someya's study that *IQSEC1* may serve a positive regulator in TNF-α mediated apoptosis (Someya A. *et al*., 2006). Sanger copy number analysis of chromosome 3 in SkHep1 cell line shows homozygous deleted region, containing *IQSEC1* gene (Figure 1.8.2). According to our real-time analysis, HepG2, PLC, SkHep1 and Snu475 cell lines have almost no *IQSEC1* expression (Figure 4.7.1). *IQSEC1* mRNA expression was also analysed in clinical HCC samples (Figure 4.7.2). We observed low *IQSEC1* mRNA expression in 16 of 23 (69,5%) primary HCCs, compared with eight normal liver tissues from the same panel.

Although there are conflicted studies about the role of *IQSEC1* in cancer development or metastasis, in the case of HCC, *IQSEC1* may act as a tumor

suppressor. It is deleted in SkHep1 HCC cell line and downregulated 69,5% of primary HCCs compare to normals.

5.8. Chromosome 14q13.3 (*MIPOL1*)

MIPOL1 is located at a 14q13 breakpoint of t(2;14) and MIPOL1-DGKB gene fusion was showed in the prostate cancer cell line, LNCAP (Maher C.A. *et al*., 2009). *MIPOL1* might be serve as a tumor suppressor in nasopharyngeal carcinoma (NPC) (Cheung A.K.L. *et al*., 2009) as all NPC cell lines have reduced levels of *MIPOL1* and in 63% of NPC tumors via promoter hypermethylation and allelic loss. Tumor suppression effect is involved the up-regulation of the p21 and p27 protein pathways (Cheung A.K.L. *et al*., 2009).

In the case of hepatocarcinoma, homozygous deletion was shown in PLC HCC cell line in SANGER database (Figure 1.9.1). Also copy number analysis at the SANGER (CONAN) showed that HLE, PLC and SkHep1 HCC cell lines have LOH in the region containing *MIPOL1* gene (Figure 1.9.2). There is still no information about *MIPOL1* gene regulation in HCC. According to our real-time analysis, Snu398 and Snu449 have high MIPOL1 mRNA expression (Figure 4.8.1).

MIPOL1 expression was also checked at the protein level (Figure 4.8.2). HepG2, Snu475, Snu387 and Hep3B was in concordance with the real-time results except PLC. Although PLC was previously shown to be reside in the homozygous deletion region (Figure 1.9.1), western results showed *MIPOL1* protein in PLC cell line. This deletion was between 36,887,100-37,030,900 bp (143.800 bp) and result in ~67 aminoacid loss in protein (Figure 4.8.3).

MIPOL1 mRNA expression was also analysed in clinical HCC samples and low *MIPOL1* mRNA expression in 12 of 23 (52,17%) primary HCCs and high *MIPOL1* mRNA expression in 11 of 23 (47,8%) primary HCCs compared with eight normal liver tissues (Figure 4.8.4, Figure 4.8.5). Although the results was not significant in the HCC samples, being reside in a deleted region, reduced mRNA expression in HCC cell lines and primary HCC samples make *MIPOL1* is a candidate tumor suppessor in hepatocarcinoma.

5.9. Chromosome 10q24 (*CHUK*)

CHUK is a part of an enzyme complex called IKK (IκB kinase) involved in the NF-κB activation. In previous studies, *CHUK* was identified as a tumor suppressor in squamous cell carcinoma (SCC) (Liu B, *et al*., 2006). Epigenetic inactivation of *CHUK* was also shown in oral carcinomas (Maeda G. *et al*., 2007). Copy number analysis of chromosome 10 in PLC and Snu475 HCC cell lines revealed LOH in the region containing *CHUK* gene (Figure 1.10.2).

We observed low *CHUK* mRNA expression in 14 of 23 (60,86%) primary HCCs, compared with eight normal liver tissues from the same panel. These findings together with the previous studies on genetic regulation and copy number analysis of *CHUK*, suggested *CHUK* as a tumor suppressor.

5.10. Chromosome 1q21 (*MCL1*)

MCL1 is a member of the BCL2 (B-cell lymphoma 2) gene family. Members of this family categorized as oncogenes. They either facilitate cell survival (pro-survival Bcl-2 subfamily) or promote cell death (Bax and Bcl-2 homologous 3 subfamilies) (Adams J.M. and Cory S., 1998; Danial N.N. and Korsmeyer S.J., 2004) (Figure 1.11.1).

There are conflicted arguments about the role of *MCL1* in cancer. It was shown that *MCL1* was not only inhibit apoptosis but also inhibit cell cycle progression in the S-phase through its interaction with PCNA (proliferating cell nuclear antigen). There are not much studies showing *MCL1* role in liver. But one recent study showed that, *MCL1* inhibition through overactivation of the MEK/ERK pathway result in resistance to TGF-B–induced cell death in liver cells (Caja L. *et al*., 2009).

According to our analysis, almost all HCC cell lines shown to express MCL1 mRNA except Snu423 (Figure 4.10.1). Western blot analysis of *MCL1* expression was also confirmed the mRNA expression. *MCL1* mRNA expression was significantly reduced in 21 of 23 (91,30%) primary HCC samples compare to normals from the same panel as calculated by the student's t-test (*P* value=0.011).

(Figure 4.10.3, Figure 4.10.4). In the light of these results, it can be concluded that MCL1 may serve as a tumor suppressor role in liver cancer progression.

5.11. Chromosome 7q21 (*MAGI-2*)

MAGI-2 is located on chromosome 7q21, a region that was shown to be deleted in prostate cancer, glioblastoma and uterine leiomyomas (Ishwad C.S. *et al*., 1995; Cui J. *et al*., 1998; Kim D.H. *et al*., 1995). In SANGER CONAN Database, homozygous deletion of this region was also described in HUH-6 cell line (Figure 1.12.1). Also, same database revealed LOH in the same region in HLE and HUH-6 HCC cell lines (Figure 1.12.2).

MAGI-2 is a multidomain scaffolding protein involved in assembling and anchoring of several cellular signaling proteins such as β-catenin, Atrophin-1, NMDA glutamate receptors, β1-adrenergic receptor, neuroligins-1, NPRAP/δ-catenin, MAGUIN-1, nRAP-GEP, SAPAP and PTEN. There are few studies showing *MAGI-2* role in the hepatocarcinogenesis possibly due to its expression mainly in neuronal cells (Xu J.G. *et al*., 2001). But, Yali H. *et al*. study showed that *MAGI-2* enhanced the stability of PTEN tumor suppressor protein which result in inhibition of cell migration and proliferation in human hepatocarcinoma cells (Yali H. *et al*., 2007). Yali H. *et al*. also showed its expression in SMMC-7721 HCC cell line among eight cell lines tested (SMMC-7721, MHCC-97H, BEL-7404, HepG2, Huh7, LM6, 7402, Chang).

According to our real-time and multiplex semi-quantitative RT-PCR analysis, *MAGI-2* mRNA expression was low in 7 out of 14 cell lines (50%). Also, significantly reduced level of *MAGI-2* mRNA expression was observed in 22 of 23 (95,65%) primary HCCs, compared with eight normal liver tissues from the same panel as calculated by the student's t-test (*P* value=0.002). According to these results, *MAGI-2* can be suggested as a tumor supressor in the progression of hepatocarcinogenesis. But, IHC studies in clinical liver tissues and functional studies in HCC cell lines could give a better view about the role of *MAGI-2*.

CHAPTER 6

CONCLUSION

Tumor suppressor role of *SIP1* was already suggested and our study strengthen this argument since all HCCs displayed no or reduced SIP1 protein and also explained the mechanism behind silencing which is not genetic but epigenetic in HCCs.

PTPRD, a novel tumor suppressor gene deleted and epigenetically downregulated in a subset of HCCs thus probably involved in hepatocarcinogenesis.

According to our results, among other candidates; *FBXL11*, *TUBA3C*, *TPTE2*, *IQSEC1*, *MIPOL1*, *CHUK*, *MCL1*, *MAGI-2* and *PTPRCAP* genes are involved in hepatocarcinogenesis.

Mutations of RAS/RAF/MAPK pathway genes; *MEK1* (*MAP2K1*), *MEK2* (*MAP2K2*), *ERK1* (*MAPK3*), *ERK2* (*MAPK1*) and *PTPN11* (*SHP2*), are not involved in hepatocarcinogenesis.

Our SNP (MDM2-SNP309) study reveals a mechanism alternative to *TP53* inactivating mutations in hepatocarcinogenesis. This finding raise the possibility that the high prevalence of HCC in some geographical regions, in addition to environmental factors, could be partly due to the high frequency of SNP309 G alleles in the people of these regions.

Bibliography

Acun T., Terzioglu-Kara E., Konu O., Ozturka M, Yakicier M.C., "Mdm2 Snp309 G allele displays high frequency and inverse correlation with somatic P53 mutations in hepatocellular carcinoma", *Mutation Research*, 684:106–108, (2010)

Adams J.M. and Cory S., "The Bcl-2 Protein Family: Arbiters of Cell Survival", *Science*, 281(5381):1322 – 1326, (1998)

Alarcon-Vargas D., Ronai Z., "p53-Mdm2-the affair that never ends", *Carcinogenesis*, 23(4): 541-547, (2002)

Alonso, A. *et al*., "Protein tyrosine phosphatases in the human genome", *Cell*, 117: 699–711, (2004).

American Cancer Society, "Cancer Facts and FIGS" (2005)

Andersen, J. N. *et al*., "Structural and evolutionary relationships among protein tyrosine phosphatase domains", *Mol. Cell. Biol.*, 21: 7117–7136, (2001)

Anthony, P. in Pathology of the Liver (eds MacSween, R., Burt, A., Portmann, B., Ishak, K., Scheuer P. & Anthony, P.) 711–775 (Churchill Livingstone, London, New York, Sydney, Toronto), (2002)

Aravalli R.N., Steer C.J., and Cressman E.N.K., "Molecular Mechanisms of Hepatocellular Carcinoma", *Hepatology*, 48(6), 2047-2063, (2008)

Barraclough J., Hodgkinson C., Hogg A., Dive C., and Welman A., "Increases in c-Yes expression level and activity promote motility but not proliferation of human colorectal carcinoma cells", *Neoplasia*, 9: 745–754, (2007)

Bekri S, Adélaïde J, Merscher S, Grosgeorge J, Caroli-Bosc F, Perucca-Lostanlen D, Kelley PM, Pébusque MJ, Theillet C, Birnbaum D, Gaudray P, "Detailed map of a region commonly amplified at 11q13-->q14 in human breast carcinoma", *Cytogenet Cell Genet.*, 79(1-2):125-31, (1997)

Beltran M. *et al*., "A natural antisense transcript regulates Zeb2/Sip1 gene expression during Snail1-induced epithelial mesenchymal transition", *Genes and Development*, 22:756-769, (2008)

Bentires-Alj M. *et al*., "Activating Mutations of the Noonan Syndrome-Associated SHP2/PTPN11 Gene in Human Solid Tumors and Adult Acute Myelogenous Leukemia", Cancer Research 64, 8816–8820, (2004)

Biden K., Young J., Buttenshaw R., Searle J., Cooksley G., Xu D.B., Leggett B., "Frequency of mutation and deletion of the tumor suppressor gene CDKN2A (MTS1/p16) in hepatocellular carcinoma from an Australian population", *Hepatology*, 25(3):593-7, (1997)

Block T.M., Mehta A.S., Fimmel C.J. & Jordan R., "Molecular viral oncology of hepatocellular carcinoma", *Oncogene*, 22:5093–5107, (2003)

Bond G.L., Hu W., Bond E.E., Robins H., Lutzker S.G., Arva N.C., Bargonetti J., Bartel F., Taubert H. , Wuerl P., Onel K., Yip L., Hwang S.J., Strong L.C., Lozano G., Levine A.J., "A single nucleotide polymorphism in the MDM2 promoter attenuates the p53 tumor suppressor pathway and accelerates tumor formation in humans", *Cell*, 119: 591-602, (2004)

Bond G.L., Hu W., Levine A., "A single nucleotide polymorphism in the MDM2 gene: from a molecular and cellular explanation to clinical effect", *Cancer Res.*, 65: 5481–5484, (2005)

Bosch, F.X., Ribes, J., Borràs, J., "Epidemiology of primary liver cancer", *Semin. Liver Dis.* 19, 271–285, (1999)

Bougeard G., Baert-Desurmont S., Tournier I., Vasseur S., Martin C., Brugieres L., Chompret A., Bressac-de Paillerets B., Stoppa-Lyonnet D., Bonaiti-Pellie C., Frebourg T., "Impact of the MDM2 SNP309 and p53 Arg72Pro polymorphism on age of tumour onset in Li-Fraumeni syndrome", *J. Med. Genet.*, 43: 531-33, (2006)

Bracken C.P. *et al*., "A Double-Negative Feedback Loop between ZEB1-SIP1 and the microRNA-200 Family Regulates Epithelial-Mesenchymal Transition", *Cancer Research*, 68(19):7846-7854, (2008)

Bressac B., Kew M., Wands J., Ozturk M., "Selective G to T mutations of p53 gene in hepatocellular carcinoma from southern Africa", *Nature,* 350:429–431,(1991)
Buendia, M.A., "Genetics of hepatocellular carcinoma", *Semin. Cancer Biol.* 10, 185–200, (2000)

Cacheux V. *et al*., "Loss-of-function mutations in SIP1 Smad interacting protein 1 result in a syndromic Hirschsprung disease", *Human Molecular Genetics*, 10(14):1503-1510 (2001)

Cagatay T., Ozturk M., "P53 mutation as a source of aberrant beta-catenin accumulation in cancer cells", *Oncogene*, 21:7971-80, (2002)

Caja L., Sancho P., Bertran E., Iglesias-Serret D., Gil J., Fabregat I., "Overactivation of the MEK/ERK Pathway in Liver Tumor Cells Confers Resistance to TGF-B–Induced Cell Death through Impairing Up-regulation of the NADPH Oxidase NOX4", *Cancer Res*, 69(19):7595-7602, (2009)

Calhoun E.S., Hucl T., Galmeier E., West K.M., Arking D.E., Maitra A., Lacobuzio-Donahue C.A., Chakravarti A., Hruban R.H., and Kern S.E., "Identifying allelic loss and homozygous deletions in pancreatic cancer without matched normals using high-density single-nucleotide polymorphism arrays", *Cancer Res.* 66:7920–7928, (2006)

Cano A. and Nieto M.A., "Non-coding RNAs take centre stage in epithelial-to-mesenchymal transition", *Trends in Cell Biology*,18(8):357-359, (2008)

Chaib H., Lina-Granade G., Guilford P., Plauchu H., Levil-liers J., Morgon A. and Petit, C., "A gene responsible for a dominant form of neurosensory non-syndromic deafness maps to the NSRD1 recessive deafness gene interval", *Hum. Mol. Genet.*, 3: 2219–2222, (1994)

Chen H., Rossier C., Morris M.A., Scott H.S., Gos A., Bairoch A., Antonarakis S.E., "A testis-specific gene, TPTE, encodes a putative transmembrane tyrosine phosphatase and maps to the pericentromeric region of human chromosomes 21 and 13, and to chromosomes 15, 22, and Y", *Hum. Genet.*, 105:399– 409, (1999)

Chen C.F., Yeh S.H., Chen D.S., Chen P.J., and Jou Y.S., "Molecular genetic evidence supporting a novel human hepatocellular carcinoma tumor suppressor locus at 13q12.1" *Genes Chromosomes. Cancer* ,*44*: 320-328, (2005)

Chen CL, Hsieh FC, Lin J., "Systemic evaluation of total Stat3 and Stat3 tyrosine phosphorylation in normal human tissues", *Exp Mol Pathol.*, 80(3):295-305, (2006)

Cheung A.K.L. *et al*., "Chromosome 14 transfer and functional studies identify a candidate tumor suppressor gene, Mirror image polydactyly 1, in nasopharyngeal carcinoma", *PNAS*, 106(34): 14478–14483, (2009)

Christoffersen N.R. *et al*., "miR-200b mediates post-transcriptional repression of ZFHX1B", *RNA*, 13:1172-1178, (2007)

Cloos P.A., Christensen J., Agger K., Helin K., “Erasing the methyl mark: histone demethylases at the center of cellular differentiation and disease”, *Genes Dev.*, 22:1115-40, (2008)

Cohen Y. and Cohen J.Y., “Statistics and Data with R: An Applied Approach Through Examples”, Wiley (2008)

Comijn J., Berx G., Vermassen P., Verschueren K., van Grunsven L., Bruyneel E., Mareel M., Huylebroeck D., van Roy F., “The two-handed E box binding zinc finger protein SIP1 downregulates E-cadherin and induces invasion”, *Mol Cell*, 7(6):1267–1278, (2001)

Cui J., Deubler D.A., Rohr L.R., Zhu X.L., Maxwell T.M., Changus J.E., Brothman A.R., “Chromosome 7 Abnormalities in Prostate Cancer Detected by Dual-Color Fluorescence In Situ Hybridization”, *Cancer Genet Cytogenet*,107(1):51–60, (1998)

Danial N.N. and Korsmeyer S.J., “Cell Death: Critical Control Points”, *Cell*, 116: 205–219, (2004)

Dastot-Le Moal F., Wilson M., Mowat D., Collot N., Niel F., Goossens M., “ZFHX1B Mutations in Patients With Mowat-Wilson Syndrome”, *Human Mutation*, 28(4):313-321, (2007)

Davies H. *et al.*,“Mutations of the BRAF gene in human cancer”, *Nature*, 417: 27, (2002)

Descargues P., Sil A.K. and Karin M., “IKKa, a critical regulator of epidermal differentiation and a suppressor of skin cancer”, *The EMBO Journal*, 27(20):2639–2647, (2008)

Dhillon A.S., Hagan S., Rath O., Kolch W., “MAP kinase signalling pathways in cancer”, *Oncogene*, 26: 3279–3290, (2007)

Dickson C., Fantla V., Gillettb C., Brookesa S., Bartekc J., Smitha R., Fisherb C., Barnesb D. and Petersa G., “Amplification of chromosome band 11q13 and a role for cyclin D1 in human breast cancer” , *Cancer Letters*, 90(1):43-50, (1995)

Ding L., *et al*., Somatic mutations affect key pathways in lung adenocarcinoma, Nature, 455:1069-75, (2008)

Dobrosotskaya I., Guy R.K., James G.L., “MAGI-1, a Membrane-associated Guanylate Kinase with a Unique Arrangement of Protein-Protein Interaction Domains”, *The Journal of Biological Chemistry*, 272, 31589-31597, (1997)

Donato F, Tagger A, Gelatti U, “Alcohol and hepatocellular carcinoma: the effect of lifetime intake and hepatitis virus infections in men and women”, *Am J Epidemiol* 155:323–331, (2002)

Downward J., “Targeting RAS signalling pathways in cancer therapy”, *Nat Rev Cancer*, 3: 11–22 (2003)

Ekstrom G, Ingelman-Sundberg M., “Rat liver microsomal NADPH-supported oxidase activity and lipid peroxidation dependent on ethanol-inducible cytochrome P-450 (P-450IIE1)”, *Biochem Pharmacol*, 38:1313, (1989)

Edamoto Y., Hara A., Biernat W., “Alterations of RB1, p53 and Wnt pathways in hepatocellular carcinomas associated with hepatitis C, hepatitis B and alcoholic liver cirrhosis”, *Int J Cancer*, 106:334, (2003)

Elloul S., Elstrand M.B., Nesland J.M., Tropé C.G., Kvalheim G., Goldberg I., Reich R., Davidson B., "Snail, Slug, and Smad-interacting protein 1 as novel parameters of disease aggressiveness in metastatic ovarian and breast carcinoma", *Cancer*, 103(8):1631-43, (2005)

El-Serag HB, Rudolph KL., "Hepatocellular carcinoma: epidemiology and molecular carcinogenesis", *Gastroenterology,*132, 2557-2576, (2007)

Essigmann J.M., Green C.L., Croy R.G., Fowler K.W., Buchi G.H., Wogan G.N., "Interactions of aflatoxin B1 and alkylating agents with DNA: structural and functional studies", *Cold Spring Harb Symp Quant Biol,* 1:327, (1983)

Esteller M, "Cancer epigenomics: DNA methylomes and histone-modification maps", *Nat Rev Genet.*, 8:286-298, (2007)

Ezzikouri S., El Feydi A.E., Afifi R., El Kihal L., Benazzouz M., Hassar M., Marchio A., Pineau P., Benjelloun S., "MDM2 SNP309T>G polymorphism and risk of hepatocellular carcinoma: a case–control analysis in a Moroccan population", *Cancer Detect. Prev.*, 32:380–385, (2009)

Farazi P.A. and DePinho R.A. "The genetic and environmental basis of hepatocellular carcinoma", *Discov. Med*. *6*: 182-186, (2006)

Feitelson M. A. *et al*., "Genetic mechanisms of hepatocarcinogenesis", *Oncogene*, 21: 2593–2604, (2002)

Ferlay, J., Bray, F., Pisani, P., Parkin, "D.M.J. GLOBOCAN 2000: Cancer Incidence, Mortality and Prevalence Worldwide, Version 1.0.", *IARC CancerBase No. 5,* Lyon, IARC Press, (2001).

Foulkes A.S., "Applied Statistical Genetics with R: For Population-Based Association Studies. Use R", Springer (2009)

Fountain J.W., *et al*., "Homozygous deletions within human chromosome band 9p21 in melanoma", *Proc Natl Acad Sci U S A*, 89: 10557-10561, (1992)

Frescas D., Guardavaccaro1 D., Kato H., Poleshko A., Katz R.A. and Pagano M., "KDM2A represses transcription of centromeric satellite repeats and maintains the heterochromatic state", *Cell Cycle*, 7(22): 3539–3547, (2008)

Fu LY., Jia HL, Dong QZ, Wu JC, Zhao Y, Zhou HJ, Ren N, Ye QH, Qin LX: "Suitable reference genes for real-time PCR in human HBV-related hepatocellular carcinoma with different clinical prognoses", *BMC Cancer*, 9(49), (2009)

Fujise K., Zhang D., Liui JL and Yeh E.T.H., "Regulation of Apoptosis and Cell Cycle Progression by MCL1", *The Journal of Biological Chemistry*, 275(50): 39458–39465, (2000)

Ghosh A.K., Steele R., Meyer K., Ray R., Ray R.B., "Hepatitis C virus NS5A protein modulates cell cycle regulatory genes and promotes cell growth", *J General Virol*, 80:1179, (1999)

Greenman C. *et al*., "Patterns of somatic mutation in human cancer genomes", *Nature*, 446: 153-158, (2007)

Gregory P.A. *et al*., "The miR-200 family and miR-205 regulate epithelial to mesenchymal transition by targeting ZEB1 and SIP1", *Nature Cell Biology*, 10(5) 593-601, (2008)

Grisham, J.W., "Molecular genetic alterations in primary hepatocellular neoplasms: hepatocellular adenoma, hepatocellular carcinoma, and hepatoblastoma", *The Molecular Basis of Human Cancer* (eds Coleman, W.B. & Tsongalis, G.J.) 269–346 (Humana Press, Totowa, New Jersey), (2001)

Guilford P., Ben Arab S., Blanchard S., Levilliers J.,Weissenbach J., Belkahia A. and Petit C., "A non-syndromic form of neurosensory, recessive deafness maps to the pericen- tromeric region of chromosome 13q", *Nature Genet.*, 6: 24–28, (1994)

Gur-Dedeoglu B., Konu O., Bozkurt B., Ergul G., Seckin S., Yulug I.G., "Identification of endogenous reference genes for qRT-PCR analysis in normal matched breast tumor tissues", *Oncol Res*., 17(8):353-65, (2009)

Haupt Y., Maya R., Kazaz A., Oren M., "Mdm2 promotes the rapid degradation of p53", *Nature*, 387: 296-99, (1997)

Herath N.I., Leggett B.A., MacDonald G.A., "Review of genetic and epigenetic alterations in hepatocarcinogenesis", *J Gastroenterol Hepatol*, 21:15-21, (2006)

Herman J.G., Baylin S.B., "Gene silencing in cancer in association with promoter Hypermethylation", *N Engl J Med* , 349:2042–2054, (2003)

Hoek J.B. & Pastorino J.G., "Ethanol, oxidative stress, and cytokine-induced liver cell injury", *Alcohol*, 27:63–68, (2002)

Huang X, Gollin SM, Raja S, Godfrey TE., "High-resolution mapping of the 11q13 amplicon and identification of a gene, TAOS1, that is amplified and overexpressed in oral cancer cells", *Proc Natl Acad Sci U S A.*, 99(17):11369-74, (2002)

IARC "Overall evaluations of carcinogenicity an updating of IARC monographs" IARC Monographs 1987;1-42[Suppl 7],83-87. Lyon: IARCPress.

Jin X., Zimmers T.A., Perez E.A., Pierce R.H., Zhang Z., Koniaris L.G., "Paradoxical effects of short- and long-term interleukin-6 exposure on liver injury and repair", *Hepatology*, 43:474, (2006)

Ishwad C.S., Ferrell R.E., Davare J., Meloni A.M., Sandberg A.A., Surti U., "Molecular and cytogenetic analysis of chromosome 7 in uterine leiomyomas", *Genes Chromosomes Cancer*, 14(1):51–55, (1995)

Jones P.A., Baylin S.B., "The fundamental role of epigenetic events in cancer", *Nature* Reviews, 3:415–428, (2002)

Ju H., Lim B., Kim M., Kim Y.S., Kim W.H., Ihm C., Noh S.M., Han D.S., Yu H.J., Choi B.Y., Kang C., "A regulatory polymorphism at position -309 in PTPRCAP is associated with susceptibility to diffuse-type gastric cancer and gene expression" *Neoplasia*, 11:1340-7, (2009)

Kew, M.C., "Synergistic interaction between aflatoxin B1 and hepatitis B virus in hepatocarcinogenesis", *Liver Int.*, 23:405–409, (2003)

Kim C.M., Koike K., Saito I., Miyamura T. & Jay G., "HBx gene of hepatitis B virus induces liver cancer in transgenic mice", *Nature*, 351:317–320, (1991)

Kim D.H., Mohapatra G., Bollen A., Waldman F.M, Feuerstein B.G., "Chromosomal-Abnormalities In Glioblastoma-Multiforme Tumors And Glioma Cell-Lines Detected By Comparative Genomic Hybridization", *Int J Cancer*, 60(6):812–819, (1995)

Kitamura K.,Maiti A., Ng D.H., Johnson P.,Maizel A.L., and Takeda A., "Characterization of the interaction between CD45 and CD45-AP", *J Biol Chem*, 270: 21151–21157, (1995)

Kohno T. *et al*., "A Catalog of Genes Homozygously Deleted in Human Lung Cancer and the Candidacy of PTPRD as a Tumor Suppressor Gene", *Genes, Chromosomes & Cancer,* 49:342–352 (2010)

Kondo Y., Kanai Y., Sakamoto M., Mizokami M., Ueda R., Hirohashi S., "Genetic instability and aberrant DNA methylation in chronic hepatitis and cirrhosis-A comprehensive study of loss of heterozygosity and microsatellite instability at 39 loci and DNA hypermethylation on 8 CpG islands in microdissected specimens from patients with hepatocellular carcinoma", *Hepatology*, 32(5):970-9, (2000)

Kondoh S. *et al*., "A novel gene is disrupted at a 14q13 breakpoint of t(2;14) in a patient with mirror-image polydactyly of hands and feet", *J.Hum. Genet.*, 47:136–139, (2002)

Kozopas K.M., Yang T., Buchan H.L., Zhou P. and Craig R.W., "MCLI, a gene expressed in programmed myeloid cell differentiation, has sequence similarity to BCL2", *Proc. Natl. Acad. Sci. USA*, 90:3516-3520, (1993)

Kurz D.J. *et al*., "Chronic oxidative stress compromises telomere integrity and accelerates the onset of senescence in human endothelial cells", *J. Cell Sci.*, 117:2417–2426, (2004)

Lauraa R.P., Rossb S., Koeppenb H., Laskya L.A., "MAGI-1: A Widely Expressed, Alternatively Spliced Tight Junction Protein", *Experimental Cell Research*, 275(2):155-170, (2002)

Li A., Omura N., Hong SM, Vincent A., Walter K., Griffith M., Borges M., Goggins M., "Pancreatic Cancers Epigenetically Silence SIP1 and Hypomethylate and Overexpress miR-200a/200b in Association with Elevated Circulating miR-200a and miR-200b Levels", Cancer Res; 70(13), (2010)

Li G. *et al*., "Allelic loss on chromosome bands 13q11-q13 in esophageal squamous cell carcinoma", *Genes Chromosomes Cancer*, 31:390–397, (2001)

Li J. *et al*., "PTEN, a putative protein tyrosine phosphatase gene mutated in human brain, breast, and prostate cancer", *Science*, 275:1943– 1947, (1997)

Li SP *et al*., "Genome-wide analyses on loss of heterozygosity in hepatocellular carcinoma in Southern China", *J Hepatol*, 34:840–849, (2001)

Li Y.J. *et al*., "Frequent loss of heterozygosity on chromosome 9, and low incidence of mutations of cyclin-dependent kinase inhibitors p15 (MTS2) and p16 (MTS1) genes in gliomas", *Oncogene*, 11:597-600, (1995)

Liew C.T., Li H.M., Lo K.W., Leow C.K., Lau W.Y., Hin L.Y., Lim B.K., Lai P.B., Chan J.Y., Wang X.Q., Wu S., Lee J.C., "Frequent allelic loss on chromosome 9 in hepatocellular carcinoma", *Int J Cancer*, 5:81(3):319-24, (1999)

Lin S.Y. and Elledge S.J., "Multiple tumor suppressor pathways negatively regulate telomerase", *Cell,*113(7):881-889, (2003)

Liu B., *et al*. "A critical role for I kappaB kinase alpha in the development of human and mouse squamous cell carcinomas", *Proc Natl Acad Sci USA*, 103(46):17202–17207, (2006)

Livak K.J. and Schmittgen T.D., "Analysis of Relative Gene Expression Data Using Real-Time Quantitative PCR and the $2^{-\Delta\Delta C}$T Method", *Methods*, 25:402–408, (2001)

Llovet J.M., Chen Y., Wurmbach E., "A molecular signature to discriminate dysplastic nodules from early hepatocellular carcinoma in HCV cirrhosis", *Gastroenterology*, 131:1758–1767, (2006)

Longnecker M.P.,"Alcohol consumption and risk of cancer in humans: an overview", *Alcohol*, 12:87, (1995)

Maeda G., Chiba T., Kawashiri S., Satoh T., Imai K. "Epigenetic inactivation of IkappaB Kinase-alpha in oral carcinomas and tumor progression", *Clin Cancer Res*, 13(17):5041–5047, (2007)

Maher C.A. *et al*., "Transcriptome Sequencing to Detect Gene Fusions in Cancer", *Nature*, 458(7234): 97–101, (2009)

Marrogi A.J. *et al*., "Oxidative stress and p53 mutations in the carcinogenesis of iron overloadassociated hepatocellular carcinoma", *J. Natl Cancer Inst.*, 93:1652–1655, (2001).

Marusawa H., Hijikata M., Chiba T., Shimotohno K., "Hepatitis C virus core protein inhibits Fas- and tumor necrosis factor alpha-mediated apoptosis via NF-kappaB activation", *J Virol.*73:4713, (1999)

Matozaki T. *et al*., "Protein tyrosine phosphatase SHP-2: A protooncogene product that promotes Ras activation", *Cancer Sci*., 100:10, 1786–1793, (2009)

McClain C.J., Hill D.B., Song Z., Deaciuc I. & Barve S., "Monocyte activation in alcoholic liver disease", *Alcohol,* 27:53–61, (2002)
McKillop I.H., Schrum L.W., "Alcohol and liver cancer", *Alcohol*, 35:195, (2005)

McKillop I.H., Moran D.M., Jin X, and Koniaris L.G., "Molecular Pathogenesis of Hepatocellular Carcinoma", *Journal of Surgical Research,* 136:125–135, (2006)

Mejlvang J., Kriajevska M., Vandewalle C., Chernova T., Sayan A.E., Berx G., Mellon J.K., Tulchinsky E., "Direct repression of cyclin D1 by SIP1 attenuates cell cycle progression in cells undergoing an epithelial mesenchymal transition", *Mol Biol Cell*, 18(11):4615-24, (2007)

Mercurio F. *et al*., "IKK-1 and IKK-2: cytokine-activated IkappaB kinases essential for NF-kappaB activation", *Science*, 278: 860–866, (1997)

Midorikawa Y, Yamamoto S, Ishikawa S, Kamimura N, Igarashi H, Sugimura H, Makuuchi M, Aburatani H, "Molecular karyotyping of human hepatocellular carcinoma using single-nucleotide polymorphism arrays", *Oncogene*, 25, 5581–5590 (2006)

Miyoshi A., Kitajima Y., Sumi K., Sato K., Hagiwara A., Koga Y., Miyazaki K., "Snail and SIP1 increase cancer invasion by upregulating MMP family in hepatocellular carcinoma cells", *Br J Cancer*, 90(6):1265-1273, (2004)

Moal DL. F. *et al*. "ZFHX1B Mutations in Patients With Mowat-Wilson Syndrome", *Human Mutation*,28(4):313-321, (2007)

Momand J., Zambetti G.P., Olson D.C., George D., Levin A.J., "The mdm-2 oncogene product forms a complex with the p53 protein and inhibits p53-mediated transactivation", *Cell*, 69: 1237-45, (1992)

Momand J., Jung D., Wilezynski S., Niland J., "The MDM2 gene amplification Database", *Nucleic Acids Res.*, 26:3453–3459, (1998)

Moncur J.T., Park J.P., Memoli V.A., Mohandas T.K., Kinlaw W.B., "The "Spot 14" gene resides on the telomeric end of the 11q13 amplicon and is expressed in lipogenic breast cancers: implications for control of tumor metabolism", *Proc Natl Acad Sci U S A.*, 95(12):6989-94, (1998)

Morishige M. *et al*., "GEP100 links epidermal growth factor receptor signalling to Arf6 activation to induce breast cancer invasion", *Nat Cell Biol.*, 10:85-92, (2008)

Moriya K., Fujie H., Shintani Y., "The core protein of hepatitis C virus induces hepatocellular carcinoma in transgenic mice", *Nat Med*, 4:1065, (1998)

Motoya S., Kitamura K., Matsuda A., Maizel A.L., Yamamoto H., and Takeda A., "Interaction between CD45-AP and protein-tyrosine kinases involved in T cell receptor signaling", *J Biol Chem*, 274: 1407–1414, (1999)

Mowat D.R., Wilson M.J., Goossens M., "Mowat-Wilson syndrome", *Journal of Medical Genetics,*40:305-310, (2003)

Murakami Y. *et al*., "Large scaled analysis of hepatitis B virus (HBV) DNA integration in HBV related hepatocellular carcinomas", *Gut*, 54:1162–1168, (2005)

Nair P., De Preter K., Vandesompele J., Speleman F., Stallings R.L.., "Aberrant splicing of the PTPRD gene mimics microdeletions identified at this locus in neuroblastomas", *Genes Chromosomes Cancer*, 47(3):197-202, (2008)

Nelles L., Van de Putte T., Van Grunsven L., Huylebroeck D., Verschuerena K., "Organization of the mouse Zfhx1b gene encoding the two-handed zinc finger repressor Smad-interacting protein-1", *Genomics*, 82:460-469, (2003)

Nijhara R., Jana S.S., Goswami S.K., Kumar V. & Sarkar D.P., "An internal segment (residues 58–119) of the hepatitis B virus X protein is sufficient to activate MAP kinase pathways in mouse liver", *FEBS Lett.,* 504: 59–64, (2001)

Puisieux A., Ozturk M., "TP53 and hepatocellular carcinoma", *Pathol. Biol. (Paris)*, 45: 864-70, (1997)

Oliner J.D., Pietenpol J.A., Thiagalingam S., Gyuris J., Kinzler K.W., Vogelstein B., "Oncoprotein MDM2 conceals the activation domain of tumour suppressor p53", *Nature*, 362: 857-60, (1993)

Osna N.A., Clemens D.L. & Donohue T.M. Jr., "Ethanol metabolism alters interferon-γ signaling in recombinant HepG2 cells", *Hepatology*, 42:1109–1117 (2005)

Ostman, A. & Böhmer, F. D., "Regulation of receptor tyrosine kinase signaling by protein tyrosine phosphatases", *Trends Cell Biol.*, 11: 258–266, (2001)

Ostman A., Hellberg C. and Böhmer F.D., "Protein-tyrosine phosphatases and cancer", *Nature Reviews, Cancer*, 6: 307-320, (2006)

Oztas E., Avci M.E., Ozcan A., Sayan A.E., Tulchinsky E., Yagci T., "Novel monoclonal antibodies detect Smad-interacting protein 1 (SIP1) in the cytoplasm of human cells from multiple tumor tissue arrays" *Exp. Mol. Pathol.*, doi:10.1016/j.yexmp.2010.05.010, (2010)

Ozturk M., "Genetic aspects of hepatocellular carcinogenesis", *Semin. Liver Dis.*, 19: 235-42, (1999)

Ozturk N., Erdal E, Mumcuoglu M, Akcali K.C., Yalcin O., Senturk S., Arslan-Ergul A., Gur B., Yulug I., Cetin-Atalay R., Yakicier C., Yagci T., Tez M., Ozturk M., "Reprogramming of replicative senescence in hepatocellular carcinoma-derived cells", *PNAS*,103: 2178–2183, (2006)

Ozturk M., "p53 mutation in hepatocellular carcinoma after aflatoxin exposure", *Lancet*, 338:1356–1359, (1991)

Park SM., Gaur A.B., Lengyel E., "The miR-200 family determines the epithelial phenotype of cancer cells by targeting the E-cadherin repressors ZEB1 and ZEB2", *Genes and Development*, 22:894–907, (2008)

Parkin, D.M., Bray, F.I., Devesa, S.S., "Cancer burden in the year 2000. The global picture", *Eur. J. Cancer*, 37, S4–S66 (2001).

Penninger J.M., Irie-Sasaki J., Sasaki T., and Oliveira-dos-Santos A.J., "CD45: new jobs for an old acquaintance", *Nat Immunol* 2: 389–396, (2001)

Pfau R., Tzatsos A., Kampranis S.C., Serebrennikova O.B., Bear S.E. and Tsichlis P.N., "Members of a family of JmjC domain-containing oncoproteins immortalize embryonic fibroblasts via a JmjC domain-dependent process", *PNAS*, 105(6): 1907–1912, (2008)

Ploner C., Kofler R. and Villunger A., "Noxa: at the tip of the balance between life and death" *Oncogene*, 27:84–92, (2009)

Ponder B.A., "Cancer genetics", *Nature*, 411:336–341, (2001)

Polakis P., "Wnt signaling and cancer", *Genes Dev.*, 4(15):1837-51, (2000)

Puisieux A., Ozturk M., "TP53 and hepatocellular carcinoma", *Pathol. Biol. (Paris)* 45:864–870, (1997)

Purdie K.J., Lambert S.R., Teh M.T., Chaplin T., Molloy G., Raghavan M., Kelsell D.P., Leigh I.M., Harwood C.A., Proby C.M., Young B.D., "Allelic imbalances and microdeletions affecting the PTPRD gene in cutaneous squamous cell carcinomas detected using single nucleotide polymorphism microarray analysis", *Genes Chromosomes Cancer*, 46(7):661-9, (2007)

Ray R.B., Lagging L.M., Meyer K., Steele R., Ray R., “Transcriptional regulation of cellular and viral promoters by the hepatitis C virus core protein", *Virus Res*,37:209, (1995)

Rehermann B. & Nascimbeni M., “Immunology of hepatitis B virus and hepatitis C virus infection”, *Nature Rev. Immunol.*, 5:215–229, (2005)

Reifenberger G., Liu L., Ichimura K., Schmidt E.E., Collins V.P., “Amplification and overexpression of the MDM2 gene in a subset of human malignant gliomas without p53 mutations”, *Cancer Res.*, 53:236–239, (1993)

Riley J., Mandel H.G., Sinha S., Judah D.J. & Neal G.E., “In vitro activation of the human Harvey-ras protooncogene by aflatoxin B1”, *Carcinogenesis,* 18:905–910, (1997).

Rodenhiser D.I. *et al*., “Epigenetic mapping and functional analysis in a breast cancer metastasis model using whole-genome promoter tiling microarrays” *Breast Cancer Research*, 10:4, (2008)

Rosivatz E., Becker I., Specht K., Fricke E., Luber B., Busch R., Höfler H., Becker K.F., “Differential expression of the epithelial-mesenchymal transition regulators snail, SIP1, and twist in gastric cancer”, *Am J Pathol.*, 161(5):1881-91, (2002)

Rudolph KL, Chang S, Millard M, Schreiber-Agus N, DePinho RA., “Inhibition of experimental liver cirrhosis in mice by telomerase gene delivery”, *Science,*287:1253–1258, (2000)

Sabe H. *et al*., “The EGFR-GEP100-Arf6-AMAP1 Signaling Pathway Specific to Breast Cancer Invasion and Metastasis”, *Traffic*, 10:982–993, (2009)

Sakamuro D., Furukawa T., Takegami T., “Hepatitis C virus nonstructural protein NS3 transforms NIH 3T3 cells”, *J Virol*; 69:3893, (1995)

Sakata K. *et al*., “Loss of heterozygosity on the short arm of chromosome 9 without p16 gene mutation in gastric carcinomas”, *Jpn J Cancer Res,* 86:333-335, (1995)

Sanchez-Carbayo M., Socci N.D., Kirchoff T., Erill N., Offit K., Bochner B.H., Cordon-Cardo C., “A polymorphism in HDM2 (SNP309) associates with early onset in superficial tumors, TP53 mutations and poor outcome in invasive bladder cancer”, *Clin. Cancer Res.*, 13:3215–3220, (2007)

Sato M., Takahashi K., Nagayama K., Arai Y., Ito N., Okada M., Minna J.D., Yokota J., and Kohno T., ”Identification of chromosome arm 9p as the most frequent target of homozygous deletions in lung cancer”, *Genes Chromosomes. Cancer*,44: 405-414, (2005)

Schubbert S., Shannon K. & Bollag G., “Hyperactive Ras in developmental disorders and cancer”, *Nature Reviews Cancer*, 7:295-308, (2007)

Schuuring E., “The involvement of the chromosome 11q13 region in human malignancies: Cyclin D1 and EMS1 are two new candidate oncogenes-a review”, *Gene*, 159(1):83-96, (1995)

Shay W.J. and Roninson I.B., “Hallmarks of senescence in carcinogenesis nad cancer therapy”, *Oncogene*, 23:2919-2933 (2004)
Simpson L., Parsons R., “PTEN: life as a tumor suppressor”, *Exp. Cell Res.*, 264:29–41, (2001)

Sivarajasingham N.S., Baker R., Tilsed J.V., Greenman J., Monson J.R., Cawkwell L. “Identifying a region of interest in site- and stage-specific colon cancer on chromosome 13”, *Ann Surg Oncol*, 10:1095–1099, (2003)

Sjoblom T., “The Consensus Coding Sequences of Human Breast and Colorectal Cancers” Science 314: 268 (2006)

Smela *et al*., “The chemistry and biology of aflatoxin B(1): from mutational spectrometry to carcinogenesis”, *Carcinogenesis*, 22(4):535–45, (2001)

Someya A., Moss J., Nagaoka I., “Involvement of a guanine nucleotide-exchange protein, ARF-GEP100/BRAG2a, in the apoptotic cell death of monocytic phagocytes”, *J Leukoc Biol.*, 80:915-21, (2006)

Solomon D.A., Kim J.S., Cronin J.C., Sibenaller Z., Ryken T., Rosenberg S.A., Ressom H., Jean W., Bigner D., Yan H., Samuels Y., Waldman T., “Mutational inactivation of PTPRD in glioblastoma multiforme and malignant melanoma”, *Cancer Res.*, 68:10300-6, (2008)

Stallings R.L., Nair P., Maris J.M., Catchpoole D., McDermott M., O'Meara A., Breatnach F., “High-resolution analysis of chromosomal breakpoints and genomic instability identifies PTPRD as a candidate tumor suppressor gene in neuroblastoma”, *Cancer Res.*, 1:66(7):3673-80, (2006)

Stark M. and Hayward N., “Genome-wide loss of heterozygosity and copy number analysis in melanoma using high-density single-nucleotide polymorphism arrays. Cancer Res. 67, 2632–2642, (2007)

Summy J.M. and Gallick G.E., “Src family kinases in tumor progression and metastasis”, *Cancer Metastasis Rev*, 22:337–358, (2003)

Sotamaa K., Liyanarachchi S., Mecklin J.P., Jarvinen H., Aaltonen L.A., Peltomaki P, Chapelle de la A., “p53 codon 72 and MDM2 SNP309 polymorphisms and age of colorectal cancer onset in Lynch syndrome”, *Clin. Cancer Res.*, 11:6840-44, (2005)

Su AI, *et al*., "A gene atlas of the mouse and human protein-encoding transcriptomes", *Proc Natl Acad Sci U S A*, 20;101(16):6062-7, (2004)

Sutton A., Nahon P., Pessayre D., Rufat P., Poire A., Ziol M., Vidaud D., Barget N., Ganne-Carrie N., Charnaux N., Trinchet J.C., Gattegno L., Beaugrand M., "Genetic polymorphisms in antioxidant enzymes modulate hepatic iron accumulation and hepatocellular carcinoma development in patients with alcohol-induced cirrhosis", *Cancer Res.*, 66: 2844-52, (2006)

Takeda A., Matsuda A., Paul R.M., and Yaseen N.R. "CD45-associated protein inhibits CD45 dimerization and up-regulates its protein tyrosine phosphatase activity", *Blood*, 103: 3440–3447, (2004)

Tamura K., Zhang X., Murakami Y., Hirohashi S., Xu HJ., Hu SX., Benedict W.F., Sekiya T. "Deletion of three distinct regions on chromosome 13q in human non-small-cell lung cancer", *Int J Cancer*, 74:45–49,(1997)

Tanaka Y., "JmjC enzyme KDM2A is a regulator of rRNA transcription in response to starvation", *The EMBO Journal* , 1–13, (2010)

Tanigami A., Tokino T., Takita K., Takiguchi S. and Nakamura Y. "A 14-Mb physical map of the region at chromosome 11q13 harboring the MEN 1 locus and the tumor amplicon region", *Genomics*, 13(1): 16-20, (1992)

Tanigami A, Tokino T, Takita K, Ueda M, Kasumi F, Nakamura Y., "Detailed analysis of an amplified region at chromosome 11q13 in malignant tumors", *Genomics*, 13(1):21-4, (1992)

Tapparel C. *et al*., "The TPTE gene family: cellular expression, subcellular localization and alternative splicing", *Gene*, 323:189–199, (2003)

Tarn C., Lee S., Hu Y., Ashendel C. & Andrisani O.M., "Hepatitis B virus X protein differentially activates RASRAF-MAPK and JNK pathways in X-transforming versus non-transforming AML12 hepatocytes", *J. Biol. Chem.*, 276:34671–34680 (2001).

Tartaglia M. *et al*., "Diversity and Functional Consequences of Germline and Somatic PTPN11 Mutations in Human Disease", *Am. J. Hum. Genet.*, 78, 279–290, (2006)

Tartaglia M., Gelb B. D., "Germ-line and somatic PTPN11 mutations in human disease", *European Journal of Medical Genetics*, 48, 81–96, (2005)

Thorgeirsson S.S. & Grisham J.W., "Molecular pathogenesis of human hepatocellular carcinoma", *Nature Genetic,*31, 339-346, (2002)

Tischoff I., Tannapfel A., "DNA methylation in hepatocellular carcinoma", *World J. Gastroenterol.*,14(11):1741-1748, (2008)

Tokino T., Tamura H., Hori N. & Matsubara K. "Chromosome deletions associated with hepatitis B virus integration", *Virology*, 185: 879–882, (1991).

Turner P.C., Sylla A., Diallo M.S., Castegnaro J.J., Hall A.J., Wild C.P., "The role of aflatoxins and hepatitis viruses in the etiopathogenesis of hepatocellular carcinoma: A basis for primary prevention in Guinea-Conakry, West Africa", *J Gastroenterol Hepatol,* 17(Suppl):S441–S448, (2002)

Ueda H. *et al*., "Functional inactivation but not structural mutation of p53 causes liver cancer", *Nature Genet*., 9:41–47, (1995)

Unsal H., Yakicier M.C., Marcais C., Kew M., Volkmann M., Zentgraf H., K.J. Isselbacher, Ozturk M., "Genetic heterogeneity of hepatocellular carcinoma", *Proc. Natl. Acad. Sci. USA*, 91:822-26, (1994)

Urushibara N., Karasaki H., Nakamura K., Mizuno Y., Ogawa K., Kikuchi K., "The selective reduction in PTPdelta expression in hepatomas", *Int. J. Oncol.* 12(3):603-7, (1998)

Valderrama F. and Ridley A.J., "Getting invasive with GEP100 and Arf6", *Nature Cell Biology*, 10(1):16-18, (2008)

Van de Putte T., Maruhashi M., Francis A., Nelles L., Kondoh H., Huylebroeck D., Higashi Y., "Mice Lacking Zfhx1b, the Gene That Codes for Smad-Interacting Protein-1, Reveal a Role for Multiple Neural Crest Cell Defects in the Etiology of Hirschsprung Disease–Mental Retardation Syndrome", *American Journal of Human Genetics*, 72:465-470, (2003)

Van der Riet P. *et al*., "Frequent loss of chromosome 9p21-22 early in head and neck cancer progression", *Cancer Res*, 54:1156-1158, (1994)

Vandewalle C., Van Roy F., Berx G., " The role of the ZEB family of transcription factors in development and disease", *Cell. Mol. Life Sci.*,66: 773 – 787, (2009)

Veeriah S., The tyrosine phosphatase PTPRD is a tumor suppressor that is frequently inactivated and mutated in glioblastoma and other human cancers, Proc Natl Acad Sci USA, 106:9435-40, (2009)

Veillette A., Soussou D., Latour S., Davidson D. and Gervais F.G., "Interactions of CD45-associated protein with the antigen receptor signaling machinery in T-lymphocytes", *J Biol Chem*, 274: 14392–14399, (1999)

Verschueren K., Remacle J.E., Collart C., Kraft H., Baker B.S., Tylzanowski P., Nelles L., Wuytens G., Su MT, Bodmer R, Smith J.C., Huylebroeck D., "SIP1, a Novel Zinc Finger/Homeodomain Repressor, Interacts with Smad Proteins and Binds to 5'-CACCT Sequences in Candidate Target Genes", *The Journal of Biological Chemistry*, 274(29):20489-20498, (1999)

Vila A.M. *et al*., "Development of a new magnetic beads-based immunoprecipitation strategy for proteomics analysis", *J Prot*, doi:10.1016/j.jprot.2010.02.015, (2010)

Vogel A., Kneip S., Barut A., Ehmer U., Tukey R.H., Manns M.P., Strassburg C.P., "Genetic link of hepatocellular carcinoma with polymorphisms of the UDP-glucuronosyltransferase UGT1A7 gene", *Gastroenterology*, 121:1136-44, (2001)

Wakamatsu N. *et al*., "Mutations in SIP1, encoding Smad interacting protein-1, cause a form of Hirschsprung disease", *Nature Genetics,* 27:369-370 (2001)

Walker S.M., Downes C.P., Leslie N.R., "TPIP: a novel phosphoinositide 3-phosphatase", *Biochem. J.*, 360,:277– 283, (2001)

Wang J., Xie L.Y., Allan S., "Myc activates telomerase", *Genes and Development*, 12:1769-1774, (1998)

Weir B.A. *et al*., "Characterizing the cancer genome in lung adenocarcinoma" Nature, 450(7171): 893–898, (2007)

Wu Y. *et al*., "Interaction of the Tumor Suppressor PTEN/MMAC with a PDZ Domain of MAGI3, a Novel Membrane-associated Guanylate Kinase", *The Journal of Biological Chemistry*, 275:21477-21485, (2000)

Yakicier M.C., Irmak M.B., Romano A., Kew M., Ozturk M., "Smad2 and Smad4 gene mutations in hepatocellular carcinoma", *Oncogene*, 18:4879-4883, (1999)

Yali H. *et al*., "MAGI-2 Inhibits cell migration and proliferation via PTEN in human hepatocarcinoma cells", *Archives of Biochemistry and Biophysics*, 467:1–9, (2007)

Yamada K. *et al*., "Nonsense and Frameshift Mutations in ZFHX1B, Encoding Smad-Interacting Protein 1, Cause a Complex Developmental Disorder with a Great Variety of Clinical Features", *American Journal of Human Genetics*, 69:1178-1185, (2001)

Yoon Y.J., Chang H.Y., Ahn S.H., Kim J.K., Park Y.K., Kang D.R., Park J.Y., Myoung S.M., Kim do Y., Chon C.Y., Han K.H., "MDM2 and p53 polymorphisms are associated with the development of hepatocellular carcinoma in patients with chronic hepatitis B virus infection", *Carcinogenesis*, 29:1192–1196, (2008)

Yu D.Y. *et al*., "Incidence of hepatocellular carcinoma in transgenic mice expressing the hepatitis B virus X-protein", *J. Hepatol.*, 31:123–132, (1999)

Yu J, Ni M, Xu J, Zhang H, Gao B, Gu J, Chen J, Zhang L, Wu M, Zhen S, Zhu J. "Methylation profiling of twenty promoter-CpG islands of genes which may contribute to hepatocellular carcinogenesis", *BMC Cancer*, 2: 29, (2002)

Yu M.W., Yang S.Y., Chiu Y.H., Chiang Y.C., Liaw Y.F., Chen C.J., "A p53 genetic polymorphism as a modulator of hepatocellular carcinoma risk in relation to chronic liver disease, familial tendency, and cigarette smoking in hepatitis B carriers", *Hepatology*, 29: 697-702, (1999)

Yuan BZ, Zhou X, Zimonjic D.B., Durkin M.E., Popescu N.C., "Amplification and overexpression of the EMS 1 oncogene, a possible prognostic marker, in human hepatocellular carcinoma", *J Mol Diagn*, 5:48-53, (2003)

Zandi E., Rothwarf D.M., Delhase M., Hayakawa M., Karin M., "The IkappaB kinase complex (IKK) contains two kinase subunits, IKKalpha and IKKbeta, necessary for IkappaB phosphorylation and NF-kappaB activation", *Cell*, 91:243–252, (1997)

Zhang Y.J., Jiang W., Chen C.J., Lee C.S., Kahn S.M., Santella R.M. and Weinstein I.B., "Amplification and Overexpression of Cyclin D1 in Human Hepatocellular Carcinoma", *Biochemical and Biophysical Research Communications*, 196:2:1010-1016, (1993)

Zhang X. *et al*., "Deletions of chromosome 13q, mutations in Retinoblastoma 1, and retinoblastoma protein state in human hepatocellular carcinoma", *Cancer Res.*,*54*: 4177-4182, (1994)

Zhao X *et al*., "Homozygous deletions and chromosome amplifications in human lung carcinomas revealed by single nucleotide polymorphism array analysis", *Cancer Res.*, 65(13):5561-70, (2005)

Zimonjic D.B., Keck C.L., Thorgeirsson S.S., Popescu N.C., "Novel Recurrent Genetic Imbalances in Human Hepatocellular Carcinoma Cell Lines Identified by Comparative Genomic Hybridization", *Hepatology,* 29(4):1208-1214, (1999)

Xiao WH, Liu WW, "Hemizygous deletion and hypermethylation of RUNX3 gene in hepatocellular carcinoma", *World J Gastroenterol*, 10(3):376-380, (2004)

Xu J.G. *et al*., "β_1-Adrenergic Receptor Association with the Synaptic Scaffolding Protein Membrane-associated Guanylate Kinase Inverted-2 (MAGI-2) Differential Regulation Of Receptor Internalization By Magi-2 And Psd-95", *The Journal of Biological Chemistry*, 276, 41310-41317, (2001)

Xu X.R., Huang J., Xu Z.G., Qian B.Z., Zhu Z.D., Yan Q., “Insight into hepatocellular carcinogenesis at transcriptome level by comparing gene expression profiles of hepatocellular carcinoma with those of corresponding noncancerous liver”, *Proc Natl Acad Sci USA,*98:15089-15094, (2001)

APPENDICES :

A. Primers Used In This Study

Primers Used To Analyse SIP1 (ZEB2) (NCBI GeneID:9839)				
Primer	**Bp**	**Sequence**	**Tm (C°)**	**Product Size (bp)**
Sip1F	20	caatgatggcactctgtgga	60.69	416
Sip1R	21	tgccaatcaaagcaatatcgt	60.47	
Sip2F	21	ctcaaacctttggcctgtct	60.65	538
Sip2R	20	tgccagttgagtttcctcag	59.01	
Sip3F	20	tggttcctacagttcgcaca	60.30	569
Sip3R	20	cgacaggcggaatattagga	60.05	
Sip4F	22	tgcagcctcatgaaaacatagt	59.77	439
Sip4R	20	agcctgagaggaggatcaca	59.94	
SE2F	23	tccctcatacggtcaggagttat	61.07	509
SE2R	20	cctcggttccttttcccttt	61.64	
SE3F	20	caattaggggtggctgatgt	59.81	415
SE3R	20	tatttggttgtgggcgatct	60.33	
SE4F	21	ttgtcactagaactgccacca	59.35	422
SE4R	20	tccttccctgcctcactaaa	59.81	
SE5F	23	atcggtcatcttcaacacttctt	59.16	422
SE5R	20	aggtaaacacccaggcatgt	59.33	
SE81F	21	ggtaccccattgtgttccttt	59.97	729
SE81R	20	cgacaggcggaatattagga	60.05	
SE82F	21	tctcaacctgaggaacaagga	59.83	543
SE82R	21	tttcagcagttcatcggagtt	59.87	
SE83F	23	tcaccatctatagcagaactcca	58.87	722
SE83R	23	aatcaaaataattgccacctctt	58.17	
SE9F	21	tgaagttgtttggtgtgagca	60.33	395
SE9R	20	agtcctactgagctcggcaa	60.16	
SE10F	23	agtggaaagagacttcatgcaaa	60.29	705
SE10R	25	cagtgttttcaagcaggtaacaata	59.66	
SIPM1dF	26	agaaaggagaacgtaggaaatgtaat	59.13	854
SIPM1dR	23	cccaacaaaacgaccaactaaaa	62.21	
SIPM1iF	25	aaggagggttagagggaggaaaagt	63.87	678
SIPM1iR	26	ccaacaaacttcaaaacccaaataaa	63.20	

SIPM1dF	26	agaaaggagaacgtaggaaatgtaat	59.13	369
SIPM1iyR1	29	aaaaataataccgaaaactaattaccata	57.6	
SIPM1iF	25	aaggagggttagagggaggaaaagt	63.87	296
SIPM1iyR1	29	aaaaataataccgaaaactaattaccata	57.6	
SIPM2dF	27	aagagaaagggtagagaattttgtttt	59.58	898
SIPM2dR	24	aaactcacatccccactcaaaata	60.95	
SIPM2iF	27	aagaagagattatttggattgaggatt	60.11	601
SIPM2iR	25	aacaactcccgaaacaaactataca	60.20	
SIPM2iyF1	20	gaggaggaagggagggaggt	63.13	380
SIPM2iR	25	aacaactcccgaaacaaactataca	60.20	
SIPM2iyF1	20	gaggaggaagggagggaggt	63.13	281
SIPM2iyR2	24	actccaaaaaacacaaacctaaaa	58.3	
SIPM3dF	26	ttagtaaatgtgtggaaattgatatt	55.43	800
SIPM3dR	24	cttttcgttctcatctttctcat	58.16	
SIPM3iF	23	cggtagagaaagggttaatggtt	59.79	631
SIPM3iR	25	aaacaacccctaaataaaacacact	58.49	
SIPM4dF	26	gagtgtgttttatttaggggttgttt	59.98	594
SIPM4dR	21	gcctcttacaccgaaaaccat	60.37	
SIPM4iF	26	atgagaaaagatgagaacgaaaagaa	60.90	418
SIPM4iR	26	aaactcgatctaacaaccaaacacaa	62.18	
SIPM5dF	26	ttgtgtttggttgttagatcgagttt	62.18	914
SIPM5dR	25	aaataacgaactcctccaaaccata	61.21	
SIPM5iF	27	ttaggaggaaaaacggtaagaagtagt	60.30	474
SIPM5iR	25	ctctcctaccttcgcaatctctcta	61.62	
SIPM6dF	25	tagagagattgcgaaggtaggagag	61.62	402
SIPM6dR	26	ccctttaatatcccacctctaatcta	59.28	
SIPM7dF	25	tatggtttggaggagttcgttattt	61.21	770
SIPM7dR	24	cgtacacacacacaaaacctaaaa	59.07	
SIPM7iF	26	ggttcgttttggagatagttagagaa	60.38	557
SIPM7iR	23	actccttccaacacctcacacta	60.08	
Sip1RTF	24	tgtagatggtccagaagaaatgaa	60.00	132
Sip1RTR	24	ttggcaaagtattcctcaaaatct	60.34	

Primers Used to Analyse ZNF198 (ZMYM2) (NCBI GeneID:7750)				
Primer	**Bp**	**Sequence**	**Tm (C°)**	**Product Size (bp)**
ZNF1981F	20	tgtacccctgaaaggaggtg	60	1550
ZNF1981R	20	cgctatgtggcctagactgg	60.8	
ZNF198Ycd1F	21	tgtgaatgatggccaattaga	59	523
ZNF198cd1R	19	ctttggagcaggcttgtgg	62	
ZNF198cd2F	25	cagcagcctactaaaccagttaaag	60	838
ZNF198cd2R	20	gcattgtggcttggtattga	59.6	
ZNF198cd3F	22	ggagccatattgttcaactgct	60.5	749
ZNF198cd3R	20	tgttgggctcattttgttga	60.1	
ZNF198cd4F	22	gattggtactacaaggctgcaa	59.3	839
ZNF198cd4R	20	ggtctgggctgttcctcata	60	
ZNF198cd5F	23	aagaactctgacccagagacaca	60.3	1307
ZNF198cd5R	20	gcgtgggtacactgctacaa	59.8	

Primers Used To Analyse Genomic Deletion/s in PTPRD Gene (NCBI GeneID:5789)				
Primer	**Bp**	**Sequence**	**Tm (C°)**	**Product Size (bp)**
PTPRD2F*	23	gtctgtcatggtgattgtgatgg	62.56	455
PTPRD2R*	22	aggaaatggtgaggaagtcacg	62.66	
PTPRD3F*	20	gtgtggttgaggatggtggg	63.62	457
PTPRD3R*	22	gagccctggcacaagtagaaac	62.38	
PTPRD4F*	23	cggatccaccactgtattgagag	63	329
PTPRD4R*	23	cccatttaagcaccatcacaatg	63.5	
PTPRD5F*	24	ggaatctcttgaatttggagcatc	62.38	417
PTPRD5R*	22	gacatcacaaacatggaccacc	62.43	
PTPRD6F	21	ctcagcttttgacctgtcctg	60	467
PTPRD6R	20	tgctacattggtgtgccata	58.6	
PTPRD7F	20	tgcctattgcggtctttacc	60.1	341
PTPRD7R	20	tggaatgacgctgaaaacag	59.8	
PTPRD8F*	22	cttccttgaagcagtctcaccc	62.55	508
PTPRD8R*	21	tataacaacacggaccctgcg	63	
PTPRD9F*	24	ttcaagtagcagttgaaagccttg	62	294
PTPRD9R*	21	agataccaccagcaagcacca	63	
PTPRD10F*	21	tgaatcgtgtctgtacggtgc	62	444
PTPRD10R*	24	tttcaaggatgggctttctagagg	64	
PTPRD11F1	23	ccttctaggaaagcaggatttgt	60.13	573
PTPRD11R1	23	ctcttcaggttccttccactgta	59.80	
PTPRD11F2	23	gaacctgtgctaacacaaacctc	60	402
PTPRD11R2	23	tttgtttttgtccttctcacctc	59.7	
PTPRD12F*	23	cgaaaggtttaagcaggttacgc	63.25	440
PTPRD12R*	22	cccaaagcctccaaataaccac	63.82	
PTPRD13F	20	tggcctctcaatcttcgtct	60	640
PTPRD13R	20	tgggaaggtgggatctgtta	60.3	
PTPRD14F	25	ttcattttgtccttattgttcgttt	60.15	689
PTPRD14R	20	gcaagaccataggagccaac	59.70	

Primer	Bp	Sequence	Tm (C°)	Product Size (bp)
PTPRD15F*	22	gaaaatgctctgatagggtggg	62	457
PTPRD15R*	25	tgtcatttcattacaattcccttcc	62.3	
PTPRD16F*	23	gcagcaaatcacacattctttgg	64	383
PTPRD16R*	22	tacgcagtcaatagcaccatgc	63.3	
PTPRD17F*	22	ctacctcccaagatgcctgaag	62.3	447
PTPRD17R*	27	ttgaccatagtccatttatttcctctg	62.6	
PTPRD18F1	24	tccacaaaggtatgtaggtcaaac	59.3	913
PTPRD18R	22	tgaaatctaaggcatccaagac	58.3	
PTPRD19F*	22	ttggctgaattggagagaaagg	62.8	391
PTPRD19R*	21	aaagtggtctgcttgctgtgc	62.8	
PTPRD20F*	23	ttccaaaagctagtgcacattgg	63.5	493
PTPRD20R*	22	tcggatagcaaaactgggagtc	62.7	
PTPRD21F	20	ccacgttttcctcctttcaa	60	296
PTPRD21R	20	ttagcatgcccatagcactg	60	
PTPRD22F*	22	caaattgcatttgggttgttcc	63.45	395
PTPRD22R*	22	tccccaaataaccacattccag	63	
PTPRD23F	26	ttacaaaacatcttccatcctttctt	60.6	436
PTPRD23R*	23	caaccacctaaggacagcagaac	62.3	
PTPRD24F*	21	cgaactgggtcacaagtcagc	63.17	465
PTPRD24R*	22	tttcttccctacccaatttccg	63.37	
PTPRD25F*	21	gcttggtgacttttcatttgg	59.6	474
PTPRD25R*	23	gtgcagacacttttaagttgacg	59	
PTPRD26F*	26	tggtggttttcagtattgattttgtg	63.14	462
PTPRD26R*	24	tcctgagtagctgggattacaggc	65	
PTPRD27F*	24	ttaggtcatgtcccaggctgtttc	65.6	468
PTPRD27R*	24	gcaaccacacacatcataacatgg	64.4	
PTPRD28F*	23	ttccttcaacagcaactcaaagc	63	327
PTPRD28R*	23	ttcattcttcactgttgccattg	62.3	
PTPRD29F*	22	gtgtcttcccaaaggctacagg	62.2	433
PTPRD29R	20	gcataggcctcatttgacca	61	

Primer	Bp	Sequence	Tm (C°)	Product Size (bp)
PTPRD30F	21	ttccctgtcctctgattatgg	59	602
PTPRD30R	20	cacctgagggaaaggtcaaa	60	
PTPRD31F	20	ctggggtacactgcattcaa	59.6	389
PTPRD31R	21	ccaagggactaaatgatgacc	58.4	
PTPRD32F*	21	gcaatttagtttgcgaagtcc	59	456
PTPRD32R	20	atggtccggattatgtccag	59.6	
PTPRD33F*	24	tactatctgccagagaccgtgctg	65	466
PTPRD33R*	24	caacagtcaagtggcaagtgcttc	65.4	
PTPRD34F*	23	tgattgttcttgtggtccgtatg	62	437
PTPRD34R*	23	tttggggctaaacattttcctct	62.20	
PTPRD35F*	23	gctggtagaagtatgtccacacc	60	305
PTPRD35R*	21	ttgagagagtatggagtccgg	59.3	
PTPRD36F*	24	ttggtcattggattagaccagttg	62.3	447
PTPRD36R*	24	gcctcatcagtcaggattctcttc	62.8	

(*) These primer sequences were obtained from Weir B.A. et al. (2007)

Bisulfite PCR Primers Used for the Analysis of PTPRD Promoter				
Primer	Bp	Sequence	Tm (C°)	Product Size (bp)
ptprdBi1F	20	tcgggattcgtatttggatt	59.23	353
ptprdBi1R	25	catttccttaacgaaccacttaata	57.91	
ptprdBi2F	27	ggggaatagtttgtgtttgatatattt	59.03	132
ptprdBi2R	21	ccaccgacccaaaactaccta	61.12	

Primers Used For Mutation Analysis of PTPRD cDNA				
Primer	**Bp**	**Sequence**	**Tm (C°)**	**Product Size (bp)**
PTPRDcd1F	20	cccgtgggatctaaagaaca	60	580
PTPRDcd1R	20	attaccactggctgcacaaa	59.2	
PTPRDcd2F	21	agttttgcgggaagatcaaat	60	595
PTPRDcd2R	21	ttcaatgacacccagtgttga	60	
PTPRDcd3F	24	ggtcaccaatgccttatgtaaagt	60.5	517
PTPRDcd3R	21	gtggtcgaactcaacattcgt	60.03	
PTPRDcd4F	23	gggttgttgctgtcaataacatt	60.16	691
PTPRDcd4R	20	cttgggctggtgcaactaat	60.13	
PTPRDcd5F	21	ctgcaaggactgaaaccaaac	59.8	784
PTPRDcd5R	20	ggttaatcacaagccgaggt	59	
PTPRDcd6F	21	aaagatgtcatgctggctgat	59.7	827
PTPRDcd6R	20	ggaatctcccaagacagcaa	60.2	
PTPRDcd7F	24	catatagtcccagtgtccagttca	60.3	724
PTPRDcd7R	20	gggctggttgcatacatctt	60	
PTPRDcd8F	23	atcccaggaagtgactatgtgaa	60	730
PTPRDcd8R	20	attcgagctccattcctgtg	60.2	
PTPRDcd8YF	20	gcatccgttatgggagagaa	60	788
PTPRDcdYR	20	tctccaaaagtccccaaatg	60	
PTPRDcd9F	22	ccatgatgcactgttagaagca	61.2	1004
PTPRDcd9R	20	aagtgccctgtatggctcag	60.3	

Primers Used To Analyse MDM2 (NCBI GeneID:4193)				
Primer	**Bp**	**Sequence**	**Tm (C°)**	**Product Size (bp)**
MDM2-F	19	gctttgcggaggttttgtt	60,24	304
MDM2-R	20	cggaacgtgtctgaacttga	59,87	

Primers Used to Analyse Chromomose 13q12 Region						
Gene	**NCBI GeneID**	**Primer**	**Bp**	**Sequence**	**Tm (C°)**	**Product Size (bp)**
BC067875	348021	BC06 F	20	aaggaaatgcaagacgatgg	60	302
		BC06 R	20	ccctctgccttctctgtcac	60	
NR_002801	266695	NR02 F	20	gcatctgtgccacgctcact	64.9	639
		NR02 R	20	gcttccccatgtaccagcag	62.9	
TUBA3C	7278	TUBA3C F	19	catcggcaaggagatcgtc	61.75	835
		TUBA3C R	20	gggctgggtaaatggcaaat	63.11	
HSMPP8	54737	HSMPP8 F	20	ggctctgtggaccgtgtagt	60.18	988
		HSMPP8 R	20	agagggtgcttctgtcaacc	59.30	
ZMYM5	9205	ZMYM5 F	20	gccaggggtggattctttat	60.15	1182
		ZMYM5 R	21	ttcttggaaggatttgcttga	59.81	
ZMYM2	7750	ZMYM2 F	20	cttgtactggttgccgaaca	59.7	650
		ZMYM2 R	21	acagttttccatcaggcattg	60	
CRYL1	51084	CRYL1 F	20	ctgcgacagatacagcgaag	59.76	579
		CRYL1 R	20	cttcaacttggcgagtctca	59.16	
IFT88	8100	IFT88 F	20	tgaaatgtatgccgaagcac	58.69	853
		IFT88 R	20	tggtctaatgccattcggta	59.69	
EFHA1	221154	EFHA1 F	20	tgctattgccatgcagatgt	60.25	941
		EFHA1 R	21	ccataaacctcgatgcattct	59.06	

RT-PCR Primers Used to Analyse TPTE2 (NCBI GeneID:93492)				
Primer	**Bp**	**Sequence**	**Tm (C°)**	**Product Size (bp)**
TPTE2F	24	ctaagcacttccataatagggtca	58.78	150
TPTE2R	21	tgcctcctttacagtgaatcg	60.26	

Primers Used To Analyse FBXL11 Mutations (NCBI GeneID:22992)				
Primer	**Bp**	**Sequence**	**Tm (C°)**	**Product Size (bp)**
FBXLex10F	24	agaagcagaatcagagtgaagagt	58	369
FBXLex10R	21	tgtgtgttcccaaaatgtcaa	59.85	
FBXLex11F	20	gtttgcaggttgactggtga	59.7	4170
FBXLex12R	26	cacacatgcatattaacttctctctg	59.3	
FBXLex13F	21	attgcagcagcctaagtttga	60	3513
FBXLex15R	20	tcctcagggtctaacgcagt	60	
FBXLex16F	21	gttcctgagggaaagtgaagg	60.1	2922
FBXLex17R	21	cactcctcataagaccccaca	60	
FBXLex18F	21	ttgtagaagaacgagcctcca	60	2648
FBXLex21R	20	tggtgtccaccaccctctct	63	
FBXLex14F	20	gaaacaagcagtgggcagat	60.3	
FBXLex17F	20	tcttctctctggtcccctga	60	
FBXLex19F	23	gactggaagtttgttcactttgc	60.2	
FBXLex20F	20	ggagccttgaagctggatta	59.4	

Primers Used For Normalization and Internal Control in the Q-Real-Time RT-PCR and Semi-Quantitative RT-PCR, respectively						
Gene	**NCBI GeneID**	**Primer**	**Bp**	**Sequence**	**Tm (C°)**	**Product Size (bp)**
GAPDH	2597	GAPDH RT F	22	agtcaacggatttggtcgtatt	59.8	611
		GAPDH RT R	22	gtagaggcagggatgatgttct	59.6	
		GAPDH_070228_cDNA_F	24	ggctgagaacgggaagcttgtcat	68.8	143
		GAPDH_070228_cDNA_R	24	cagccttctccatggtggtgaaga	68.8	
TBP	6908	TBP RT F[a]	21	tgcacaggagccaagagtgaa	64.4	132
		TBP RT R[a]	20	cacatcacagctccccacca	65.6	
ACTB	60	ACTB RT F*	24	cagccatgtacgttgctatccagg	66.8	151
		ACTB RT R*	23	aggtccagacgcaggatggcatg	71.7	

([a]) These primer sequences were obtained from Gur-Dedeoglu B. *et al.* (2009)

(*) Primers Purchased From Origene

Primers Used To Analyse RAS/RAF/MAPK Pathway						
Gene	**NCBI GeneID**	**Primer**	**Bp**	**Sequence**	**Tm (C°)**	**Product Size (bp)**
MEK1 (MAP2K1)	5604	MEK1-1F	18	ggagttggaagcgcgtta	59.95	634
		MEK1-1R	22	cacgggagttgactaggatgtt	60.42	
		MEK1-2F	23	acatatctgagggagaagcacaa	60.14	709
		MEK1-2R	20	aaaagcgacatggcaaacca	63.74	
MEK2 (MAP2K2)	5605	MEK2-1F	18	ctatgggccccggctaga	63.33	626
		MEK2-1R	19	ggtgcatgatctggtgctt	59.65	
		MEK2-2F	20	tggaccaggtgctgaaagag	61.39	823
		MEK2-2R	20	cagcctgtcctcagctggaa	64.01	
ERK1 (MAPK3)	5595	ERK1-eks1F	19	gggtggctctggtaggtca	61.09	580
		ERK1-eks1R	18	gtctccacgtcccggaaa	62.07	
		ERK1-2F	18	ggggaggagtggagatgg	60.42	680
		ERK1-2R	20	atagcccttggagttcagca	59.84	
		ERK1-3F	20	tccaacctgctcatcaacac	59.68	705
		ERK1-3R	20	ctaacagtctggcgggagag	60.01	
ERK2 (MAPK1)	5594	ERK2-eks1F	20	aatccgcatgcacacttctt	60.67	528
		ERK2-eks1R	18	gaagtccgggttcgaggt	60.05	
		ERK2-2F	21	acaccaacctctcgtacatcg	60.04	550
		ERK2-2R	20	gacttggtgtagcccttgga	60.11	
		ERK2-3F	20	gttgcagatccagaccatga	59.64	609
		ERK2-3R	20	gtctgagcacgtccagtcct	60.47	
PTPN11 (SHP2)	5781	PTPN2F	22	gaggcattgaccaaggagaaga	62.8	381
		PTPN2R	20	actcgaaatgcaggcagcaa	64.25	
		PTPN3F	23	ttccttgggtttctttcaacact	61.21	416
		PTPN3R	23	gtcacaagcctttggagtcaga	61.75	
		PTPN4F	23	ttgtgtttaggagagctgactgt	58.20	347
		PTPN4R	23	gaaaaatcacccaaaggtaacat	58.37	
		PTPN5F	22	cactgcacccagcctattatct	60.52	393
		PTPN5R	20	aatgggtacatggaggctga	60.34	
		PTPN6F	20	cctctgtccgtgcctttatg	60.65	337
		PTPN6R	23	cgtcagtttcaagtctctcaggt	59.97	

Gene	NCBI GeneID	Primer	Bp	Sequence	Tm (C°)	Product Size (bp)
PTPN11 (SHP2)	5781	PTPN7F	22	gtaatgctgatccaggcttttt	59.64	248
		PTPN7R	22	tgaggaaaggtacagaggtgct	60.30	
		PTPN8F	22	gactaggctggggagtaactga	59.77	247
		PTPN8R	22	ttcaggacatgaggaaggattt	59.94	
		PTPN9F	23	aagctttgcttttcacagtgttt	59.53	479
		PTPN9R	20	tcaacaaatcccaagcagaa	59.25	
		PTPN10F	20	ccgaatgcctgcttttctta	60.34	522
		PTPN10R	20	tgagggcaggaacactacct	59.72	
		PTPN11F	20	gagttctgggaacctcacga	60.24	443
		PTPN11R	20	tgcagttgctctatgcctca	60.71	
		PTPN12F	22	atgattctgttgtccctgcttt	60.00	262
		PTPN12R	22	tctgttctcaggcagacacact	60.10	
		PTPN13F	22	aaacaacttcatcctggctctg	60.66	261
		PTPN13R	22	gaggcctagcaagagaatgaga	60.12	

Primers Used to Analyse TUBA3C (NCBI GeneID:7278)				
Primer	Bp	Sequence	Tm (C°)	Product Size (bp)
tuba3cex1F	20	cttagcagctgggatggtgt	60.23	517
tuba3cex1R	20	tgcaggaggattcaaaggag	60.3	
tuba3cex2F	20	cctggaatgtgtccatcttg	59	319
tuba3cex2R	20	ccaacgcactggtctaggtt	60.2	
tuba3cex3 1F	23	caagtcttcagaggcagagaagt	59.3	501
tuba3cex3 1R	20	ggcactaggttggtctggaa	60.1	
tuba3cex3 2F	20	gtcccacgtacaccaacctc	60.3	508
tuba3cex3 2R	20	gcccatggaatagggtagt	60	
tuba3cex4F	21	cctgttcacctacagggtgtc	59.5	519
tuba3cex4R	21	ggcaaagctaggcagtacgat	60.8	
tuba3CRTF	17	gcagcggaggagctcaa	61.4	145
tuba3CRTR	23	caatggttttatcacttggcatc	60.6	

Primers Purchased From OriGene Technologies						
Gene	**Accession**	**Primer**	**Bp**	**Sequence**	**Tm (C°)**	**Product Size (bp)**
PTPRCAP	NM_005608	PTPRCAP-F	22	caggacacagactatgaccacg	60,6	132
		PTPRCAP-R	22	gtcactgtctctggcttcctca	60,2	
FBXL11	NM_012308	FBXL11-F	22	caaggagagtgtggtgtttgcc	64,2	143
		FBXL11-R	22	acctctccacagagggaacatg	62,7	
MCL1	NM_021960	MCL1-F	23	ccaagaaagctgcatcgaaccat	66,7	151
		MCL1-R	22	cagcacattcctgatgccacct	66,8	
CHUK	NM_001278	CHUK-F	22	ctcggaaaccagcctctcaatg	65,4	121
		CHUK-R	24	gataaacttctggaagcaaatggc	62,3	
IQSEC1	NM_014869	IQSEC1-F	22	cagaaactcggactacaccagc	61,2	154
		IQSEC1-R	22	actggttctcgaagagcaggac	62,2	
MAGI-2	NM_012301	MAGI2-F	22	caccgctatgtcatcgacctca	65,6	129
		MAGI2-R	22	ggatacagagcctggacttctc	59,4	
MIPOL1	NM_138731	MIPOL1-F	23	actgcaacaagctctgacagagc	63,4	120
		MIPOL1-R	23	ctcagtacatccaccagcctttc	62,3	

B. Clinical Informations of the Samples in the TissueScan Liver Cancer Tissue qPCR Panel I (Cat No: LVRT 501, OriGene)

Detailed information can be found on the OriGene web site;

http://www.origene.com/assets/documents/TissueScan/LVRT-01.xls

Well	gender	age	appearance	verification	diagnosis	stage	tumorgrade
C1	Male	81	Normal	Within normal limits	Carcinoma of liver, hepatocellular	0	Not Applicable
C2	Male	73	Normal	Within normal limits	Carcinoma of liver, hepatocellular	0	Not Applicable
C3	Male	71	Normal	Within normal limits	Carcinoma of liver, hepatocellular	0	Not Applicable
C4	Male	86	Normal	Within normal limits	Carcinoma of liver, hepatocellular	0	Not Applicable
C5	Male	52	Normal	Within normal limits	Granuloma of liver	0	Not Applicable
C6	Female	33	Normal	Within normal limits	Nodular hyperplasia of liver, focal	0	Not Applicable
C7	Male	66	Normal	Within normal limits	Carcinoma of liver, hepatocellular	0	Not Applicable
C8	Male	68	Normal	Within normal limits	Carcinoma of liver, hepatocellular	0	Not Applicable
C9	Male	81	Tumor	Carcinoma of liver, hepatocellular	Carcinoma of liver, hepatocellular	I	AJCC G1: Well differentiated
C10	Male	79	Tumor	Carcinoma of liver, hepatocellular	Carcinoma of liver, hepatocellular	I	AJCC G2: Moderately differentiated
C11	Female	61	Tumor	Carcinoma of liver, hepatocellular	Carcinoma of liver, hepatocellular	I	AJCC G1: Well differentiated
C12	Female	58	Tumor	Carcinoma of liver, hepatocellular	Carcinoma of liver, hepatocellular	I	Not Reported
D1	Male	66	Tumor	Carcinoma of liver, hepatocellular	Carcinoma of liver, hepatocellular	I	AJCC G3: Poorly differentiated
D2	Female	62	Tumor	Cholangiocarcinoma of liver	Cholangiocarcinoma of liver	I	AJCC G2: Moderately differentiated
D3	Female	78	Tumor	Cholangiocarcinoma of liver	Cholangiocarcinoma of liver	I	AJCC G2: Moderately differentiated
D4	Female	63	Tumor	Carcinoma of liver, hepatocellular	Carcinoma of liver, hepatocellular	II	AJCC G2: Moderately differentiated
D5	Male	73	Tumor	Carcinoma of liver, hepatocellular	Carcinoma of liver, hepatocellular	II	AJCC G2: Moderately differentiated
D6	Male	68	Tumor	Carcinoma of liver, hepatocellular	Carcinoma of liver, hepatocellular	II	Not Reported
D7	Male	60	Tumor	Carcinoma of liver, hepatocellular	Carcinoma of liver, hepatocellular	II	AJCC G3: Poorly differentiated
D8	Female	62	Tumor	Carcinoma of liver, hepatocellular	Carcinoma of liver, hepatocellular	II	AJCC G1: Well differentiated
D9	Male	60	Tumor	Carcinoma of liver, hepatocellular	Carcinoma of liver, hepatocellular	II	AJCC G2: Moderately differentiated
D10	Male	77	Tumor	Carcinoma of liver, hepatocellular	Carcinoma of liver, hepatocellular	II	AJCC G1: Well differentiated
D11	Male	63	Tumor	Carcinoma of liver, hepatocellular	Carcinoma of liver, hepatocellular	II	AJCC G2: Moderately differentiated
D12	Female	39	Tumor	Carcinoma of liver, hepatocellular	Carcinoma of liver, hepatocellular	IIIA	AJCC G1: Well differentiated
E1	Male	43	Tumor	Carcinoma of liver, hepatocellular	Carcinoma of liver, hepatocellular	IIIA	AJCC G3: Poorly differentiated
E2	Female	79	Tumor	Carcinoma of liver, hepatocellular	Carcinoma of liver, hepatocellular	IIIA	AJCC G2: Moderately differentiated
E3	Male	56	Tumor	Carcinoma of liver, hepatocellular	Carcinoma of liver, hepatocellular	IIIA	AJCC G2: Moderately differentiated
E4	Male	71	Tumor	Carcinoma of liver, hepatocellular	Carcinoma of liver, hepatocellular	IIIA	AJCC G2: Moderately differentiated
E5	Male	86	Tumor	Carcinoma of liver, hepatocellular	Carcinoma of liver, hepatocellular	IIIA	AJCC G1: Well differentiated
E6	Male	26	Tumor	Carcinoma of liver, hepatocellular	Carcinoma of liver, hepatocellular	IIIA	AJCC G2: Moderately differentiated
E7	Male	68	Tumor	Carcinoma of liver, hepatocellular	Carcinoma of liver, hepatocellular	IIIA	AJCC G2: Moderately differentiated
E8	Male	21	Tumor	Carcinoma of liver, hepatocellular	Carcinoma of liver, hepatocellular	IV	AJCC G2: Moderately differentiated
E9	Male	70	Tumor	Carcinoma of liver, hepatocellular, metastatic	Carcinoma of liver, hepatocellular, metastatic	IV	AJCC G3: Poorly differentiated
E10	Male	66	Tumor	Cholangiocarcinoma of liver, metastatic	Cholangiocarcinoma of liver, metastatic	IV	Not Reported
E11	Male	71	Lesion	Cirrhosis of liver	Carcinoma of liver, hepatocellular	see path report	Not Applicable
E12	Male	43	Lesion	Cirrhosis of liver	Carcinoma of liver, hepatocellular	see path report	Not Applicable
F1	Male	60	Lesion	Cirrhosis of liver	Carcinoma of liver, hepatocellular	see path report	Not Applicable
F2	Male	50	Lesion	Cirrhosis of liver	Carcinoma of liver, hepatocellular	see path report	Not Applicable
F3	Male	77	Lesion	Cirrhosis of liver	Carcinoma of liver, hepatocellular	see path report	Not Applicable
F4	Male	73	Lesion	Fatty changes to liver	Carcinoma of liver, hepatocellular	see path report	Not Applicable
F5	Female	32	Lesion	Fatty changes to liver	Nodular hyperplasia of liver, focal	see path report	Not Applicable
F6	Male	79	Lesion	Fatty changes to liver	Carcinoma of liver, hepatocellular	see path report	Not Applicable
F7	Male	56	Lesion	Fatty changes to liver	Carcinoma of liver, hepatocellular	see path report	Not Applicable
F8	Male	26	Lesion	Fatty changes to liver	Carcinoma of liver, hepatocellular	see path report	Not Applicable
F9	Female	79	Lesion	Hepatitis	Carcinoma of liver, hepatocellular	see path report	Not Applicable
F10	Male	68	Lesion	Hepatitis, chronic	Carcinoma of liver, hepatocellular	see path report	Not Applicable
F11	Female	58	Lesion	Hepatitis, chronic	Carcinoma of liver, hepatocellular	see path report	Not Applicable
F12	Female	31	Tumor	Adenoma of liver	Adenoma of liver	Not Reported	Not Reported

C. Permissions for figures

Permission for Figure 1.1.1.

Logged in as:
TOLGA ACUN
Account #:
3000330041
LOGOUT

License Details

This is a License Agreement between TOLGA ACUN ("You") and Elsevier ("Elsevier"). The license consists of your order details, the terms and conditions provided by Elsevier, and the payment terms and conditions.

Get the printable license.

License Number	2481981305081
License date	Aug 04, 2010
Licensed content publisher	Elsevier
Licensed content publication	Gastroenterology
Licensed content title	Hepatocellular Carcinoma: Epidemiology and Molecular Carcinogenesis
Licensed content author	Hashem B. El-Serag, K. Lenhard Rudolph
Licensed content date	June 2007
Licensed content volume number	132
Licensed content issue number	7
Number of pages	20
Type of Use	reuse in a thesis/dissertation
Requestor type	Not specified
Intended publisher of new work	n/a
Portion	figures/tables/illustrations
Number of figures/tables/illustrations	1
Format	both print and electronic
Are you the author of this Elsevier article?	No
Will you be translating?	No
Order reference number	
Title of your thesis/dissertation	GENETIC AND EPIGENETIC EVALUATION OF THE CANDIDATE GENES IN HUMAN HEPATOCELLULAR CARCINOMAS
Expected completion date	Sep 2010
Estimated size (number of pages)	240
Elsevier VAT number	GB 494 6272 12
Permissions price	0.00 USD
Value added tax 0.0%	0.0 USD / 0.0 GBP
Total	0.00 USD

BACK

Permission for Figure 1.1.2.

Powered by RIGHTSLINK COPYRIGHT CLEARANCE CENTER, INC. | Home | Account Info | Help

OXFORD JOURNALS
OXFORD UNIVERSITY PRESS

Title:	The chemistry and biology of aflatoxin B1: from mutational spectrometry to carcinogenesis
Author:	Maryann E. Smela, et. al.
Publication:	Carcinogenesis
Publisher:	Oxford University Press
Date:	April 1, 2001

Copyright © 2001, Copyright (c) 2001 by the Oxford University Press.

Logged in as:
TOLGA ACUN
LOGOUT

Order Completed

Thank you very much for your order.

This is a License Agreement between TOLGA ACUN ("You") and Oxford University Press ("Oxford University Press"). The license consists of your order details, the terms and conditions provided by Oxford University Press, and the payment terms and conditions.

Get the printable license.

License Number	2481990633519
License date	Aug 04, 2010
Licensed content publisher	Oxford University Press
Licensed content publication	Carcinogenesis
Licensed content title	The chemistry and biology of aflatoxin B1: from mutational spectrometry to carcinogenesis
Licensed content author	Maryann E. Smela, et. al.
Licensed content date	April 1, 2001
Volume number	22
Issue number	4
Type of Use	Thesis/Dissertation
Requestor type	Academic/Educational institute
Format	Print and electronic
Portion	Figure/table
Number of figures/tables	1
Will you be translating?	No
Author of this OUP article	No
Order reference number	
Title of your thesis / dissertation	GENETIC AND EPIGENETIC EVALUATION OF THE CANDIDATE GENES IN HUMAN HEPATOCELLULAR CARCINOMAS
Expected completion date	Sep 2010
Estimated size(pages)	240
Total	0.00 USD

ORDER MORE... | CLOSE WINDOW

Permission for Figure 1.1.3.

Powered by RIGHTSLINK COPYRIGHT CLEARANCE CENTER, INC. Home | Account Info | Help

Title: Molecular Pathogenesis of Hepatocellular Carcinoma
Author: Iain H. McKillop, Diarmuid M. Moran, Xiaoling Jin, Leonidas G. Koniaris
Publication: Journal of Surgical Research
Publisher: Elsevier
Date: November 2006
Copyright © 2006, Elsevier

Logged in as:
TOLGA ACUN
Account #: 3000330041
LOGOUT

Order Completed

Thank you very much for your order.

This is a License Agreement between TOLGA ACUN ("You") and Elsevier ("Elsevier"). The license consists of your order details, the terms and conditions provided by Elsevier, and the payment terms and conditions.

Get the printable license.

License Number	2481991036441
License date	Aug 04, 2010
Licensed content publisher	Elsevier
Licensed content publication	Journal of Surgical Research
Licensed content title	Molecular Pathogenesis of Hepatocellular Carcinoma
Licensed content author	Iain H. McKillop, Diarmuid M. Moran, Xiaoling Jin, Leonidas G. Koniaris
Licensed content date	November 2006
Licensed content volume number	136
Licensed content issue number	1
Number of pages	11
Type of Use	reuse in a thesis/dissertation
Requestor type	Not specified
Intended publisher of new work	other
Portion	figures/tables/illustrations
Number of figures/tables/illustrations	1
Format	both print and electronic
Are you the author of this Elsevier article?	No
Will you be translating?	No
Order reference number	
Title of your thesis/dissertation	GENETIC AND EPIGENETIC EVALUATION OF THE CANDIDATE GENES IN HUMAN HEPATOCELLULAR CARCINOMAS
Expected completion date	Sep 2010
Estimated size (number of pages)	240
Elsevier VAT number	GB 494 6272 12
Permissions price	0.00 USD
Value added tax 0.0%	0.0 USD / 0.0 GBP
Total	0.00 USD

ORDER MORE... CLOSE WINDOW

Permission for Figure 1.1.4.

Title:	Molecular pathogenesis of human hepatocellular carcinoma
Author:	Snorri S. Thorgeirsson, Joe W. Grisham
Publication:	Nature Genetics
Publisher:	Nature Publishing Group
Date:	Aug 1, 2002

Copyright © 2002, Nature Publishing Group

Logged in as:
TOLGA ACUN
Account #:
3000330041

LOGOUT

Order Completed

Thank you very much for your order.

This is a License Agreement between TOLGA ACUN ("You") and Nature Publishing Group ("Nature Publishing Group"). The license consists of your order details, the terms and conditions provided by Nature Publishing Group, and the payment terms and conditions.

Get the printable license.

License Number	2481991443972
License date	Aug 04, 2010
Licensed content publisher	Nature Publishing Group
Licensed content publication	Nature Genetics
Licensed content title	Molecular pathogenesis of human hepatocellular carcinoma
Licensed content author	Snorri S. Thorgeirsson, Joe W. Grisham
Volume number	
Issue number	
Pages	
Year of publication	2002
Portion used	Figures / tables
Number of figures / tables	1
Requestor type	Student
Type of Use	Thesis / Dissertation
Billing type	Invoice
Company	TOLGA ACUN
Billing address	Elvankent Banka Evleri B/19 No:34 Ankara, other 06790 Turkey
Customer reference info	
Total	0.00 USD

ORDER MORE... CLOSE WINDOW

Permission for Figure 1.1.5.

Powered by RIGHTSLINK COPYRIGHT CLEARANCE CENTER, INC. Home | Account Info | Help

nature publishing group

Title:	Hepatocellular carcinoma pathogenesis: from genes to environment
Author:	Paraskevi A. Farazi, Ronald A. DePinho
Publication:	Nature Reviews Cancer
Publisher:	Nature Publishing Group
Date:	Sep 1, 2006

Copyright © 2006, Nature Publishing Group

Logged in as:
TOLGA ACUN
Account #:
3000330041

LOGOUT

Order Completed

Thank you very much for your order.

This is a License Agreement between TOLGA ACUN ("You") and Nature Publishing Group ("Nature Publishing Group"). The license consists of your order details, the terms and conditions provided by Nature Publishing Group, and the payment terms and conditions.

Get the printable license.

License Number	2482340705787
License date	Aug 05, 2010
Licensed content publisher	Nature Publishing Group
Licensed content publication	Nature Reviews Cancer
Licensed content title	Hepatocellular carcinoma pathogenesis: from genes to environment
Licensed content author	Paraskevi A. Farazi, Ronald A. DePinho
Volume number	
Issue number	
Pages	
Year of publication	2006
Portion used	Figures / tables
Number of figures / tables	1
Requestor type	Student
Type of Use	Thesis / Dissertation
Billing type	Invoice
Company	TOLGA ACUN
Billing address	Elvankent Banka Evleri B/19 No:34 Ankara, other 06790 Turkey
Customer reference info	
Total	0.00 USD

ORDER MORE... CLOSE WINDOW

Permission for Figure 1.2.2.

Powered by RIGHTSLINK COPYRIGHT CLEARANCE CENTER, INC. Home | Account Info | Help

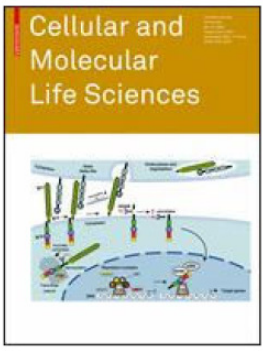

Title: The role of the ZEB family of transcription factors in development and disease
Author: C. Vandewalle
Publication: Cellular and Molecular Life Sciences
Publisher: Springer
Date: Mar 1, 2009
Copyright © 2009, Birkhäuser Basel

Logged in as:
TOLGA ACUN
Account #:
3000330041
LOGOUT

Order Completed

Thank you very much for your order.

This is a License Agreement between TOLGA ACUN ("You") and Springer ("Springer"). The license consists of your order details, the terms and conditions provided by Springer, and the payment terms and conditions.

Get the printable license.

License Number	2482000828977
License date	Aug 04, 2010
Licensed content publisher	Springer
Licensed content publication	Cellular and Molecular Life Sciences
Licensed content title	The role of the ZEB family of transcription factors in development and disease
Licensed content author	C. Vandewalle
Licensed content date	Mar 1, 2009
Volume number	66
Issue number	5
Type of Use	Thesis/Dissertation
Portion	Figures
Author of this Springer article	No
Title of your thesis / dissertation	GENETIC AND EPIGENETIC EVALUATION OF THE CANDIDATE GENES IN HUMAN HEPATOCELLULAR CARCINOMAS
Expected completion date	Sep 2010
Estimated size(pages)	240
Total	0.00 USD

CLOSE WINDOW

Permission for Figure 1.4.1.

OXFORD JOURNALS
OXFORD UNIVERSITY PRESS

Title:	p53-Mdm2--the affair that never ends
Author:	Dania Alarcon-Vargas, et. al.
Publication:	Carcinogenesis
Publisher:	Oxford University Press
Date:	April 1, 2002

Copyright © 2002, Copyright (c) 2002 by the Oxford University Press.

Logged in as:
TOLGA ACUN
Account #:
3000330041

LOGOUT

Order Completed

Thank you very much for your order.

This is a License Agreement between TOLGA ACUN ("You") and Oxford University Press ("Oxford University Press"). The license consists of your order details, the terms and conditions provided by Oxford University Press, and the payment terms and conditions.

Get the printable license.

License Number	2482001135235
License date	Aug 04, 2010
Licensed content publisher	Oxford University Press
Licensed content publication	Carcinogenesis
Licensed content title	p53-Mdm2--the affair that never ends
Licensed content author	Dania Alarcon-Vargas, et. al.
Licensed content date	April 1, 2002
Volume number	23
Issue number	4
Type of Use	Thesis/Dissertation
Requestor type	Academic/Educational institute
Format	Print and electronic
Portion	Figure/table
Number of figures/tables	1
Will you be translating?	No
Author of this OUP article	No
Order reference number	
Title of your thesis / dissertation	GENETIC AND EPIGENETIC EVALUATION OF THE CANDIDATE GENES IN HUMAN HEPATOCELLULAR CARCINOMAS
Expected completion date	Sep 2010
Estimated size(pages)	240
Total	0.00 USD

ORDER MORE... CLOSE WINDOW

Permission for Figure 1.5.1.

Powered by RIGHTSLINK COPYRIGHT CLEARANCE CENTER, INC. Home | Account Info | Help

nature publishing group

Title:	Hyperactive Ras in developmental disorders and cancer
Author:	Suzanne Schubbert , Kevin Shannon and Gideon Bollag
Publication:	Nature Reviews Cancer
Publisher:	Nature Publishing Group
Date:	Jul 1, 2007

Copyright © 2007, Nature Publishing Group

Logged in as:
TOLGA ACUN
Account #:
3000330041

LOGOUT

Order Completed

Thank you very much for your order.

This is a License Agreement between TOLGA ACUN ("You") and Nature Publishing Group ("Nature Publishing Group"). The license consists of your order details, the terms and conditions provided by Nature Publishing Group, and the payment terms and conditions.

Get the printable license.

License Number	2482010380075
License date	Aug 04, 2010
Licensed content publisher	Nature Publishing Group
Licensed content publication	Nature Reviews Cancer
Licensed content title	Hyperactive Ras in developmental disorders and cancer
Licensed content author	Suzanne Schubbert , Kevin Shannon and Gideon Bollag
Volume number	7
Issue number	7
Pages	pp
Year of publication	2007
Portion used	Figures / tables
Number of figures / tables	1
Requestor type	Student
Type of Use	Thesis / Dissertation
Billing type	Invoice
Company	TOLGA ACUN
Billing address	Elvankent Banka Evleri B/19 No:34 Ankara, other 06790 Turkey
Customer reference info	
Total	0.00 USD

ORDER MORE... CLOSE WINDOW

Permission for Figure 1.8.1.

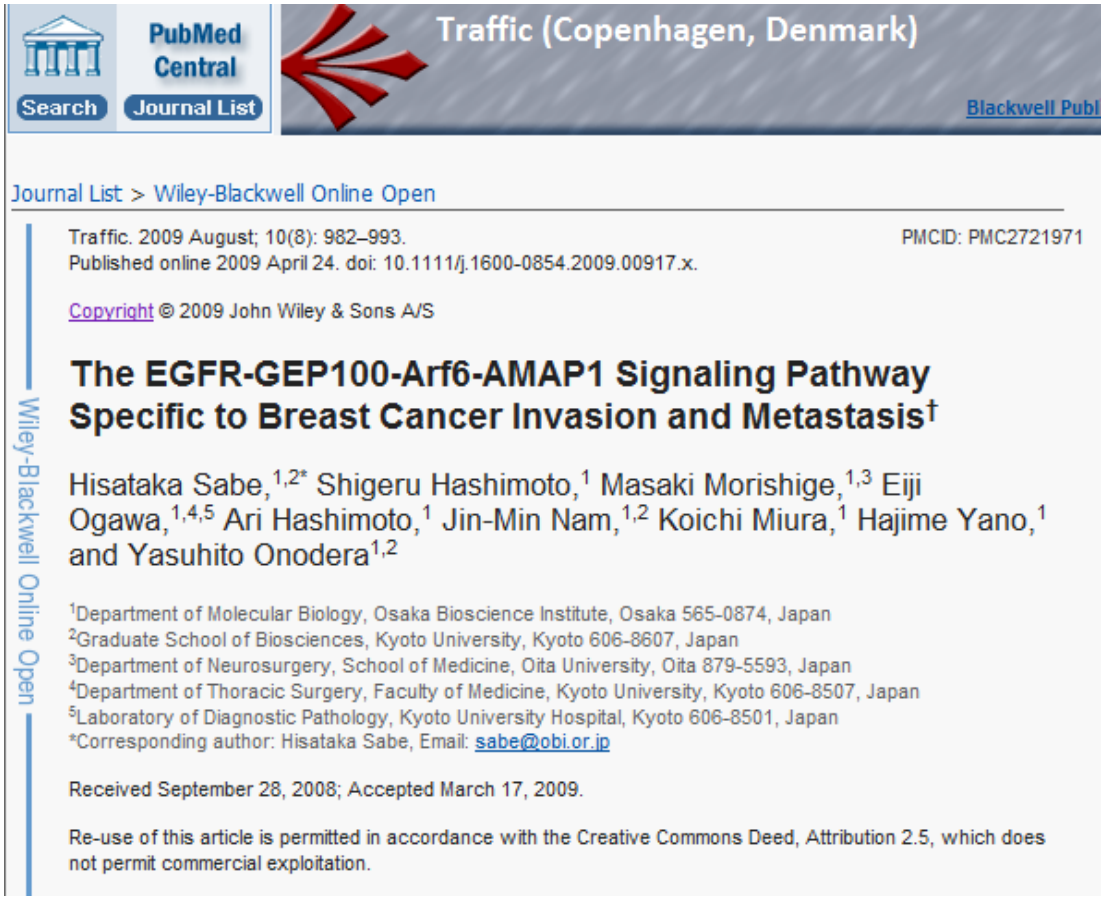

PubMed Central Search Journal List

Traffic (Copenhagen, Denmark)

Blackwell Publ

Journal List > Wiley-Blackwell Online Open

Wiley-Blackwell Online Open

Traffic. 2009 August; 10(8): 982–993. PMCID: PMC2721971
Published online 2009 April 24. doi: 10.1111/j.1600-0854.2009.00917.x.

The EGFR-GEP100-Arf6-AMAP1 Signaling Pathway Specific to Breast Cancer Invasion and Metastasis†

Hisataka Sabe,[1,2*] Shigeru Hashimoto,[1] Masaki Morishige,[1,3] Eiji Ogawa,[1,4,5] Ari Hashimoto,[1] Jin-Min Nam,[1,2] Koichi Miura,[1] Hajime Yano,[1] and Yasuhito Onodera[1,2]

[1]Department of Molecular Biology, Osaka Bioscience Institute, Osaka 565-0874, Japan
[2]Graduate School of Biosciences, Kyoto University, Kyoto 606-8607, Japan
[3]Department of Neurosurgery, School of Medicine, Oita University, Oita 879-5593, Japan
[4]Department of Thoracic Surgery, Faculty of Medicine, Kyoto University, Kyoto 606-8507, Japan
[5]Laboratory of Diagnostic Pathology, Kyoto University Hospital, Kyoto 606-8501, Japan
*Corresponding author: Hisataka Sabe, Email: sabe@obi.or.jp

Received September 28, 2008; Accepted March 17, 2009.

Permission for Figure 1.10.1.

Powered by RIGHTSLINK COPYRIGHT CLEARANCE CENTER, INC. Home | Account Info | Help

nature publishing group

Title:	IKK[alpha], a critical regulator of epidermal differentiation and a suppressor of skin cancer
Author:	Pascal Descargues , Alok K Sil and Michael Karin
Publication:	The EMBO Journal
Publisher:	Nature Publishing Group
Date:	Oct 22, 2008

Copyright © 2008, Nature Publishing Group

Logged in as:
TOLGA ACUN
Account #:
3000330041

LOGOUT

Order Completed

Thank you very much for your order.

This is a License Agreement between TOLGA ACUN ("You") and Nature Publishing Group ("Nature Publishing Group"). The license consists of your order details, the terms and conditions provided by Nature Publishing Group, and the payment terms and conditions.

Get the printable license.

License Number	2482020039941
License date	Aug 04, 2010
Licensed content publisher	Nature Publishing Group
Licensed content publication	The EMBO Journal
Licensed content title	IKK[alpha], a critical regulator of epidermal differentiation and a suppressor of skin cancer
Licensed content author	Pascal Descargues , Alok K Sil and Michael Karin
Volume number	
Issue number	
Pages	
Year of publication	2008
Portion used	Figures / tables
Number of figures / tables	1
Requestor type	Student
Type of Use	Thesis / Dissertation
High-res requested	No
Billing type	Invoice
Company	TOLGA ACUN
Billing address	Elvankent Banka Evleri B/19 No:34 Ankara, other 06790 Turkey
Customer reference info	
Total	0.00 USD

ORDER MORE... CLOSE WINDOW

Permission for Figure 1.11.1.

Powered by RIGHTSLINK COPYRIGHT CLEARANCE CENTER, INC. Home | Account Info | Help

nature publishing group

Title:	Noxa: at the tip of the balance between life and death
Author:	C Ploner, R Kofler and A Villunger
Publication:	Oncogene
Publisher:	Nature Publishing Group
Date:	Dec 1, 2008

Copyright © 2008, Nature Publishing Group

Logged in as:
TOLGA ACUN
Account #:
3000330041

LOGOUT

Order Completed

Thank you very much for your order.

This is a License Agreement between TOLGA ACUN ("You") and Nature Publishing Group ("Nature Publishing Group"). The license consists of your order details, the terms and conditions provided by Nature Publishing Group, and the payment terms and conditions.

Get the printable license.

License Number	2482020193159
License date	Aug 04, 2010
Licensed content publisher	Nature Publishing Group
Licensed content publication	Oncogene
Licensed content title	Noxa: at the tip of the balance between life and death
Licensed content author	C Ploner, R Kofler and A Villunger
Volume number	27
Issue number	S1
Pages	
Year of publication	2008
Portion used	Figures / tables
Number of figures / tables	1
Requestor type	Student
Type of Use	Thesis / Dissertation
High-res requested	No
Billing type	Invoice
Company	TOLGA ACUN
Billing address	Elvankent Banka Evleri B/19 No:34 Ankara, other 06790 Turkey
Customer reference info	
Total	0.00 USD

ORDER MORE... CLOSE WINDOW

D. Authors' rights of published paper

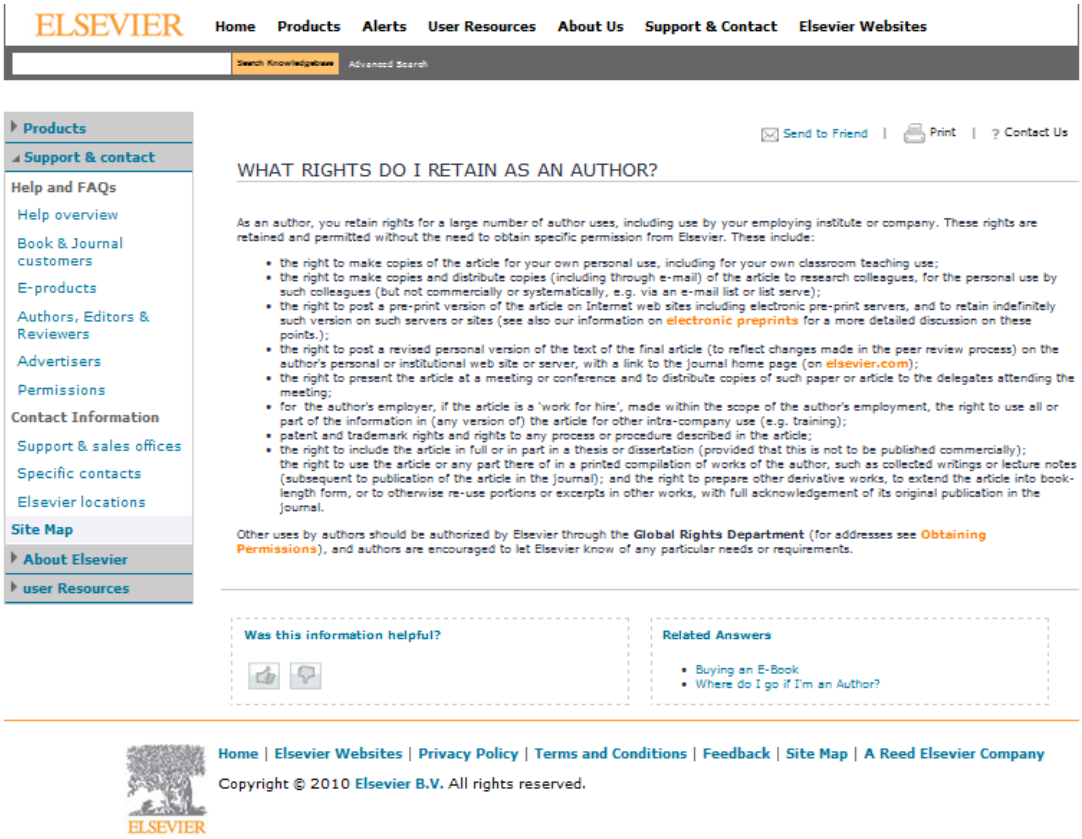

ELSEVIER Home Products Alerts User Resources About Us Support & Contact Elsevier Websites

Search Knowledgebase Advanced Search

- Products
- Support & contact

Help and FAQs
- Help overview
- Book & Journal customers
- E-products
- Authors, Editors & Reviewers
- Advertisers
- Permissions

Contact Information
- Support & sales offices
- Specific contacts
- Elsevier locations

Site Map
- About Elsevier
- user Resources

Send to Friend | Print | Contact Us

WHAT RIGHTS DO I RETAIN AS AN AUTHOR?

As an author, you retain rights for a large number of author uses, including use by your employing institute or company. These rights are retained and permitted without the need to obtain specific permission from Elsevier. These include:

- the right to make copies of the article for your own personal use, including for your own classroom teaching use;
- the right to make copies and distribute copies (including through e-mail) of the article to research colleagues, for the personal use by such colleagues (but not commercially or systematically, e.g. via an e-mail list or list serve);
- the right to post a pre-print version of the article on Internet web sites including electronic pre-print servers, and to retain indefinitely such version on such servers or sites (see also our information on electronic preprints for a more detailed discussion on these points.);
- the right to post a revised personal version of the text of the final article (to reflect changes made in the peer review process) on the author's personal or institutional web site or server, with a link to the journal home page (on elsevier.com);
- the right to present the article at a meeting or conference and to distribute copies of such paper or article to the delegates attending the meeting;
- for the author's employer, if the article is a 'work for hire', made within the scope of the author's employment, the right to use all or part of the information in (any version of) the article for other intra-company use (e.g. training);
- patent and trademark rights and rights to any process or procedure described in the article;
- the right to include the article in full or in part in a thesis or dissertation (provided that this is not to be published commercially);
- the right to use the article or any part there of in a printed compilation of works of the author, such as collected writings or lecture notes (subsequent to publication of the article in the journal); and the right to prepare other derivative works, to extend the article into book-length form, or to otherwise re-use portions or excerpts in other works, with full acknowledgement of its original publication in the journal.

Other uses by authors should be authorized by Elsevier through the **Global Rights Department** (for addresses see Obtaining Permissions), and authors are encouraged to let Elsevier know of any particular needs or requirements.

Was this information helpful?

Related Answers
- Buying an E-Book
- Where do I go if I'm an Author?

Home | Elsevier Websites | Privacy Policy | Terms and Conditions | Feedback | Site Map | A Reed Elsevier Company

Copyright © 2010 Elsevier B.V. All rights reserved.

ELSEVIER

Mutation Research 684 (2010) 106–108

Contents lists available at ScienceDirect

Mutation Research/Fundamental and Molecular Mechanisms of Mutagenesis

journal homepage: www.elsevier.com/locate/molmut
Community address: www.elsevier.com/locate/mutres

Short communication

Mdm2 Snp309 G allele displays high frequency and inverse correlation with somatic P53 mutations in hepatocellular carcinoma

Tolga Acun[a], Ece Terzioğlu-Kara[a,b], Ozlen Konu[a], Mehmet Ozturk[a,c], Mustafa Cengiz Yakicier[a,*]

[a] Department of Molecular Biology and Genetics, Bilkent University, 06533 Bilkent, Ankara, Turkey
[b] Department of Molecular Biology and Genetics, Bogazici University, 34342 Istanbul, Turkey
[c] Centre de Recherche INSERM-Université Joseph Fourrier U823, 06800 Grenoble, France

ARTICLE INFO

Article history:
Received 30 July 2009
Received in revised form
23 November 2009
Accepted 24 November 2009
Available online 30 November 2009

Keywords:
Hepatocellular carcinoma
MDM2 SNP309
TP53
Polymorphism

ABSTRACT

Loss of function of the p53 protein, which may occur through a range of molecular events, is critical in hepatocellular carcinoma (HCC) evolution. MDM2, an oncogene, acts as a major regulator of the p53 protein. A polymorphism in the MDM2 promoter, SNP309 (T/G), has been shown to alter protein expression and may thus play a role in carcinogenesis. MDM2 SNP309 is also associated with HCC. However, the role of SNP309 in hepatocarcinogenesis with respect to TP53 mutations is unknown. In this study, we investigated the distribution of the MDM2 SNP309 genotype and somatic TP53 (the p53 tumor suppressor gene) mutations in 99 human HCC samples from Africa, Europe, China and Japan. Samples exhibited striking geographical differences in their distribution of SNP309 genotypes. The frequency and spectrum of p53 mutations also varied geographically; TP53 mutations were frequent in Africa, where the SNP309 T/T genotype predominated but were rare in Europe and Japan, where the SNP309 G allele was present more frequently.

TP53 mutations were detected in 18% (4/22) of SNP309 T/G and G/G and 82% (18/22) of SNP309 T/T genotype holders; this difference was statistically highly significant (P-value = 0.0006).

Our results indicated that the presence of the SNP309 G allele is inversely associated with the presence of somatic TP53 mutations because they only coincided in 4% of HCC cases. This finding suggests that the SNP309 G allele may functionally replace p53 mutations, and in addition to known etiological factors, may be partly responsible for differential HCC prevalence.

1. Introduction

Hepatocellular carcinoma (HCC), the most common liver malignancy, is among the five leading causes of cancer death in the world. The incidence of HCC varies greatly worldwide, depending on the distribution of well-known environmental risk factors such as hepatitis B virus (HBV) and hepatitis C virus (HCV) infections and dietary exposure to aflatoxins [1]. HCC is thought to be mainly an environmental disease; however, not all individuals with exposure to risk factors develop cancer even over the long term. On the other hand, familial clustering and early onset of HCCs in some populations suggest an inherited genetic predisposition to liver cancer [2]. Germline polymorphisms of several genes have been studied as potential risk factors for HCCs [3–5]. However, the pathogenesis of human HCC is a multistage process with the involvement of a series of genes, including oncogenes and tumor suppressor genes; germline polymorphisms of these genes may also determine individual susceptibility to HCC.

The p53 tumor suppressor gene (TP53) is of critical importance for regulating cell cycles and maintaining genomic integrity. TP53 also is a common target for inactivation during liver carcinogenesis. Although this inactivation may be largely due to mutations in the p53 gene, recent evidence suggests that other mechanisms may be involved in p53 inactivation. For instance, the hepatitis B virus-encoded X antigen (HBxAg) binds to and inactivates wild-type p53 [6,7]. Interaction of p53 with a cellular oncoprotein, MDM2, also inactivates p53, via increasing its degradation and/or blocking p53 transcriptional activation [8–10].

In a recent study, a functional single nucleotide polymorphism at nucleotide 309 (T > G) in the promoter region of MDM2 has been reported. Interestingly, cells with the 309 G/G genotype have an enhanced affinity to bind stimulatory protein Sp1 and also show heightened MDM2 expression and a significant attenuation of the p53 pathway compared with those carrying the 309 T/T genotype [11]. Furthermore, SNP309 has been shown to be associated with earlier age of onset of certain hereditary and sporadic cancers in humans [11,12].

In this study, we investigated the distribution of the SNP309 genotype in 99 human HCCs that were previously characterized for TP53 alterations from HCC endemic and rare geographical areas.

* Corresponding author. Tel.: +90 3122902138; fax: +90 3122665097.
E-mail address: yakicier@fen.bilkent.edu.tr (M.C. Yakicier).

0027-5107/$ – see front matter © 2009 Elsevier B.V. All rights reserved.
doi:10.1016/j.mrfmmm.2009.11.008

Table 1
Distribution of P53 mutations and SNP309 genotypes in HCC samples from different geographical regions and Hardy–Weinberg equilibrium states of MDM2 genotypes.

Samples	P53 Mut.	SNP309 genotypes			Hardy–Weinberg Equilibrium			
		T/T	T/G	G/G	p	q	Chi-square	*P*-value
Africa (n = 33)	11 (33%)	31	2	0	0.97	0.03	0.03	1
Japan (n = 13)	1 (8%)	0	10	3	0.38	0.62	5.08	0.08
China (n = 21)	5 (23%)	7	3	11	0.40	0.60	10.39	0.001
Europe (n = 32)	5 (16%)	11	16	5	0.59	0.41	0.04	1
Total (n = 99)	22 (22%)	49	31	19	0.65	0.35	9.54	0.0015

Mut, mutations; p and q refer to allele frequencies of T and G, respectively.

Table 2
Inverse relationship between p53 mutation and SNP309 G genotype of MDM2 gene in all HCC samples and without African samples.

		Genotype Frequency		OR (95%CI)	*P*-value
		T/T	T/G + G/G		
All HCC samples	p53 Wt	31	46	0.15 (0.03–0.52)	0.0006
	p53 Mut	18	4		
African samples excluded	p53 Wt	11	44	0.15 (0.03–0.7)	0.0065
	p53 Mut	7	4		

Wt, wild-type; Mut, mutant; OR, odds-ratio; CI, confidence interval.

Our findings revealing the differential occurrence of the SNP309 genotype in mutant and wild-type p53 carriers enhance the understanding of HCC aetiology in a multi-regional context.

2. Materials and methods

We analyzed a total of 99 DNA samples (isolated from histologically confirmed tumor and nontumor liver tissue of the patients) from HCC patients living in different geographical regions, including Mozambique (n = 16), South Africa (excluding Mozambique: n = 17), China (n = 21), Japan (n = 13), Europe (Germany, France, Spain, Turkey, Israel and USA: n = 32). Characteristics of these tumors and methods for DNA isolation have been described previously [13,14].

SNP309 (T/G) of MDM2 were genotyped using PCR amplification of the first intron of the MDM2, followed by MspA1I (Promega) digestion as described elsewhere [15].

All statistical analyses were conducted using R functions in 'genetics' and 'stats' packages (http://www.r-project.org) [16,17]. Pearson's Chi-squared test with simulated *P*-value (based on 10,000 replicates) was applied to test whether the populations were in Hardy–Weinberg equilibrium with respect to MDM2 SNP309 polymorphism. The association between the P53 mutation status and the SNP309 genotypes was assessed using Fishers' exact tests.

3. Results

Ninety-nine samples with known p53 status (n = 99) were genotyped for SNP309. The observed genotypic frequency of SNP309 in HCC patients was distributed as 49% T/T genotype carriers (n = 49), 31% T/G genotype carriers (n = 31), and 19% G/G genotype carriers (n = 19).

Remarkable differences in the allele frequencies for each SNP309 genotype between patients from different geographical regions were observed. The G allele was the most common in the 13 Japanese HCC patients (100%); three of them were homozygous (23%) and 10 of them (77%) were heterozygous (Table 1). Interestingly, there was no wild-type SNP309 genotype carrier (T/T) among Japanese HCC patients (n = 13), although the Japanese population was in HW equilibrium (*P*-value = 0.08). Contrastingly, 31 out of 33 South African patients were wild-type for SNP309 (94%), but only two were heterozygous (6%), while there was no patient with the G/G genotype. Genotypic distributions of African and European populations did not exhibit HW disequilibrium (Table 1). The allele frequencies were highly divergent between African and other populations in which G allele was frequent (Table 1).

Distribution of T/T and T/G – G/G genotypes together was similar between patients from two geographically distant regions: China and Europe [wild-type genotype frequency 33% (7/21) vs. 34% (11/32); mutant genotype frequency 67% (14/21) vs. 66% (21/32), respectively]. However, heterozygote genotype frequency varied drastically between Chinese and European HCC patients [15% (3/21) vs. 50% (16/32)].

We then analyzed whether a significant correlation between the TP53 mutation and SNP309 genotypes existed. Interestingly, 18 of 22 (82%) TP53 mutations were concentrated in 49 (37%) HCC cases displaying the T/T genotype (Table 2). Among the 19 cases homozygous for G/G, three of them had TP53 mutations (16%) and only one of 31 cases of heterozygous T/G displayed somatic TP53 mutations (3%) (Table 2). Considering both T/G and G/G genotypes together (dominant model), only 4% of the 99 HCCs were positive for both p53 gene mutation and the G genotype (Tables 1 and 2).

We next examined whether there was a statistical interaction between the G genotype and TP53 mutations using Fisher's exact test. There was a highly significant inverse relationship between the presence of TP53 mutation and the G allele (*P*-value, two-sided = 0.0006; odds-ratio = 0.153; 95% CI = 0.03–0.52).

We next excluded African patients from the statistical analysis to prevent the potential bias from the high percentage of p53 mutations and SNP309 wild-type genotype carriers in Africa. The inverse relationship between the presence of TP53 mutation and the G genotype was sustained (*P*-value, two-sided = 0.0065; odds-ratio = 0.148; 95% CI = 0.03–0.7).

4. Discussion

Given the importance of the p53 pathway in HCC development, it is of interest to investigate the potential impact of the SNP309 genotype on its own and in combination with p53 mutation status in hepatocellular carcinomas. Here, we analyzed two genetic alterations, one of which is somatic and another of which is germline: TP53 mutations and SNP309 polymorphism. We evaluated dominant and additive models (G/G and G/T genotypes together) because Bond et al. showed a twofold increase in the MDM2 protein for cell lines with the heterozygous (G/T) genotype and a fourfold increase for cell lines with the homozygous variant (SNP309 G/G) genotype [11].

Our study provides evidence for an inverse association between the presence of the SNP309 mutant genotype and p53 mutation in HCC patients. However 4% of our HCC population displayed TP53 mutations despite having SNP309 G allele. The presence of the TP53

mutations in these samples could at least partly be explained by direct affect of known and unknown environmental factors in the etiology of these four HCC samples. Indeed, one of these patients displays G > T mutation in codon 249 of TP53, which is strongly associated with diatery aflatoxin B1 intake [6,7].

Given the functional role of SNP309 in the inhibition of the p53 pathway, the mutant genotype of this SNP may be functionally equivalent to the inactivating p53 mutations in hepatocarcinogenesis. In fact, numerous studies have shown that overexpression of MDM2 is an important event in carcinogenesis; in addition, MDM2 amplification occurs mostly in the absence of p53 mutation, supporting the concept that MDM2 amplification and p53 mutation are alternative mechanisms of p53 dysfunction [8,18,19]. In agreement with our hypothesis, a recent study shows that invasive bladder cancer patients with wild-type SNP309 (T/T) were prone to displaying p53 mutations [20].

On the other hand, our study also provides evidence that the p53 pathway was disrupted either by p53 mutation or the SNP309 G allele in 68/99 HCCs (68%). Thus, the p53 pathway may be more frequently altered in HCCs than previously thought.

Previous studies proposed that high levels of MDM2 resulting from the SNP309 G allele and just one wild-type p53 allele in Li-Fraumeni patients produce a severely weakened p53 tumor suppressor pathway, resulting in a higher mutation rate, poorer DNA repair processes and reduced apoptosis, which lead to faster and more frequent tumor formation [11,21]. Because the G genotype might substitute the need for p53 gene mutation or weaken the p53 tumor suppressor pathway, we suggest that this genotype may contribute to hepatocellular carcinoma risk. Because of lack of healthy control samples in corresponding ethnic groups or countries, we were not able to test this hypothesis with a case–control study. However, in a recent study, Dharel et al. reported that SNP309 is associated with the presence of hepatocellular carcinoma in Japanese patients with chronic hepatitis C [22]. In concordance with the study by Dharel et al., two recent studies indicated an association between the G genotype and risk for hepatocellular carcinoma in Moroccan and Korean patients with chronic hepatitis B infections [23,24].

Our study, together with the studies by Dharel et al., Yoon et al. and Ezzikouri et al., infers that the variations in HCC development not only depend on somatic mutations occurring in the tumor itself but also host genetic factors. Although additional work is necessary to confirm, these findings may raise the possibility that the high prevalence of HCC in some geographical regions, in addition to environmental factors, could be partly due to the high frequency of SNP309 G alleles in the people of these regions.

Conflict of interest

There is no conflict of interest.

Acknowledgment

This work is supported by TUBITAK (Grand No. 107S174).

Appendix A. Supplementary data

Supplementary data associated with this article can be found, in the online version, at doi:10.1016/j.mrfmmm.2009.11.008.

References

[1] F.X. Bosch, J. Ribes, M. Diaz, R. Cleries, Primary liver cancer: worldwide incidence and trends, Gastroenterology 127 (5 Suppl. 1) (2004) S5–S16.
[2] K. Hemminki, X. Li, Familial liver and gall bladder cancer: a nationwide epidemiological study from Sweden, Gut 52 (2003) 592–596.
[3] A. Sutton, P. Nahon, D. Pessayre, P. Rufat, A. Poire, M. Ziol, D. Vidaud, N. Barget, N. Ganne-Carrie, N. Charnaux, J.C. Trinchet, L. Gattegno, M. Beaugrand, Genetic polymorphisms in antioxidant enzymes modulate hepatic iron accumulation and hepatocellular carcinoma development in patients with alcohol-induced cirrhosis, Cancer Res. 66 (2006) 2844–2852.
[4] A. Vogel, S. Kneip, A. Barut, U. Ehmer, R.H. Tukey, M.P. Manns, C.P. Strassburg, Genetic link of hepatocellular carcinoma with polymorphisms of the UDP-glucuronosyltransferase UGT1A7 gene, Gastroenterology 121 (2001) 1136–1144.
[5] M.W. Yu, S.Y. Yang, Y.H. Chiu, Y.C. Chiang, Y.F. Liaw, C.J. Chen, A p53 genetic polymorphism as a modulator of hepatocellular carcinoma risk in relation to chronic liver disease, familial tendency, and cigarette smoking in hepatitis B carriers, Hepatology 29 (1999) 697–702.
[6] M. Ozturk, Genetic aspects of hepatocellular carcinogenesis, Semin. Liver Dis. 19 (1999) 235–242.
[7] A. Puisieux, M. Ozturk, TP53 and hepatocellular carcinoma, Pathol. Biol. (Paris) 45 (1997) 864–870.
[8] J.D. Oliner, J.A. Pietenpol, S. Thiagalingam, J. Gyuris, K.W. Kinzler, B. Vogelstein, Oncoprotein MDM2 conceals the activation domain of tumour suppressor p53, Nature 362 (1993) 857–860.
[9] J. Momand, G.P. Zambetti, D.C. Olson, D. George, A.J. Levin, The mdm-2 oncogene product forms a complex with the p53 protein and inhibits p53-mediated transactivation, Cell 69 (1992) 1237–1245.
[10] Y. Haupt, R. Maya, A. Kazaz, M. Oren, Mdm2 promotes the rapid degradation of p53, Nature 387 (1997) 296–299.
[11] G.L. Bond, W. Hu, E.E. Bond, H. Robins, S.G. Lutzker, N.C. Arva, J. Bargonetti, F. Bartel, H. Taubert, P. Wuerl, K. Onel, L. Yip, S.J. Hwang, L.C. Strong, G. Lozano, A.J. Levine, A single nucleotide polymorphism in the MDM2 promoter attenuates the p53 tumor suppressor pathway and accelerates tumor formation in humans, Cell 119 (2004) 591–602.
[12] G. Bougeard, S. Baert-Desurmont, I. Tournier, S. Vasseur, C. Martin, L. Brugieres, A. Chompret, B. Bressac-de Paillerets, D. Stoppa-Lyonnet, C. Bonaiti-Pellie, T. Frebourg, Impact of the MDM2 SNP309 and p53 Arg72Pro polymorphism on age of tumour onset in Li-Fraumeni syndrome, J. Med. Genet. 43 (2006) 531–533.
[13] H. Unsal, C. Yakicier, C. Marcais, M. Kew, M. Volkmann, H. Zentgraf, K.J. Isselbacher, M. Ozturk, Genetic heterogeneity of hepatocellular carcinoma, Proc. Natl. Acad. Sci. U.S.A. 91 (1994) 822–826.
[14] T. Cagatay, M. Ozturk, P53 mutation as a source of aberrant beta-catenin accumulation in cancer cells, Oncogene 21 (2002) 7971–7980.
[15] K. Sotamaa, S. Liyanarachchi, J.P. Mecklin, H. Jarvinen, L.A. Aaltonen, P. Peltomaki, A. de la Chapelle, p53 codon 72 and MDM2 SNP309 polymorphisms and age of colorectal cancer onset in Lynch syndrome, Clin. Cancer Res. 11 (2005) 6840–6844.
[16] A.S. Foulkes, Applied Statistical Genetics with R: For Population-Based Association Studies. Use R, Springer, 2009.
[17] Y. Cohen, J.Y. Cohen, Statistics and Data with R: An Applied Approach Through Examples, Wiley, 2008.
[18] J. Momand, D. Jung, S. Wilezynski, J. Niland, The MDM2 gene amplification database, Nucleic Acids Res. 26 (1998) 3453–3459.
[19] G. Reifenberger, L. Liu, K. Ichimura, E.E. Schmidt, V.P. Collins, Amplification and overexpression of the *MDM2* gene in a subset of human malignant gliomas without *p53* mutations, Cancer Res. 53 (1993) 236–239.
[20] M. Sanchez-Carbayo, N.D. Socci, T. Kirchoff, N. Erill, K. Offit, B.H. Bochner, C. Cordon-Cardo, A polymorphism in HDM2 (SNP309) associates with early onset in superficial tumors, TP53 mutations and poor outcome in invasive bladder cancer, Clin. Cancer Res. 13 (2007) 3215–3220.
[21] G.L. Bond, W. Hu, A. Levine, A single nucleotide polymorphism in the MDM2 gene: from a molecular and cellular explanation to clinical effect, Cancer Res. 65 (2005) 5481–5484.
[22] N. Dharel, N. Kato, R. Muroyama, M. Moriyama, R.X. Shao, T. Kawabe, M. Omata, MDM2 promoter SNP309 is associated with the risk of hepatocellular carcinoma in patients with chronic hepatitis C, Clin. Cancer Res. 12 (2006) 4867–4871.
[23] S. Ezzikouri, A.E. El Feydi, R. Afifi, L. El Kihal, M. Benazzouz, M. Hassar, A. Marchio, P. Pineau, S. Benjelloun, MDM2 SNP309T>G polymorphism and risk of hepatocellular carcinoma: a case–control analysis in a Moroccan population, Cancer Detect. Prev. 32 (2009) 380–385.
[24] Y.J. Yoon, H.Y. Chang, S.H. Ahn, J.K. Kim, Y.K. Park, D.R. Kang, J.Y. Park, S.M. Myoung, Y. Kim do, C.Y. Chon, K.H. Han, MDM2 and p53 polymorphisms are associated with the development of hepatocellular carcinoma in patients with chronic hepatitis B virus infection, Carcinogenesis 29 (2008) 1192–1196.